Measurement of the inclusive isolated-γ production cross section in Pb–Pb collisions with ALICE

Gustavo CONESA BALBASTRE
LPSC Grenoble — IN2P3-CNRS-UGA
for the ALICE Collaboration

- ➡ Differential p_{T} cross section
  - **pp & Pb–Pb at $\sqrt{s_{\mathrm{NN}}}$ = 5.02 TeV arXiv:2409.12641, ALICE-PUBLIC-2024-003** New
  - pp at $\sqrt{s}$ = 13 TeV arXiv:2407.01165 *accepted by EPJ C!* New
- ➡ Isolated γ-hadron correlation
  - **Pb–Pb at $\sqrt{s_{\mathrm{NN}}}$ = 5.02 TeV preliminary**

LPSC GRENOBLE | MODANE

EP seminar | CERN | 21/01/2025

IN2P3 Les deux infinis

Probing the QGP in heavy-ion collisions

➡ In heavy-ion collisions at the LHC, a dense, hot and strongly interacting coloured QCD medium is produced → the *"**quark-gluon plasma**"* (***QGP***)

➡ The ALICE experiment aims at the characterisation of the QGP (temperature, energy density, etc., the equation of state) via the measurements of different types of probes

➡ **Hard probes**: high-*E* partons (quarks and gluons) and electroweak particles (γ, Z^0 & $W^{\pm}$) emitted in the first stages of the collision:
→ "*bullets*" passing through the QGP

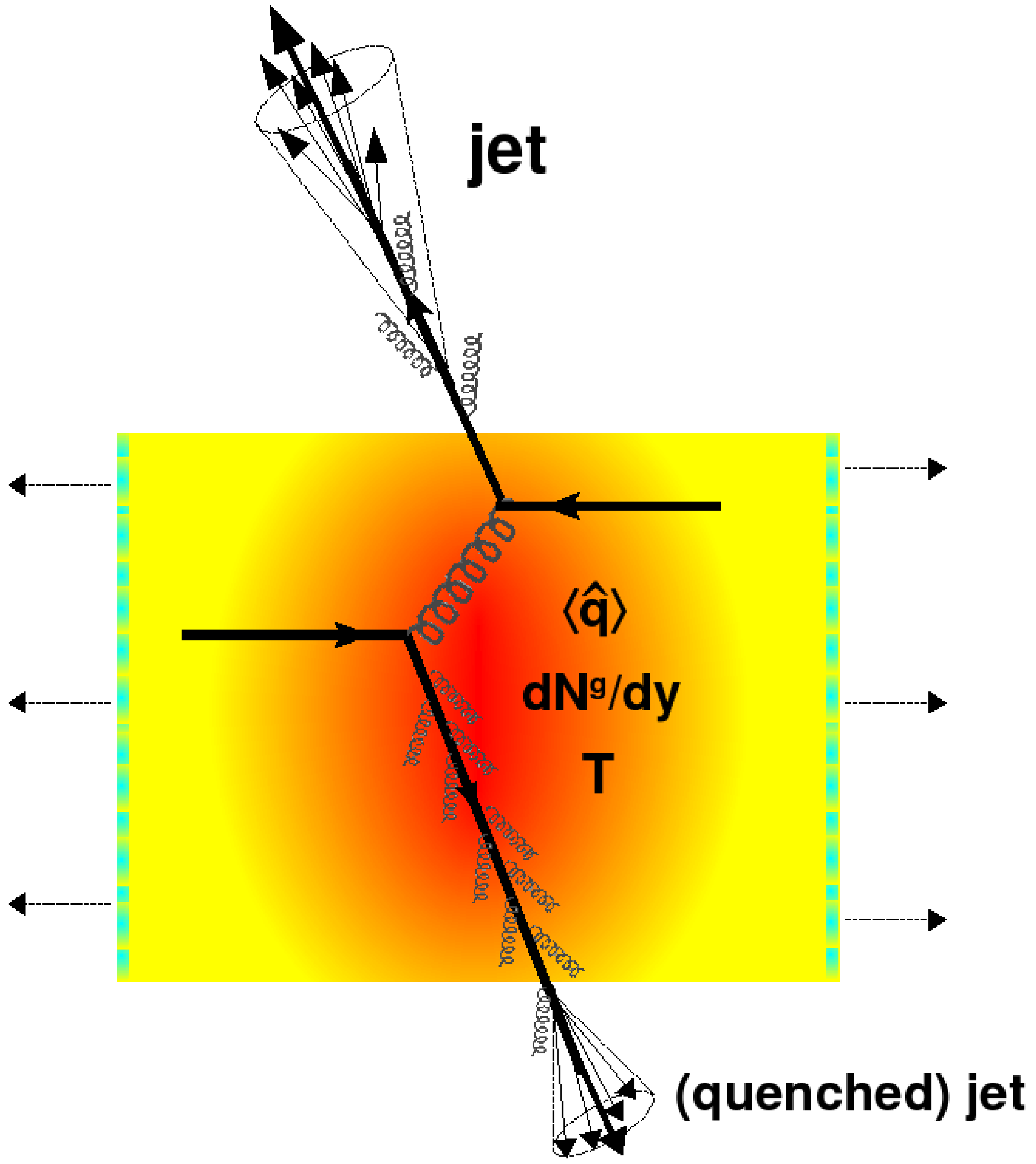

- **Partons lose energy** via radiational (gluonstrahlung) or collisional processes → **"jet quenching"**

- γ, Z^0 & $W^{\pm}$ are **colourless: not affected** by the *QGP* → **Candle particles**

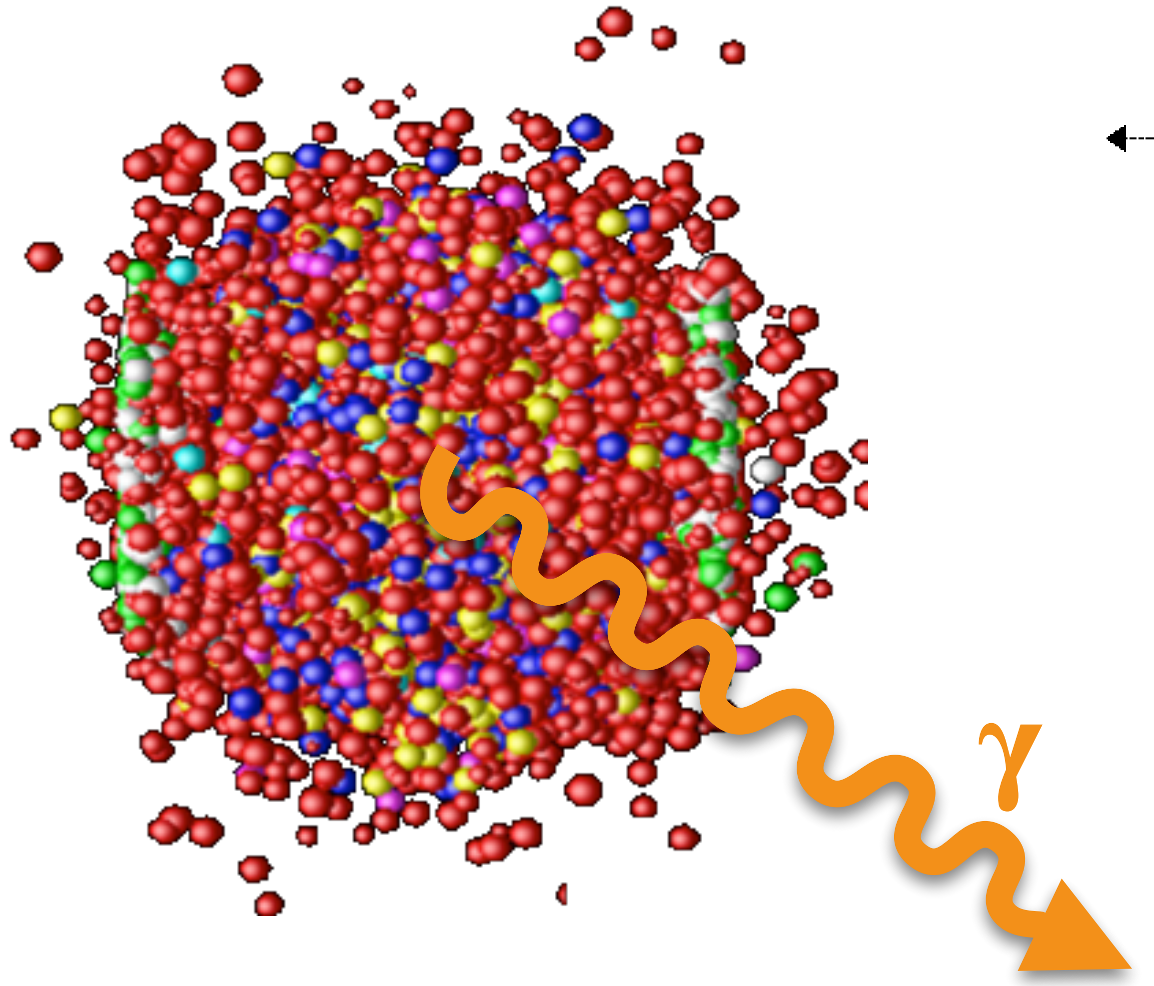

Observation of QGP effects: The nuclear modification factor

ALICE

➡ Consequence of jet-quenching: modification of jets and high p_T particle cross sections with respect to pp collisions

➡ Observation via the nuclear modification factor

$$R_{AA} = \frac{1}{\langle N_{coll} \rangle} \frac{d^2\sigma_{AA} / (dp_T \, d\eta)}{d^2\sigma_{pp} / (dp_T \, d\eta)}$$

$R_{AA} > 1$	Generation in the medium: Thermal γ
$R_{AA} = 1$	Transparent to the medium: Prompt γ
$R_{AA} < 1$	“Suppressed” by the medium: Coloured partons

If no QGP, a Pb–Pb collision is roughly N_{coll} × pp collisions

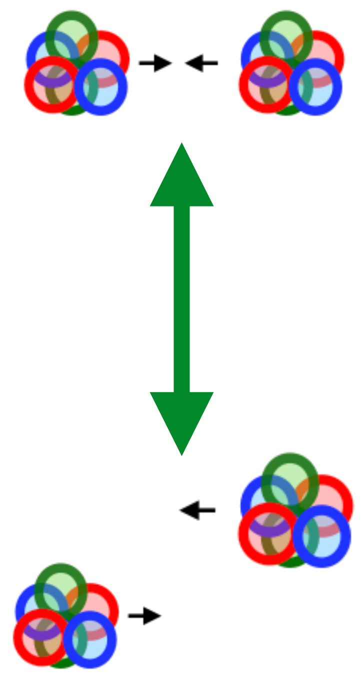

Centrality	$\langle N_{coll} \rangle$
0–10%	1572 ± 17
10–30%	783 ± 7
30–50%	265 ± 3
50–70%	65.9 ± 1.2
70–90%	10.9 ± 0.2

$\sqrt{s_{NN}}$ = 5.02 TeV

➡ Collision centrality (impact parameter *b*) variation: Change of the QGP volume → change of R_{AA}

- Higher centrality (larger *b*) implies smaller modification of the hadronic cross section

Photon sources probing the QGP

- Direct γ, *not originating from hadronic decays*
  - ➡ **Direct thermal γ: $R_{AA} >> 1$**
    - QGP thermal radiation
    - Measure ***T* & time/size evolution**

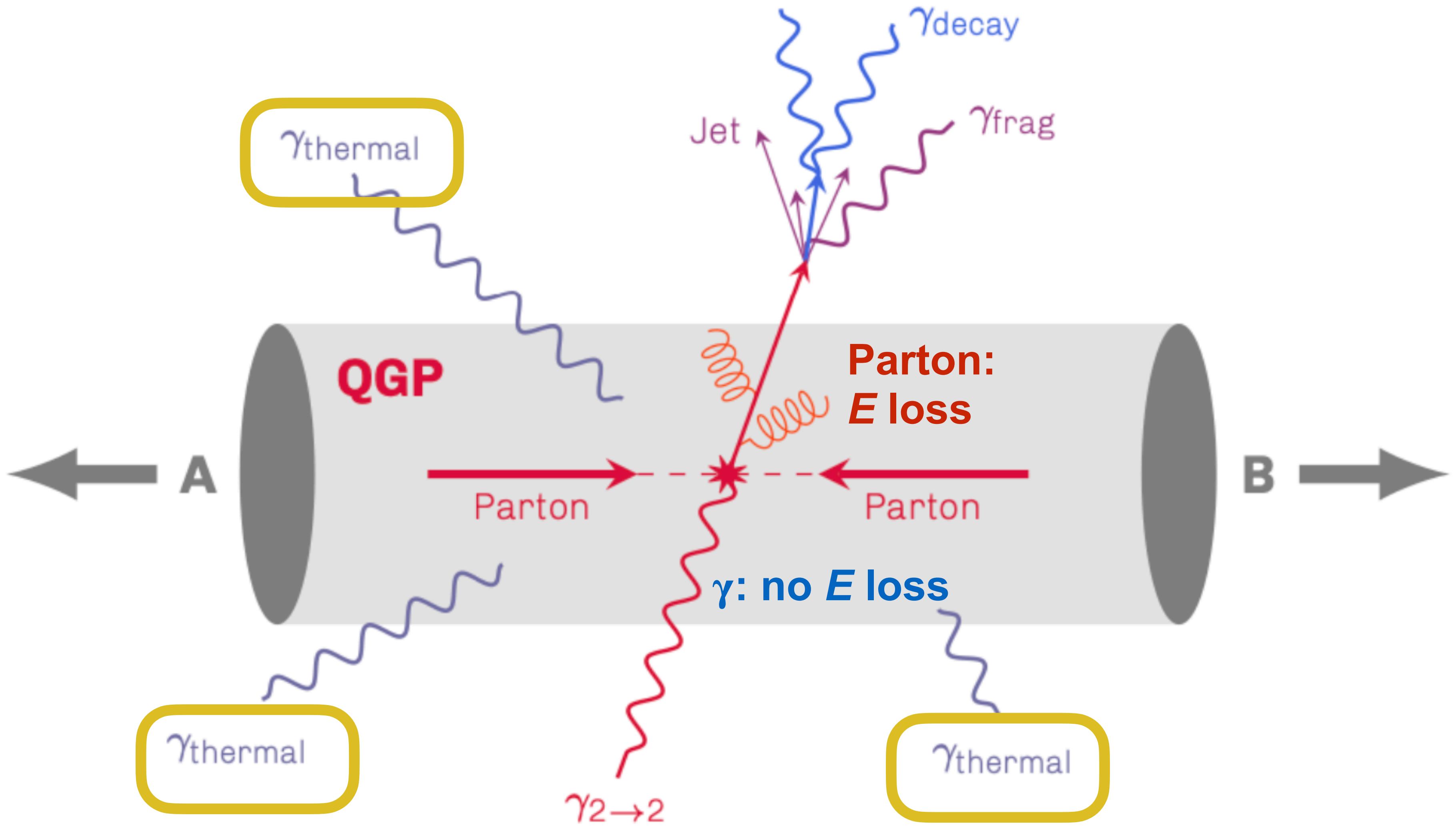

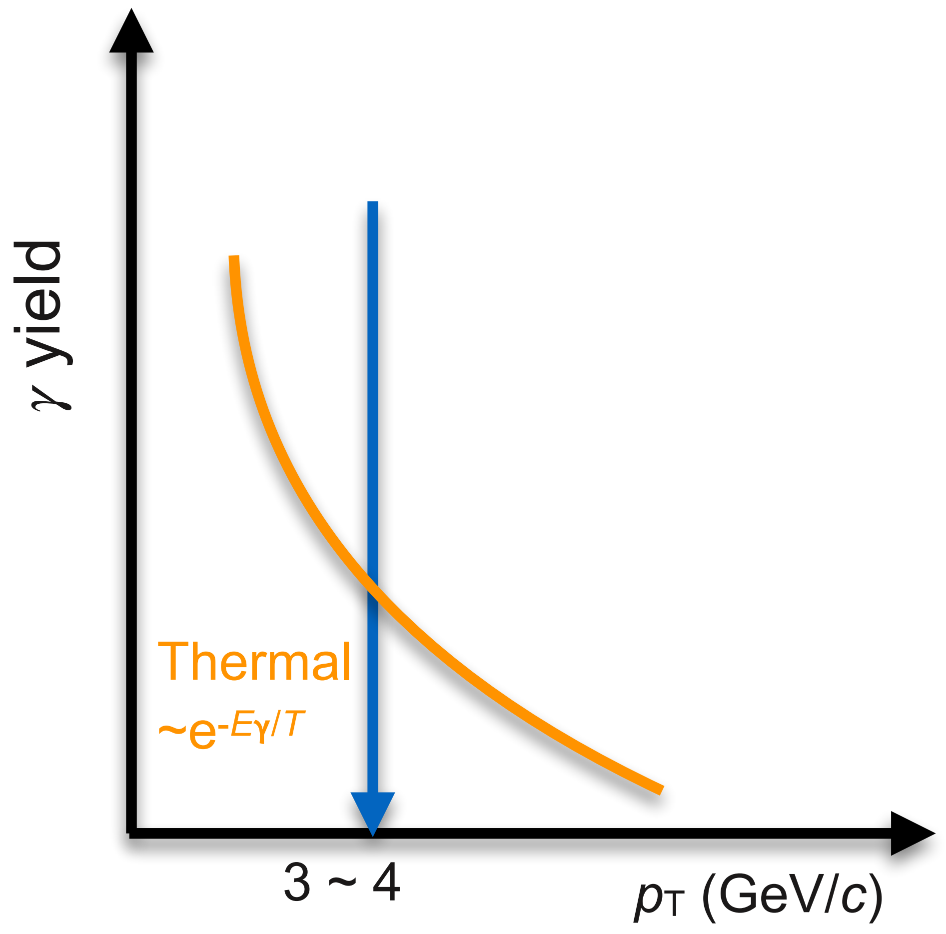

Photon sources probing the QGP

- Direct γ, *not originating from hadronic decays*

  ➡ **Direct thermal γ**: R_{AA} >> 1
  – QGP thermal radiation
  – Measure ***T* & time/size evolution**

  ➡ **Direct prompt γ**: $R_{AA} \approx 1$
  – Initial hard scattering, processes at LO:

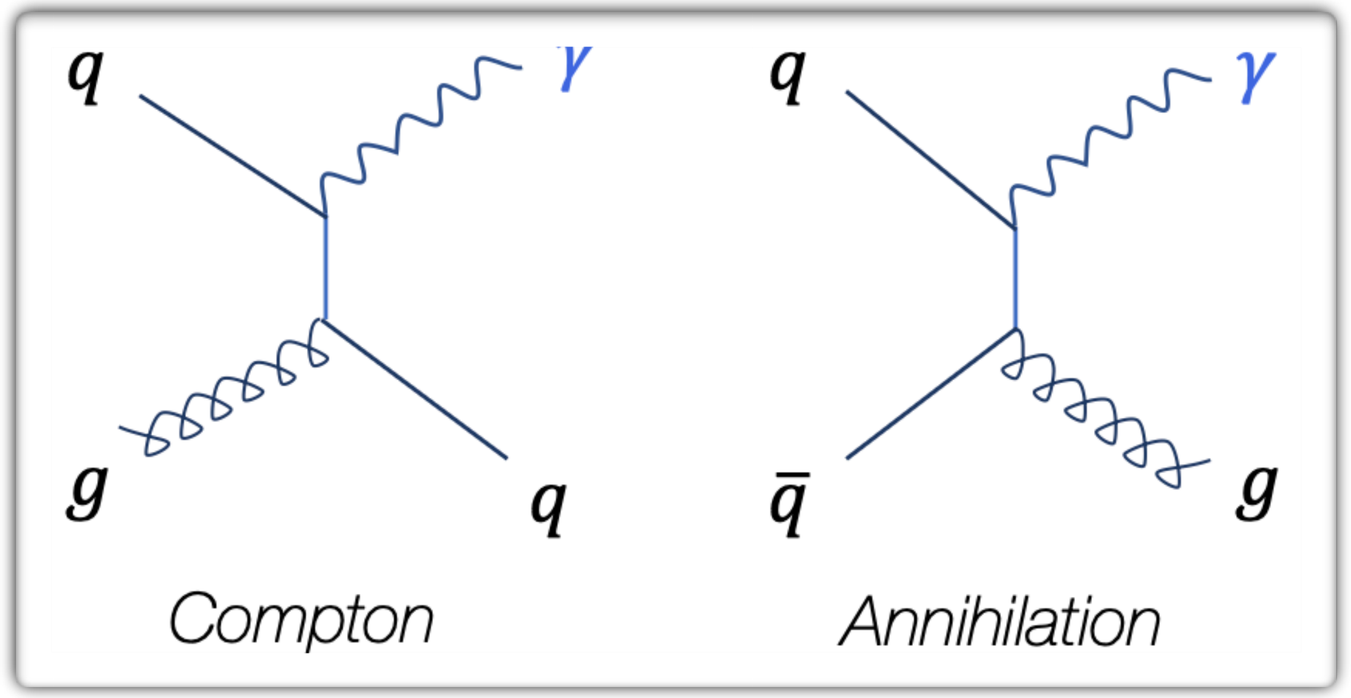

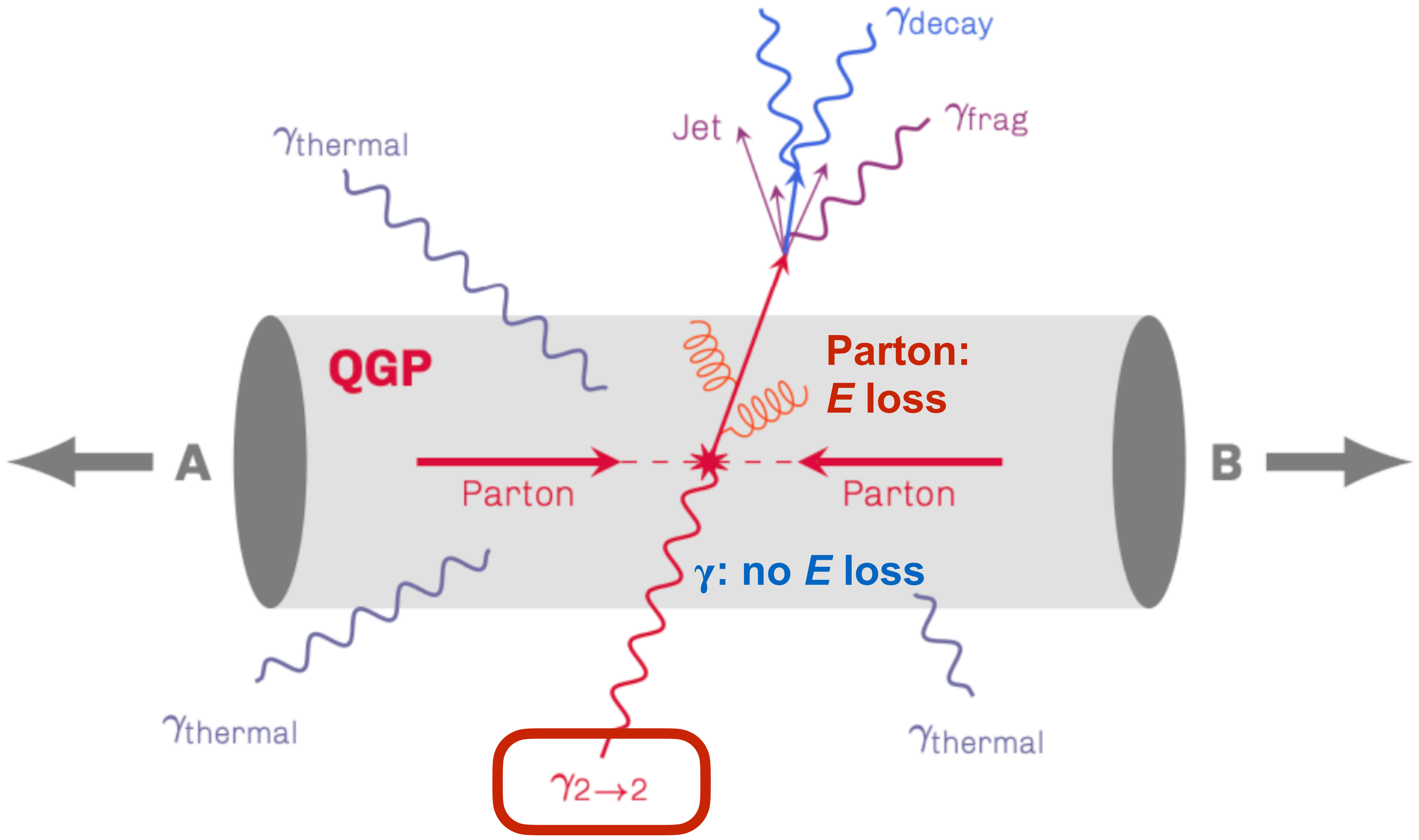

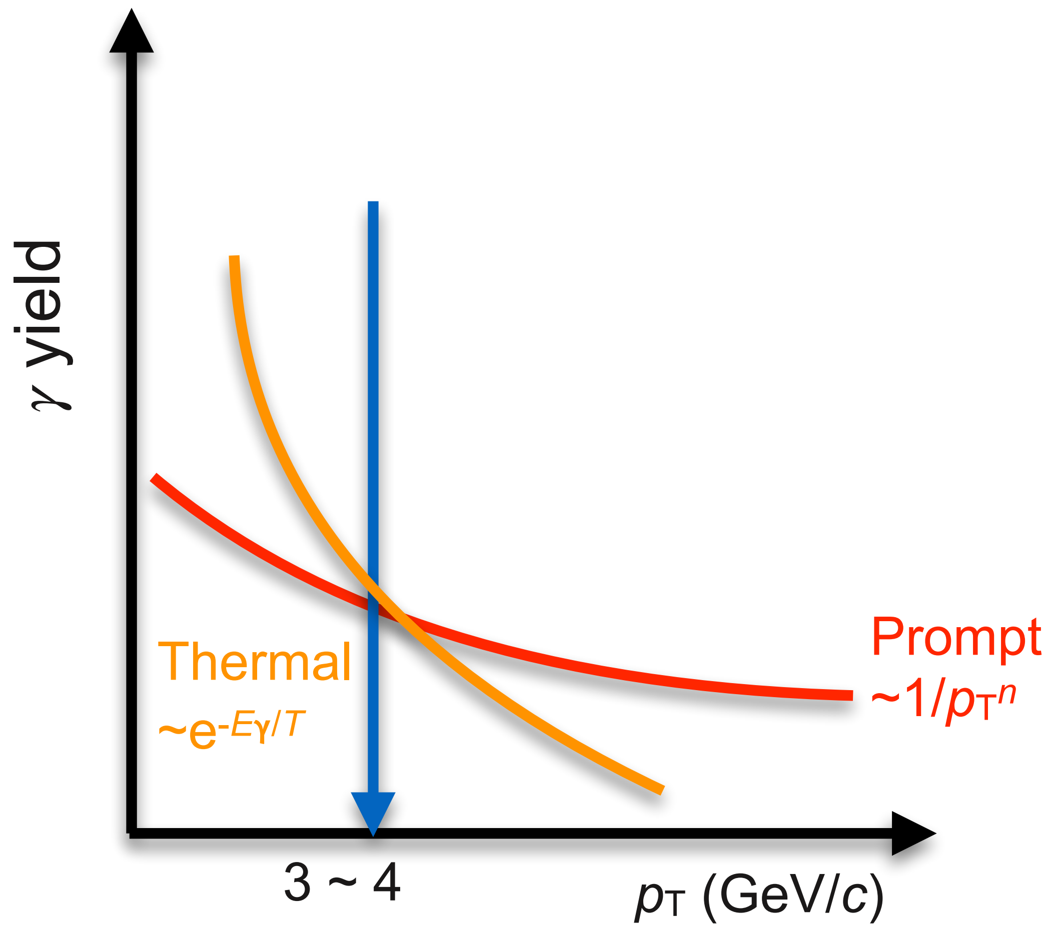

  – **Test pQCD** predictions, **constrain (n)PDFs & FF**
    ▷ Cold nuclear matter (nPDF) effects can lead to $R_{AA} \neq 1$
  – $p_{\mathrm{T}}^{\gamma} \simeq p_{\mathrm{T}}^{\mathrm{parton}}$, before parton loses ΔE in QGP
  – Measure **FF modifications**, where is the ΔE radiated?

$$d\sigma^{hard}_{AB\to h} = f_{a/A}(x_1, Q^2) \otimes f_{b/B}(x_2, Q^2) \otimes d\sigma^{hard}_{ab\to c}(x_1, x_2, Q^2) \otimes D_{c\to h}(z, Q^2)$$

PDFs | Hard scattering (pQCD) | Fragmentation function (FF)

Main focus of today's presentation!

Photon sources probing the QGP

- Direct γ, *not originating from hadronic decays*
  - ➡ **Direct thermal γ**: R_{AA} >> 1
    - QGP thermal radiation
    - Measure ***T* & time/size evolution**
  - ➡ **Direct prompt γ**: $R_{AA} \approx 1$
    - Initial hard scattering, processes at LO:

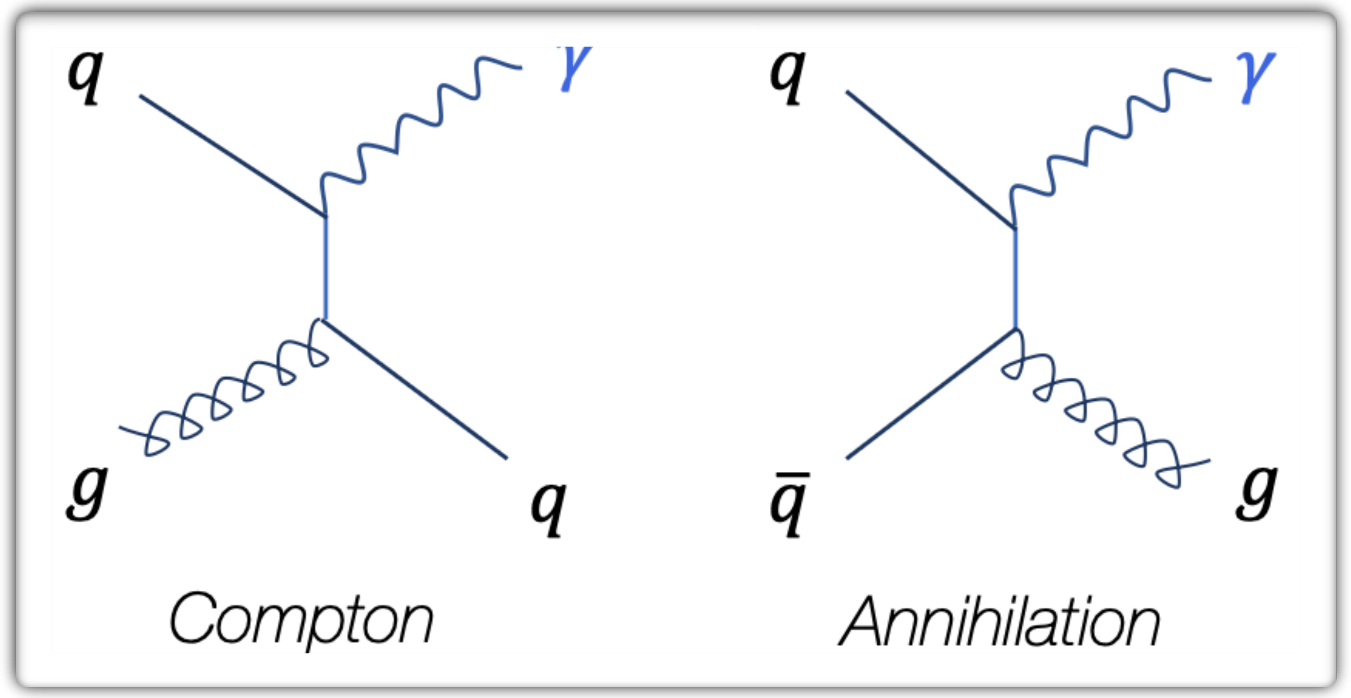

    - **Test pQCD** predictions, **constrain (n)PDFs & FF**
      - Cold nuclear matter (nPDF) effects can lead to $R_{AA} \neq 1$
    - $p_T^{\gamma} \simeq p_T^{\text{parton}}$, before parton loses Δ*E* in QGP
    - Measure **FF modifications**, where is the Δ*E* radiated?

- **Decay γ (π^0 & η)**: R_{AA} << 1
  - Main background for direct γ measurements
    - ◉ ***N*prompt / *N*decay ~ 0.01 (pp)**

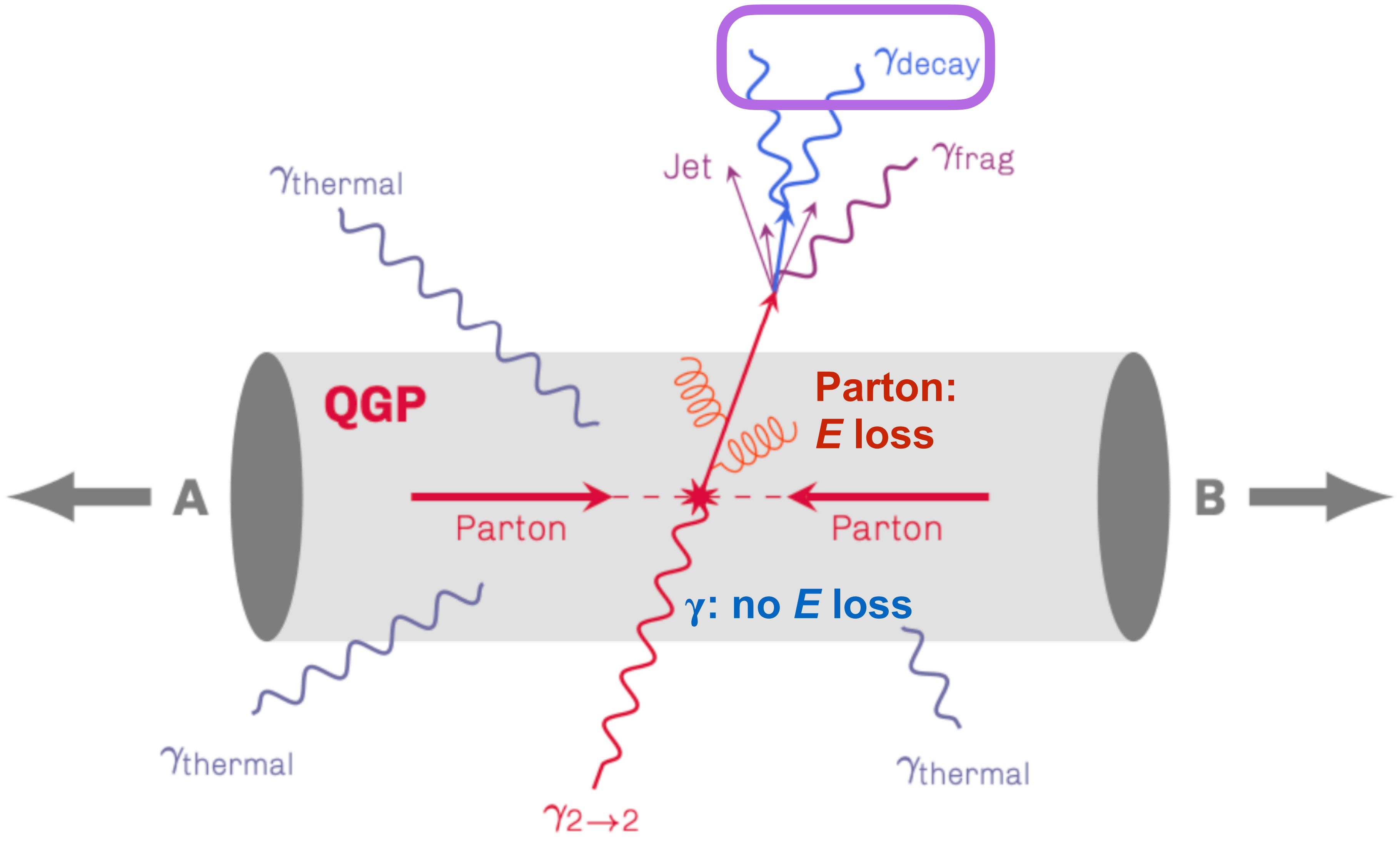

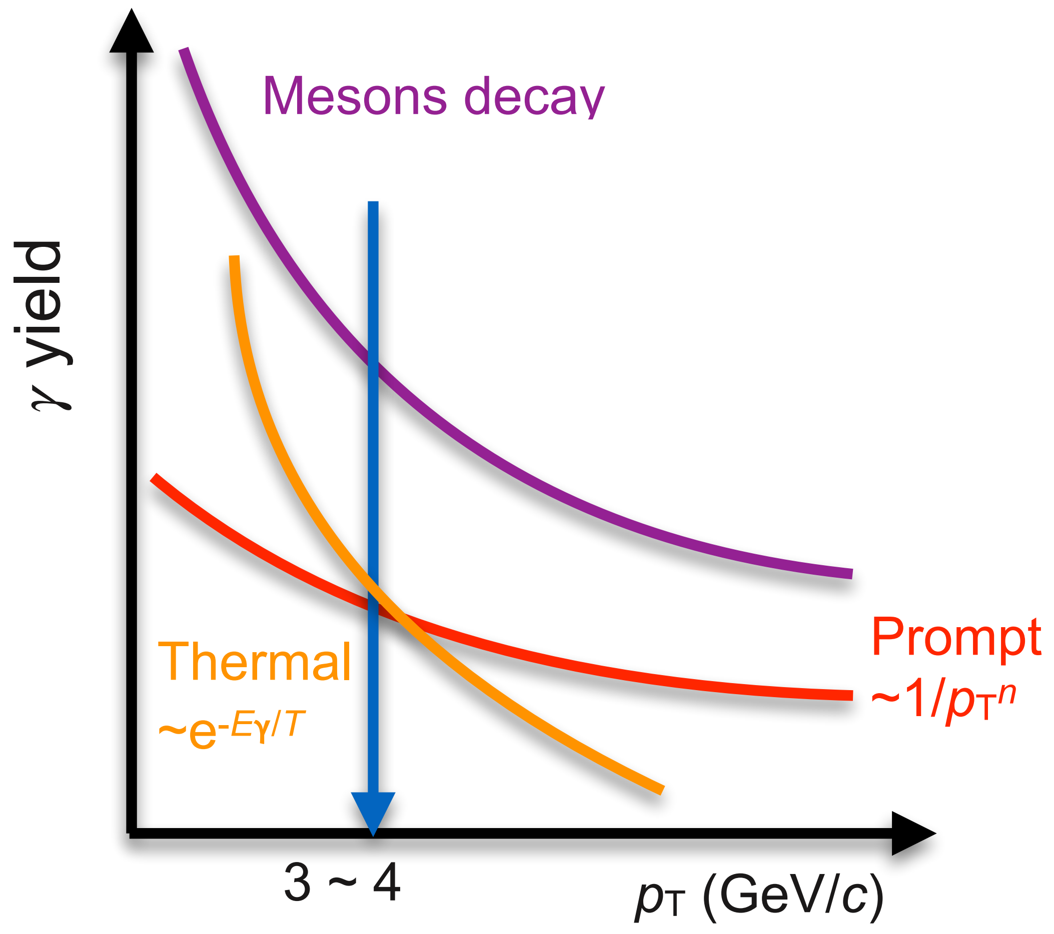

$$d\sigma^{hard}_{AB\to h} = f_{a/A}(x_1, Q^2) \otimes f_{b/B}(x_2, Q^2) \otimes d\sigma^{hard}_{ab\to c}(x_1, x_2, Q^2) \otimes D_{c\to h}(z, Q^2)$$

PDFs — Hard scattering (pQCD) — Fragmentation function (FF)

Photon sources probing the QGP

- Direct γ, *not originating from hadronic decays*

➡ **Direct thermal γ**: R_{AA} >> 1

– QGP thermal radiation

– Measure ***T* & time/size evolution**

➡ **Direct prompt γ**: $R_{AA} \approx 1$

– Initial hard scattering, processes at LO:

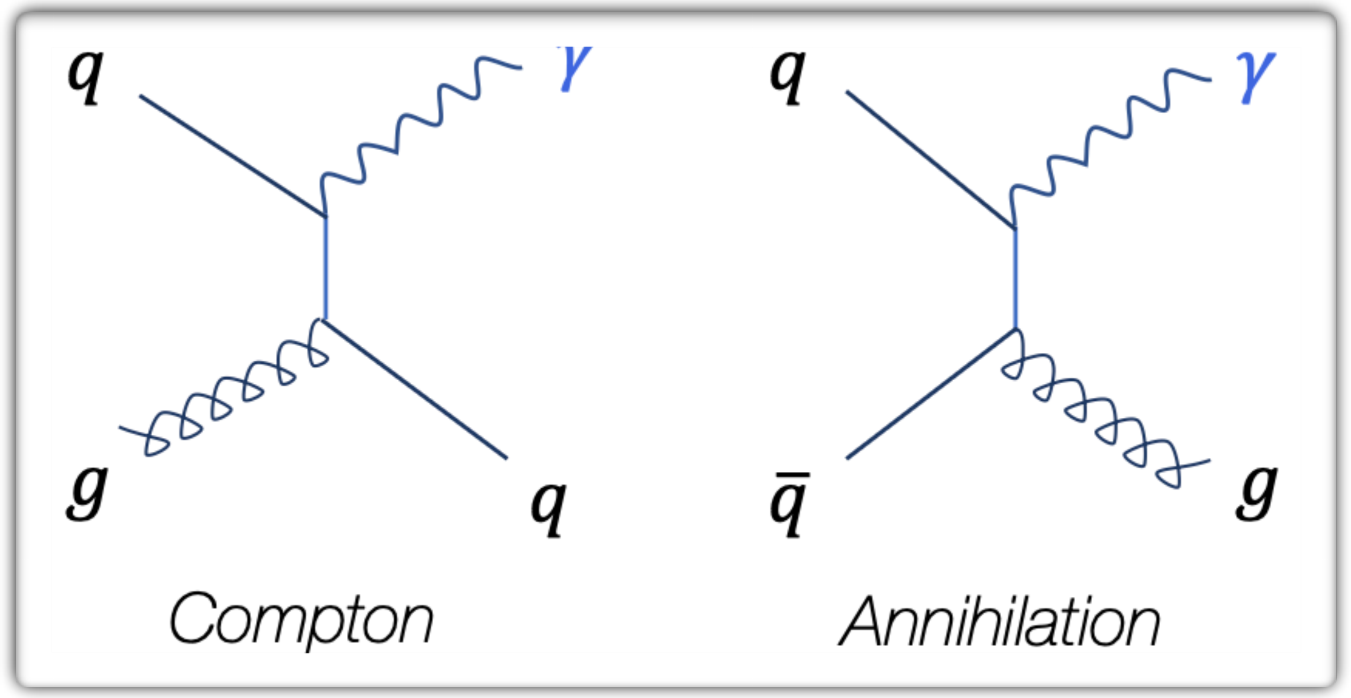

– **Test pQCD** predictions, **constrain (n)PDFs & FF**

▸ Cold nuclear matter (nPDF) effects can lead to $R_{AA} \neq 1$

– $p_{T}^{\gamma} \simeq p_{T}^{\mathrm{parton}}$, before parton loses Δ*E* in QGP

– Measure **FF modifications**, where is the Δ*E* radiated?

- **Decay γ** (π^0 & η): R_{AA} << 1

– Main background for direct γ measurements

◉ N_{prompt} / N_{decay} ~ 0.01 (pp)

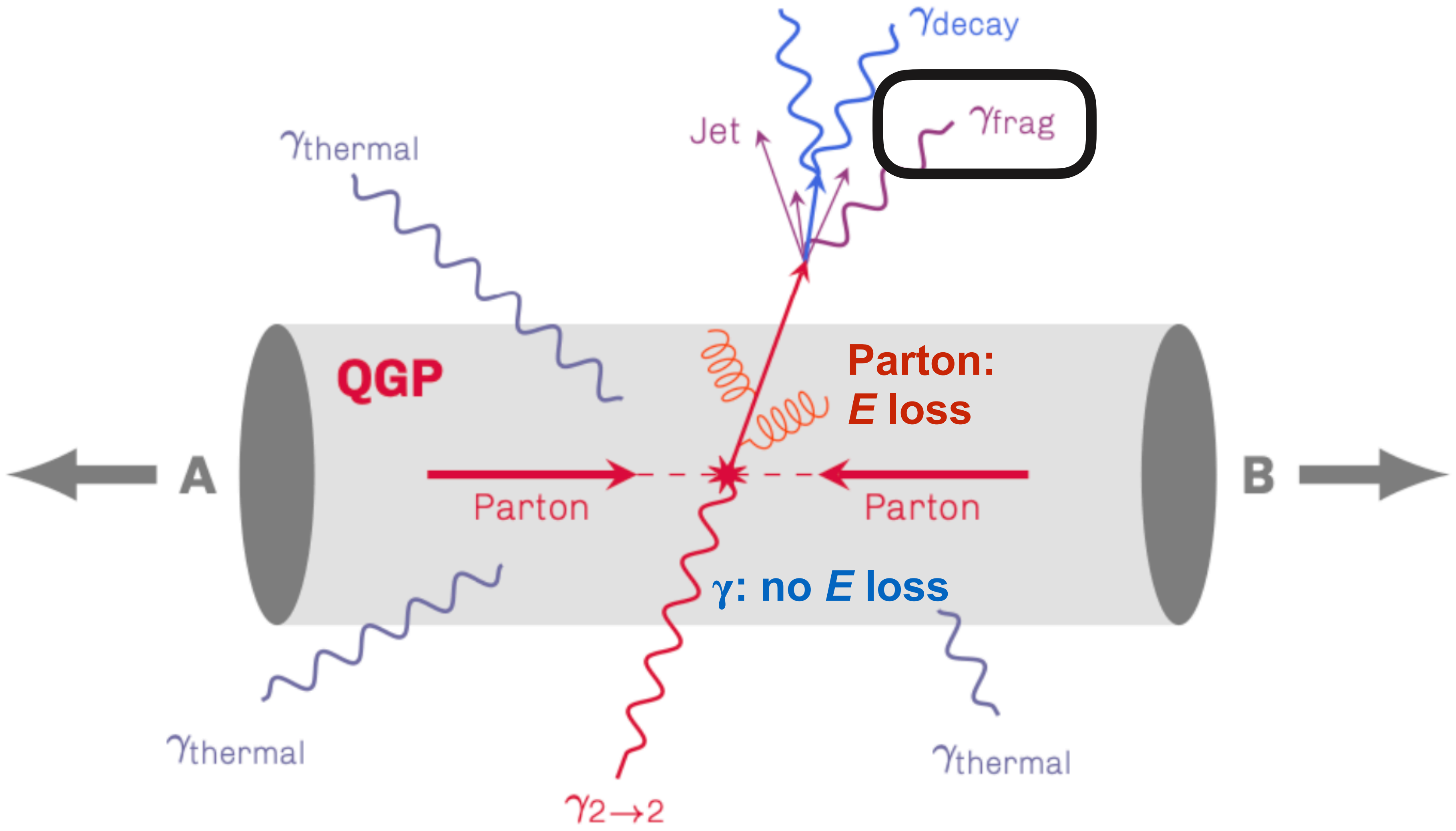

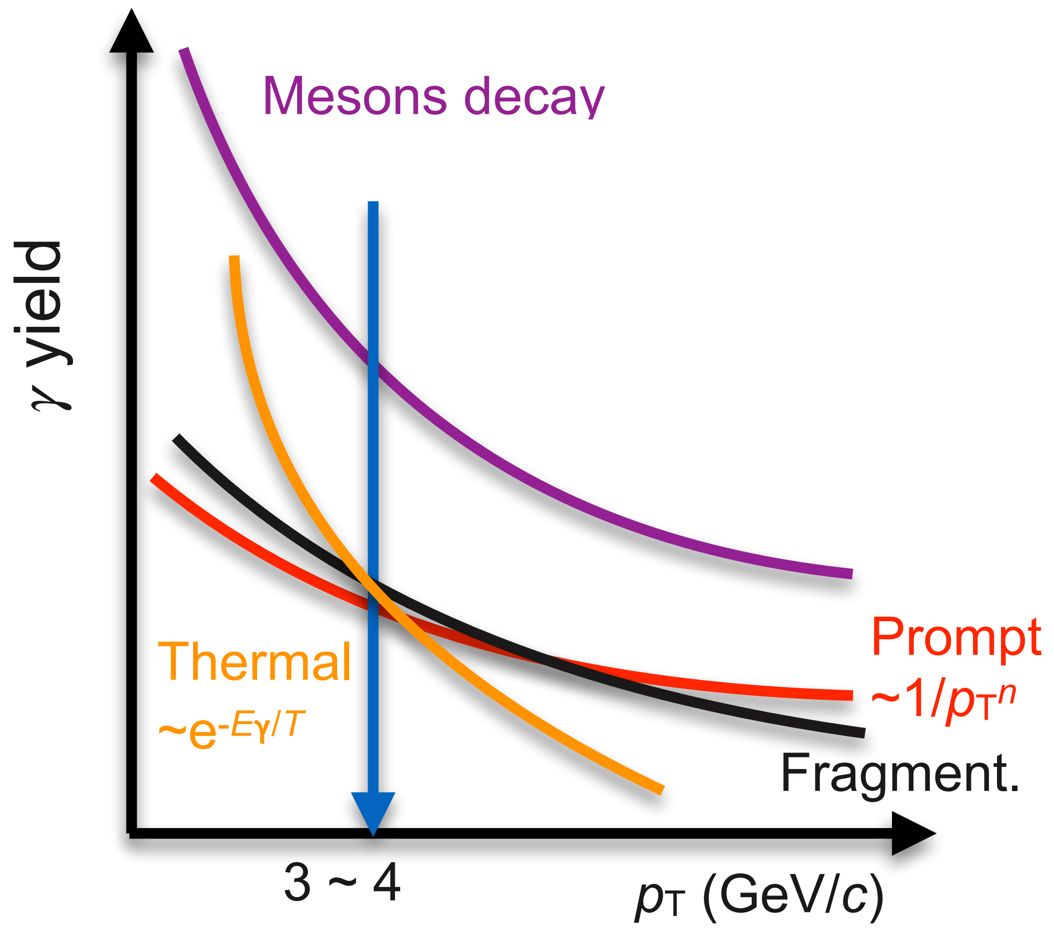

$$d\sigma^{hard}_{AB\to h} = f_{a/A}(x_1, Q^2) \otimes f_{b/B}(x_2, Q^2) \otimes d\sigma^{hard}_{ab\to c}(x_1, x_2, Q^2) \otimes D_{c\to h}(z, Q^2)$$

PDFs — Hard scattering (pQCD) — Fragmentation function (FF)

➡ **Other direct γ sources:**

– **Fragmentation γ**: $R_{AA} < 1$? comparable yield to direct prompt γ

– QGP pre-equilibrium γ? $R_{AA} >> 1$ (glasma phase)

– Jet-QGP interaction γ? $R_{AA} >> 1$ (hard partons scattering)

How to measure and identify prompt γ in ALICE?

- For the measurements presented here:

➡ Calorimeter, EMCal/DCal:
  - Pb/scintillator towers (6 × 6 cm)
  - 4.4 m from interaction point (IP)
  - $|\eta| < 0.67$ for $\Delta\varphi = 107^\circ$,
    $0.22 < |\eta| < 0.67$ for $\Delta\varphi = 60^\circ$ (DCal);
  - Identification: EM shower dispersion
  - E_γ > 700 MeV

➡ Tracking, TPC & ITS
  - $|\eta| < 0.9$ for $\Delta\varphi = 360^\circ$
  - E_γ > 100 MeV

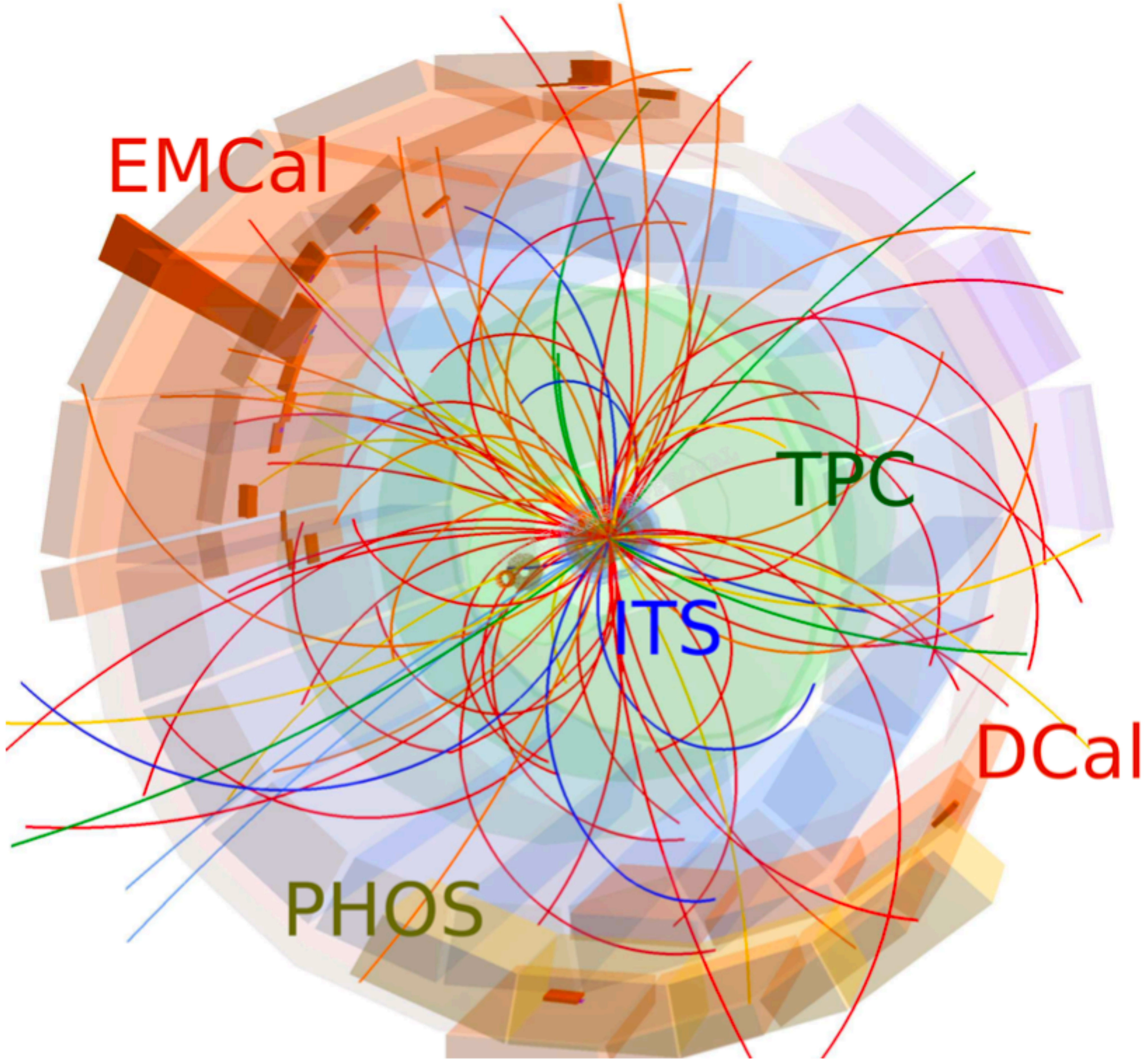

- γ identification combining tracking+calorimeter

➡ Inclusive γ: Charged particle veto

➡ Prompt γ: **Isolation** (next slides)

Prompt γ identification in ALICE: EM shower spread shape

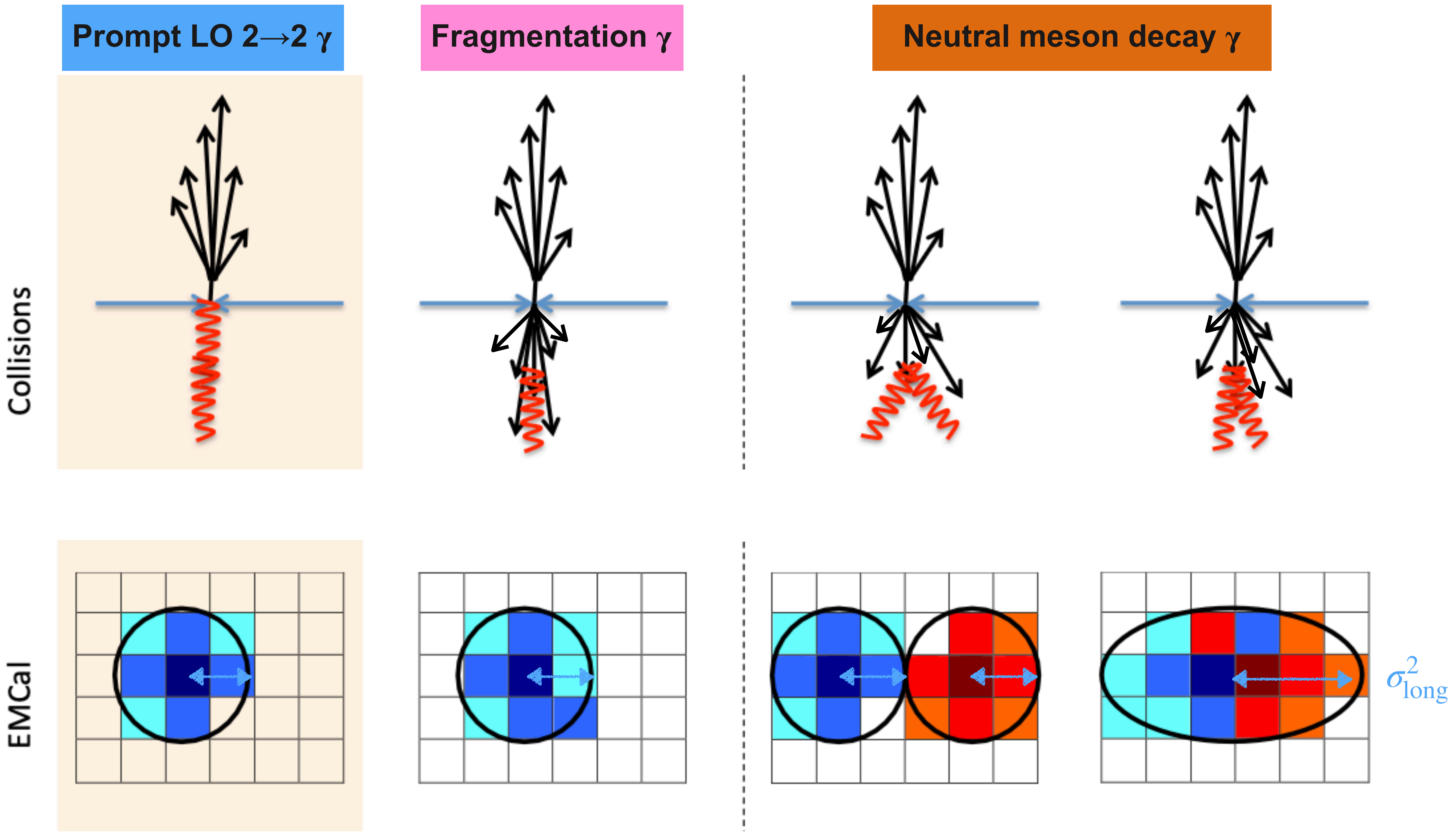

EM shower discrimination

γ single vs merged decays

- ➡ **EMCal**
- ➡ Shower elongation σ^2_{long}: longest ellipse axis size

➡ **circular "narrow" cluster**

➡ circular narrow clusters, potentially wider due to jet particles nearby merging

➡ decay γ merge, E_{π^0} > 6 GeV **elliptical "wide" cluster**

Prompt γ identification in ALICE: EM shower spread shape & isolation with tracks

Prompt γ at LO 2→2: ***isolated***

- ➡ **TPC+ITS charged tracks**
- ➡ Select γ with low hadronic activity in R, small $p_{\mathrm{T}}^{\mathrm{iso,\,ch}}$

$$\sqrt{(\eta_{\mathrm{track}}-\eta_{\gamma})^2+(\varphi_{\mathrm{track}}-\varphi_{\gamma})^2} < R = 0.4 \text{ or } 0.2$$

$$p_{\mathrm{T}}^{\mathrm{iso,\,ch}} = \sum p_{\mathrm{T}}^{\mathrm{tracks\ in\ cone}} - \rho_{\mathrm{UE}}\cdot\pi\cdot R^2 < 1.5\ \mathrm{GeV}/c$$

✱ Underlying event (UE) subtracted event-by-event, ρ_{UE} density estimation

EM shower discrimination

γ single vs merged decays

- ➡ **EMCal**
- ➡ Shower elongation σ^2_{long}: longest ellipse axis size

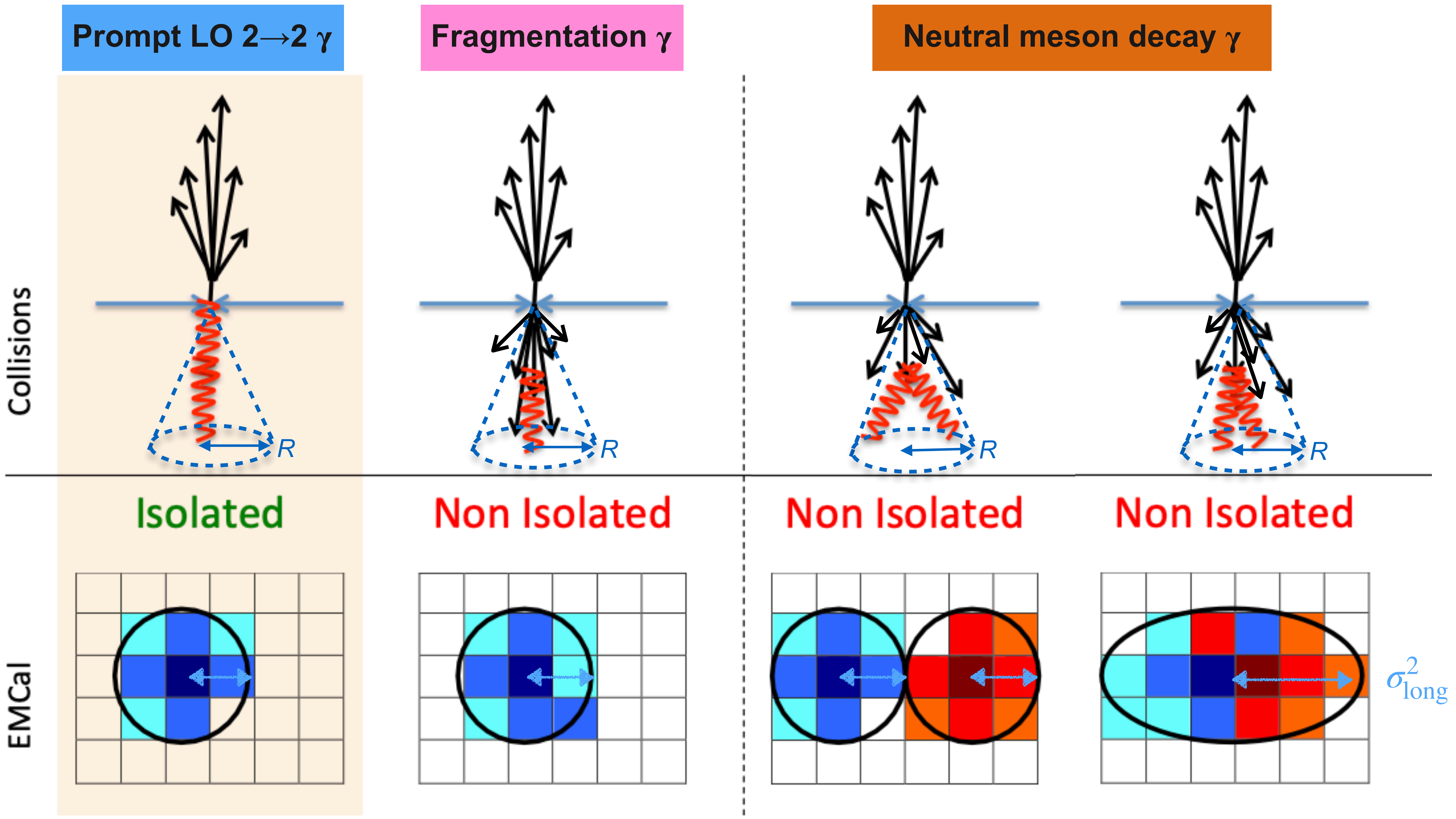

- ➡ **circular "narrow" cluster**
- ➡ circular narrow clusters, potentially wider due to jet particles nearby merging
- ➡ decay γ merge, E_{π^0} > 6 GeV **elliptical "wide" cluster**

Prompt γ identification in ALICE: isolation with tracks

Prompt γ at LO 2→2: *isolated*

- ➡ **TPC+ITS charged tracks**
- ➡ Select γ with low hadronic activity in R, small $p_{\mathrm{T}}^{\text{iso, ch}}$

$$\sqrt{(\eta_{\text{track}} - \eta_{\gamma})^2 + (\varphi_{\text{track}} - \varphi_{\gamma})^2} < R = 0.4 \text{ or } 0.2$$

$$p_{\mathrm{T}}^{\text{iso, ch}} = \sum p_{\mathrm{T}}^{\text{tracks in cone}} - \rho_{\text{UE}} \cdot \pi \cdot R^2 < 1.5 \text{ GeV}/c$$

✱ Underlying event (UE) subtracted event-by-event, ρ_{UE} density estimation

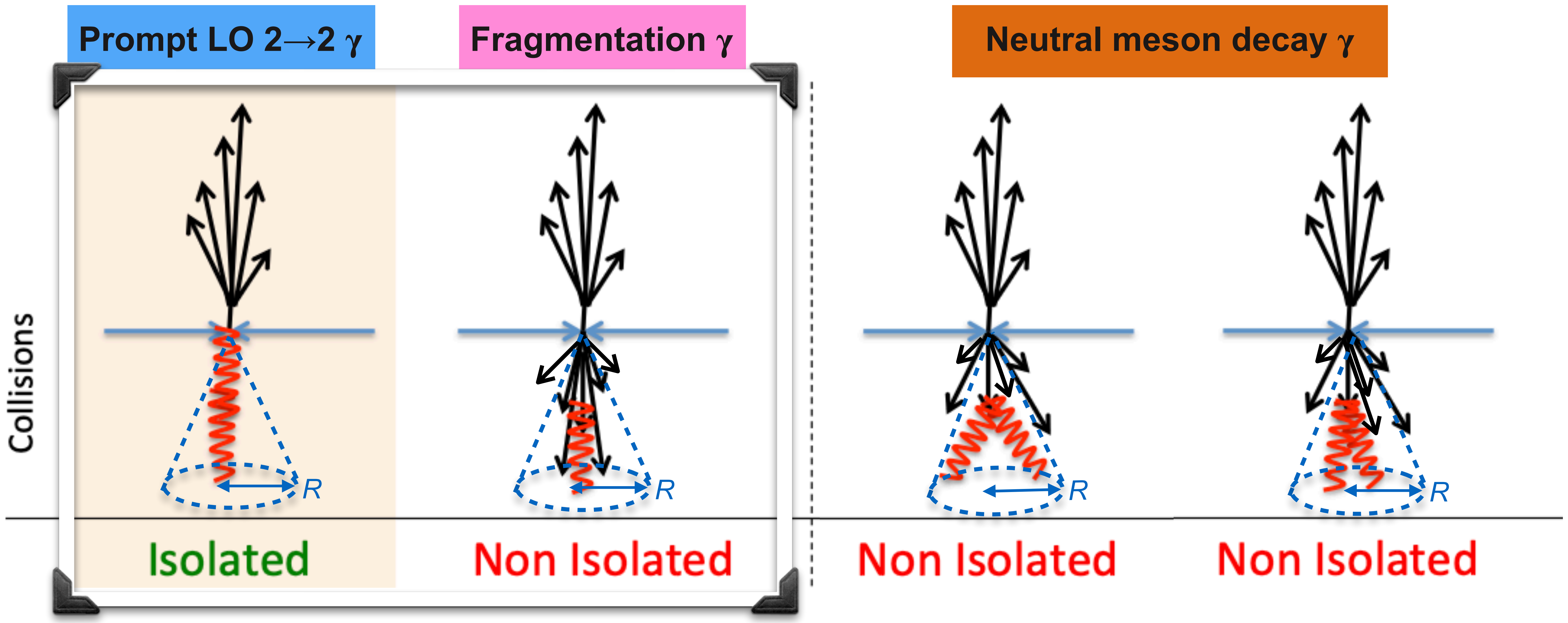

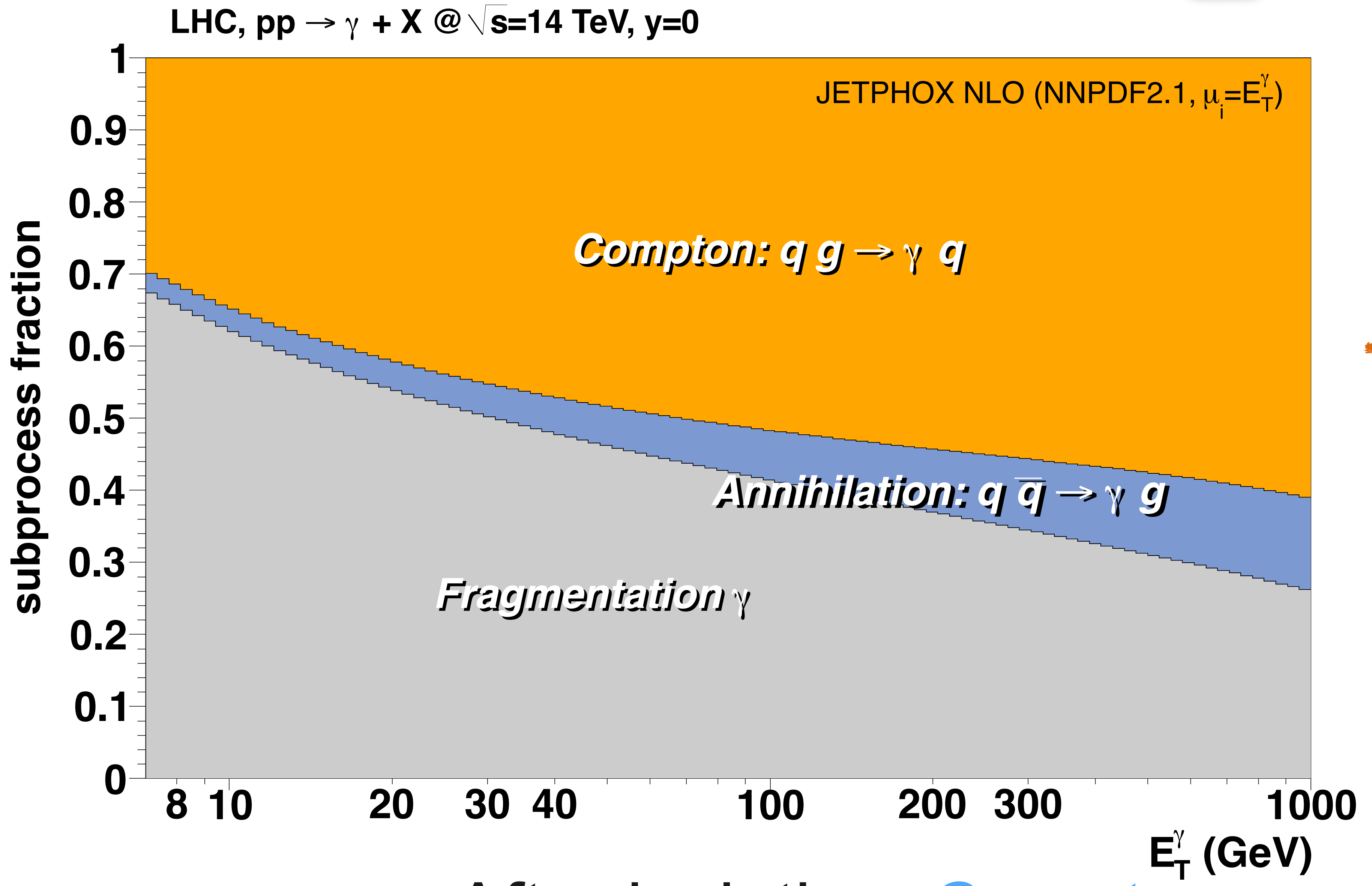

pp, $\sqrt{s}$ = 14 TeV

Isolation

R = 0.4, $E_{\mathrm{T}}^{\text{had}} < 4$ GeV

D. D'Enterria & J. Rojo
Nucl. Phys. B 860 (2012),
arXiv:1202.1762 [hep-ph]

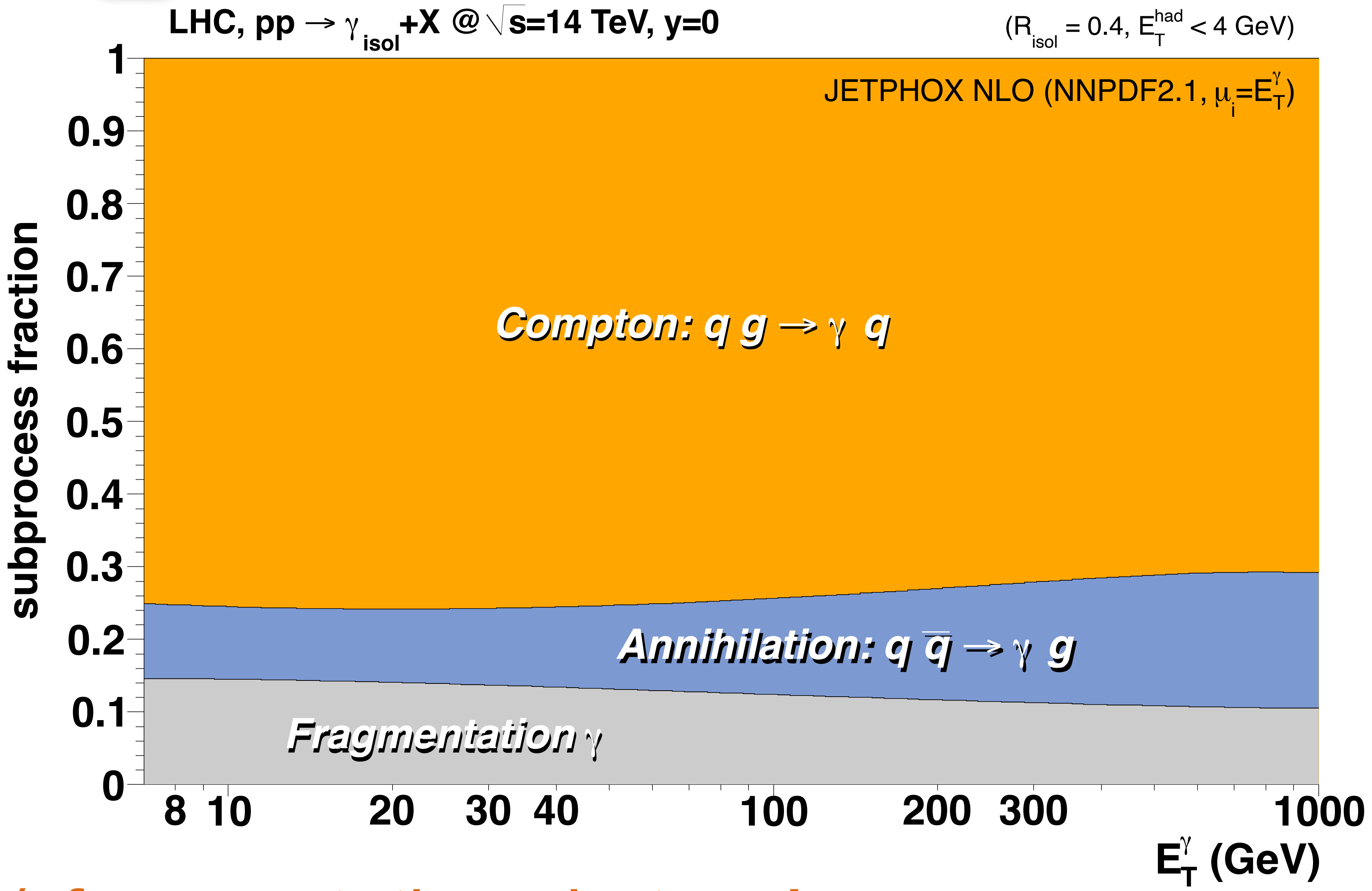

After isolation: Compton process dominance, 10-15% fragmentation photons!

Prompt γ identification in ALICE: isolation with tracks

Prompt γ at LO 2→2: *isolated*

- ➡ **TPC+ITS charged tracks**
- ➡ Select γ with low hadronic activity in R, small $p_{\mathrm{T}}^{\mathrm{iso,\,ch}}$

$$\sqrt{(\eta_{\mathrm{track}}-\eta_{\gamma})^2+(\varphi_{\mathrm{track}}-\varphi_{\gamma})^2} < R = 0.4 \text{ or } 0.2$$

$$p_{\mathrm{T}}^{\mathrm{iso,\,ch}} = \sum p_{\mathrm{T}}^{\mathrm{tracks\ in\ cone}} - \rho_{\mathrm{UE}}\cdot\pi\cdot R^2 < 1.5\ \mathrm{GeV}/c$$

✱ Underlying event (UE) subtracted event-by-event, ρ_{UE} density estimation

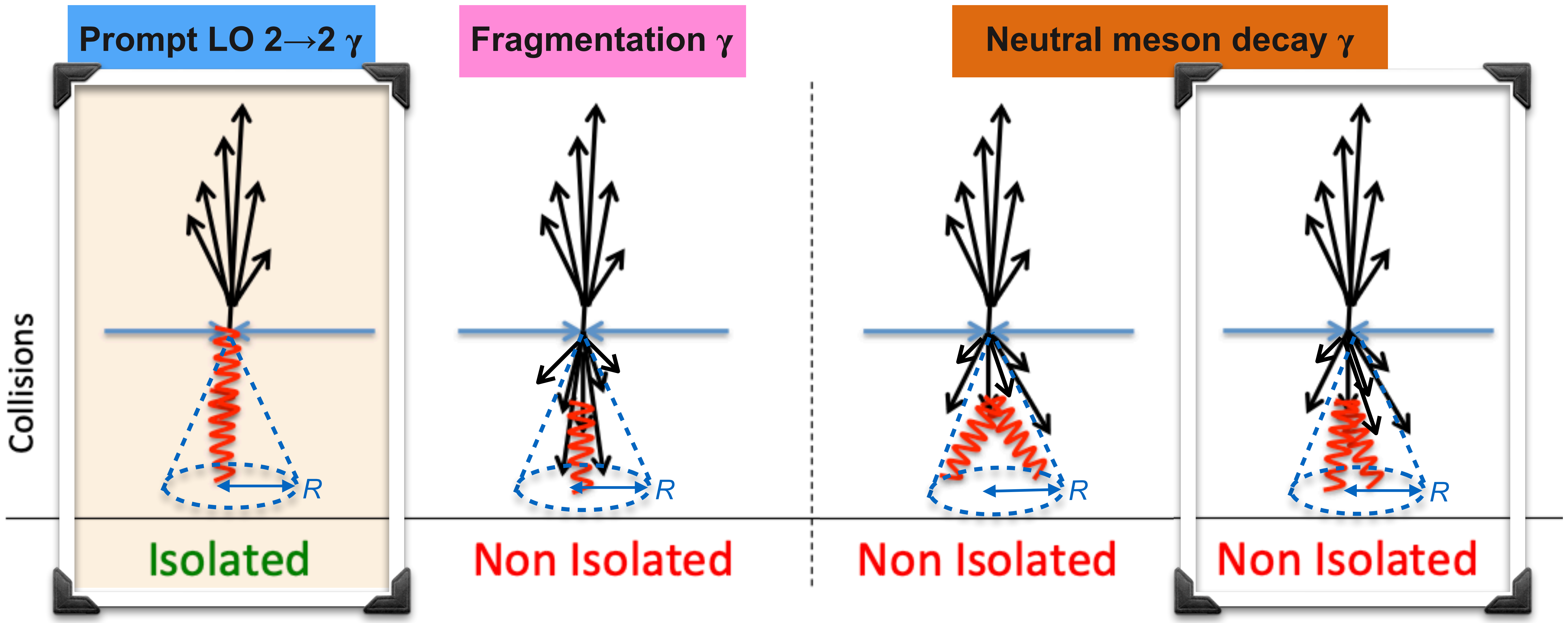

- ➡ Strong neutral meson background rejection
  ◉ Remaining cases: parton fragments into meson plus few low p_{T} particles → low $p_{\mathrm{T}}^{\mathrm{iso,\,ch}}$
- ➡ Strong effect in central Pb–Pb in signal rejection due to UE fluctuations

ALICE-PUBLIC-2024-003

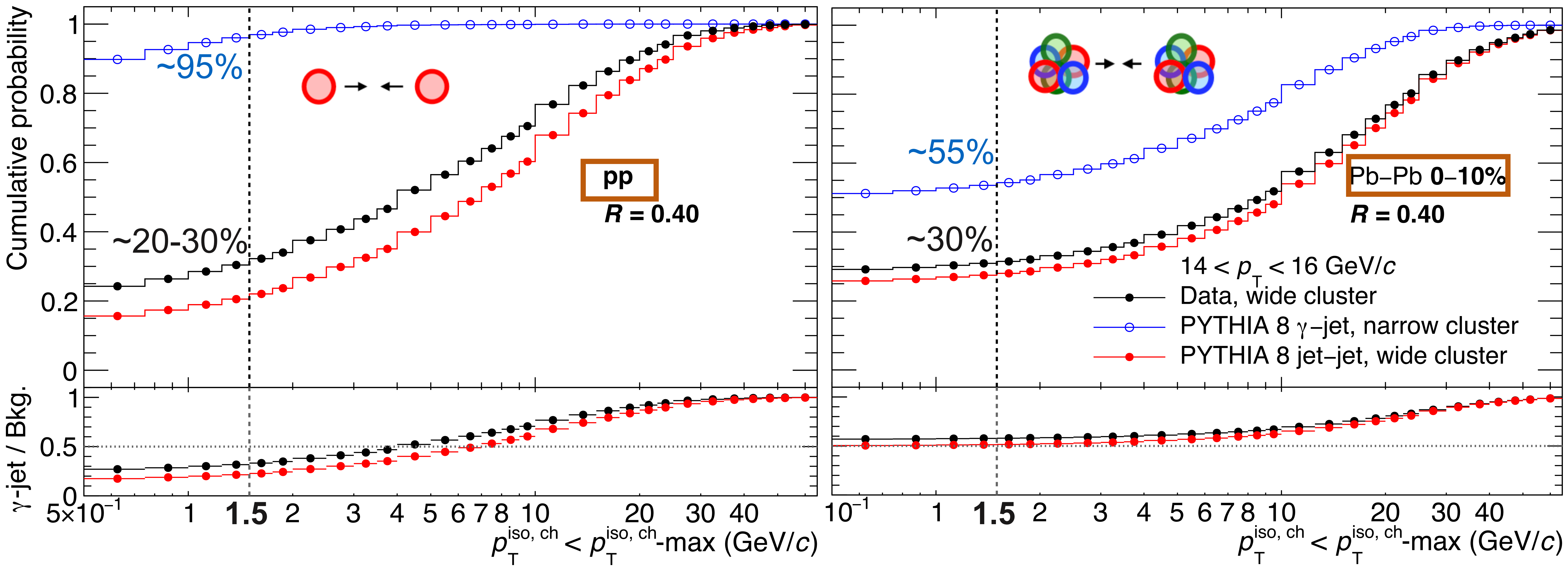

Underlying event estimation

Track p_T UE density estimated on Pb–Pb & pp collisions at $\sqrt{s_{NN}}$ = 5.02 TeV:

- ➡ Sum of tracks p_T normalised by ***η*-band** area
  → *Avoid flow effects*
- ➡ Gap between cone and band of $\Delta R_{\mathrm{UE\ gap}}$= 0.1
  → *Avoid jet remnants*

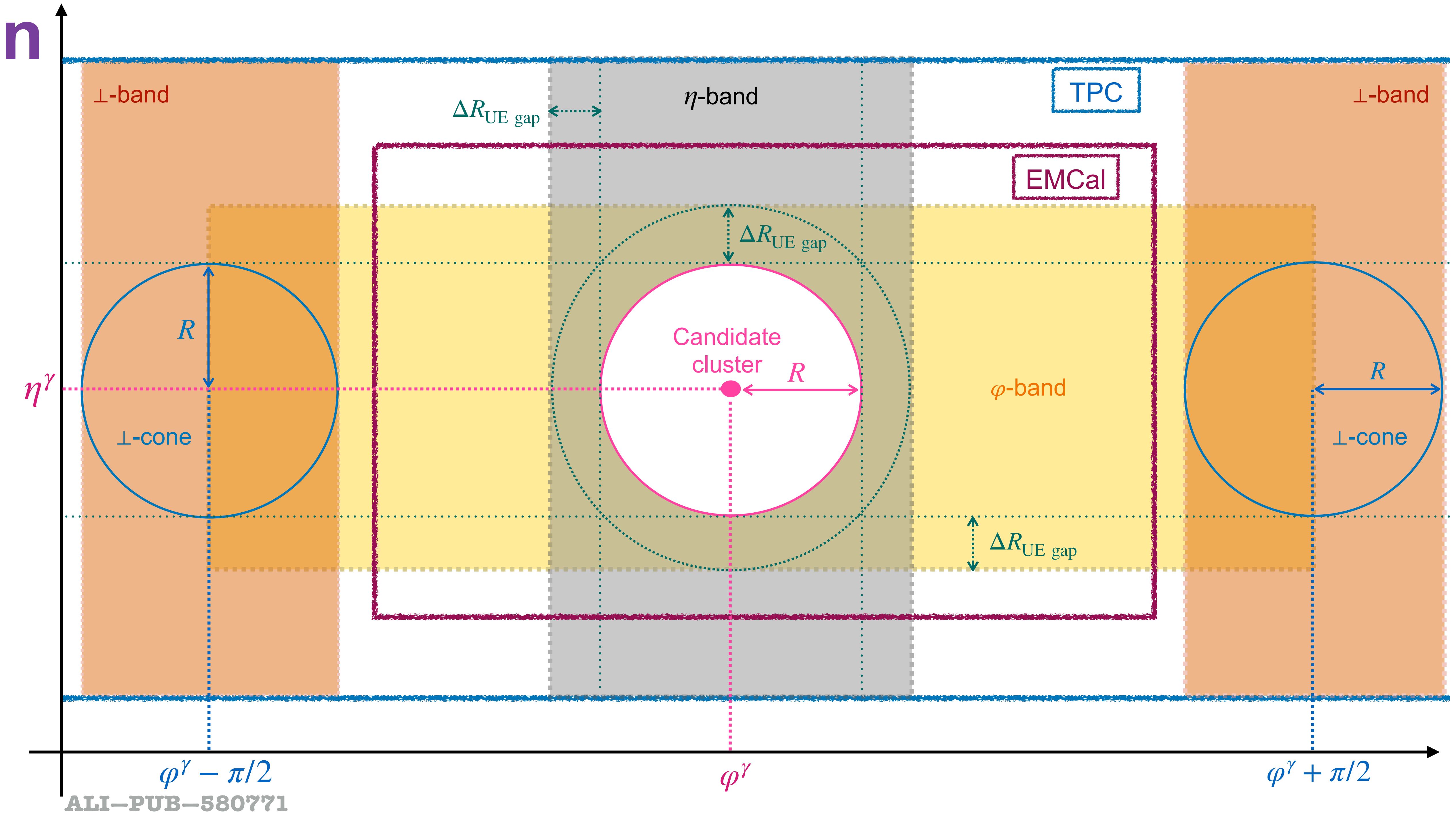

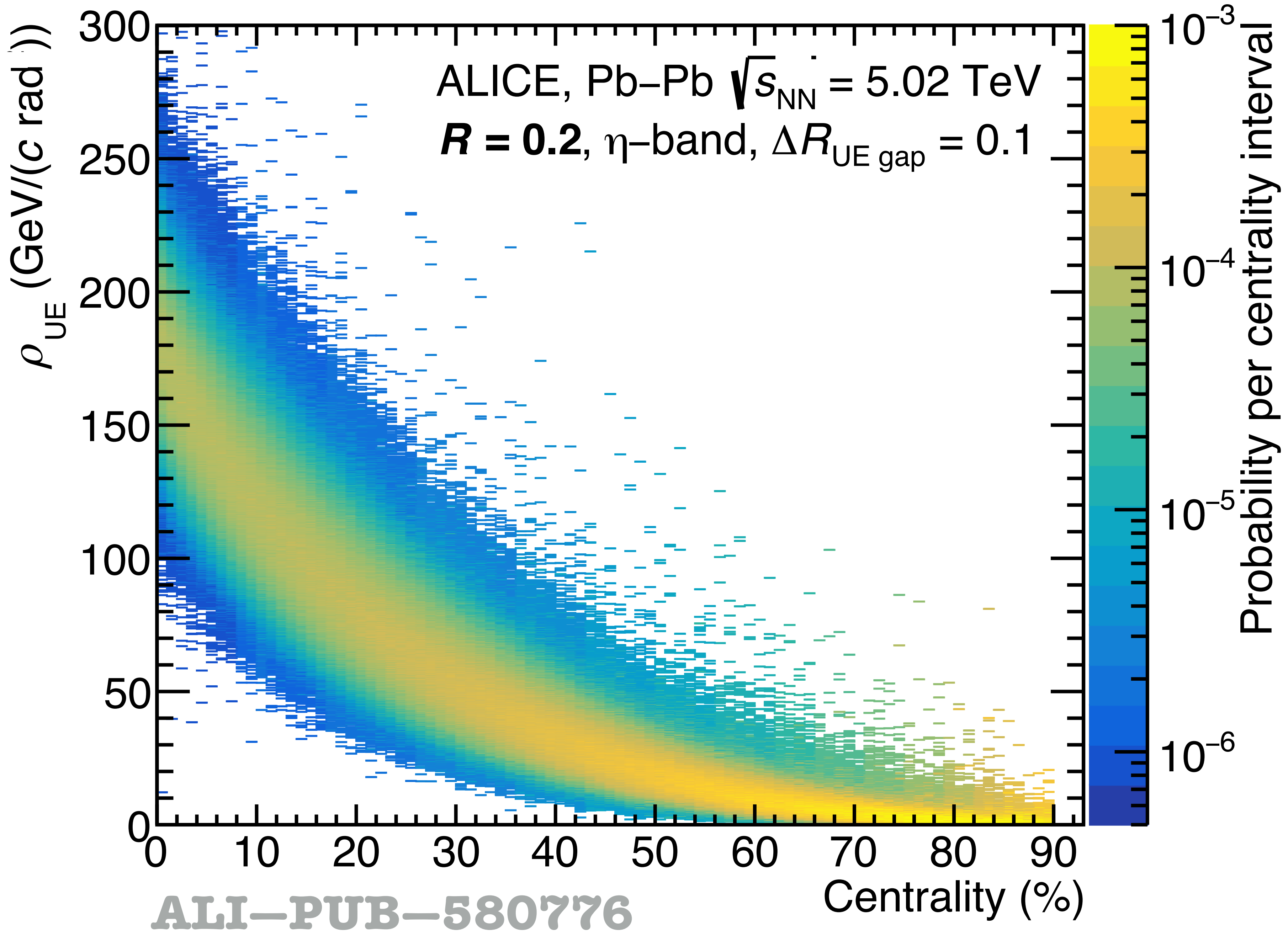

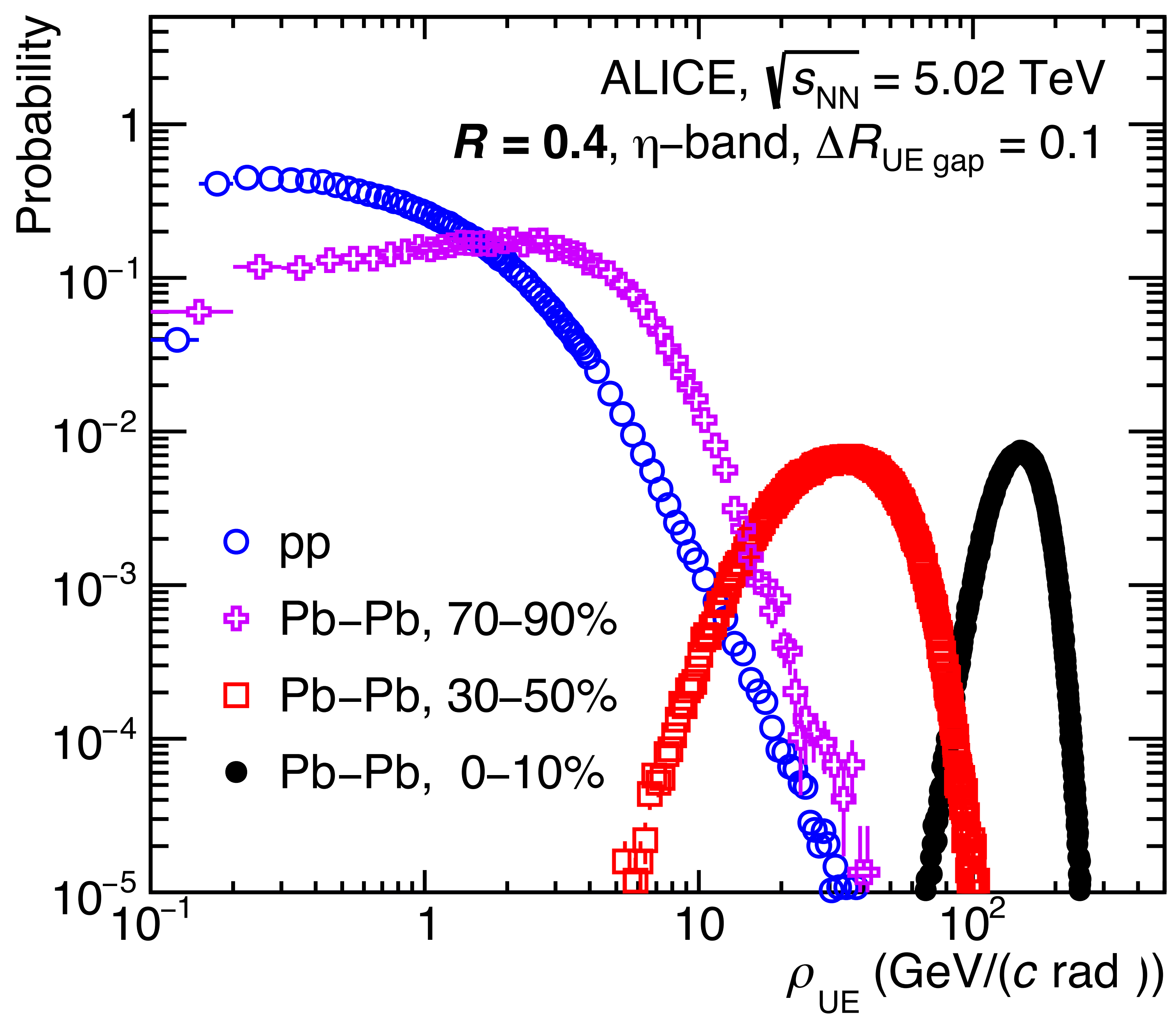

Remark: UE was not subtracted in pp $\sqrt{s}$ = 7 & 13 TeV measurements, UE small

Prompt γ identification in ALICE: EM shape & isolation

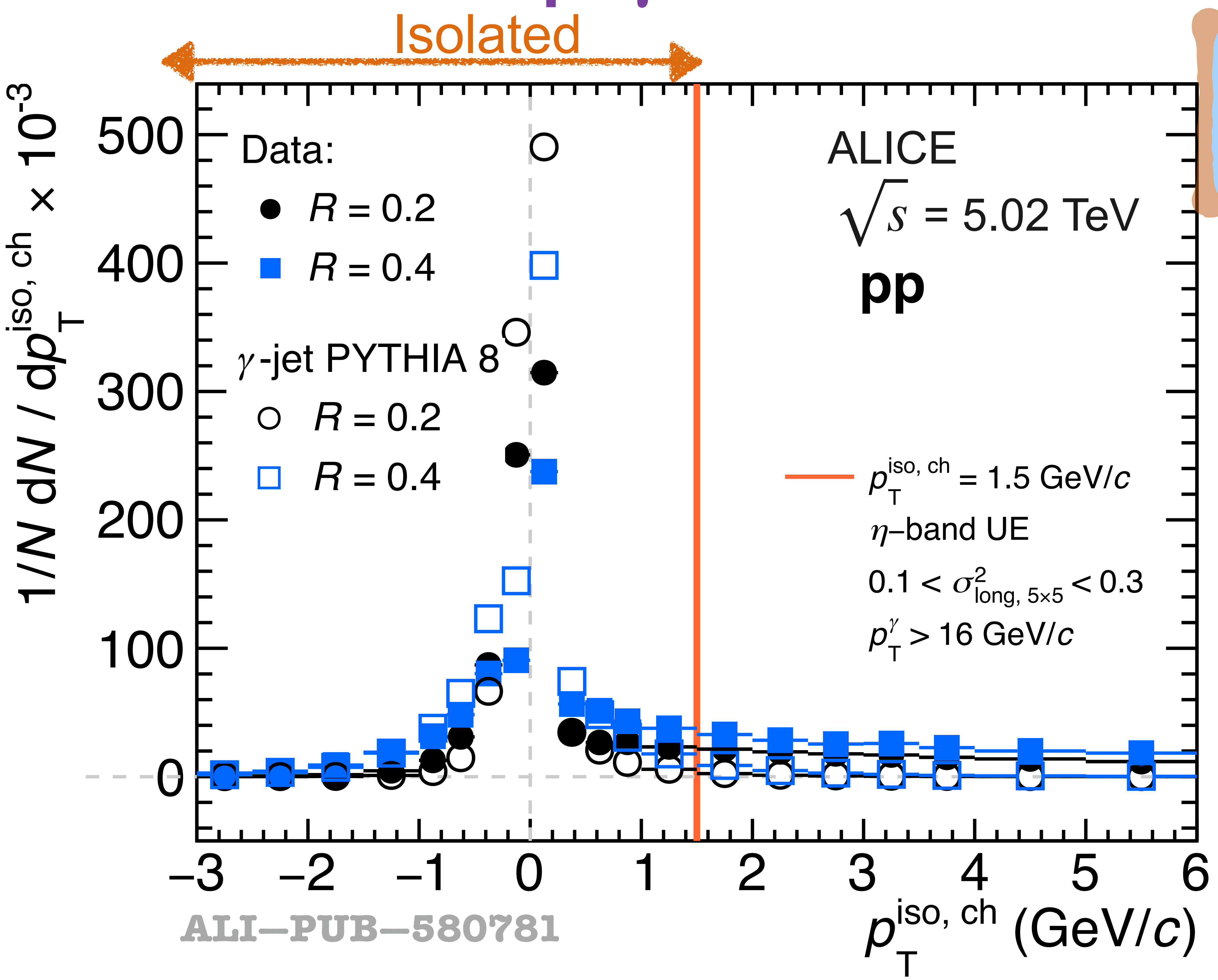

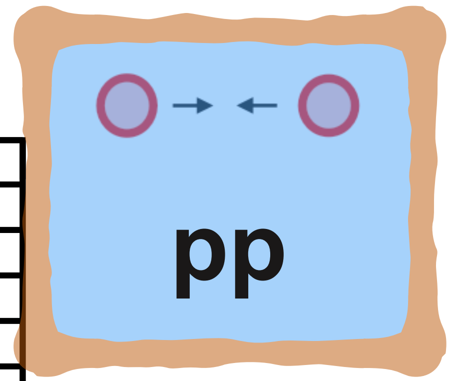

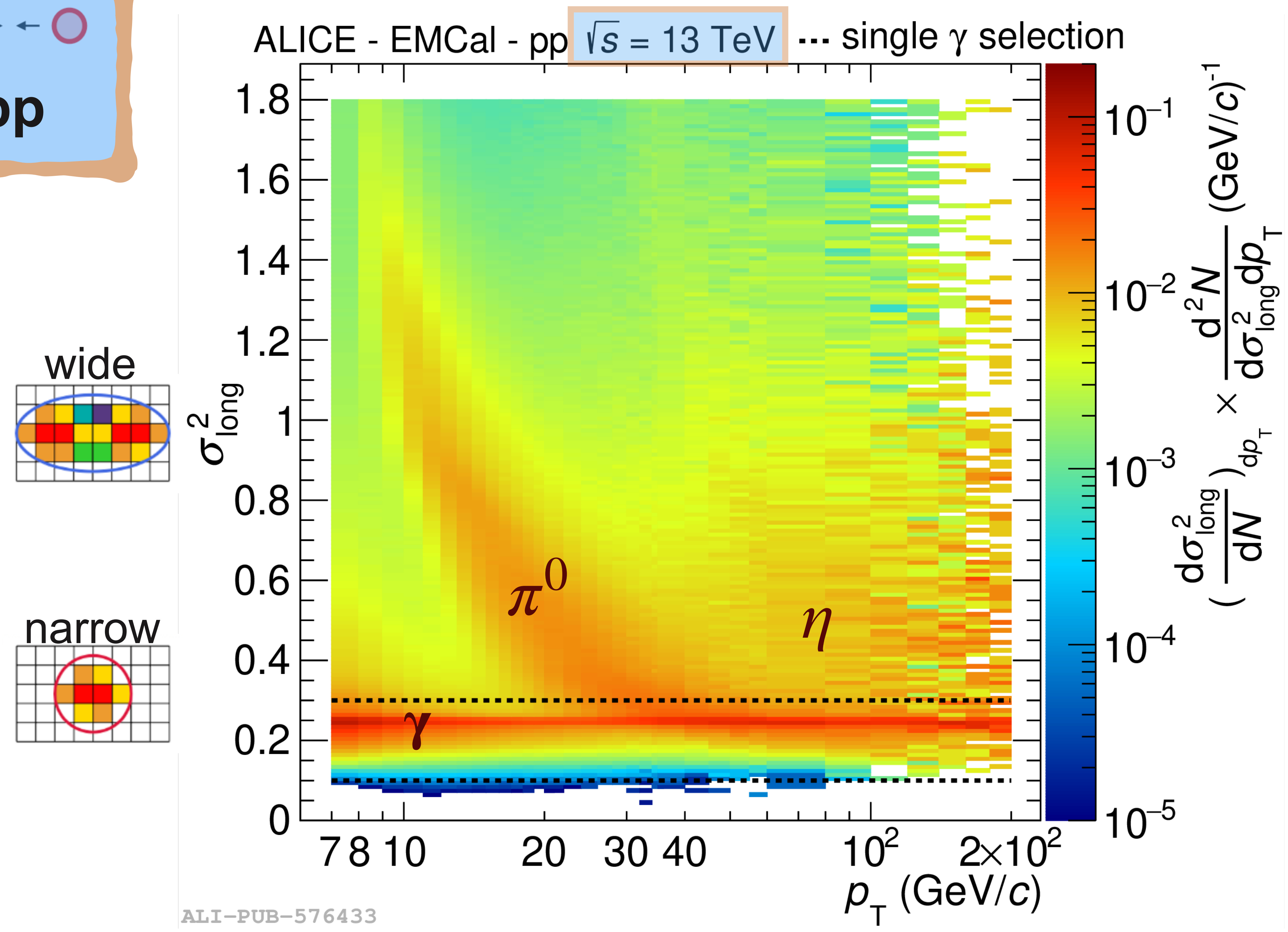

- Isolated if $p_{\mathrm{T}}^{\mathrm{iso,\,ch}}$ < 1.5 GeV/c with R = 0.4 or 0.2
- Symmetric in PYTHIA 8 **γ**-jet process simulation
- In data, more asymmetric and less peaked distribution due to jet contribution
- Wider for R = 0.4 due to UE fluctuations

- Visible bands for **γ** (narrow clusters) & π^0 (wide clusters)
- Select as **γ** clusters with $0.1 < \sigma^2_{\mathrm{long,\,5\times5}} < 0.3$

Prompt γ identification in ALICE: EM shape & isolation

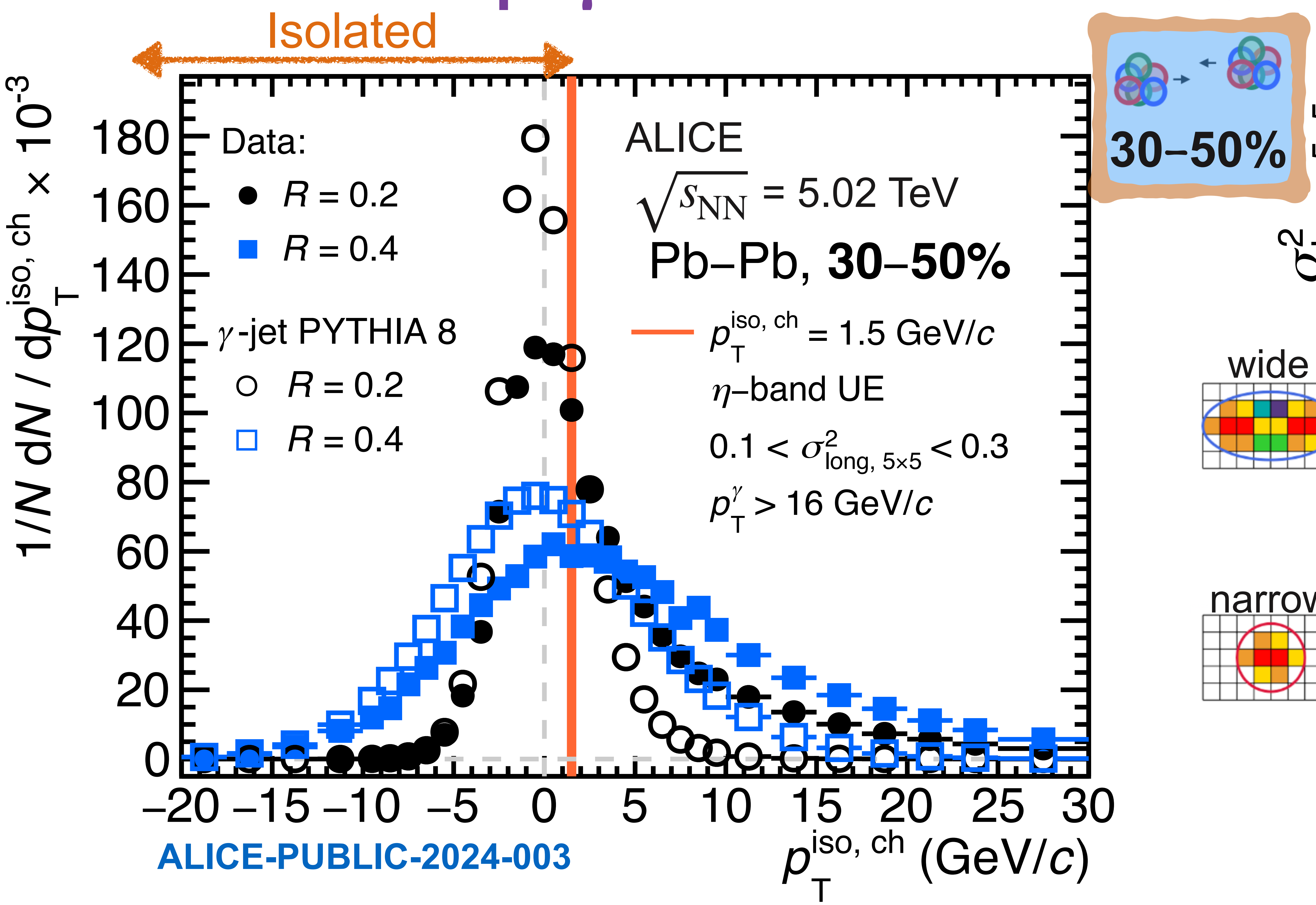

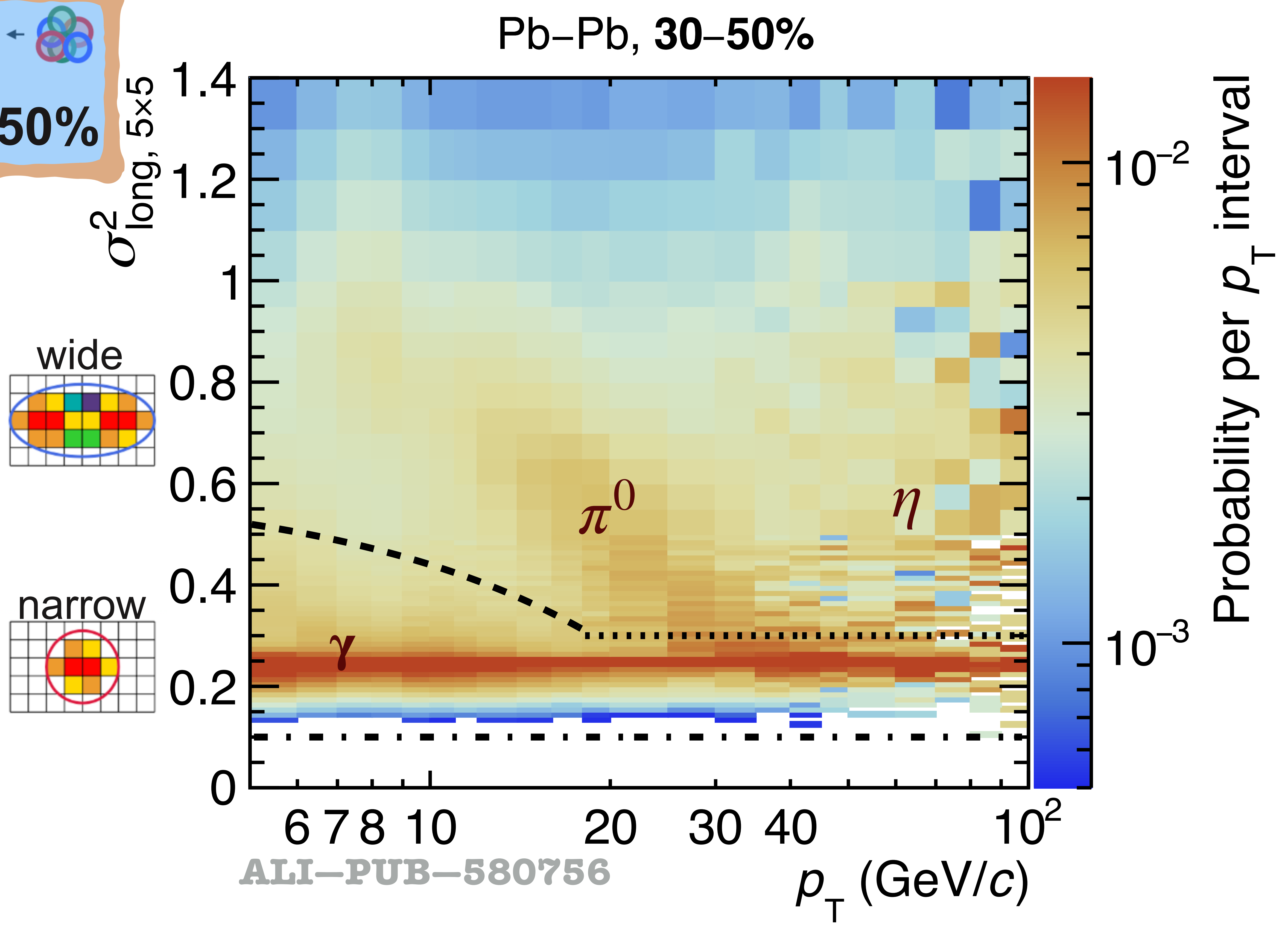

- Isolated if $p_T^{iso, ch}$ < 1.5 GeV/*c* with *R* = 0.4 or 0.2
- Embedded pp PYTHIA 8 γ-jet process simulation into MB data, symmetric distribution
- In data, more asymmetric distribution due to jet contribution
- Significantly wider distributions for *R* = 0.4 due to UE fluctuations

- Visible bands for **γ** (narrow clusters) & π^0 (wide clusters)
- Select as **γ** clusters with
  - Pb–Pb:
    - $p_T < 18$ GeV/*c*: $0.1 < \sigma^2_{long, 5\times5} < 0.6 - 0.016 \cdot p_T$
    - $p_T > 18$ GeV/*c*: $0.1 < \sigma^2_{long, 5\times5} < 0.3$
  - pp:
    - $0.1 < \sigma^2_{long, 5\times5} < 0.3$

Prompt γ identification in ALICE: EM shape & isolation

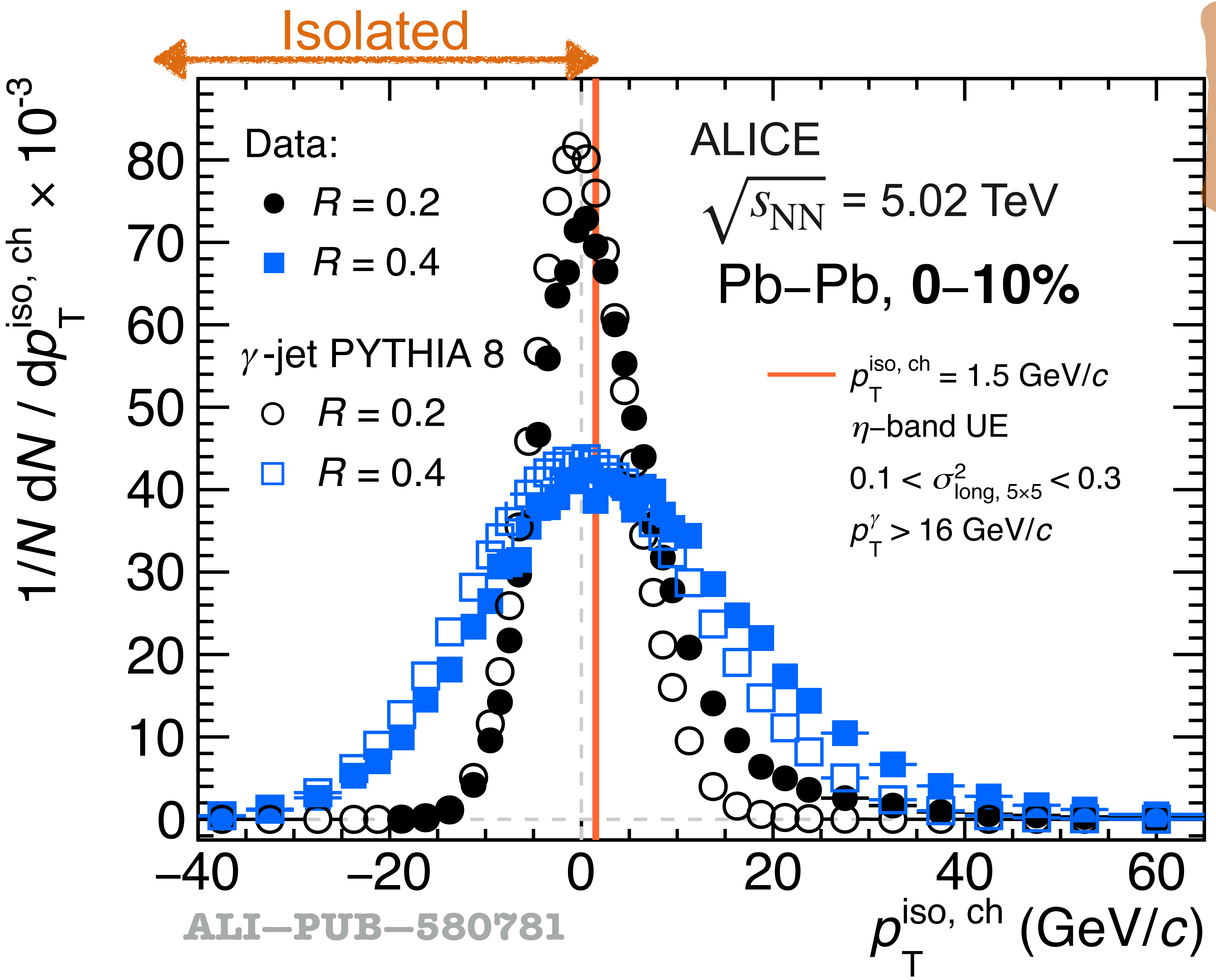

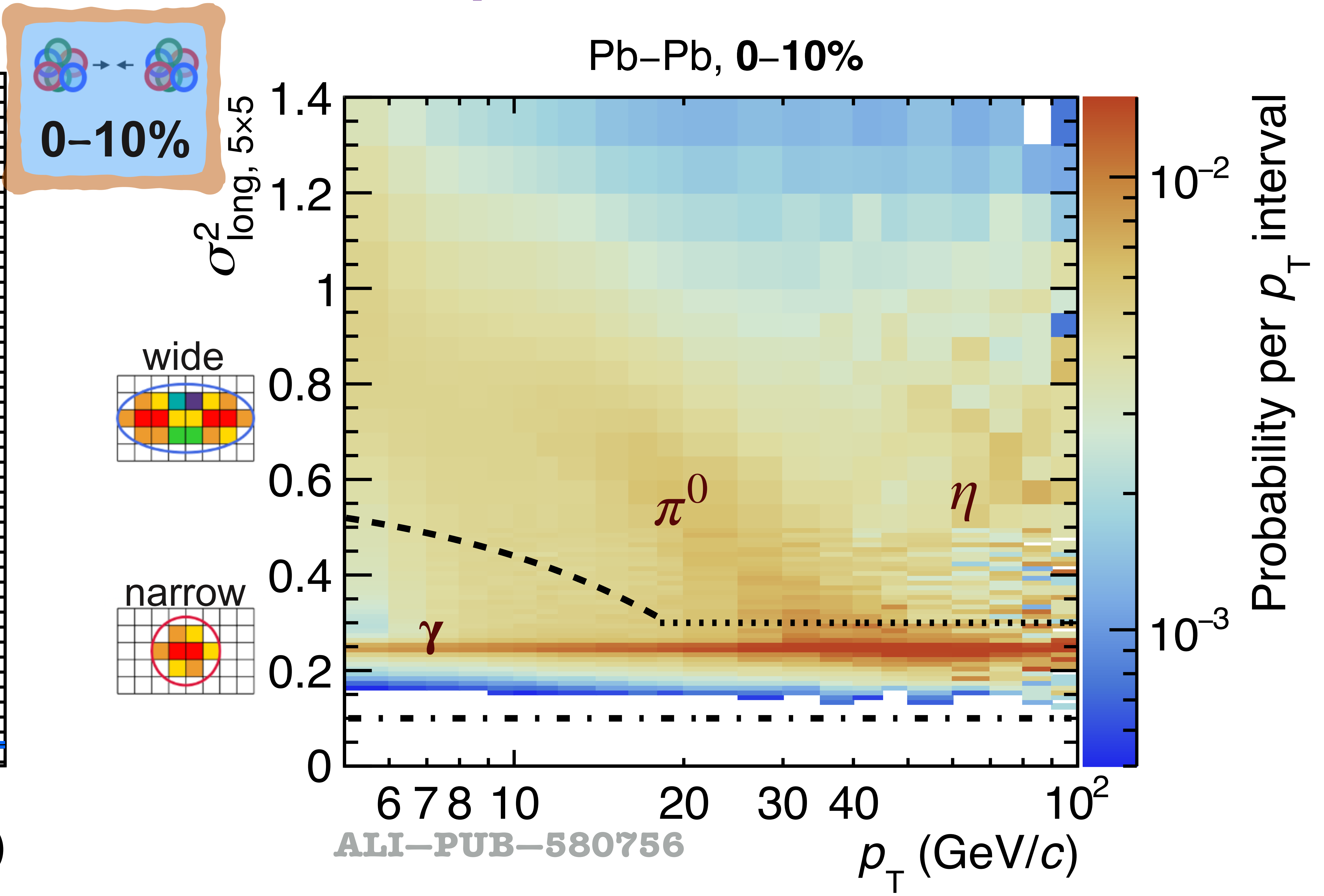

- Isolated if $p_{\mathrm{T}}^{\mathrm{iso,\,ch}} < 1.5$ GeV/c with $R = 0.4$ or 0.2
- Embedded pp PYTHIA 8 γ-jet process simulation into MB data, symmetric distribution
- In data, more asymmetric distribution due to jet contribution
- Significantly **much** wider distributions for $R = 0.4$ due to UE fluctuations

- Visible bands for **γ** (narrow clusters) & π^0 (wide clusters)
- Select as γ clusters with
  - Pb–Pb:
    - ➡ $p_{\mathrm{T}} < 18$ GeV/c: $0.1 < \sigma^2_{\mathrm{long,\,5\times5}} < 0.6 - 0.016 \cdot p_{\mathrm{T}}$
    - ➡ $p_{\mathrm{T}} > 18$ GeV/c: $0.1 < \sigma^2_{\mathrm{long,\,5\times5}} < 0.3$
  - pp:
    - ➡ $0.1 < \sigma^2_{\mathrm{long,\,5\times5}} < 0.3$

γ increase their $\sigma^2_{\mathrm{long,\,5\times5}}$ due to the UE

Purity

- Purity, ABCD method: Phase space of calorimeter clusters divided in 4 regions: $\mathbb{A}$, signal dominated & $\mathbb{B}$-$\mathbb{C}$-$\mathbb{D}$, background dominated

Data driven — PYTHIA

$$P = 1 - \left(\frac{N_{\rm n}^{\overline{\rm iso}} / N_{\rm n}^{\rm iso}}{N_{\rm w}^{\overline{\rm iso}} / N_{\rm w}^{\rm iso}} \right)_{\rm data} \times \left(\frac{B_{\rm n}^{\rm iso} / N_{\rm n}^{\overline{\rm iso}}}{N_{\rm w}^{\rm iso} / N_{\rm w}^{\overline{\rm iso}}} \right)_{\rm MC}$$

$N_{\rm n,w}^{\rm iso,\overline{iso}}$ = jet-jet ($B_{\rm n,w}^{\rm iso,\overline{iso}}$) + γ-jet ($S_{\rm n,w}^{\rm iso,\overline{iso}}$)

($\sigma^2_{\rm long}$ cluster n: narrow, w: wide)

➡ Semi data-driven approach, simulation used to correct correlations between $p_{\rm T}^{\rm iso,\ ch}$ and $\sigma^2_{\rm long}$

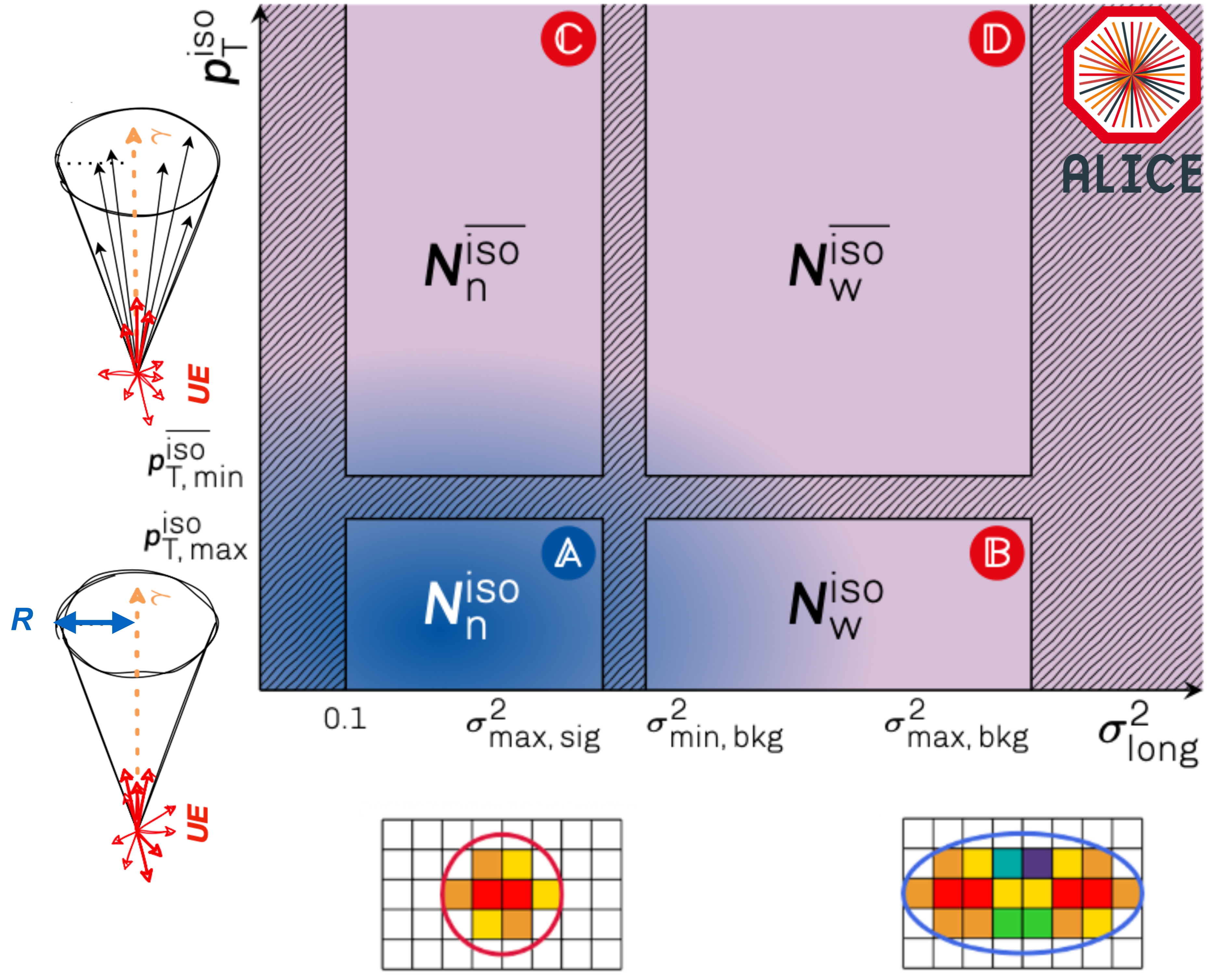

Purity, pp $\sqrt{s}$ = 13 TeV

- Purity, ABCD method: Phase space of calorimeter clusters divided in 4 regions: 𝔸, signal dominated & 𝔹-ℂ-𝔻, background dominated

Data driven — PYTHIA

$$P = 1 - \left(\frac{N_{n}^{\overline{iso}}/N_{n}^{iso}}{N_{w}^{\overline{iso}}/N_{w}^{iso}}\right)_{data} \times \left(\frac{B_{n}^{iso}/N_{n}^{\overline{iso}}}{N_{w}^{iso}/N_{w}^{\overline{iso}}}\right)_{MC}$$

$N_{n,w}^{iso,\overline{iso}}$ = jet-jet ($B_{n,w}^{iso,\overline{iso}}$) + γ-jet ($S_{n,w}^{iso,\overline{iso}}$)

(σ^2_{long} cluster n: narrow, w: wide)

➡ Semi data-driven approach, simulation used to correct correlations between $p_{T}^{iso,\,ch}$ and σ^2_{long}

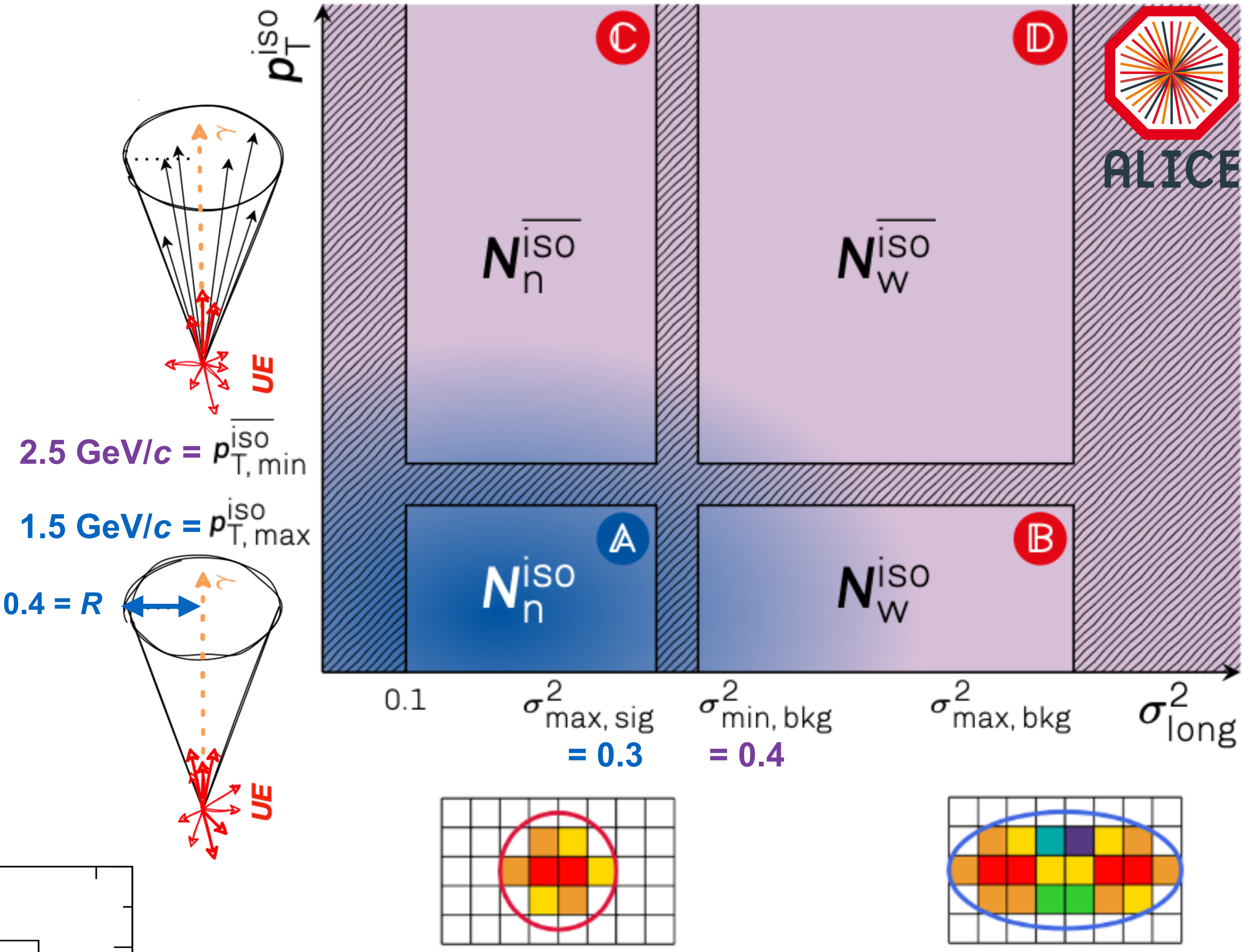

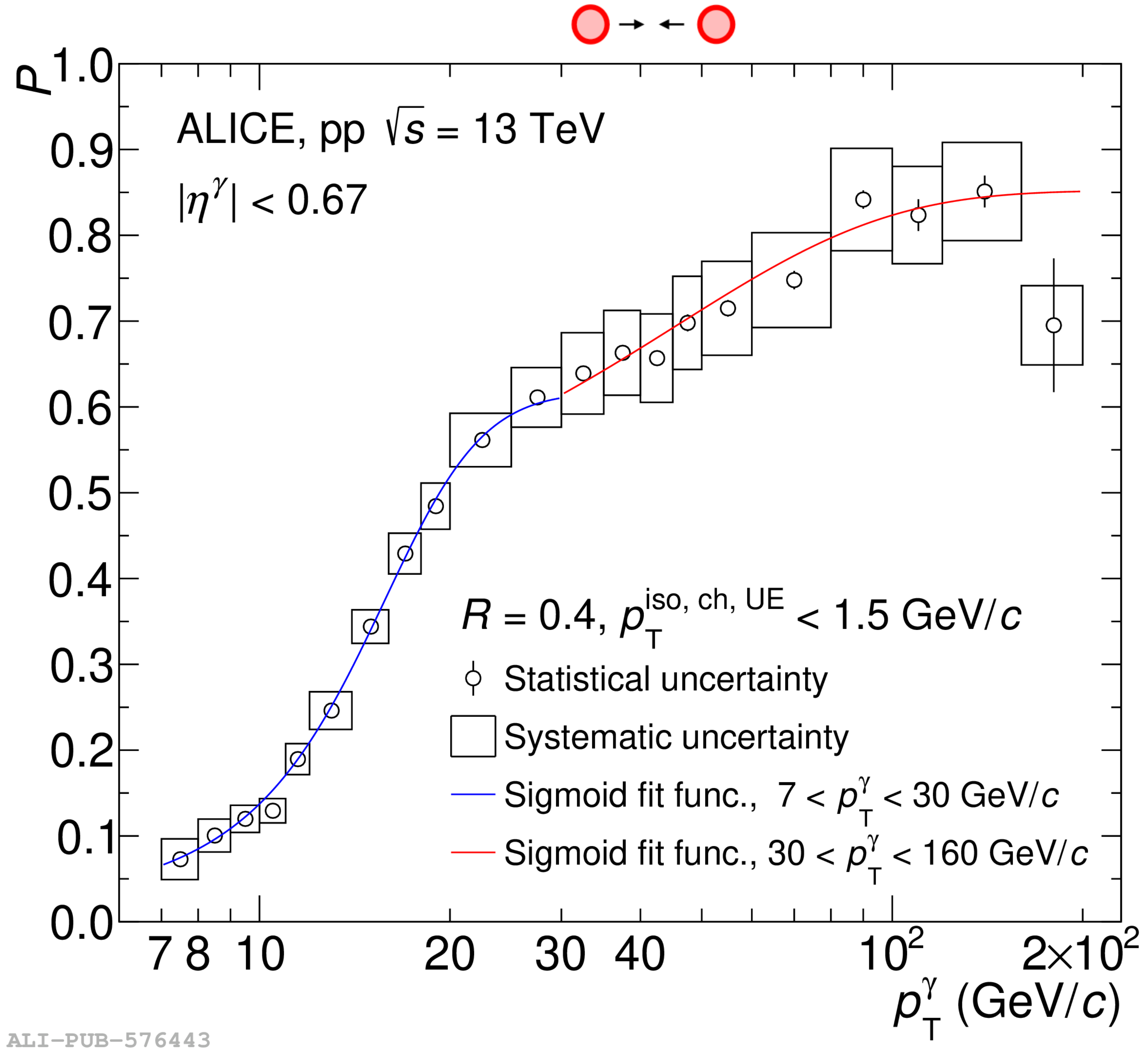

▹ Reduce the influence of statistical fluctuations with sigmoid function fits

Purity, Pb–Pb $\sqrt{s_{NN}}$ = 5.02 TeV

- Purity, ABCD method: Phase space of calorimeter clusters divided in 4 regions: 𝔸, signal dominated & 𝔹-ℂ-𝔻, background dominated

Data driven | PYTHIA

$$P = 1 - \left(\frac{N_{n}^{\overline{iso}}/N_{n}^{iso}}{N_{w}^{\overline{iso}}/N_{w}^{iso}}\right)_{data} \times \left(\frac{B_{n}^{iso}/N_{n}^{\overline{iso}}}{N_{w}^{iso}/N_{w}^{\overline{iso}}}\right)_{MC}$$

$N_{n,w}^{iso,\overline{iso}}$ = jet-jet ($B_{n,w}^{iso,\overline{iso}}$) + γ-jet ($S_{n,w}^{iso,\overline{iso}}$)
(σ^2_{long} cluster n: narrow, w: wide)

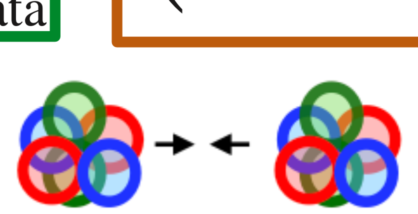

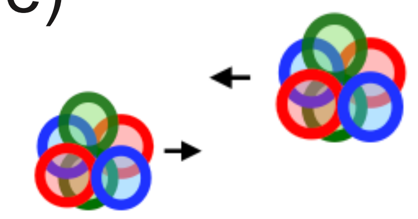

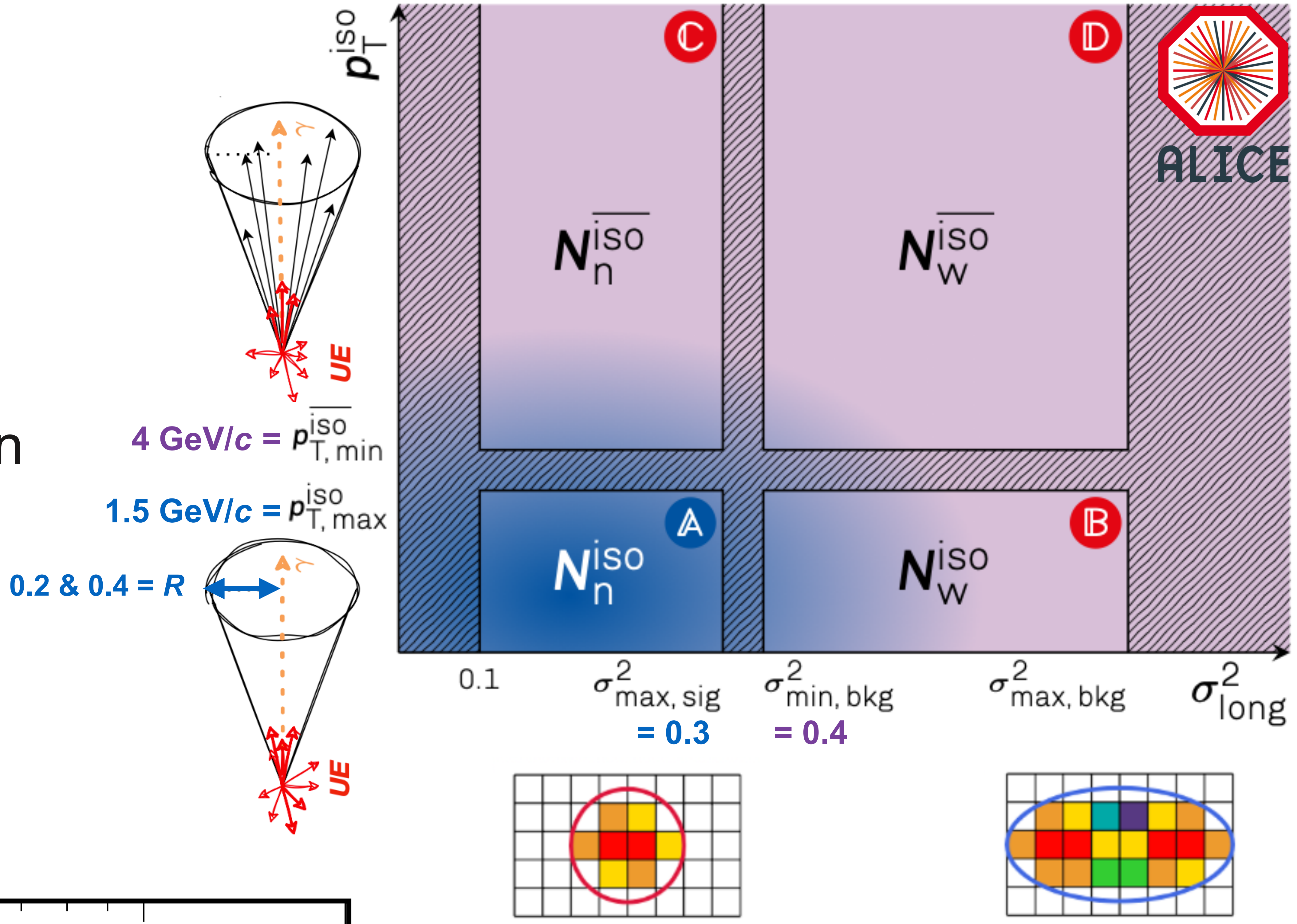

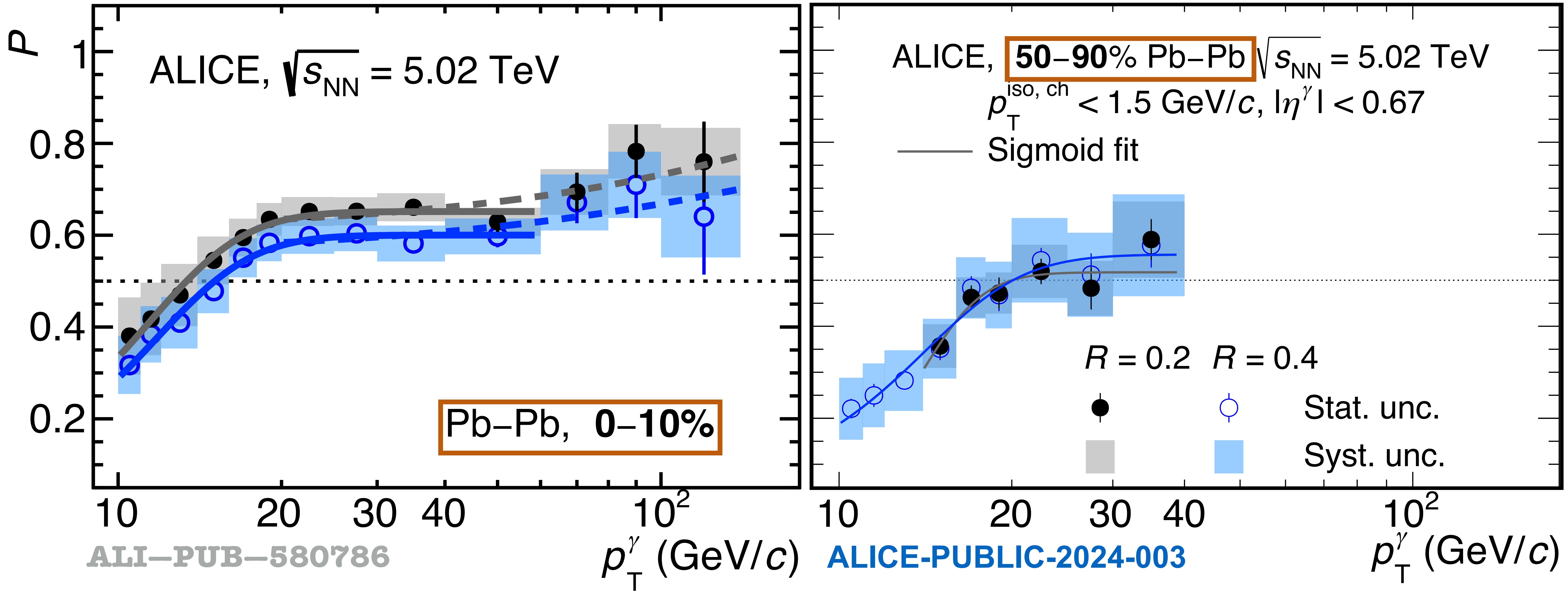

ALI–PUB–580786

ALICE-PUBLIC-2024-003

- Reduce the influence of statistical fluctuations with sigmoid function fits
- Higher purity in central vs peripheral collisions due to neutral meson background suppression due to QGP
- Higher purity in central collisions for R = 0.2 vs R = 0.4 due to lower UE fluctuations in $p_T^{iso, ch}$

Efficiency, R = 0.2 & 0.4, pp & Pb–Pb $\sqrt{s_{NN}}$ = 5.02 TeV

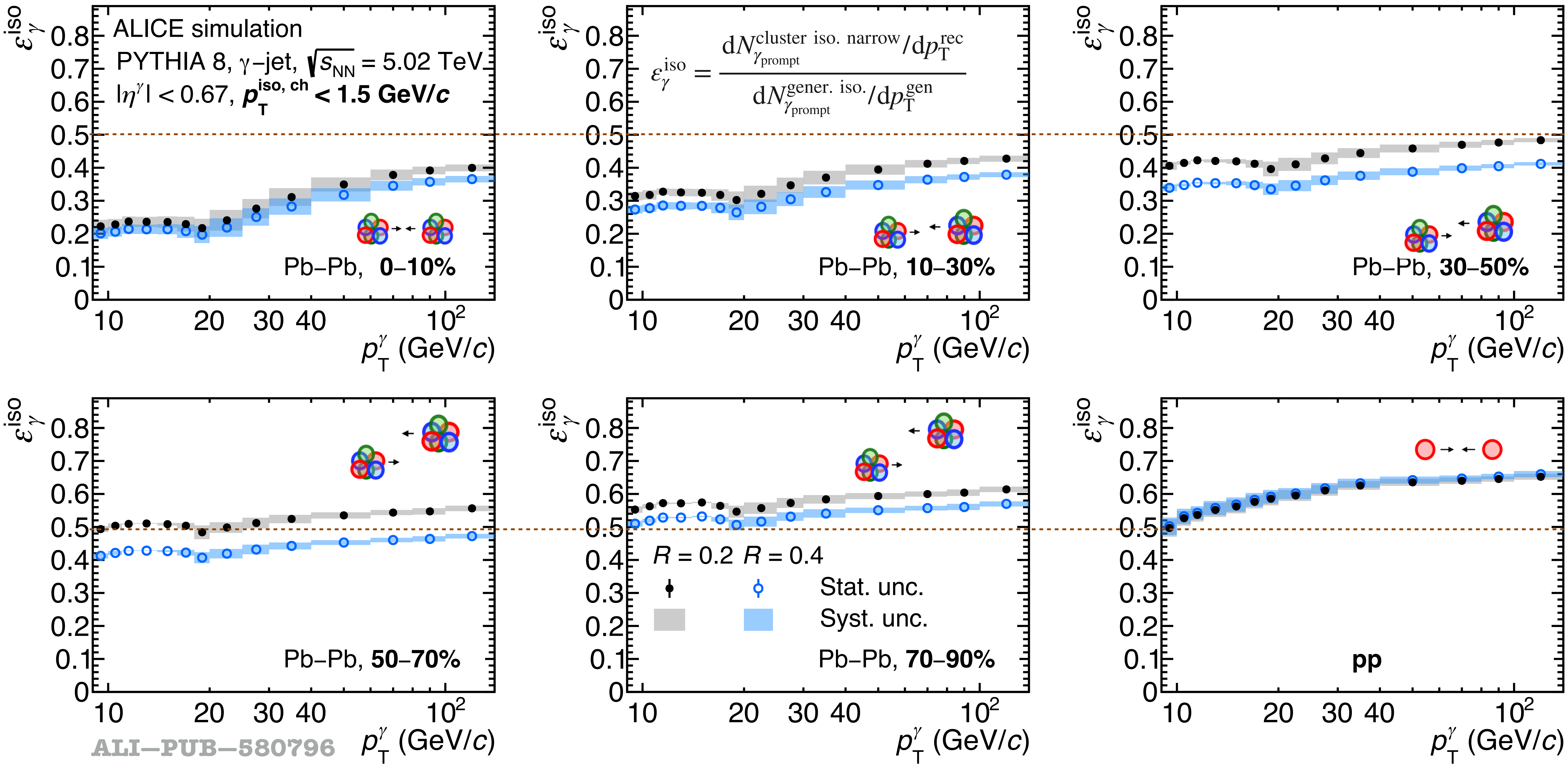

- $\varepsilon_{\gamma}^{iso}$ (0-10%) < $\varepsilon_{\gamma}^{iso}$ (70-90%): UE fluctuations ($p_T^{iso,\ ch}$) and cluster size increase (σ^2_{long}) (see backup)
- In Pb–Pb, $\varepsilon_{\gamma}^{iso}$ (R = 0.2) > $\varepsilon_{\gamma}^{iso}$ (R = 0.4) a factor ~0.9 due to lower UE fluctuations ($p_T^{iso,\ ch}$)
- In pp, $\varepsilon_{\gamma}^{iso}$ (R = 0.2) ≈ $\varepsilon_{\gamma}^{iso}$ (R = 0.4), due to the less performing ITS-only tracks (TPC+ITS in Pb–Pb)

Inclusive isolated-γ production cross section in pp collisions at $\sqrt{s}$ = 13 TeV

arXiv:2407.01165

Publication accepted by EPJ C

Cross section, pp $\sqrt{s}$ = 13 TeV

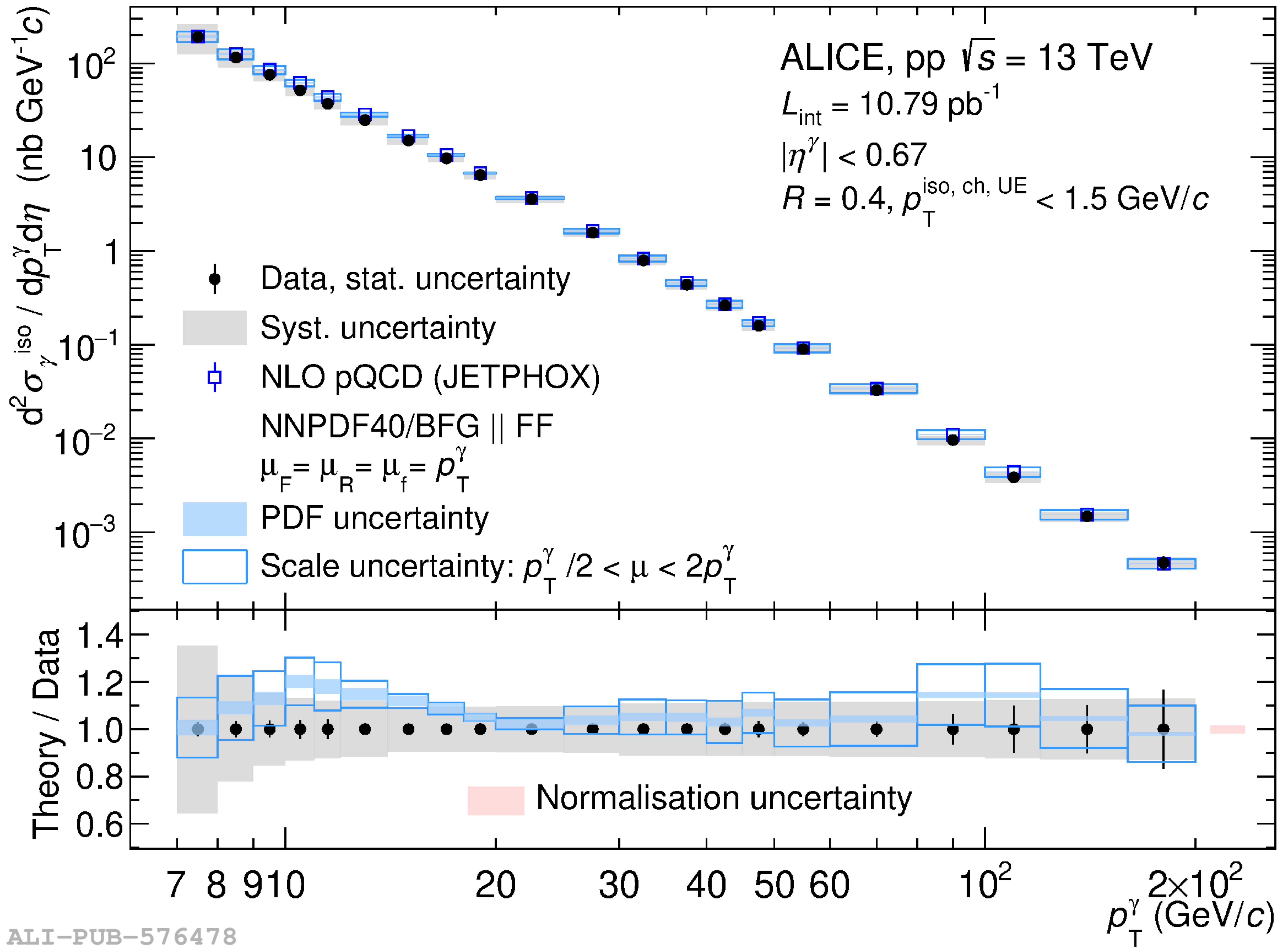

➡ NLO pQCD predictions (JETPHOX) and data agree

Cross section, pp $\sqrt{s}$ = 13 TeV

ALICE

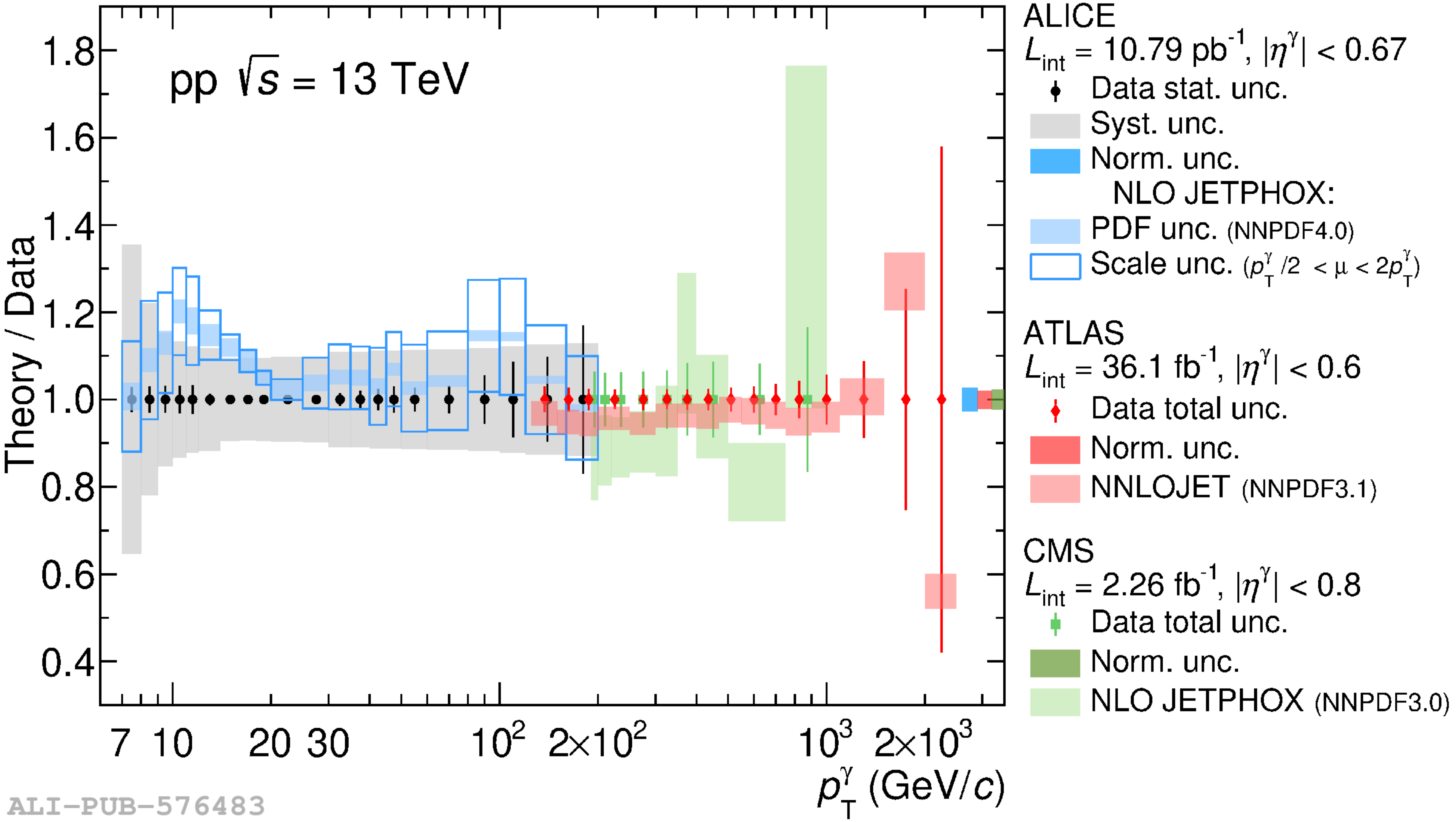

ATLAS JHEP 2019 (2019) 203
arXiv:1908.02746 [hep-ex]

CMS Eur. Phys. J. C 79 (2019) 20
arXiv:1807.00782 [hep-ex]

- ➡ NLO pQCD predictions (JETPHOX) and data agree
- ➡ Significantly lower p_T than CMS and ATLAS at $\sqrt{s}$ = 13 TeV

Cross section, pp $\sqrt{s}$ = 13 TeV

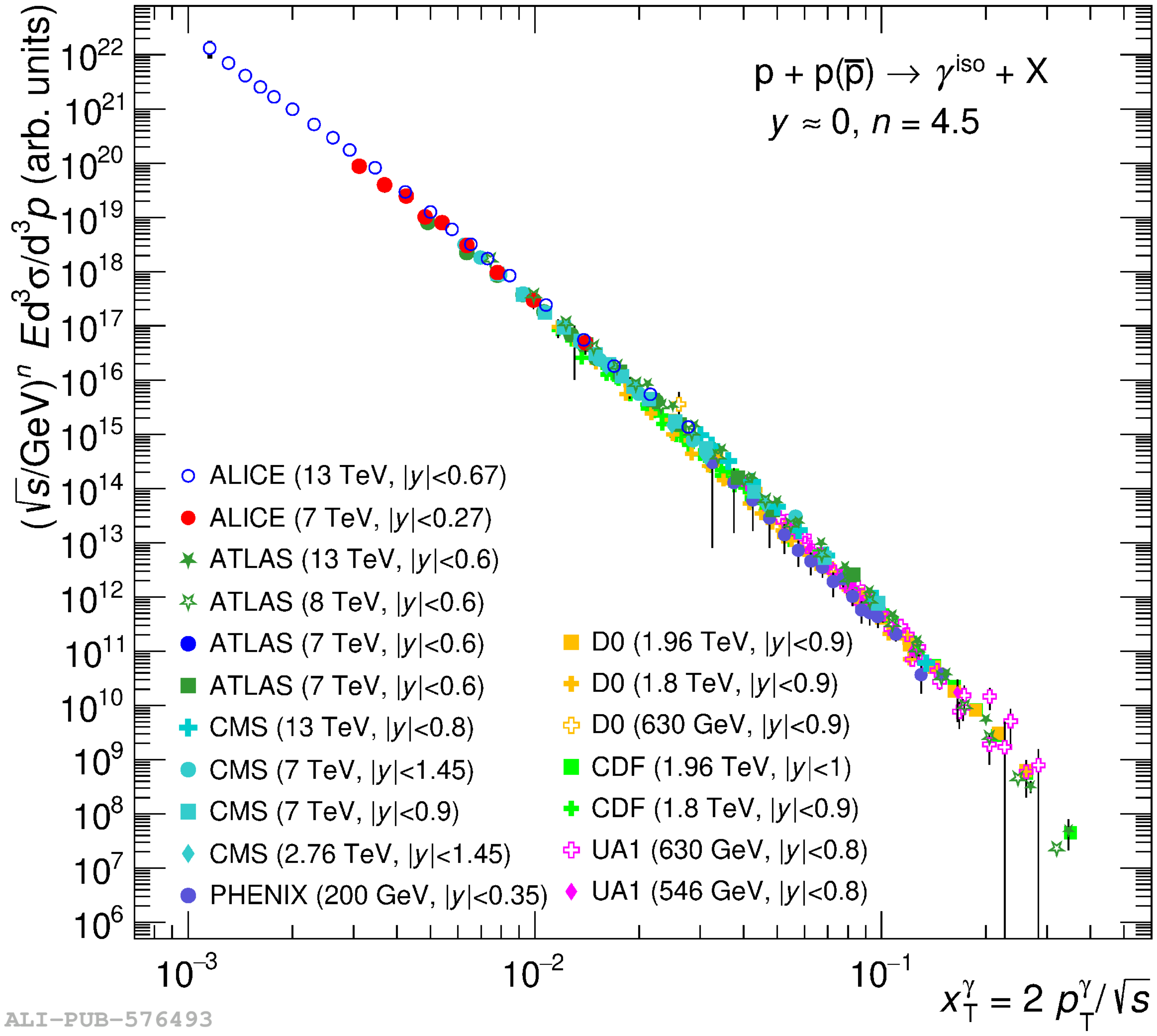

- NLO pQCD predictions (JETPHOX) and data agree
- Significantly lower p_T than CMS and ATLAS at $\sqrt{s}$ = 13 TeV
- Lowest x_T at mid-rapidity $(\sqrt{s})^{4.5}$ scale from x_T ~10^{-3} to 10^{-1}

Full list of older results compiled in D. D'Enterria & J. Rojo Nucl. Phys. B 860 (2012), arXiv:1202.1762 [hep-ph]

Cross section, pp $\sqrt{s}$ = 13 TeV

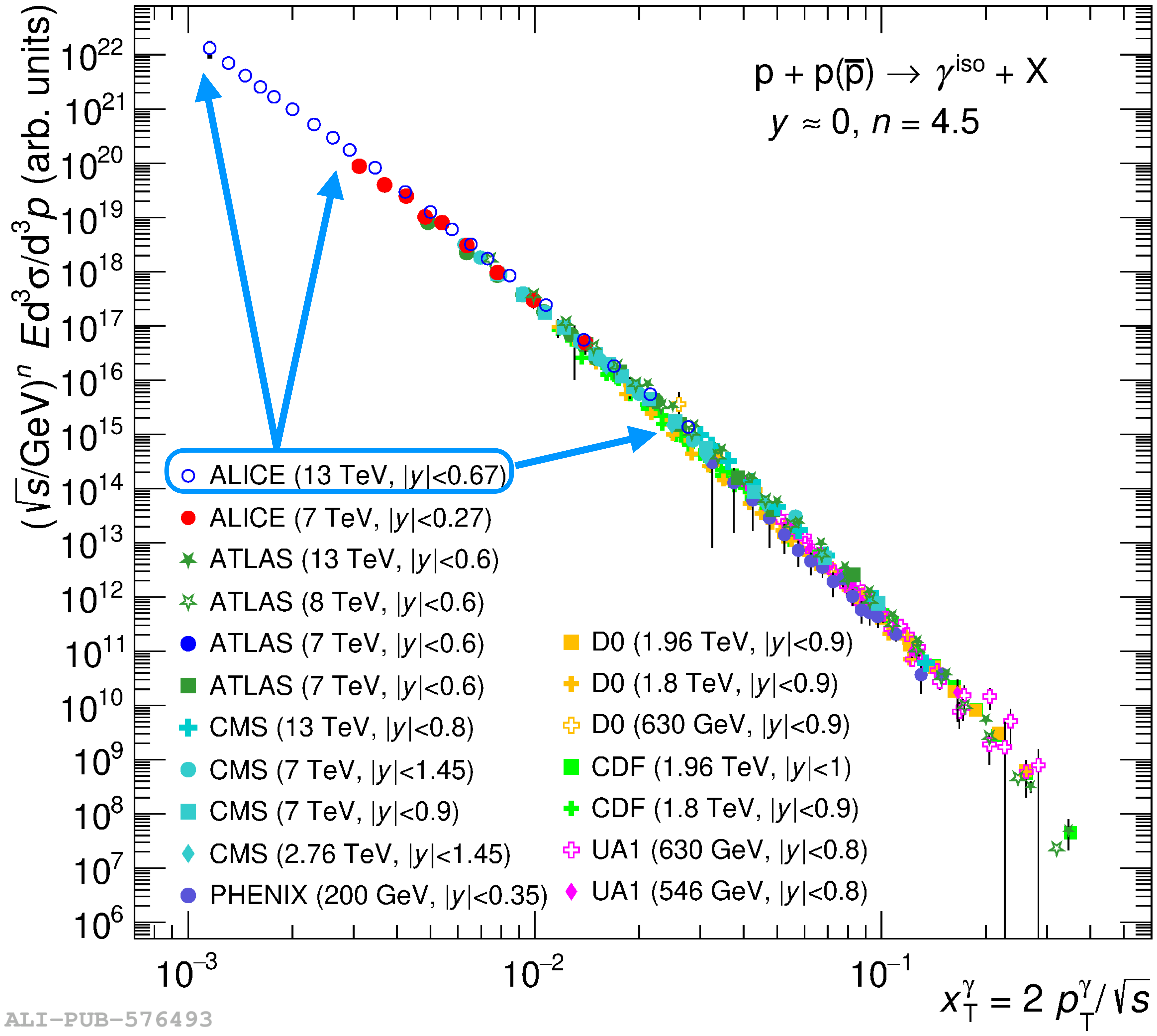

- NLO pQCD predictions (JETPHOX) and data agree
- Significantly lower p_T than CMS and ATLAS at $\sqrt{s}$ = 13 TeV
- Lowest x_T at mid-rapidity $\left(\sqrt{s}\right)^{4.5}$ scale from x_T ~10^{-3} to 10^{-1}
- Additional constrains to the gluon PDF at low Bjorken-x

Full list of older results compiled in D. D'Enterria & J. Rojo Nucl. Phys. B 860 (2012), arXiv:1202.1762 [hep-ph]

Foreseen story for the Jan/Feb 2025 issue of the CERN Courier

Inclusive isolated-γ production cross section in pp & Pb–Pb collisions at $\sqrt{s_{NN}}$ = 5.02 TeV

arXiv:2409.12641, Supplementary note ALICE-PUBLIC-2024-003

Publication submitted EPJ C

Cross section, pp & Pb–Pb at $\sqrt{s_{NN}}$ = 5.02 TeV

$$\frac{d^2\sigma^{\gamma\ iso}}{dp_T\ d\eta} = \frac{\sigma^{INEL}_{NN}}{N_{events} \times RF_{\varepsilon_{trig}}} \times \frac{d^2N}{dp_T\ d\eta} \times \frac{P}{Acc \times \varepsilon^{iso}_{\gamma} \times \varepsilon_{trig}}$$

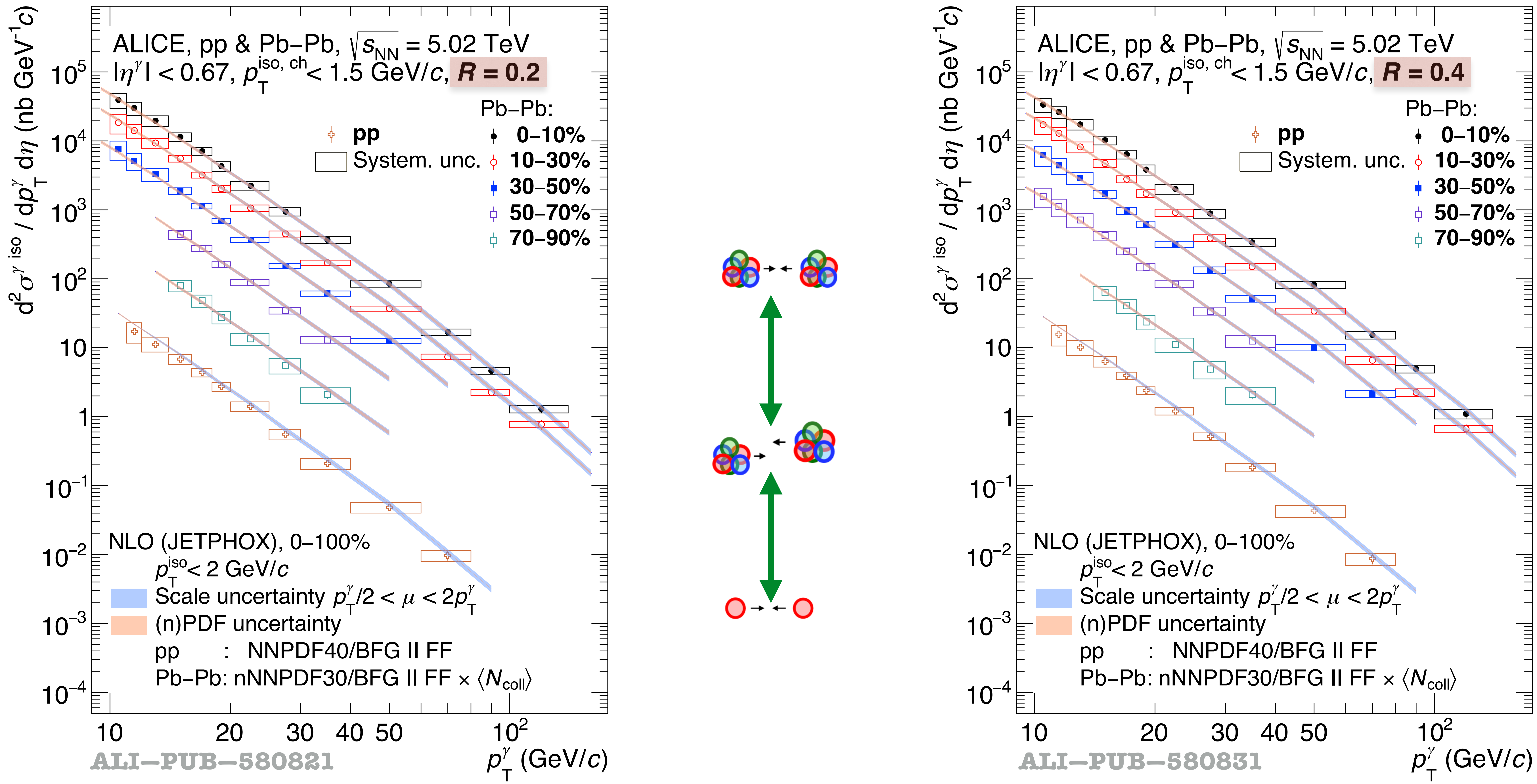

- Wide range: 10 < p_T < 140 GeV/c in Pb–Pb 0-30% & 11 < p_T < 80 GeV/c in pp
- NLO pQCD predictions (JETPHOX)

➡ Note: Theory calculated for 0–100%, **PDF (pp) & nPDF** $\times N_{coll}$ **(Pb–Pb)**

Cross section, pp & Pb–Pb at $\sqrt{s_{NN}}$ = 5.02 TeV

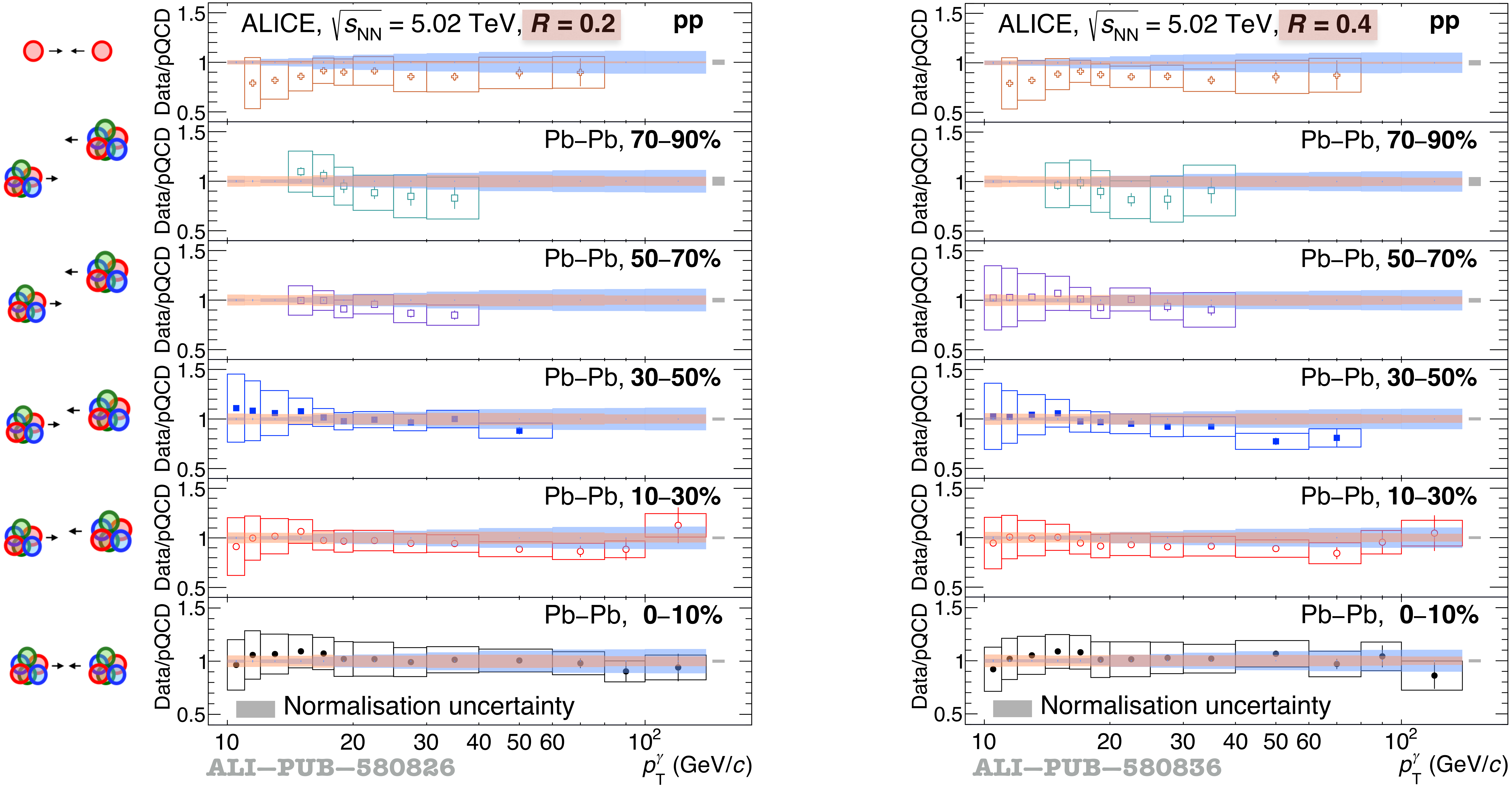

- NLO pQCD predictions (JETPHOX)
  - ➡ Note: Theory calculated for 0–100%, **PDF (pp) & nPDF** $\times N_{coll}$ **(Pb–Pb)**
- Theory & data agreement for both *R* and collision system

Cross section R ratio, pp & Pb–Pb at $\sqrt{s_{NN}}$ = 5.02 TeV

$$f_{R(0.4/0.2)} = \left.\frac{d^2\sigma}{dp_T\, d\eta}\right|_{(R=0.4)} \Big/ \left.\frac{d^2\sigma}{dp_T\, d\eta}\right|_{(R=0.2)}$$

- Sensitive to fraction of fragmentation γ surviving the isolation selection
  - ➡ Interesting for theory models
- Agreement with theory and between collision systems
  - ➡ Theory (NLO): controls the isolation mechanism, fragmentation γ & prompt γ production even in Pb–Pb

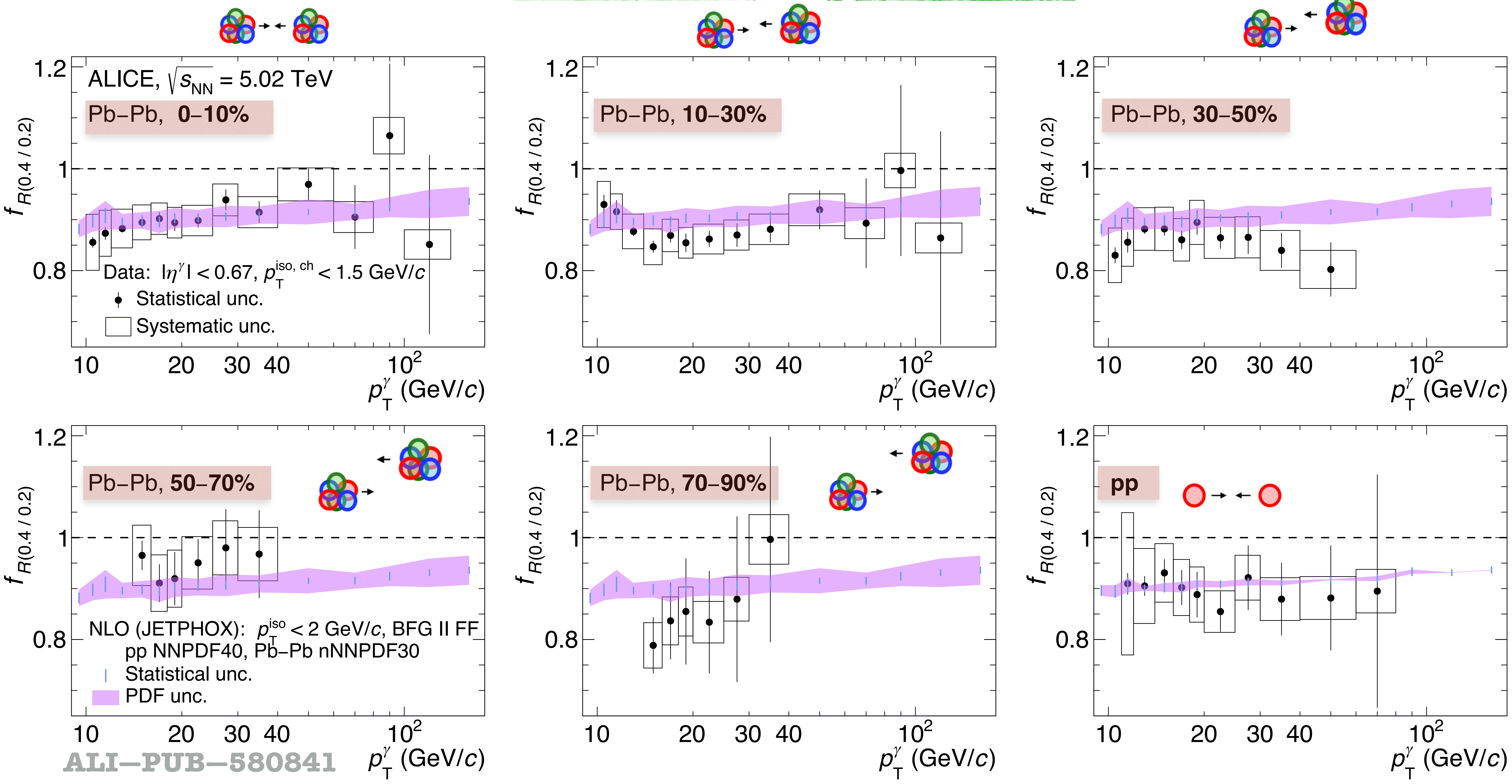

✳ Not shown (backup): ATLAS pp $\sqrt{s}$ =13 TeV, for p_T > 250 GeV/c
JHEP 07 (2023) 86 arXiv:2302.00510

Cross section R ratio, pp & Pb–Pb at $\sqrt{s_{\rm NN}}$ = 5.02 TeV

$$f_{R(0.4/0.2)} = \left.\frac{d^2\sigma}{dp_T\, d\eta}\right|_{(R=0.4)} \Big/ \left.\frac{d^2\sigma}{dp_T\, d\eta}\right|_{(R=0.2)}$$

- Sensitive to fraction of fragmentation γ surviving the isolation selection
  ➡ Interesting for theory models

- Agreement with theory and between collision systems
  ➡ Theory (NLO): controls the isolation mechanism, fragmentation γ & prompt γ production even in Pb–Pb
  ➡ Intriguing: No modification from central Pb–Pb to pp collisions in data

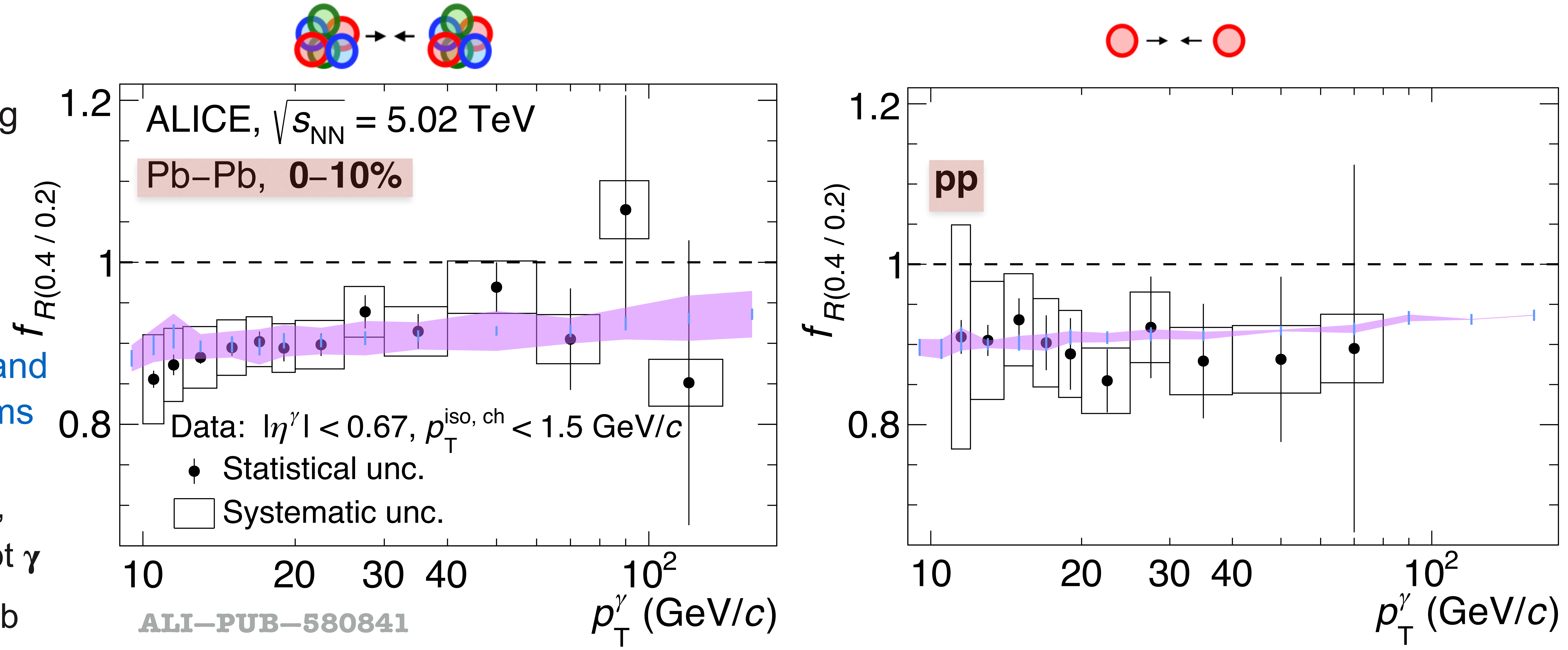

✳ Not shown (backup): ATLAS pp $\sqrt{s}$ =13 TeV, for p_T > 250 GeV/c
JHEP 07 (2023) 86 arXiv:2302.00510

Nuclear modification factor R_{AA}, pp & Pb–Pb at $\sqrt{s_{NN}}$ = 5.02 TeV

$$R_{AA} = \frac{1}{\langle N_{coll} \rangle} \frac{d^2\sigma_{AA} / (dp_T\, d\eta)}{d^2\sigma_{pp} / (dp_T\, d\eta)}$$

- 0-70%
  - ➡ Consistent with unity within the unc. for both R
    - ✤ No modification of the prompt γ yield due to the QGP as expected
  - ➡ Agreement with NLO pQCD incorporating cold nuclear matter effects: PDF vs nPDF

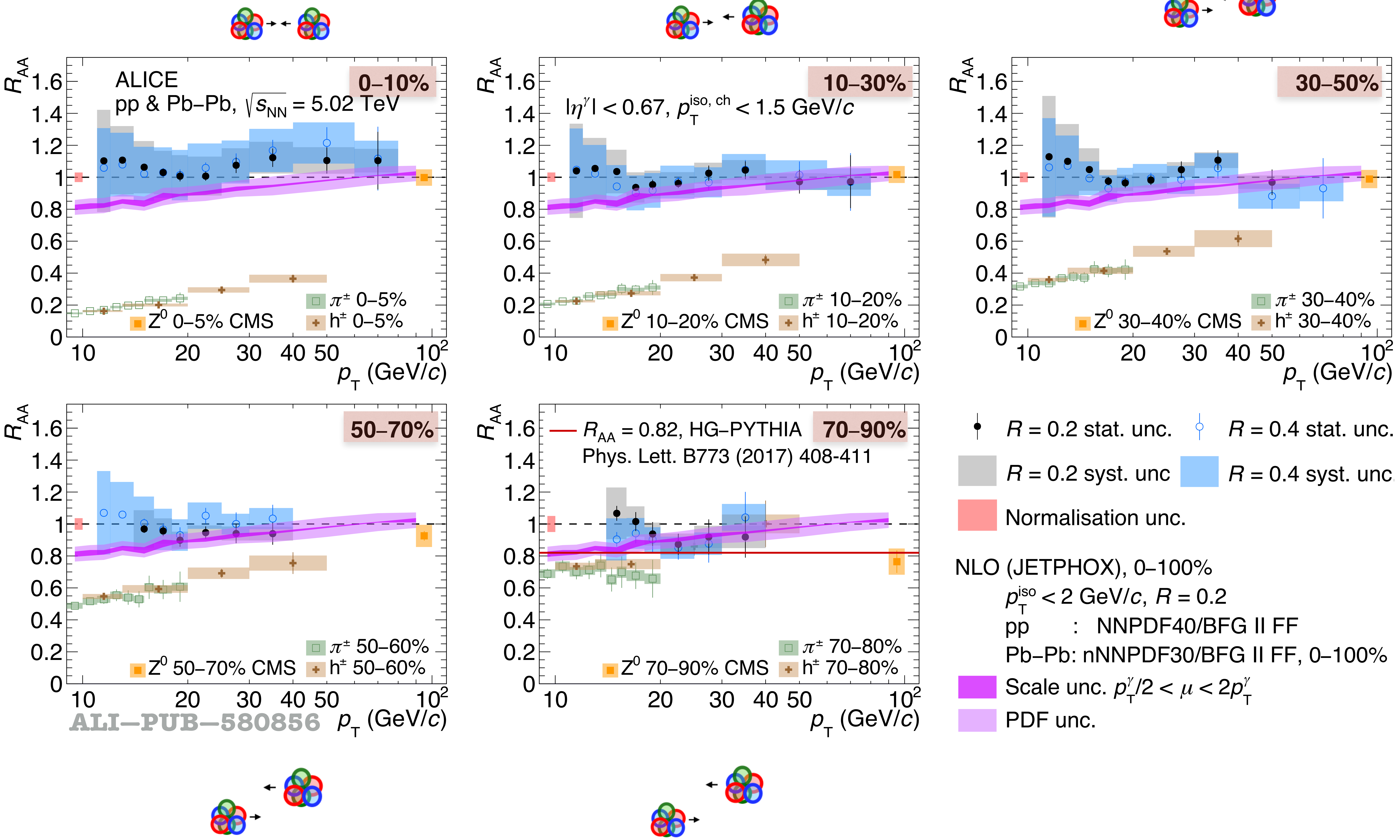

Nuclear modification factor R_{AA}, pp & Pb–Pb at $\sqrt{s_{NN}}$ = 5.02 TeV

$$R_{AA} = \frac{1}{\langle N_{coll} \rangle} \frac{d^2\sigma_{AA} / (dp_T\, d\eta)}{d^2\sigma_{pp} / (dp_T\, d\eta)}$$

- 0-70%
  - ➡ Consistent with unity within the unc. for both *R*
    - ✤ No modification of the prompt γ yield due to the QGP as expected
  - ➡ Agreement with NLO pQCD incorporating cold nuclear matter effects: PDF vs nPDF
- 70-90%
  - ➡ Closer to 0.9 than 1 for both *R* likely due to centrality selection bias of Glauber model
  - ➡ Model by C. Loizides & A. Morsch (Phys. Lett. B773 (2017) 408-411) yields a value at 0.82
    - ✤ In agreement within the uncertainties
  - ➡ Seen by CMS with Z^0 bosons

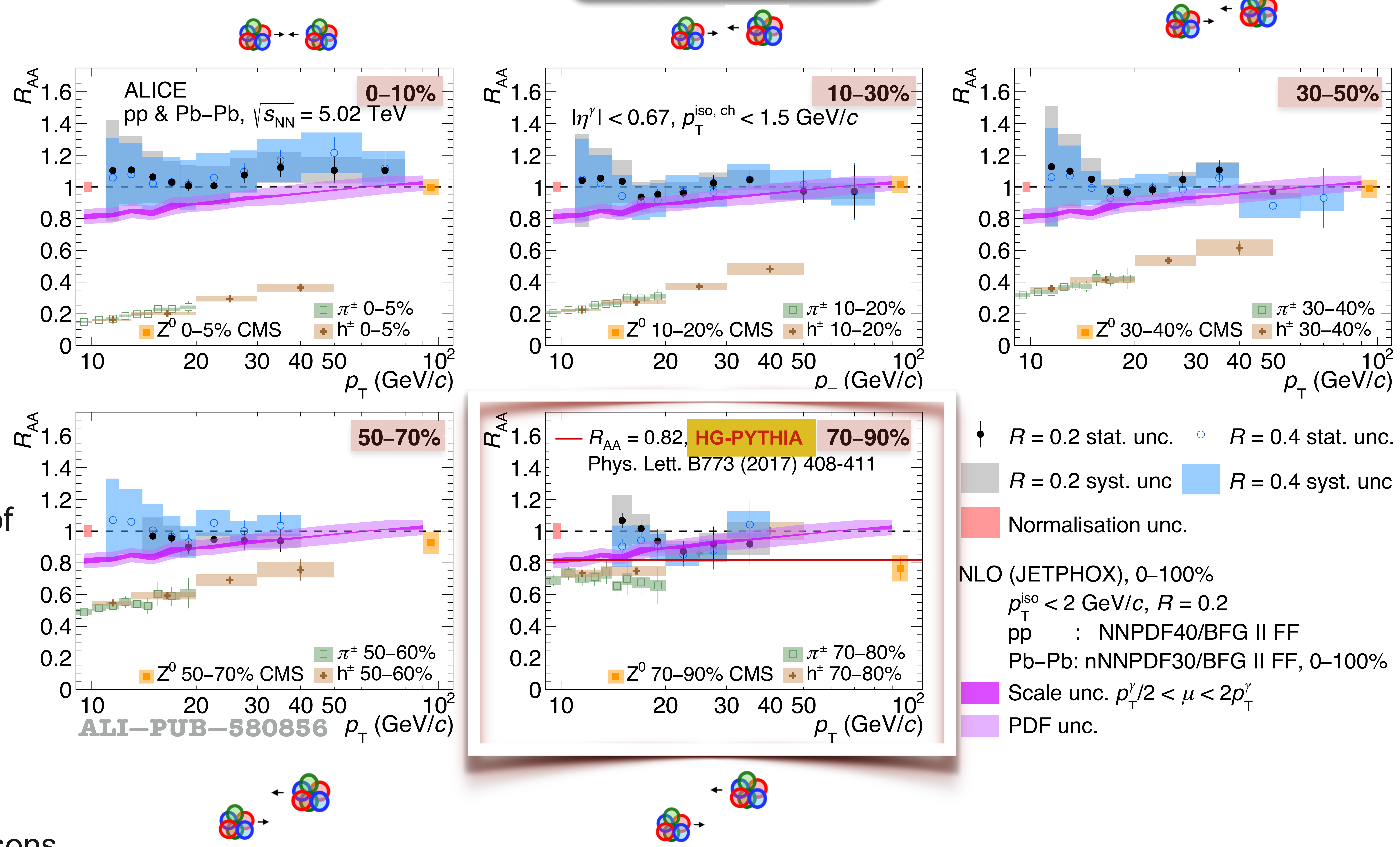

Nuclear modification factor R_{AA} in peripheral Pb–Pb at $\sqrt{s_{NN}}$ = 5.02 TeV: Centrality election bias

- ➡ Centrality calculation in data based typically in the event particle multiplicity and the Glauber model
- ➡ Early unexpected observation of rather suppressed hadron cross section in peripheral collision
- ➡ Glauber model breaks in peripheral collisions (above ~70%), effects not considered:
  - ➡ Colliding ions fluctuating geometry
  - ➡ Presence of jets, multi-parton interactions, in the event affects the particle multiplicity
- ➡ **HG-PYTHIA** model includes those effects and reproduces observations for charged hadrons and for Z^0 bosons and photons

Charged particles

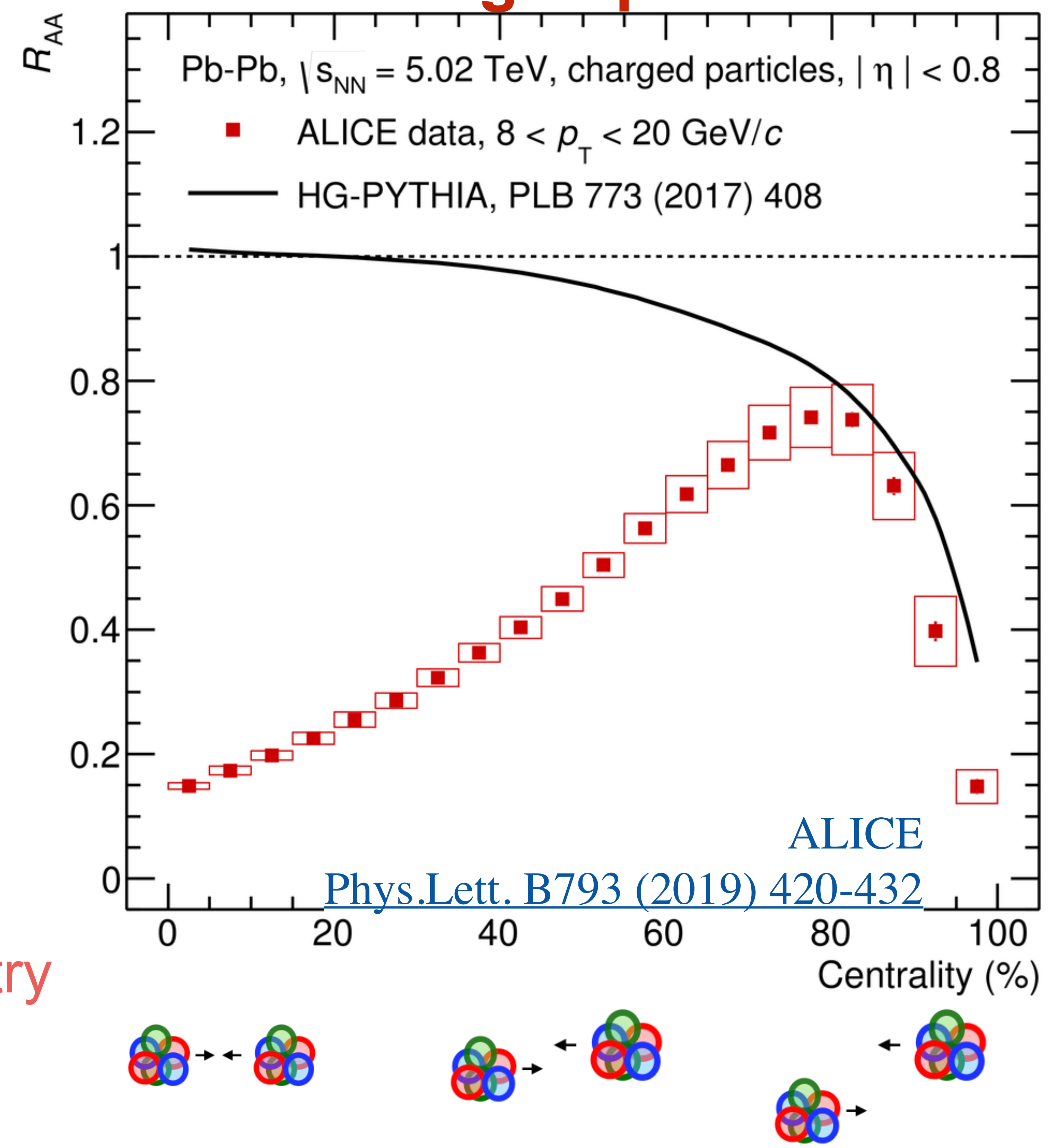

Z^0 (CMS) and isolated γ

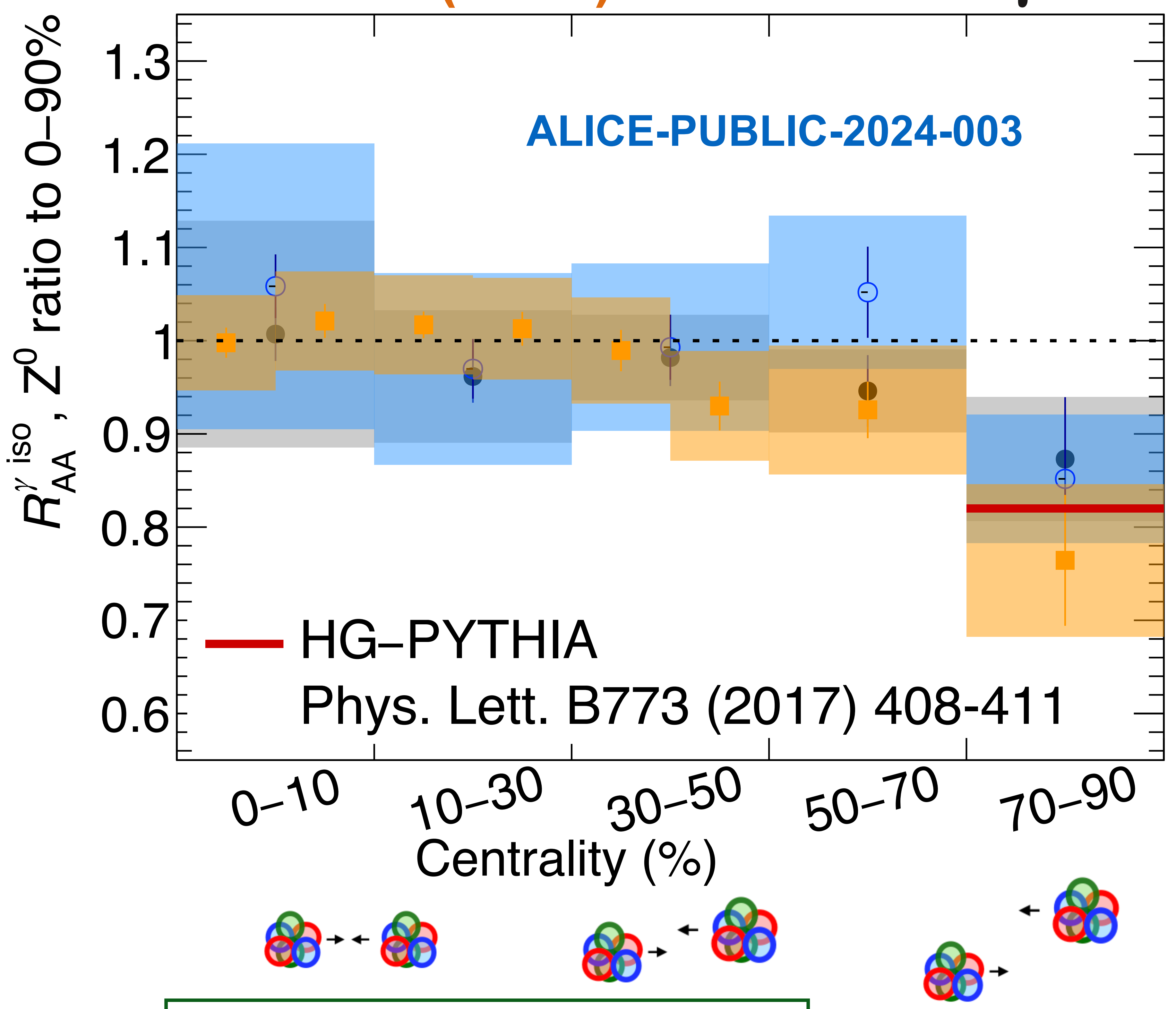

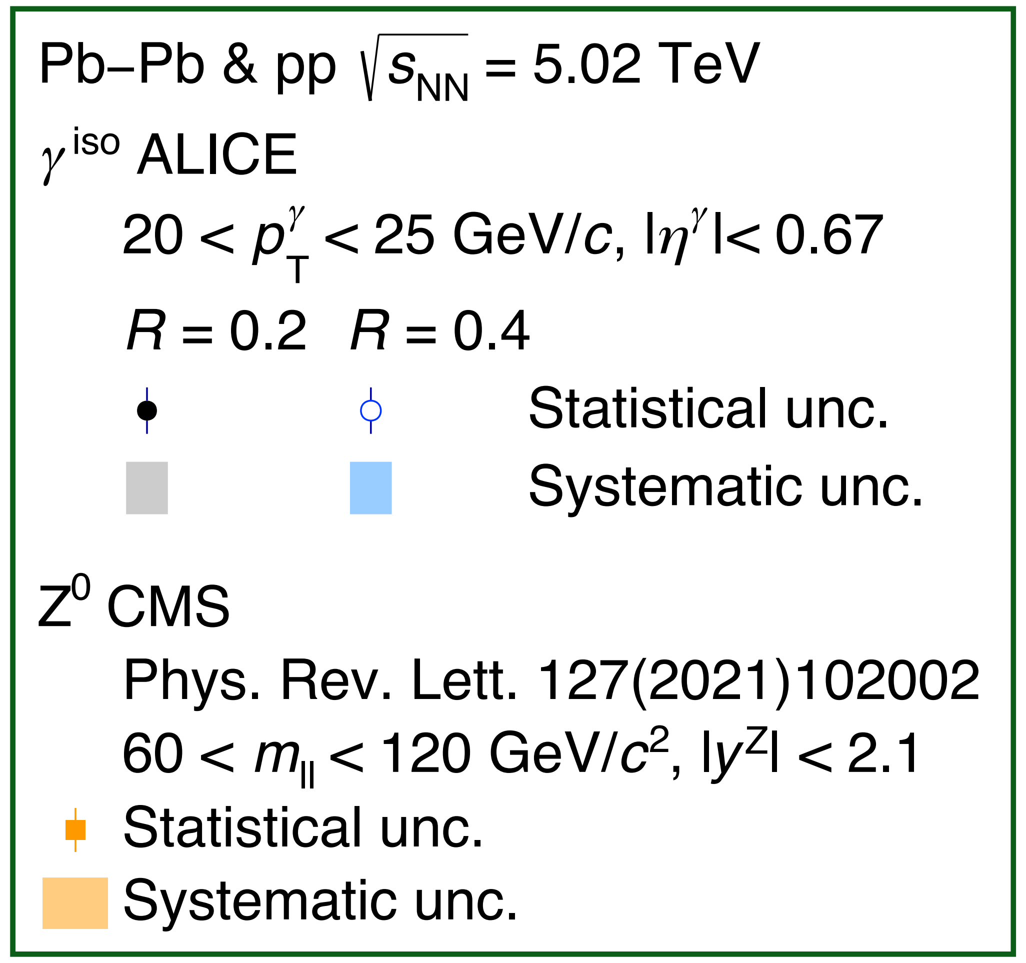

γ: Lowest uncertainty p_T bin

Z^0: Integrated p_T

Nuclear modification factor R_{AA}, pp & Pb–Pb at $\sqrt{s_{NN}}$ = 5.02 TeV

$$R_{AA} = \frac{1}{\langle N_{coll} \rangle} \frac{d^2\sigma_{AA} / (dp_T\, d\eta)}{d^2\sigma_{pp} / (dp_T\, d\eta)}$$

- **ALICE** & **CMS**: good agreement in the overlapping region 25 < p_T < 40–80 GeV/c

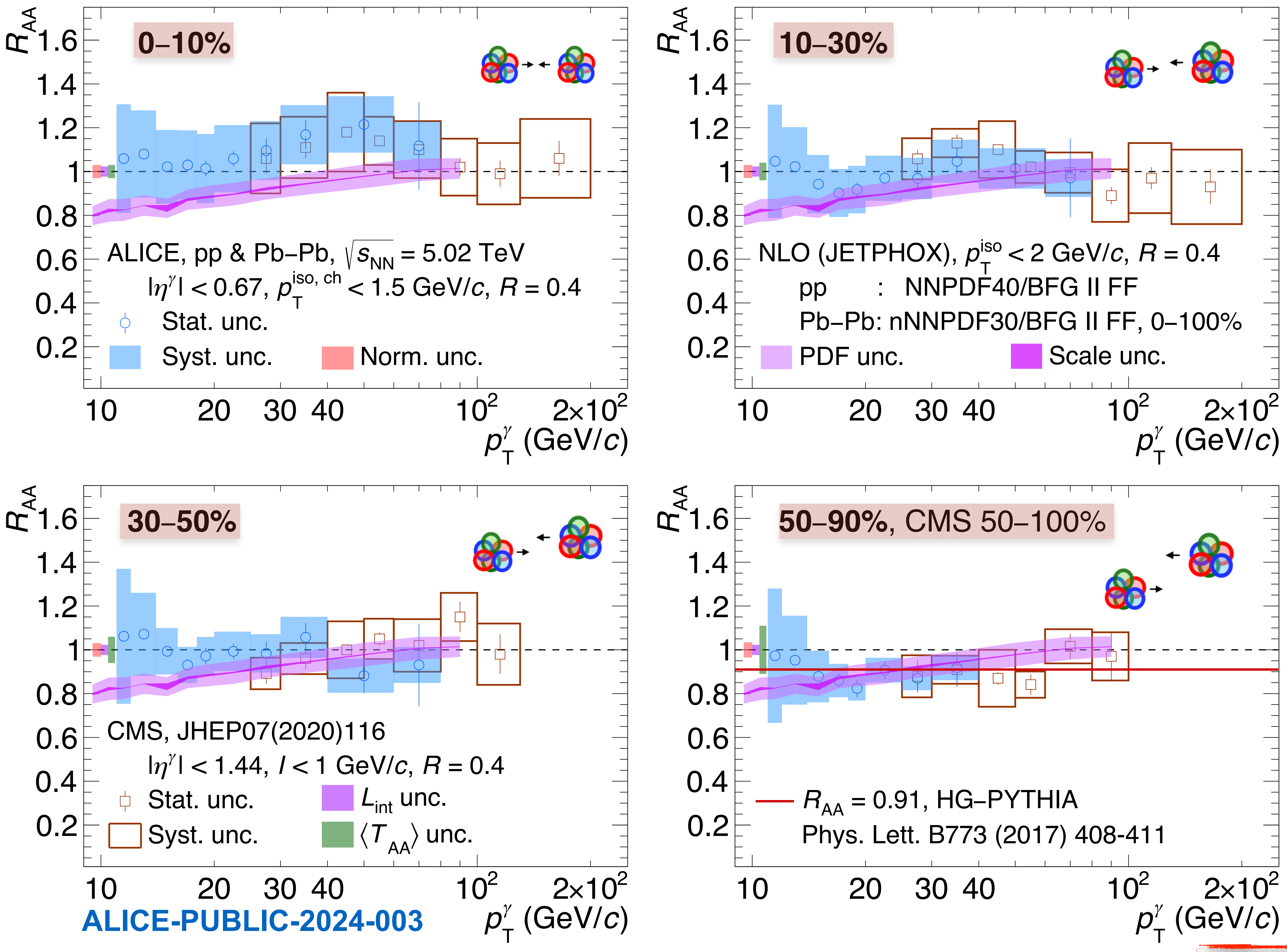

ALICE-PUBLIC-2024-003

Nuclear modification factor R_{AA}, pp & Pb–Pb at $\sqrt{s_{NN}}$ = 5.02 TeV

$$R_{AA} = \frac{1}{\langle N_{coll} \rangle} \frac{d^2\sigma_{AA} / (dp_T\, d\eta)}{d^2\sigma_{pp} / (dp_T\, d\eta)}$$

- **ALICE & CMS**: good agreement in the overlapping region 25 < p_T < 40–80 GeV/c

- 50-90%
  - ➡ Closer to 0.9 than 1 for both R likely due to centrality selection bias of Glauber model
  - ➡ Model by C. Loizides & A. Morsch (Phys. Lett. B773 (2017) 408-411) yields a value at 0.91
    - ✤ In agreement within the uncertainties

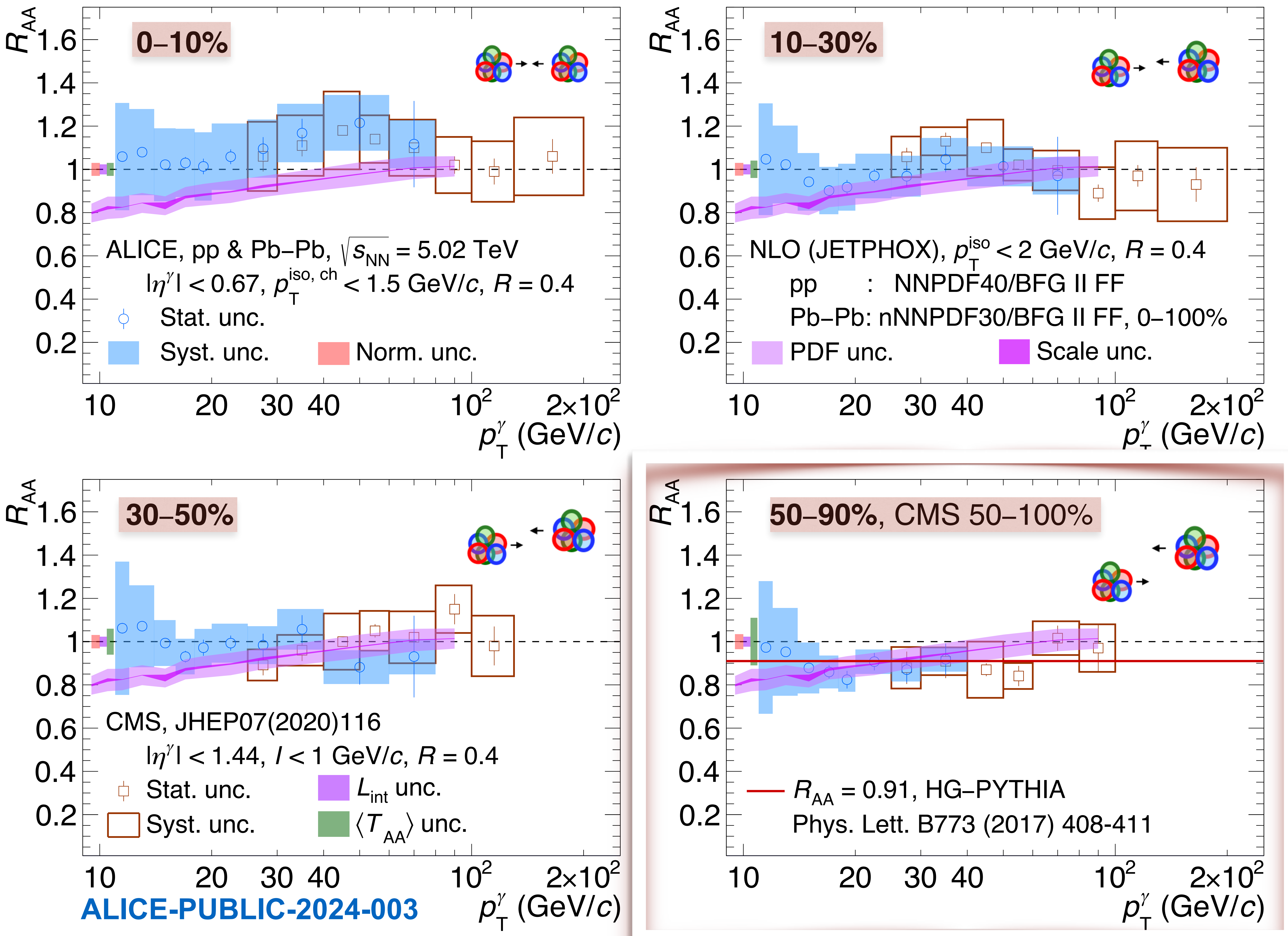

ALICE-PUBLIC-2024-003

Nuclear modification factor R_{AA}, pp & Pb–Pb at $\sqrt{s_{NN}}$ = 5.02 TeV

$$R_{AA} = \frac{1}{\langle N_{coll} \rangle} \frac{d^2\sigma_{AA} / (dp_T\, d\eta)}{d^2\sigma_{pp} / (dp_T\, d\eta)}$$

- **ALICE** & **CMS**: good agreement in the overlapping region 25 < p_T < 40–80 GeV/c
- 50-90%
  - ➡ Closer to 0.9 than 1 for both R likely due to centrality selection bias of Glauber model
  - ➡ Model by C. Loizides & A. Morsch (Phys. Lett. B773 (2017) 408-411) yields a value at 0.91
    - ✤ In agreement within the uncertainties

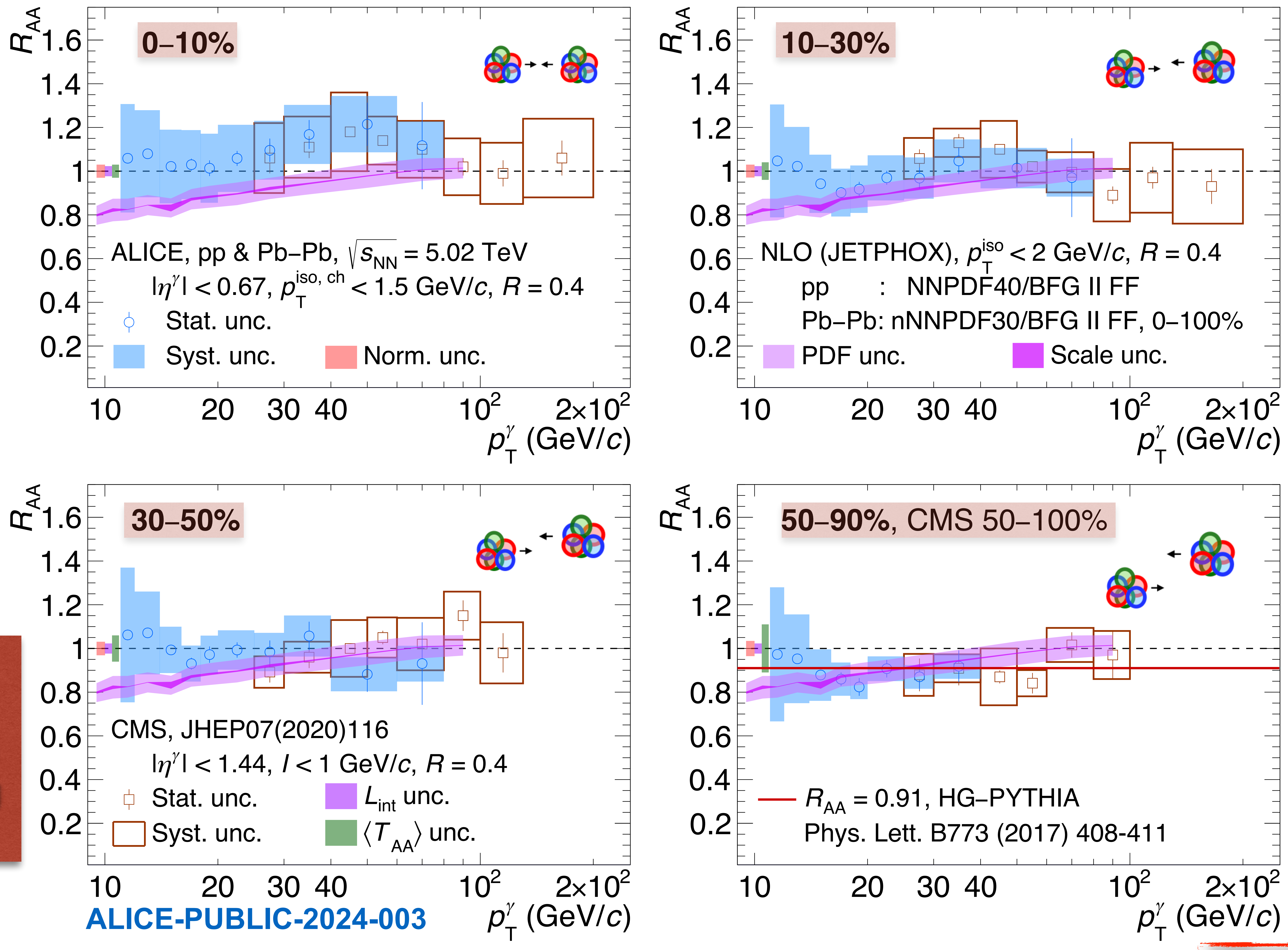

Isolated photons are not modified by the QGP from central to peripheral collisions and are candle/calibrated probes to test the interpretation of other particles R_{AA} and study the jet-quenching of the back-to-back correlated partons

Isolated-γ hadron correlation Pb–Pb collisions at $\sqrt{s_{NN}}$ = 5.02 TeV

Preliminary results

Isolated γ-hadron correlations in Pb–Pb at $\sqrt{s_{\rm NN}}$ = 5.02 TeV, R = 0.2

- Prompt γ associated to a parton emitted in opposite side
- **Tags the parton initial energy** $p_{\rm T}^{\gamma} \simeq p_{\rm T}^{\rm parton}$, before losing Δ*E* in QGP
  - ➡ Aim: Measure jet fragmentation function modifications**,** *where is the ΔE radiated?*

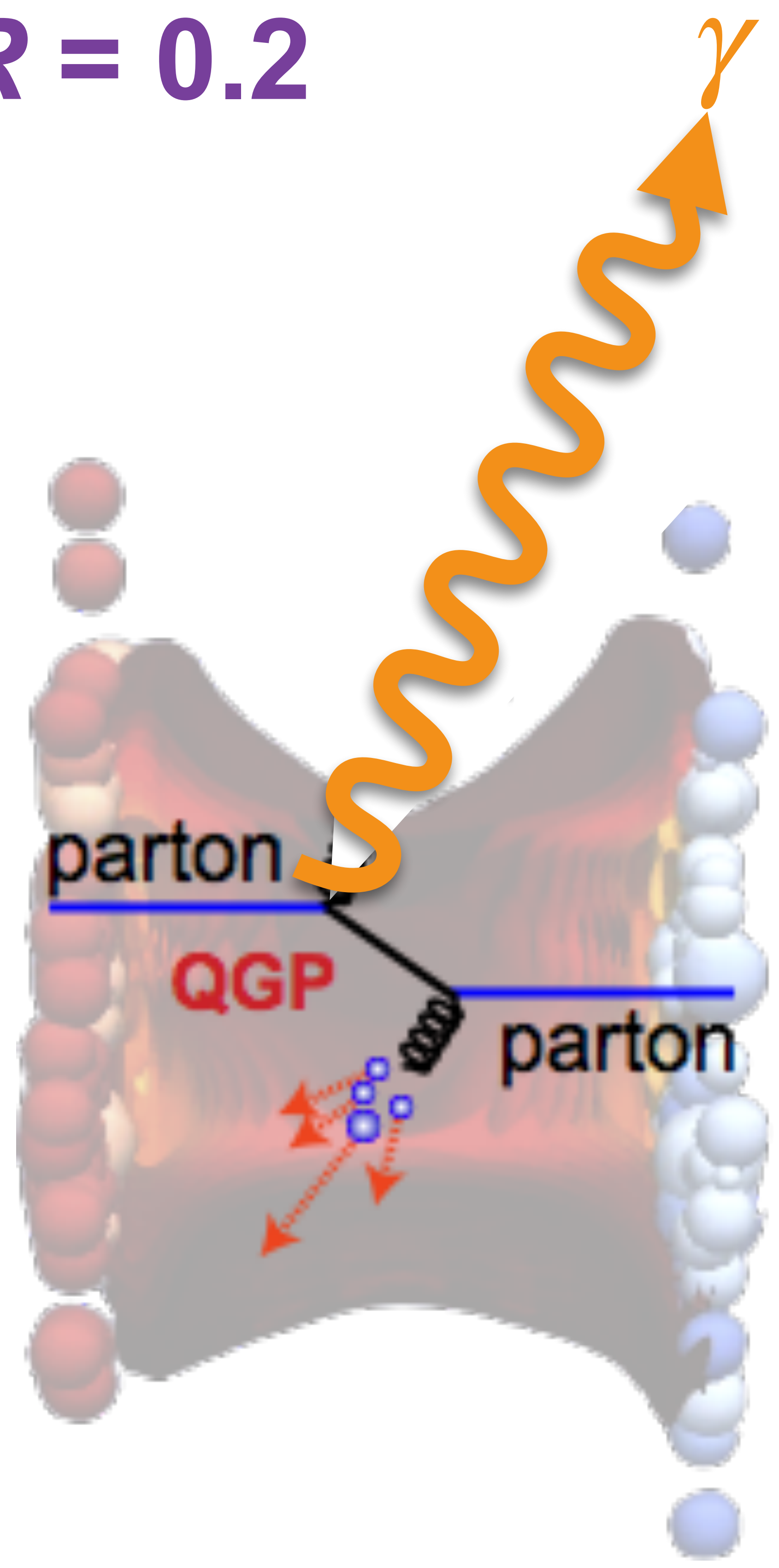

Isolated γ-hadron correlations in Pb–Pb at $\sqrt{s_{\rm NN}}$ = 5.02 TeV, R = 0.2

- Prompt γ associated to a parton emitted in opposite side
- **Tags the parton initial energy** $p_{\rm T}^{\gamma} \simeq p_{\rm T}^{\rm parton}$, before losing Δ*E* in QGP
  - ➡ Aim: Measure jet fragmentation function modifications**,** *where is the ΔE radiated?*

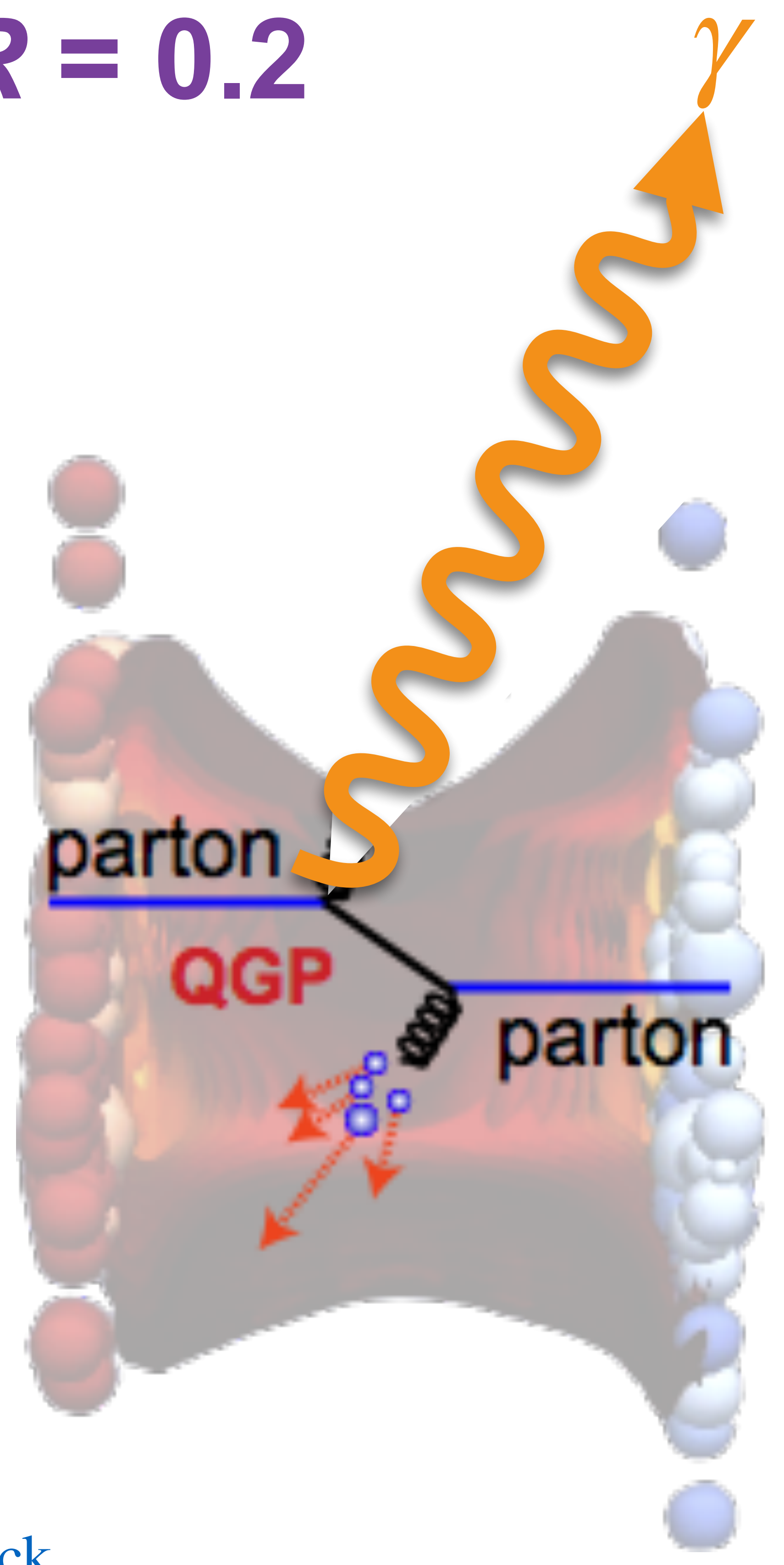

- Observables:
  - ➡ Trigger: isolated narrow or wide clusters, $18 < p_T^{\rm trigger} < 40$ GeV/*c*
    - ◉ $R = 0.2$ & $p_{\rm T}^{\rm iso\ ch} < 1.5$ GeV/*c*: Higher isolation purity and efficiency in central collisions
  - ➡ Azimuthal correlation: $\Delta\varphi = \varphi^{\rm trigger} - \varphi^{\rm track}$, $p_T^{\rm track} > 0.5$ GeV/*c*
  - ➡ Per trigger yield $\mathrm{D}(z_{\rm T}) = \dfrac{1}{N^{\rm trigger}} \dfrac{{\rm d}\, N^{\rm track}}{{\rm d}\ z_{\rm T}}$ for tracks in $|\Delta\varphi| > 3/5\pi$ rad (mirrored) with $z_{\rm T} = \dfrac{p_{\rm T}^{\rm track}}{p_T^{\rm trigger}}$
    - ◉ When trigger = prompt γ, $\mathrm{D}(z_{\rm T})$ is a proxy for the jet fragmentation function
  - ➡ Study $\mathrm{D}(z_{\rm T})$ modification due to jet-quenching via $I_{\rm AA} = \dfrac{D(z_{\rm T})_{\rm \ Pb-Pb}}{D(z_{\rm T})_{\rm \ pp}} \approx \dfrac{D(z_{\rm T})_{\rm \ Pb-Pb}}{D(z_{\rm T})_{\rm \ NLO\ pQCD}}$

(similar to $R_{\rm AA}$ but no need of $N_{\rm col}$, per trigger yields)

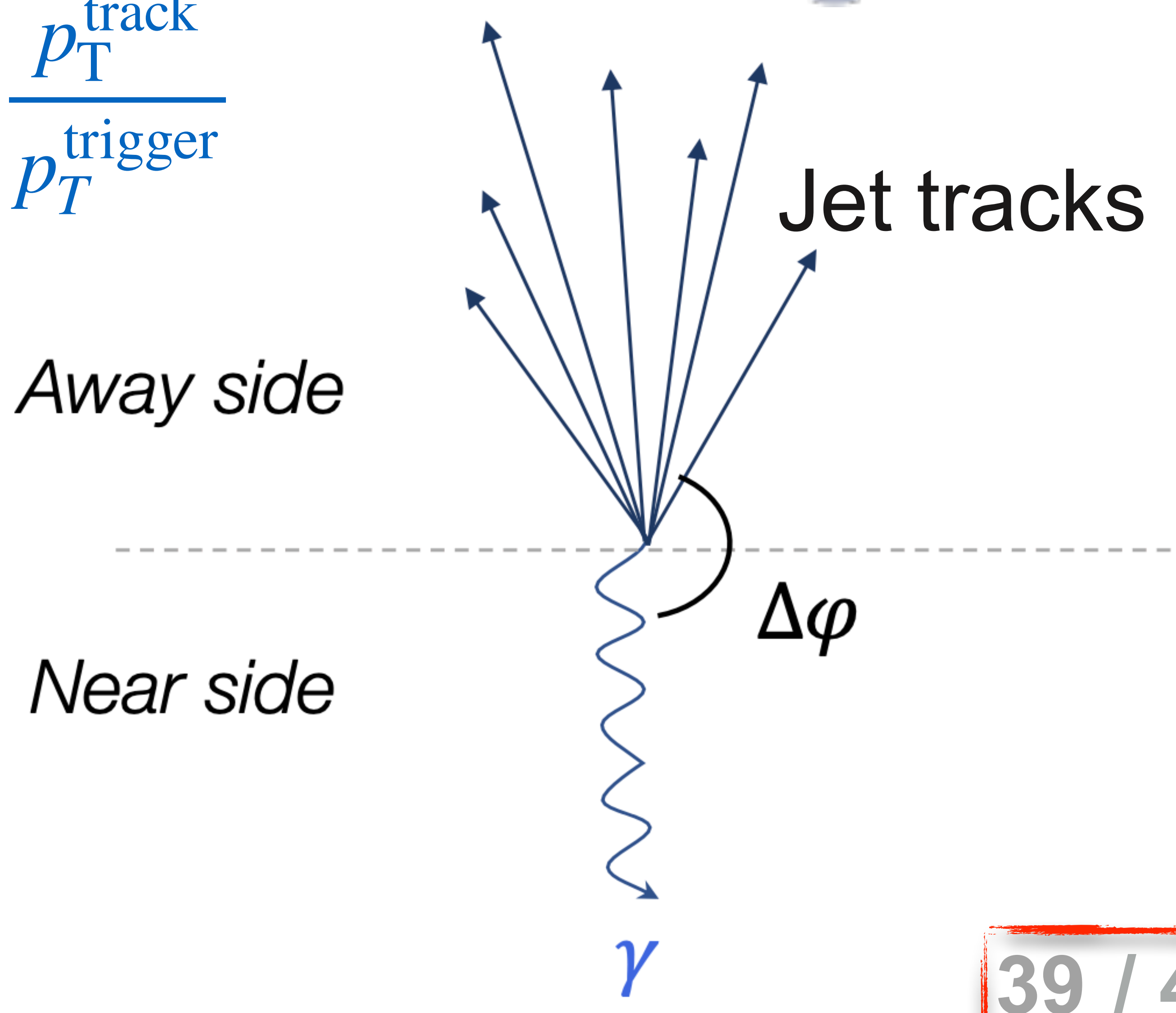

Isolated γ-hadron correlations in Pb–Pb: Azimuthal distribution

20 < p_T < 25 GeV/c & 0.2 < z_T < 0.3

- UE in $\Delta\varphi$: uncorrelated tracks shift up the distribution
- *<u>UE subtraction with mixed event</u>*: artificial dataset created combining the trigger cluster with tracks on different collisions

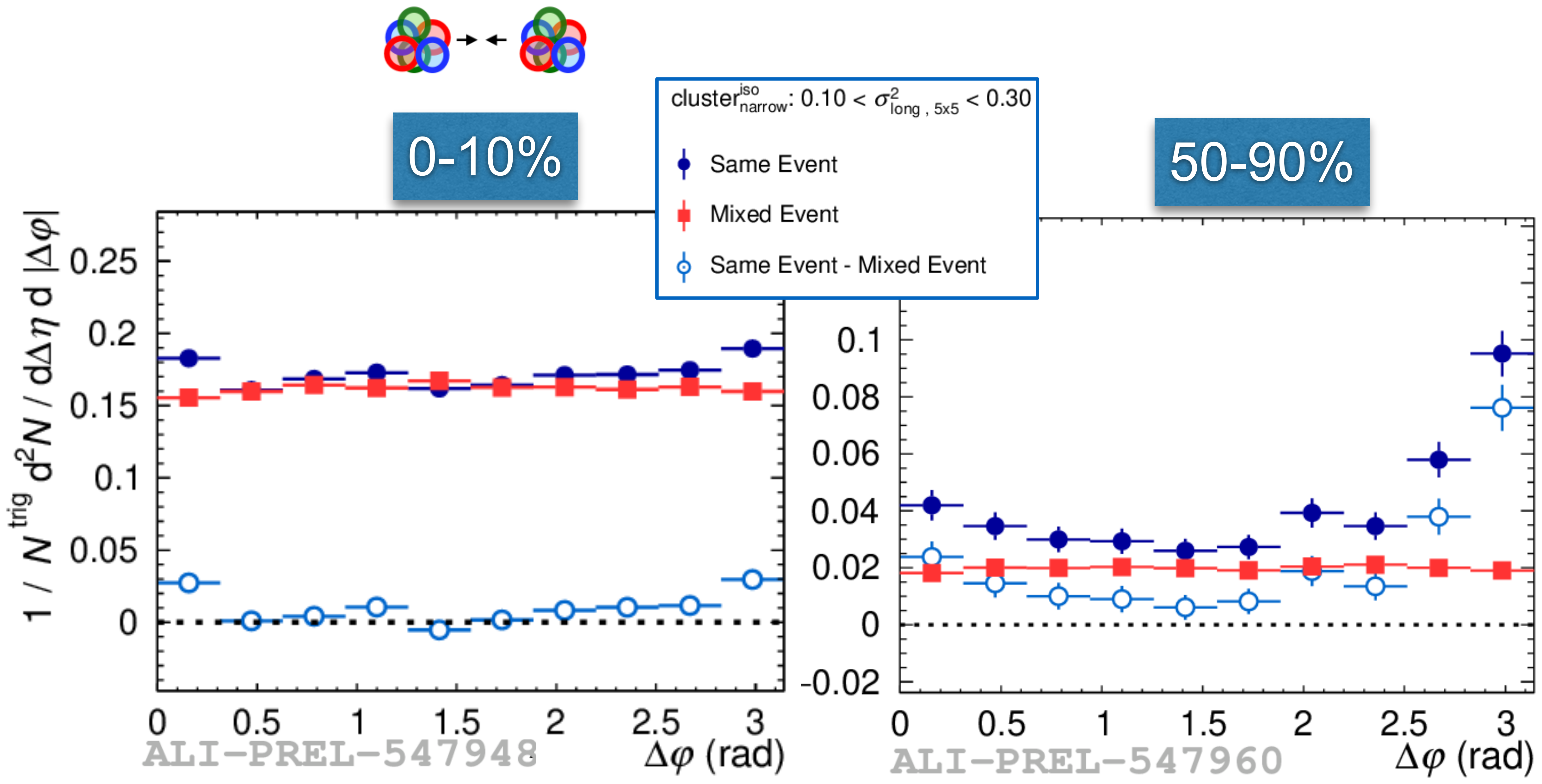

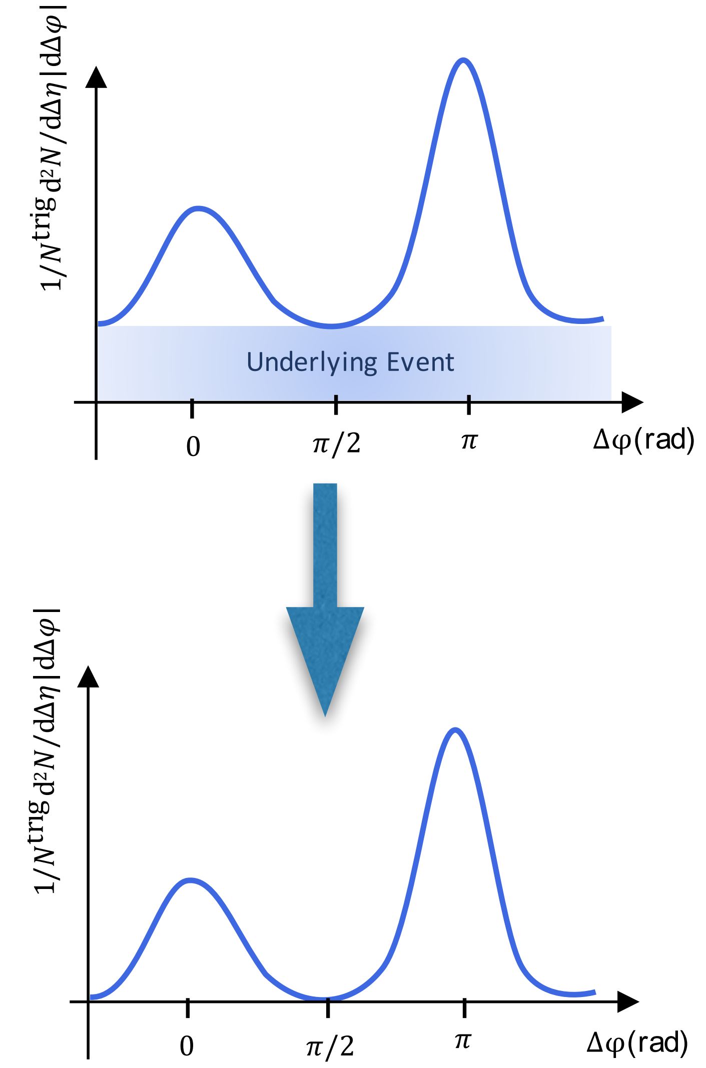

Isolated γ-hadron correlations in Pb–Pb: Azimuthal distribution

- UE in $\Delta\varphi$: uncorrelated tracks shift up the distribution
- *UE subtraction with mixed event*: artificial dataset created combining the trigger cluster with tracks on different collisions
- Purity < 1, considering $f(\Delta\varphi^{\mathrm{cls}^{\mathrm{iso}}_{\mathrm{narrow}}})$ bkg = $f(\Delta\varphi^{\mathrm{cls}^{\mathrm{iso}}_{\mathrm{wide}}})$:

$$f(\Delta\varphi^{\gamma^{\mathrm{iso}}}) = \frac{f(\Delta\varphi^{\mathrm{cls}^{\mathrm{iso}}_{\mathrm{narrow}}}) - (1-P)\cdot f(\Delta\varphi^{\mathrm{cls}^{\mathrm{iso}}_{\mathrm{wide}}})}{P}$$

➡ Subtraction of two close distributions → large statistical uncertainty

➡ $D(z_T)$: Integrate $f(\Delta\varphi^{\gamma^{\mathrm{iso}}})$ in $3/5\pi < |\Delta\varphi| < \pi$ rad

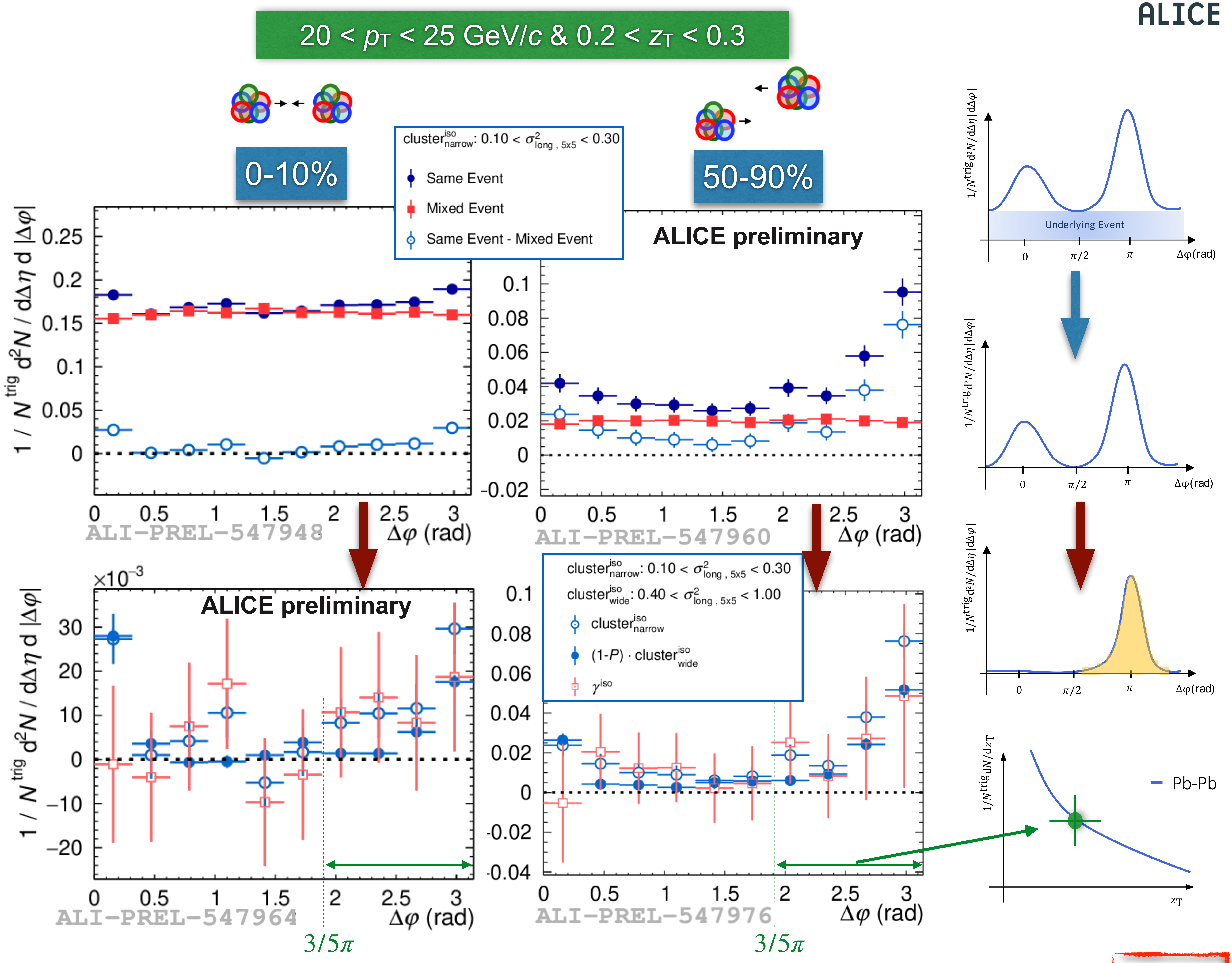

Isolated γ-hadron correlations in p–Pb & pp, R = 0.4: $D(z_T)$

Previous published results in p–Pb and pp collisions

➡ Agreement between systems and with PYTHIA

➡ Note: Pb–Pb collisions measurement (next slides) done in different p_T ranges and is compared directly to pQCD predictions

Phys Rev C 102 (2020) 044908

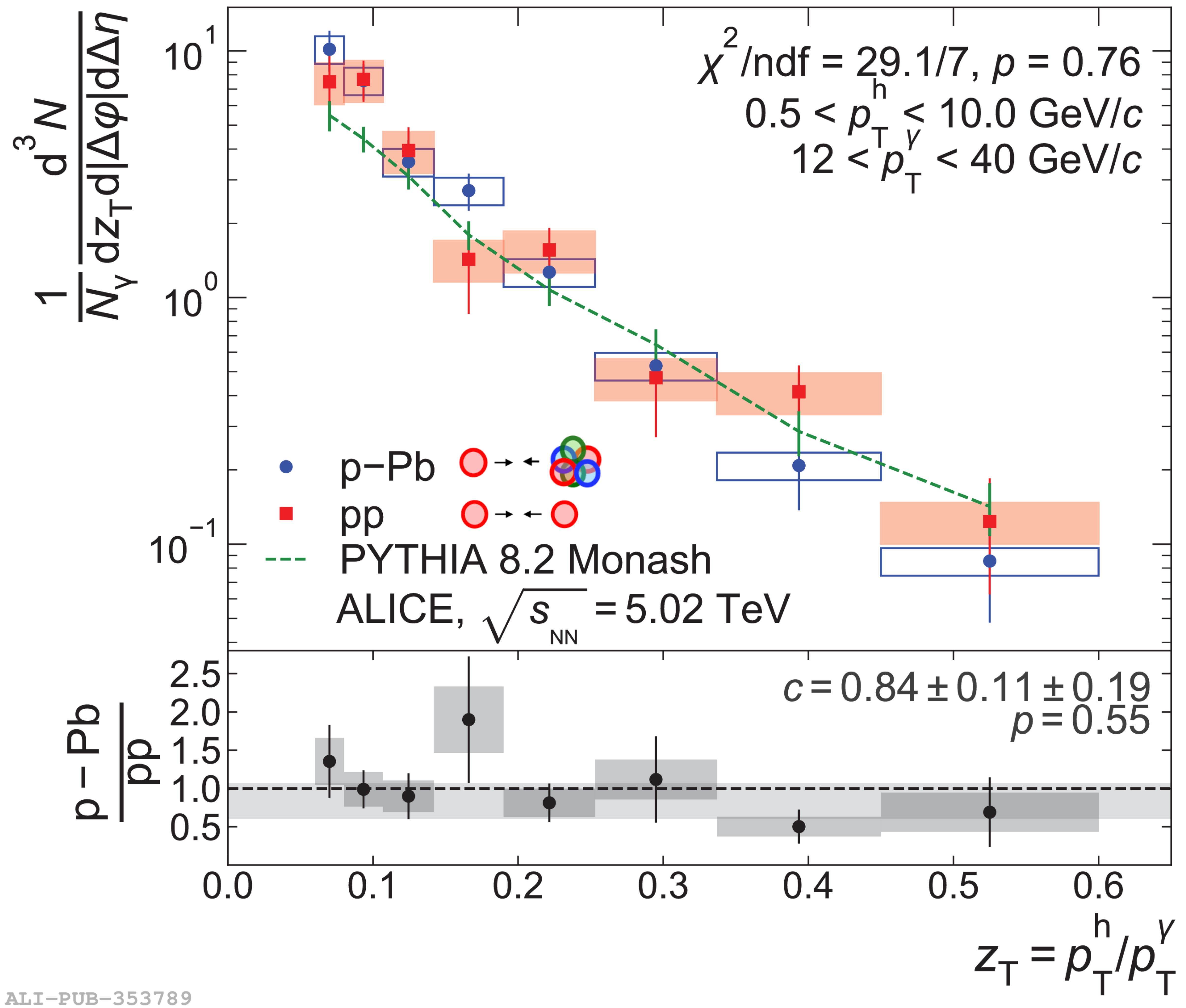

Isolated γ-hadron correlations in Pb–Pb: $D(z_T)$

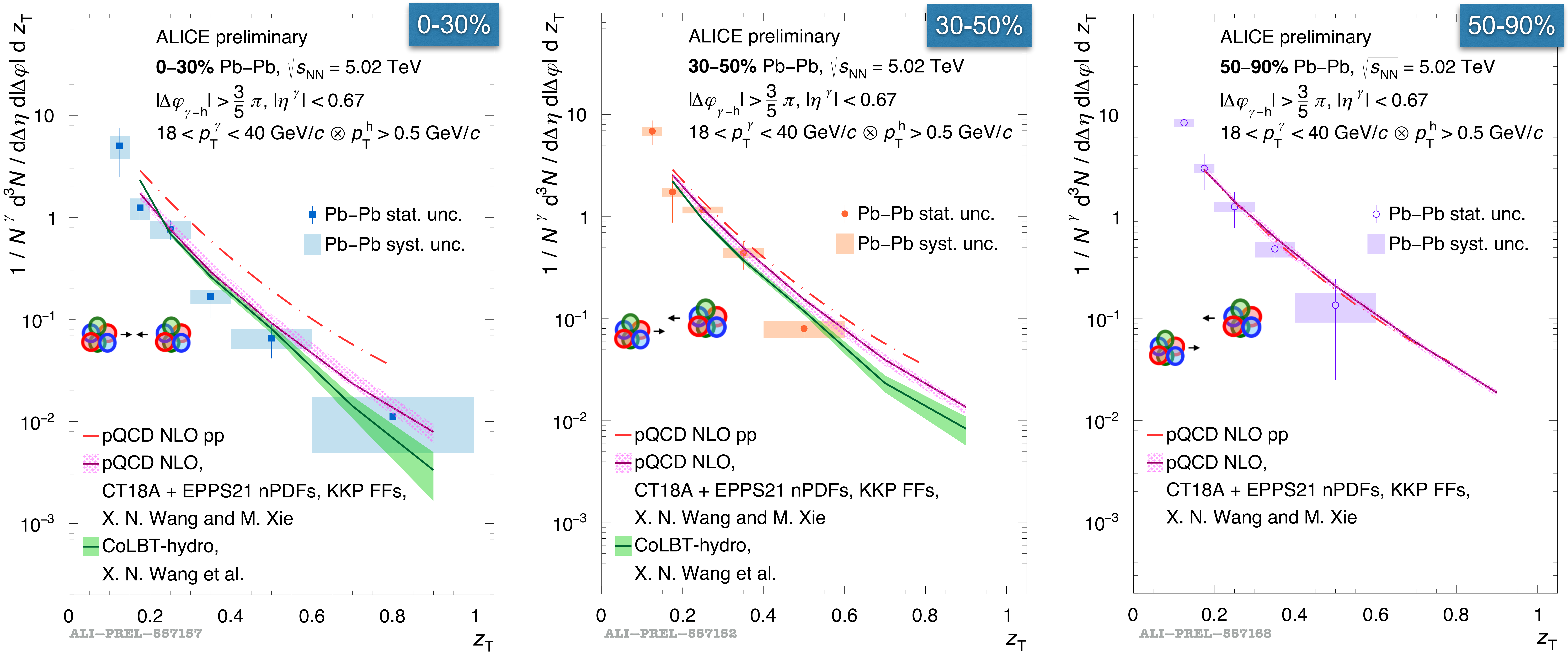

- Pb–Pb data compared with theory: *NLO pQCD* and *CoLBT* (0-50% only)
  - ➡ In agreement with both models
  - ➡ Discrimination not possible yet

- *Phys. Rev. C 103, 034911, Xie, Wang and Zhang,*
- *Phys. Rev. Lett. 103, 032302, Xie, Wang and Zhang*
- *Phys.Lett.B 777 (2018) 86-90 , Chen et al.*

Isolated γ-hadron correlations in Pb–Pb: $D(z_T)$

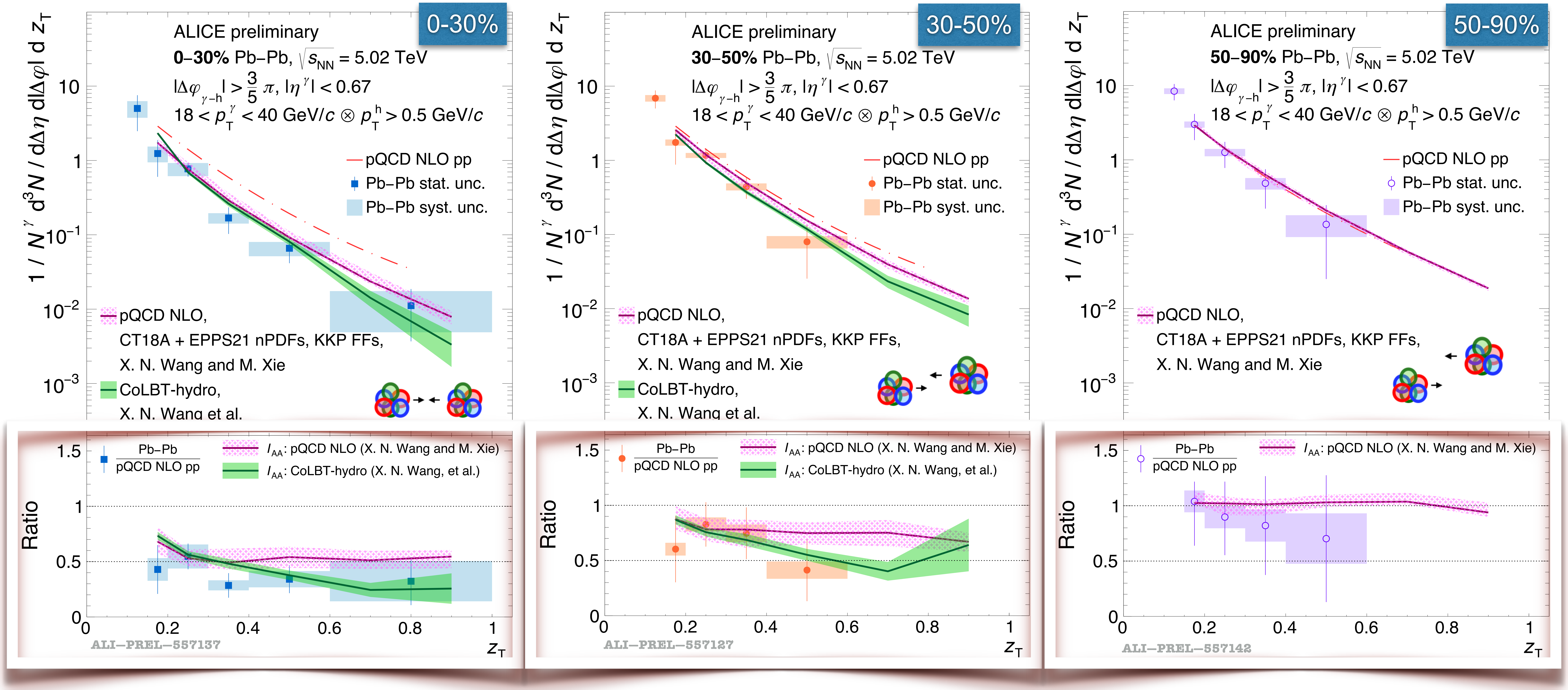

- Ratio with respect to NLO pQCD pp collision simulation → A proxy for $I_{AA} = \frac{D(z_T)_{\text{Pb-Pb}}}{D(z_T)_{\text{pp}}}$
- Clear modifications in data with respect to NLO pQCD pp simulation
- Comparison with I_{AA} from NLO pQCD and CoLBT models → agreement

Isolated γ-hadron correlations in Pb–Pb: RHIC & LHC

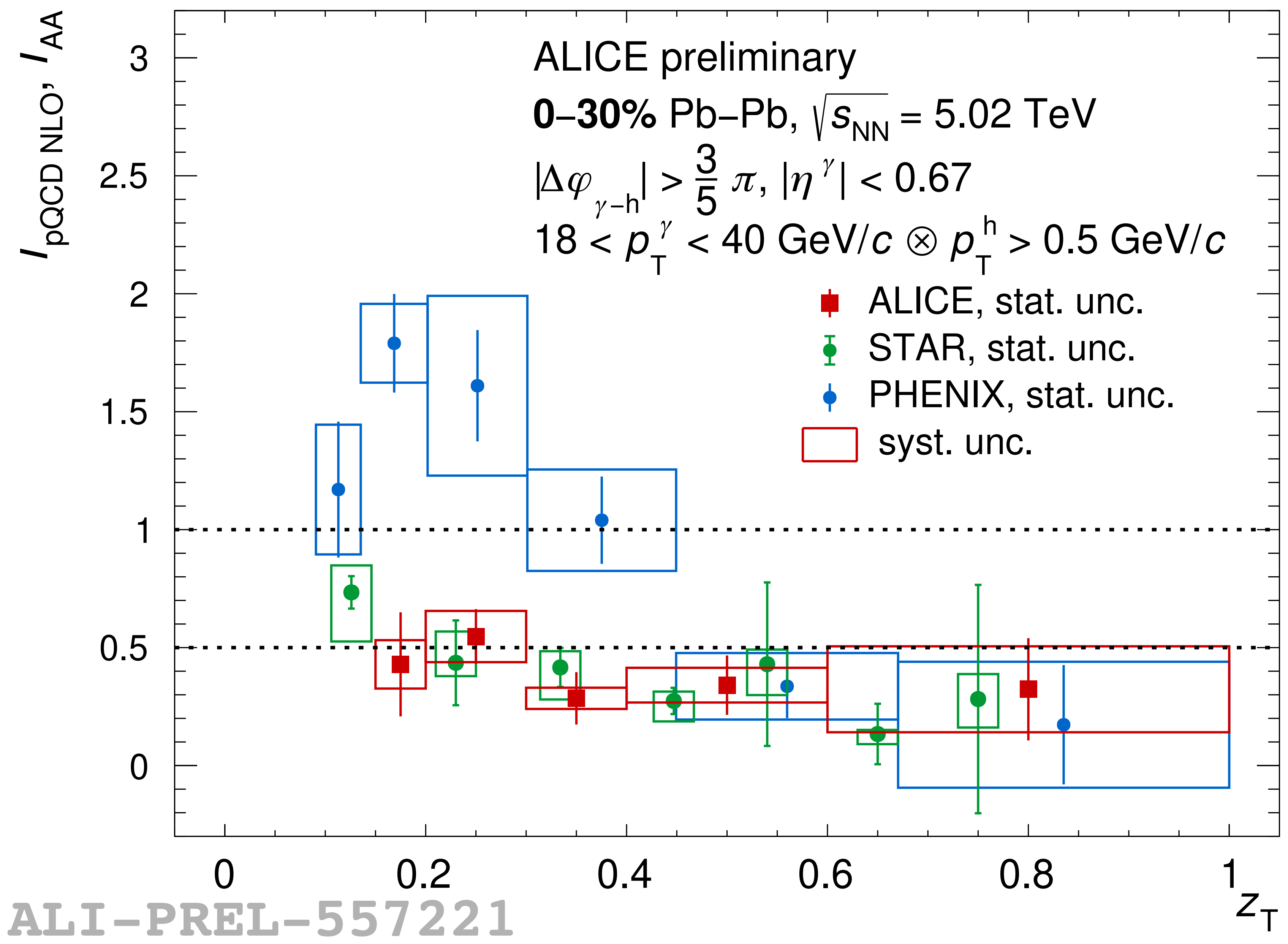

STAR, Phys.Lett.B 760 (2016) 689-696

0–12% Au–Au, $\sqrt{s_{NN}}$ = 200 GeV

$|\Delta\varphi_{\gamma\text{-h}} - \pi| \leq 1.4$

$12 < p_T^{\gamma} < 20$ GeV/c ⊗ $p_T^{h} > 1.2$ GeV/c

PHENIX, PRL 111, 032301 (2013)

0–40% Au–Au, $\sqrt{s_{NN}}$ = 200 GeV

$|\Delta\varphi_{\gamma\text{-h}} - \pi| < \pi/2$, $|y| < 0.35$

$5 < p_T^{\gamma} < 9$ GeV/c ⊗ $0.5 < p_T^{h} < 7$ GeV/c

Central

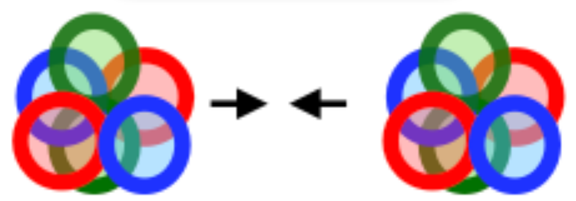

$$I_{AA}(z_T) = \frac{D(z_T, \mathbf{Pb-Pb})}{D(z_T, \mathbf{pp})}$$

- Similar behaviour as observed at RHIC and LHC experiments

➡ Note: <u>not completely apple-to-apple comparisons!</u>

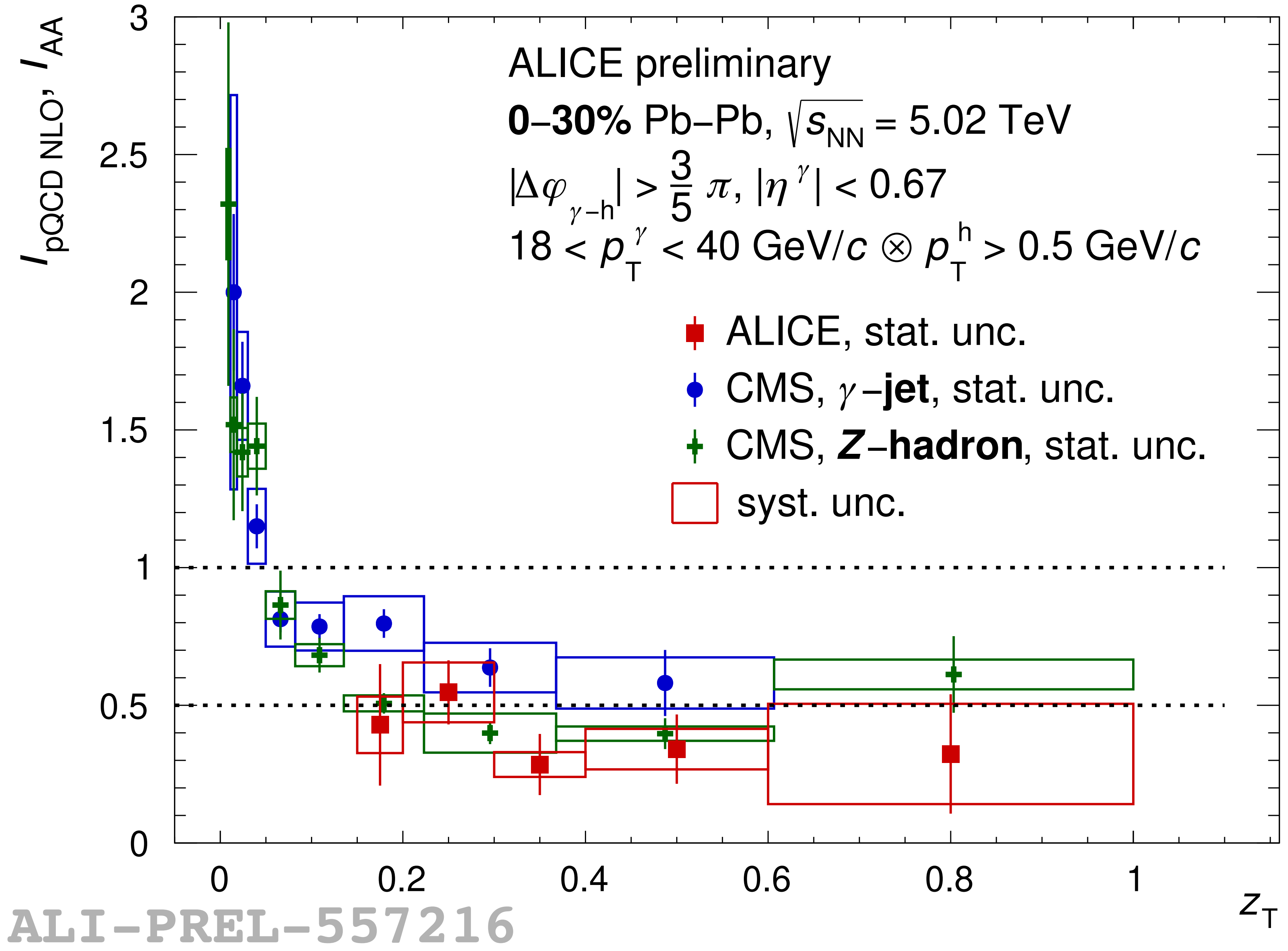

CMS, Phys.Rev.Lett. 121 (2018) 242301, 2018

γ–**jet**, **0–10%**

anti-k_T jet R = 0.3, $p_T^{jet} > 30$ GeV/c, $|\eta^{jet}| < 1.6$

$|\Delta\varphi_{\gamma\text{-jet}}| > \frac{7}{8}\pi$, $|\eta^{\gamma}| < 1.44$ $p_T^{\gamma} > 60$ GeV/c ⊗ $p_T^{h} > 1$ GeV/c

CMS, Phys.Rev.Lett. 128 (2022) 122301, 2022

***Z*–hadron**, **0–30%**

$|\Delta\varphi_{Z\text{-h}}| > \frac{7}{8}\pi$, $p_T^{Z} > 30$ GeV/c ⊗ $p_T^{h} > 1$ GeV/c

Summary

➡ **Cross section**

✱ Data in agreement with NLO pQCD in multiple collision systems & $\sqrt{s_{NN}}$

✱ Lowest measured x_T at mid-rapidity in pp collisions at $\sqrt{s}$ = 13 TeV

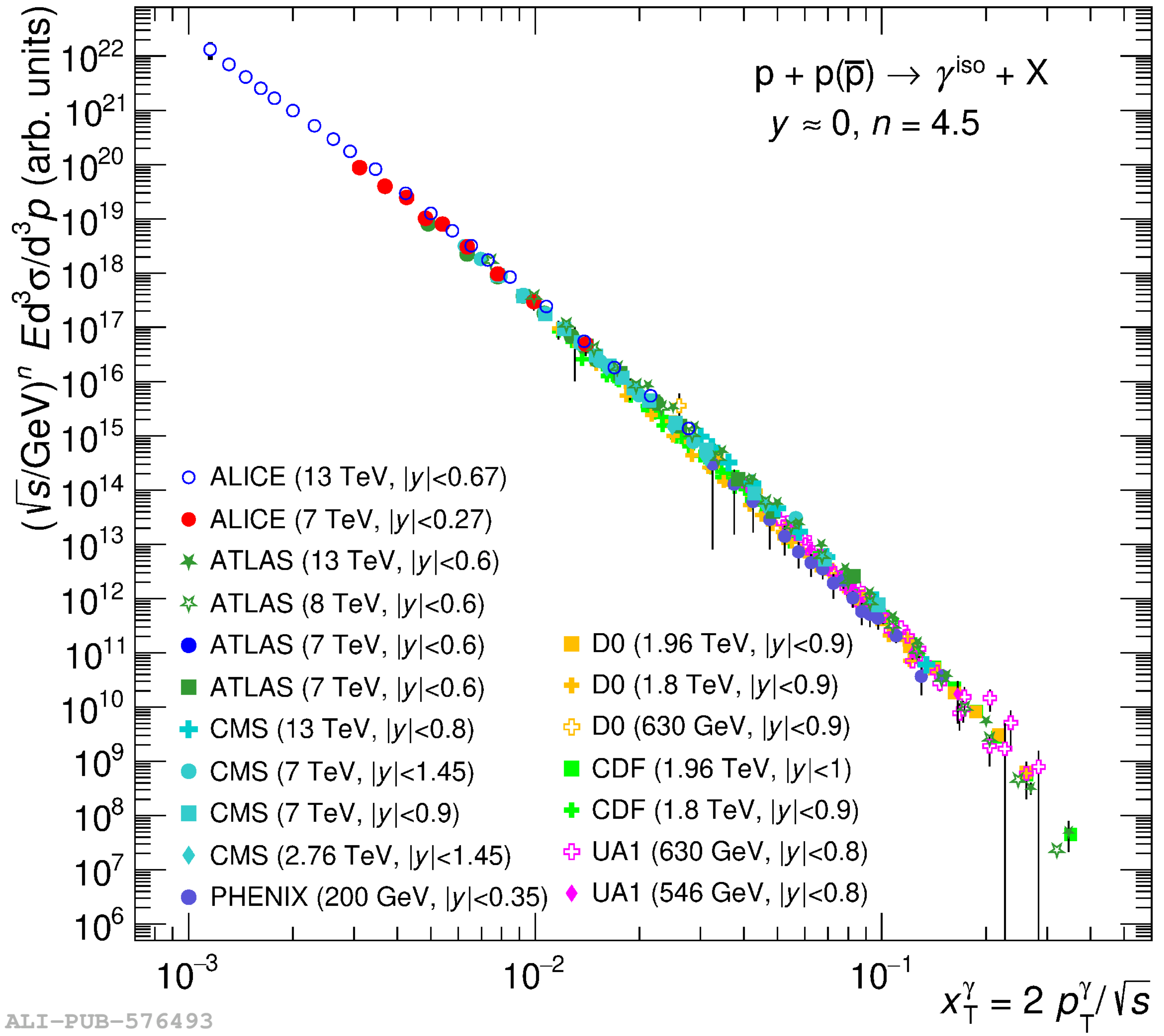

Summary

➡ **Cross section**

- Ratio of cross sections for different R in agreement with theory and within the different collision systems
- $R_{AA} \simeq 1$, no γ production modification by QGP
  - but for 50–90% & 70–90%: $R_{AA} \simeq 0.9$, agreement (1σ) with HG-PYTHIA, model of the centrality selection bias
  - Pb-Pb col. agree with nPDF prediction

ALICE-PUBLIC-2024-003

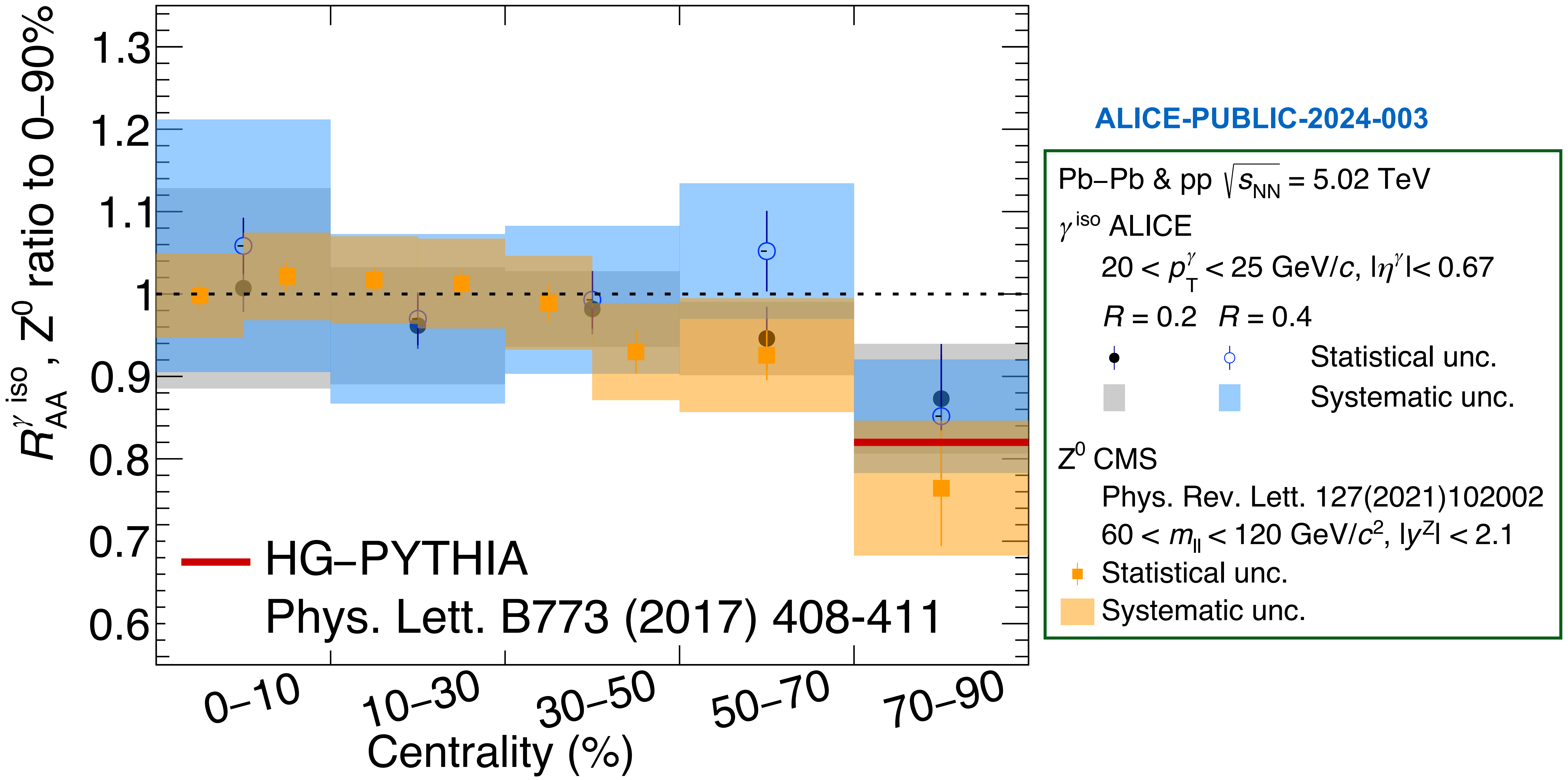

Summary

➡ **γ–hadron corr. in Pb–Pb at $\sqrt{s_{NN}}$ = 5.02 TeV**

- **Very statistically limited, challenging!**
- z_T distribution significantly lower than pp NLO pQCD in central
  - FF modification: stronger for central compared to peripheral
- Results described by two models, model discrimination not possible yet

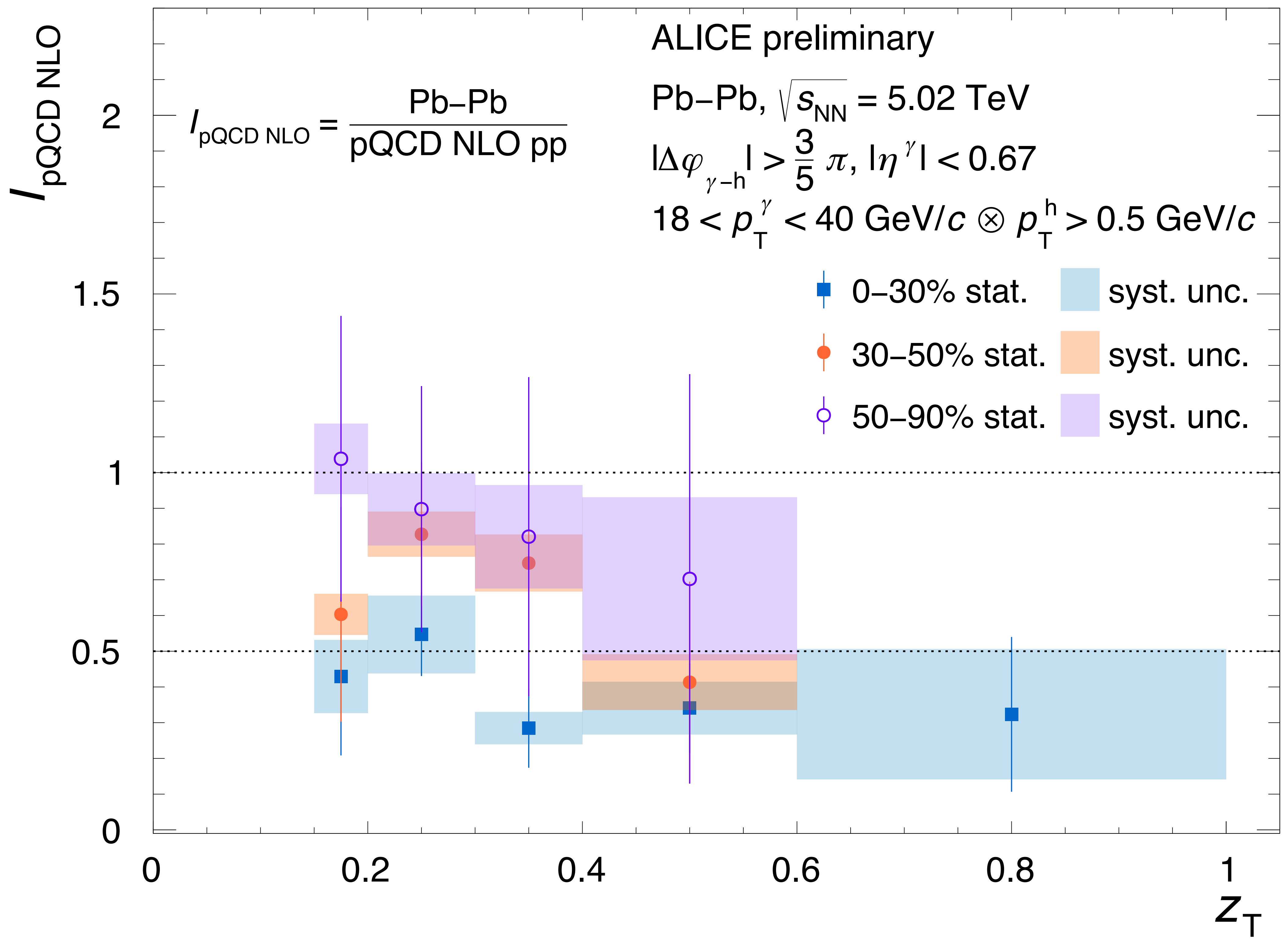

Expected improvement with Run 3 + Run 4 data samples, in particular γ-hadron correlations

ALI−PREL−556595

Thank you for your attention!

Table 1: Cluster reconstruction and selection criteria. Description and discussion can be found in Ref. [80].

Cluster seed threshold	$E_{seed} > 500$ MeV
Cluster aggregation threshold	$E_{agg} > 100$ MeV
Number of cells	$N_{cell} > 1$
N cells from highest E cell to SM border	$N_{border} > 1$
Cluster time - bunch crossing time	$\lvert\Delta t_{cluster}\rvert < 20$ ns
Abnormal signal removal	$F_{+} = 1 - \frac{\Sigma_{cell} E_{adjacent\ to\ highest\ E}}{E_{highest\ E\ cell}} < 0.95$
Charged particle veto (Pb–Pb only):	
when	$E_{cluster}/p^{track} < 1/7$
track–cluster η residual	$\Delta\eta^{residual} > 0.010 + (p_{T}^{track} + 4.07)^{-2.5}$
track–cluster φ residual	$\Delta\varphi^{residual} > 0.015 + (p_{T}^{track} + 3.65)^{-2}$ rad
Acceptance:	
Top section	$81.2^{\circ} < \varphi < 185.8^{\circ}$ $\quad \lvert\eta\rvert < 0.67$
Bottom section	$261.2^{\circ} < \varphi < 318.8^{\circ}$ $\quad 0.25 < \lvert\eta\rvert < 0.67$

Table 2: Trigger $RF^{trig}_{\varepsilon_{trig}}$ (Eq. (8)) fits to a constant in Fig. 9-right, $\mathscr{L}^{trig}_{NN}$, and $\mathscr{L}^{trig}_{int}$ (Eq. (9)), for pp and Pb–Pb collisions per centrality class and per trigger inclusive cluster p_{T} range. The $\mathscr{L}^{trig}_{NN}$ uncertainty contains both the $\sigma_{NN}^{col.\ system}$ and rejection factor uncertainties. The integrated luminosity uncertainty includes in addition the $\langle N_{coll}\rangle$ uncertainty.

Trigger	System	p_{T} (GeV/c)	$RF^{trig}_{\varepsilon_{trig}}$	$\mathscr{L}^{trig}_{NN}$ (nb^{-1})	$\mathscr{L}^{trig}_{int}$ (nb^{-1})
L1-γ	pp	$p_{T} > 11$	997 ± 10	265 ± 7	265 ± 7
	Pb–Pb:				
MB	0–10%	$p_{T} < 12$		1.189 ± 0.011	1869 ± 26
MB	10–30%	$p_{T} < 12$		0.522 ± 0.005	409 ± 5
MB	30–50%	$p_{T} < 12$		1.163 ± 0.010	308 ± 5
MB+L1-γ-high	0–10%	$p_{T} > 12$	45.0 ± 0.2	2.50 ± 0.02	3936 ± 55
MB+L1-γ-high	10–30%	$p_{T} > 12$	79.2 ± 0.4	4.90 ± 0.05	3834 ± 51
MB+L1-γ-high	30–50%	$p_{T} > 12$	179.3 ± 1.5	5.01 ± 0.05	1325 ± 21
MB+L1-γ-low	50–70%	$p_{T} < 12$	72.2 ± 1.2	3.5 ± 0.5	230 ± 5
MB+L1-γ-low	70–90%	$p_{T} < 12$	315 ± 13	3.62 ± 0.11	39.5 ± 1.3
MB+L1-γ-high+low	50–70%	$p_{T} > 12$	98.2 ± 1.2	4.88 ± 0.07	322 ± 7
MB+L1-γ-high+low	70–90%	$p_{T} > 12$	410 ± 20	5.1 ± 0.2	55 ± 2

Pb–Pb 50-90%: cross section and ratios

ALICE-PUBLIC-2024-003

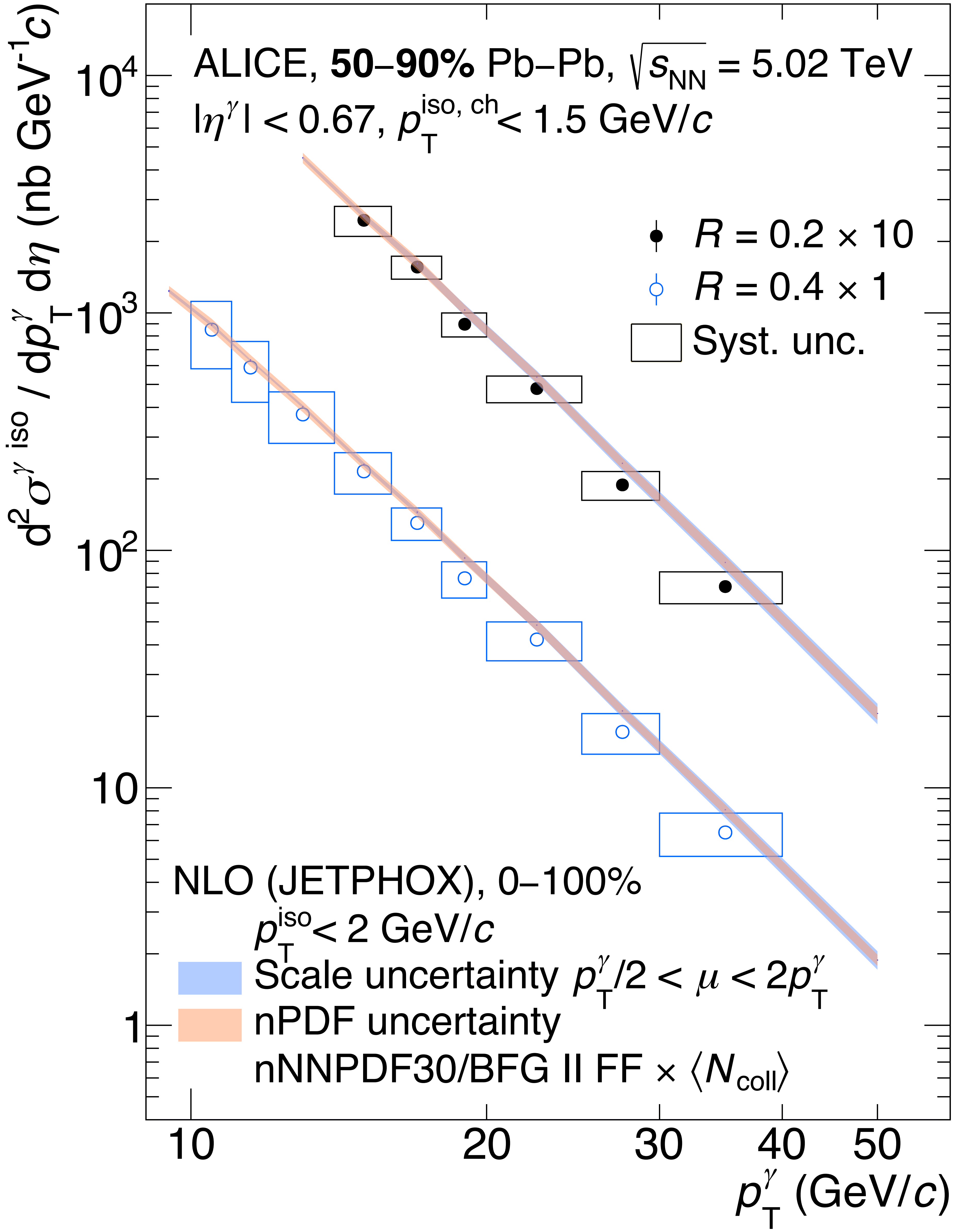

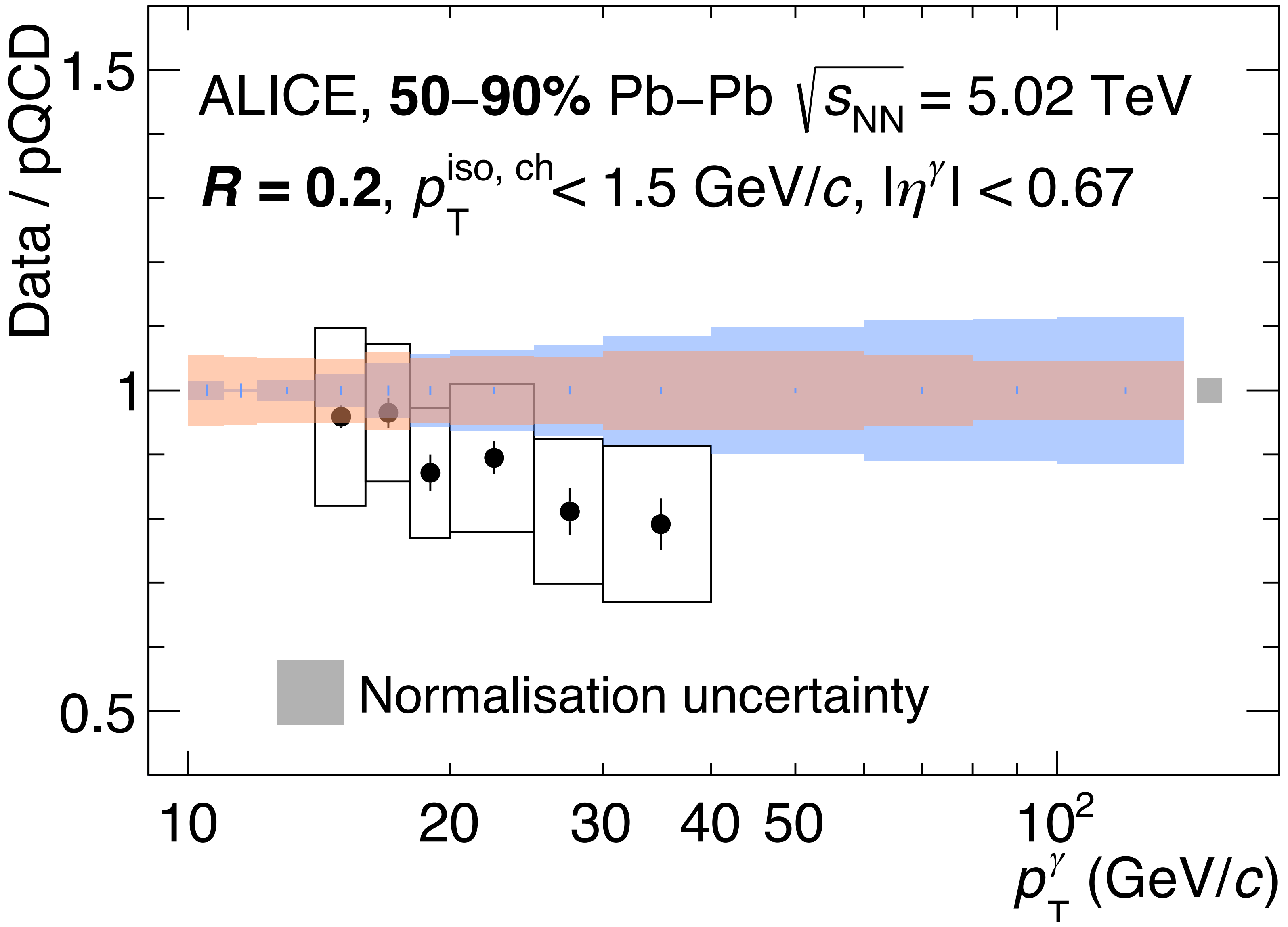

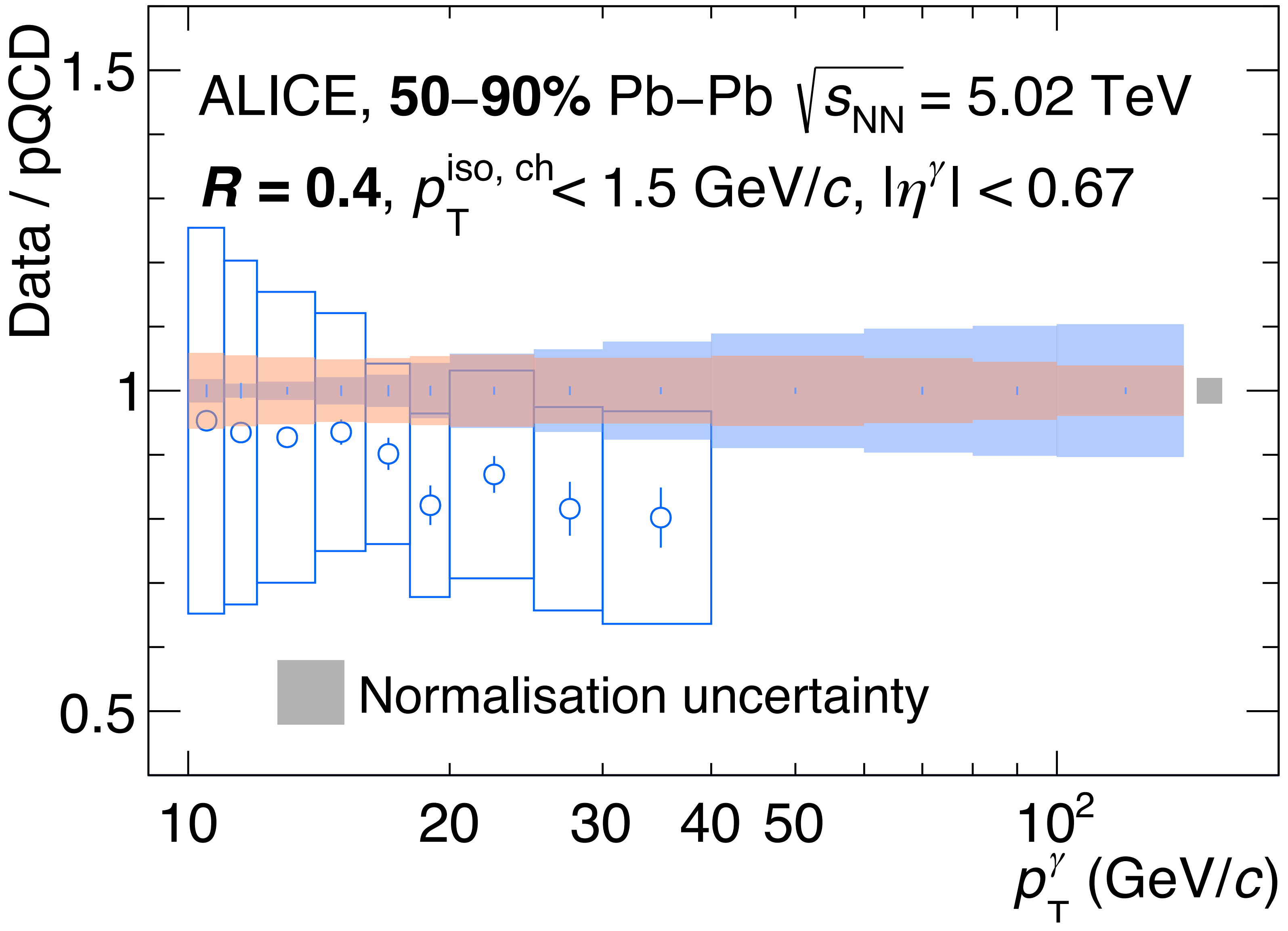

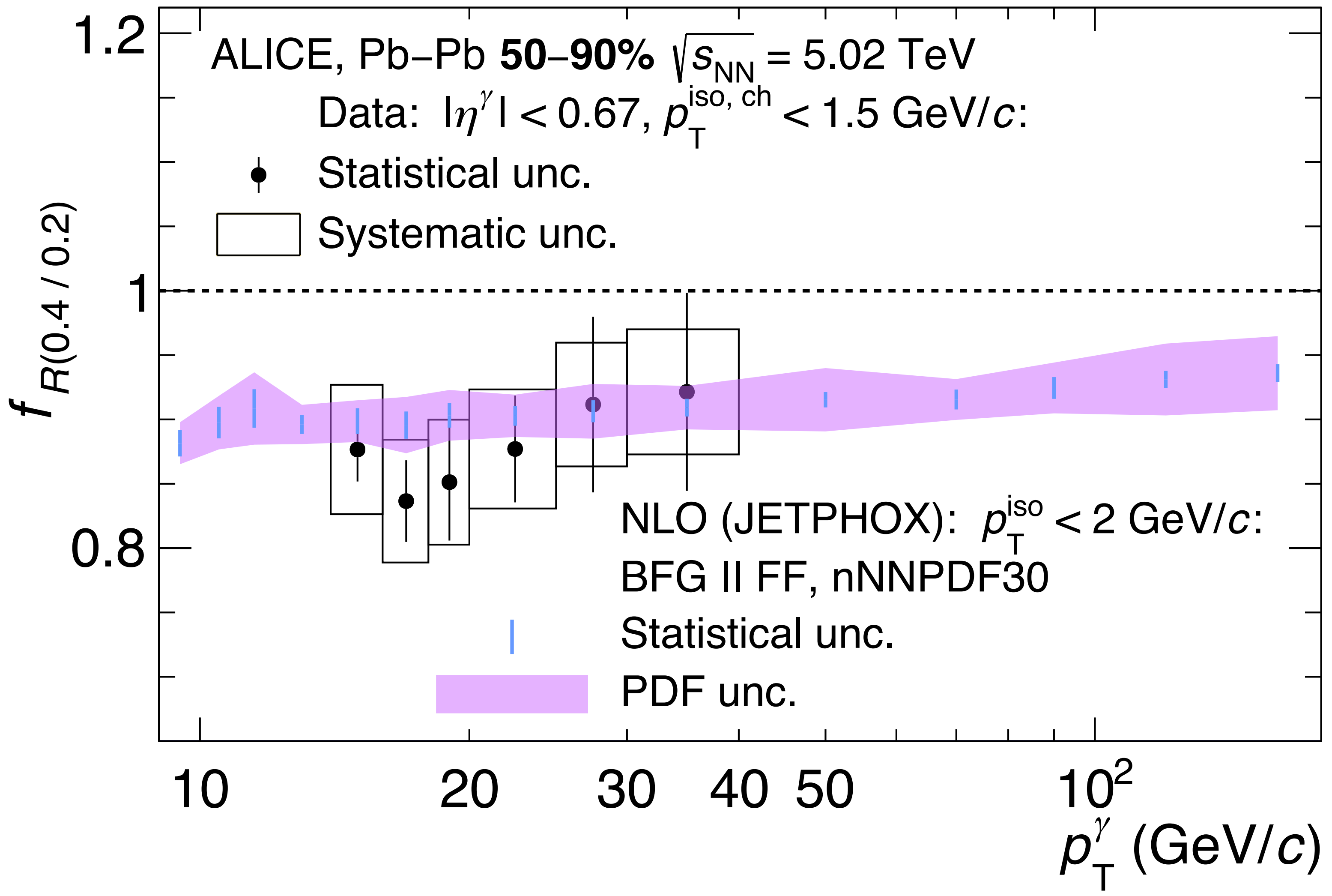

Nuclear modification factor R_{AA}, pp & Pb–Pb at $\sqrt{s_{NN}}$ = 5.02 TeV

$$R_{AA} = \frac{1}{\langle N_{coll} \rangle} \frac{d^2\sigma_{AA} / (dp_T\, d\eta)}{d^2\sigma_{pp} / (dp_T\, d\eta)}$$

- **ALICE** & **CMS**: good agreement in the overlapping region 25 < p_T < 40–80 GeV/c
- 50-90%
  - ➡ Closer to 0.9 than 1 for both R likely due to centrality selection bias of Glauber model
  - ➡ Model by C. Loizides & A. Morsch (Phys. Lett. B773 (2017) 408-411) yields a value at 0.91
    - ✤ In agreement within the uncertainties

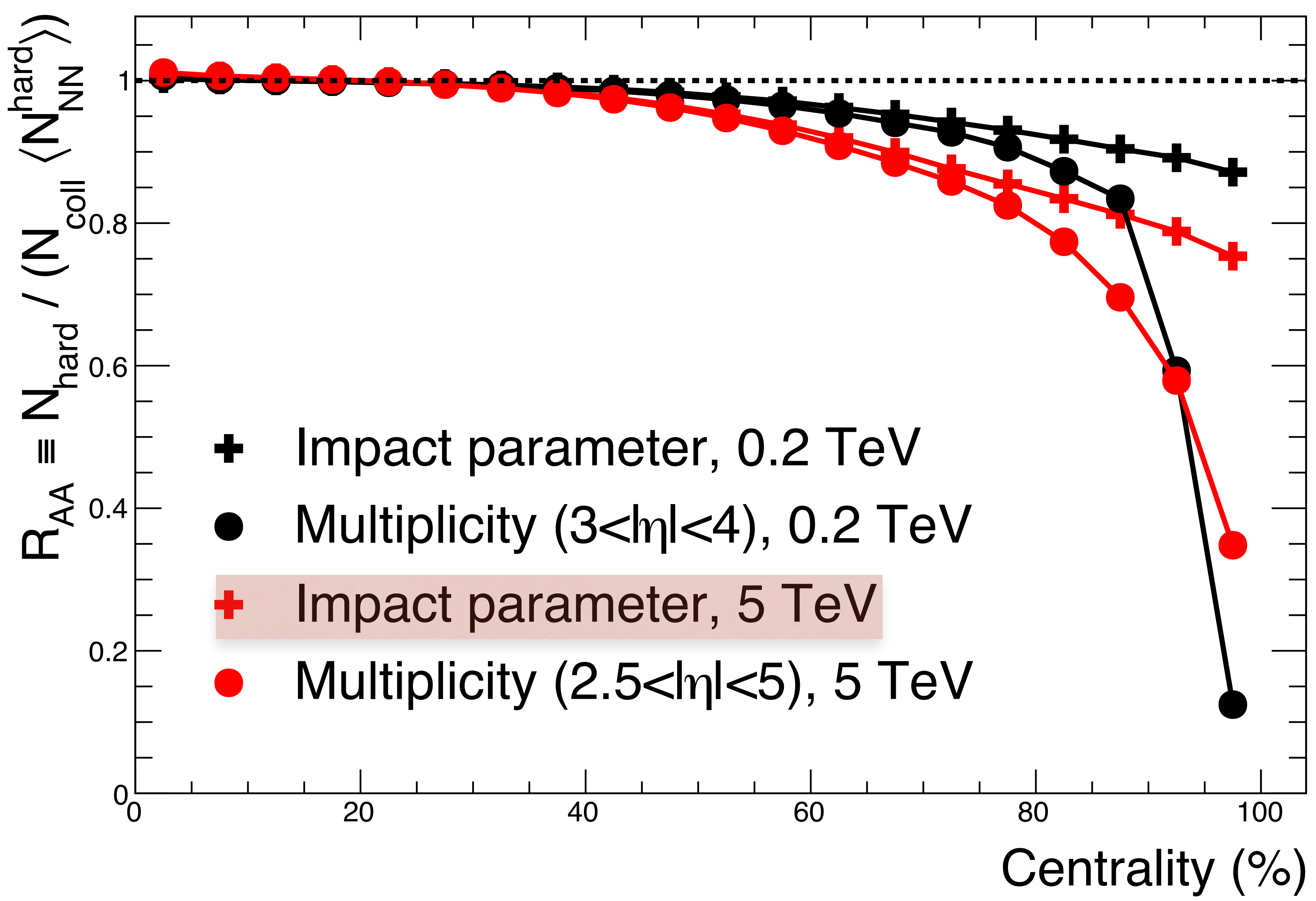

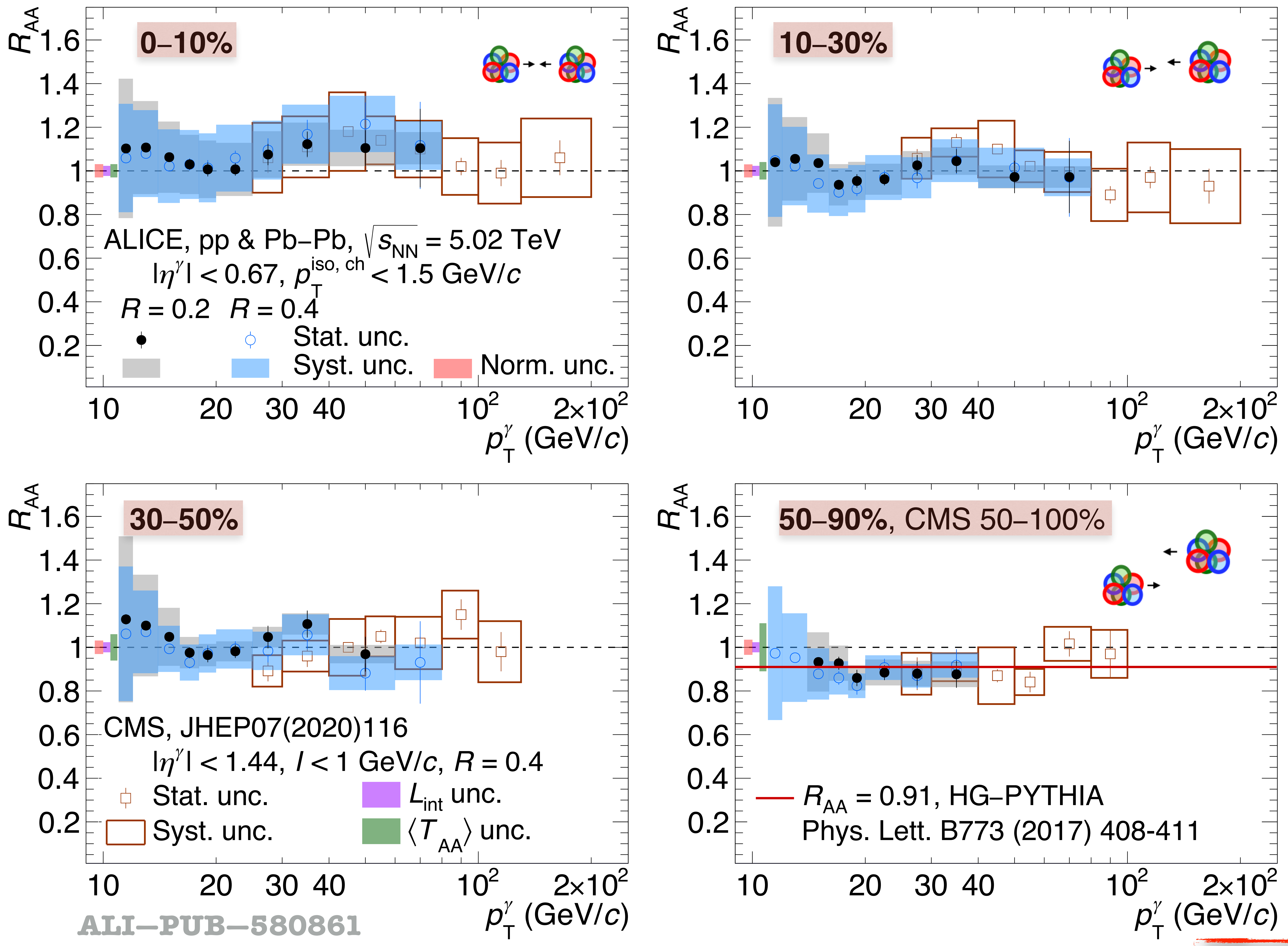

Data over theory, R = 0.4, pp & Pb–Pb at $\sqrt{s_{NN}}$ = 5.02 TeV

ALICE

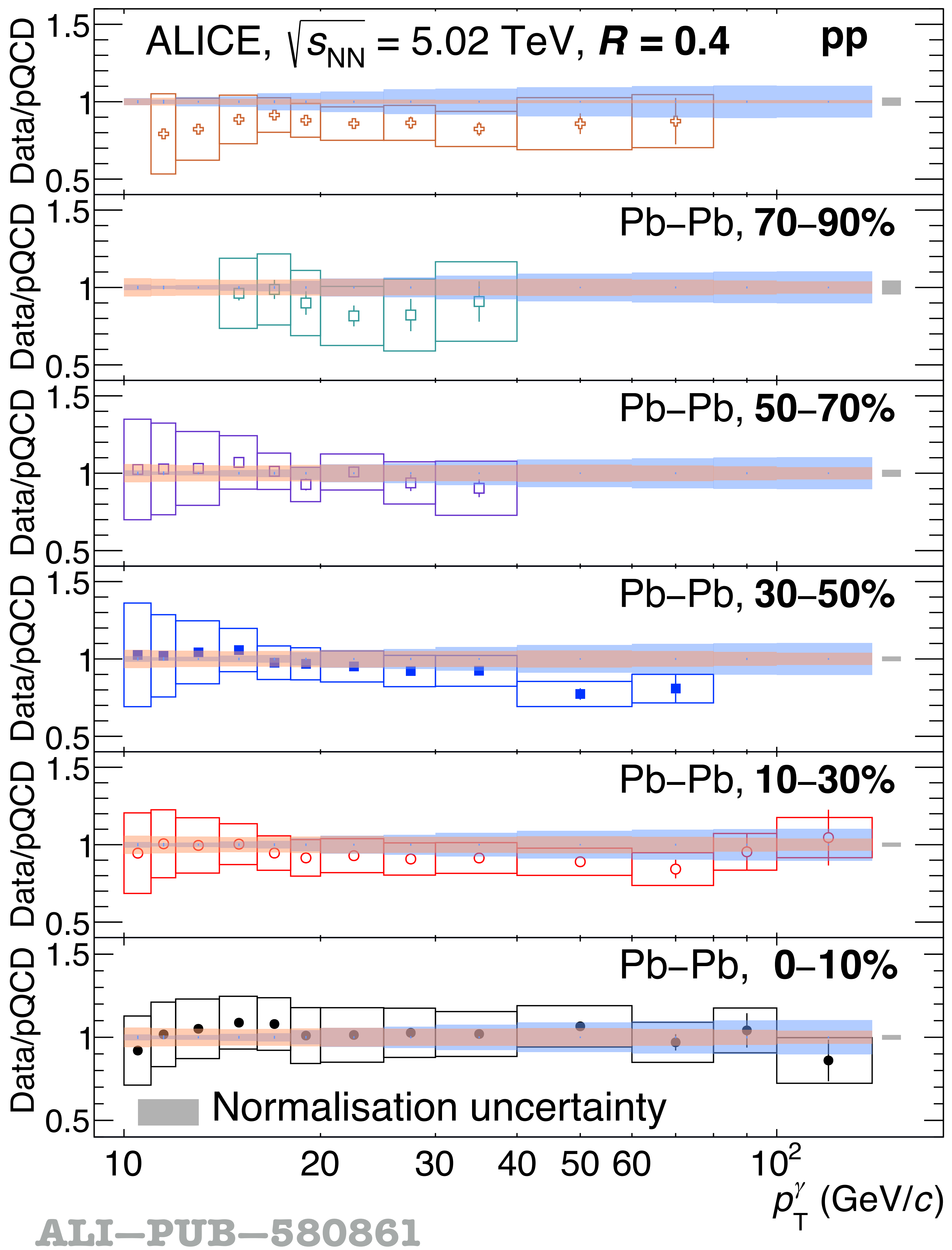

ALI–PUB–580861

CMS

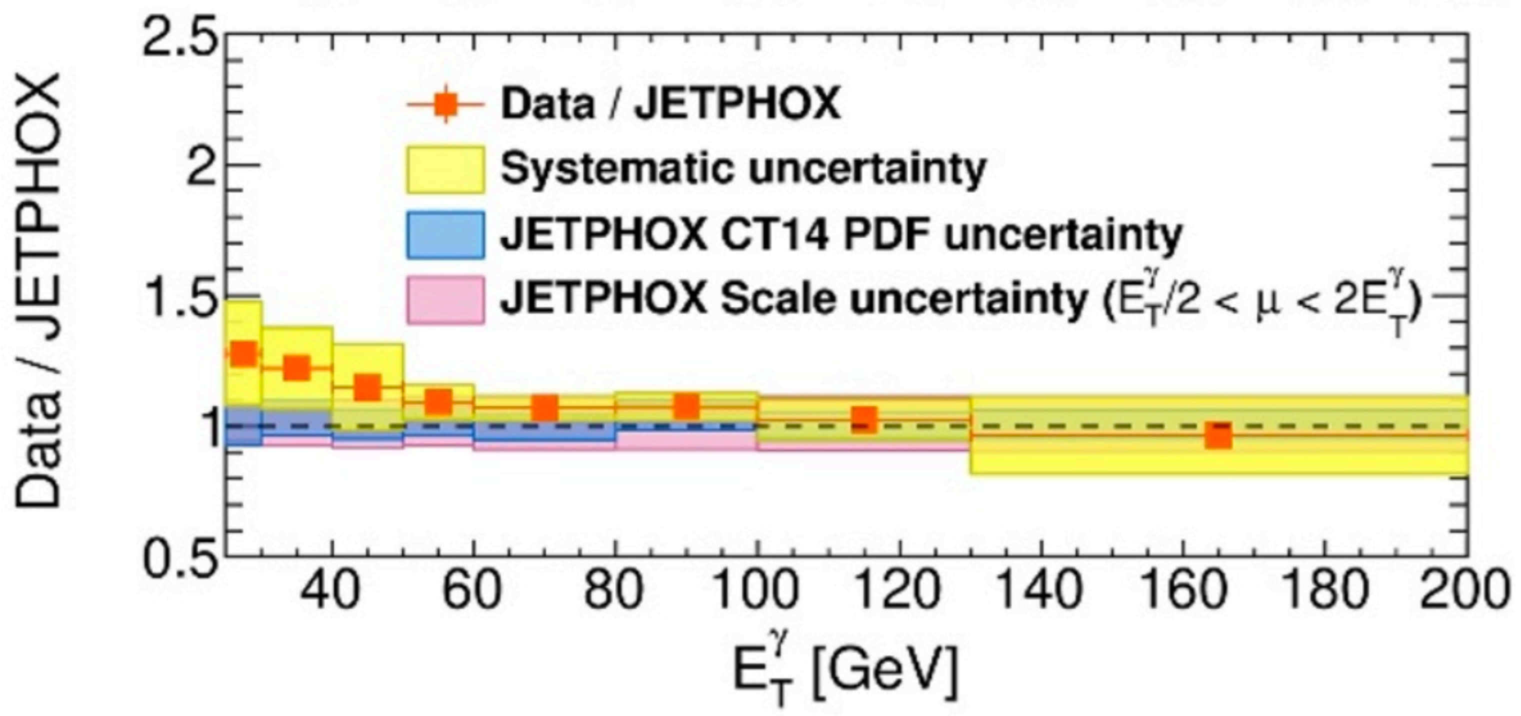

pp

CMS JHEP 07 (2020) 116
arXiv:2003.12797 [hep-ex]

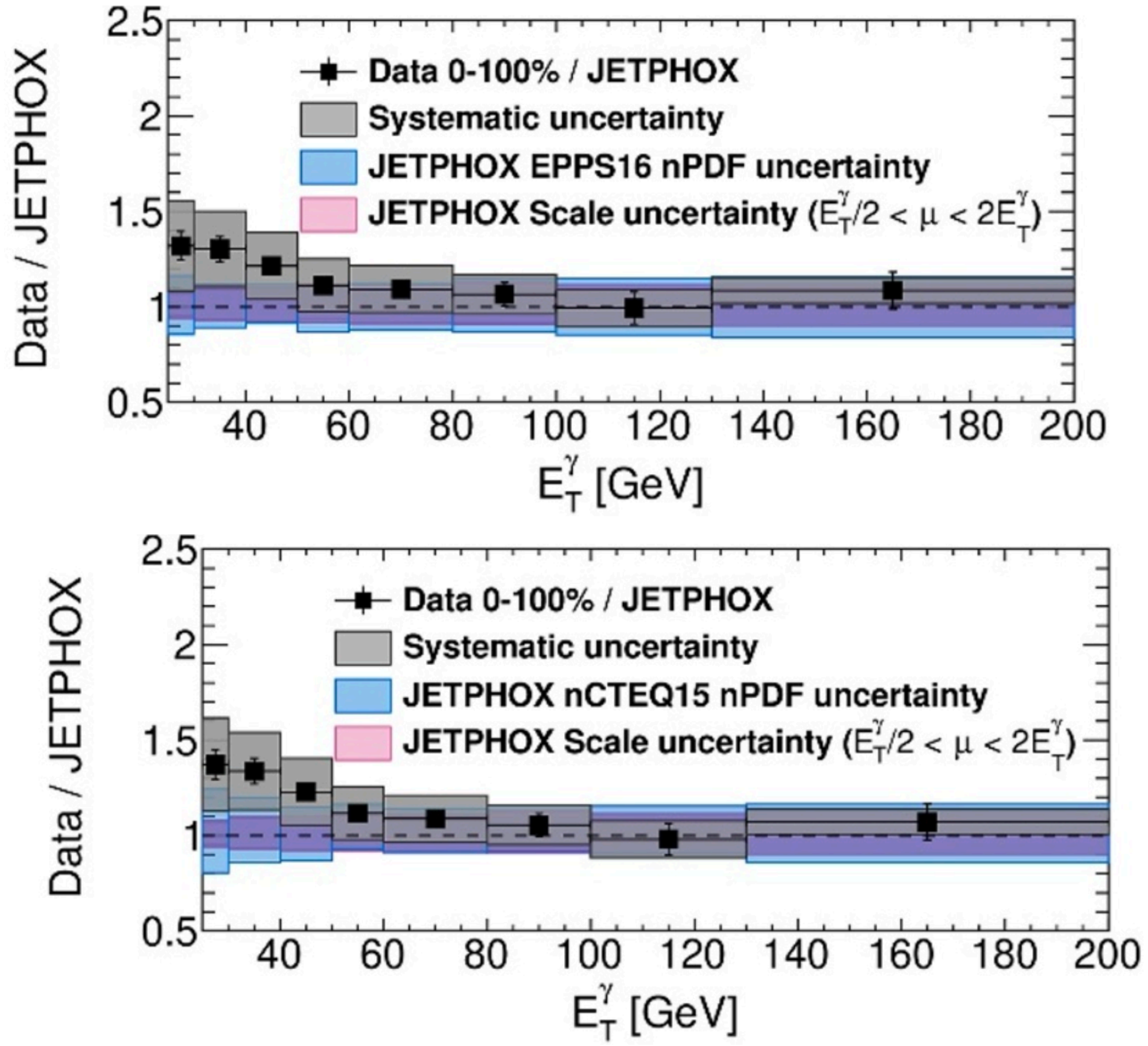

Pb–Pb 0–100%

Nuclear modification factor
pp data denominator replaced by pp NLO pQCD

ALICE-PUBLIC-2024-003

Pb–Pb cross section ratios

$$R_{\mathrm{CSP}} = \frac{\langle N_{\mathrm{coll}}\rangle^{50-70\%}}{\langle N_{\mathrm{coll}}\rangle^{k}} \frac{\mathrm{d}^2\sigma^{\gamma\,\mathrm{iso}}_{\mathrm{Pb-Pb}}/(\mathrm{d}p_{\mathrm{T}}\,\mathrm{d}\eta)|_k}{\mathrm{d}^2\sigma^{\gamma\,\mathrm{iso}}_{\mathrm{Pb-Pb}}/(\mathrm{d}p_{\mathrm{T}}\,\mathrm{d}\eta)|_{50-70\%}}, \qquad R_{\mathrm{CSC}} = \frac{\langle N_{\mathrm{coll}}\rangle^{30-50\%}}{\langle N_{\mathrm{coll}}\rangle^{k}} \frac{\mathrm{d}^2\sigma^{\gamma\,\mathrm{iso}}_{\mathrm{Pb-Pb}}/(\mathrm{d}p_{\mathrm{T}}\,\mathrm{d}\eta)|_k}{\mathrm{d}^2\sigma^{\gamma\,\mathrm{iso}}_{\mathrm{Pb-Pb}}/(\mathrm{d}p_{\mathrm{T}}\,\mathrm{d}\eta)|_{30-50\%}}$$

ALICE-PUBLIC-2024-003

Nuclear modification factor R_{AA}, pp & Pb–Pb at $\sqrt{s_{NN}}$ = 5.02 TeV

ALICE-PUBLIC-2024-003

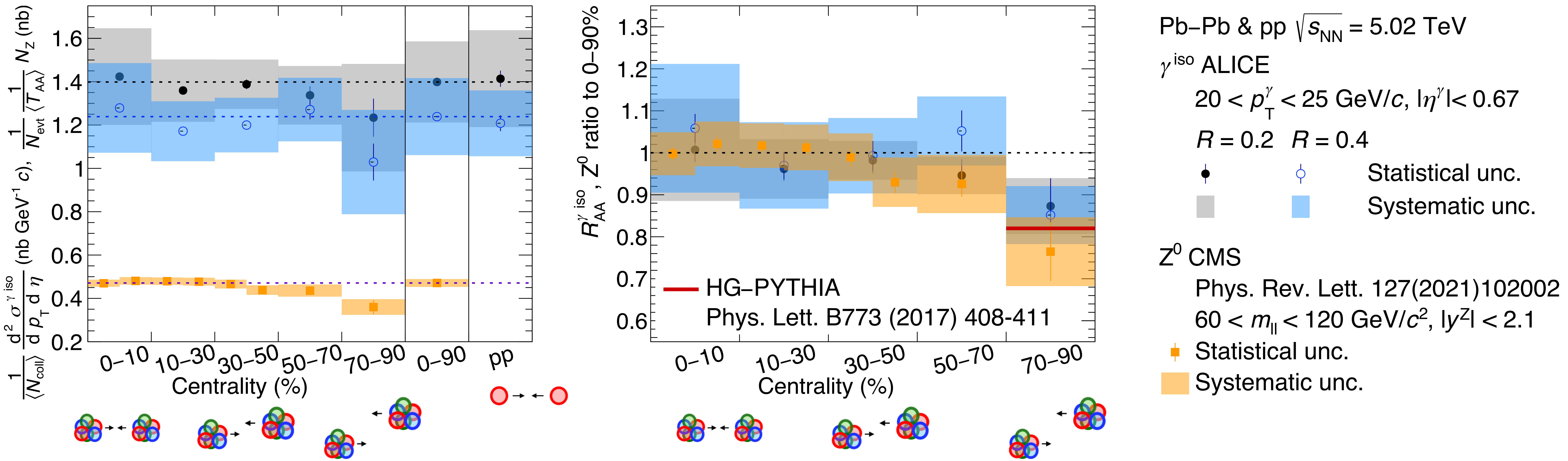

Cross section, pp $\sqrt{s}$ = 7 TeV

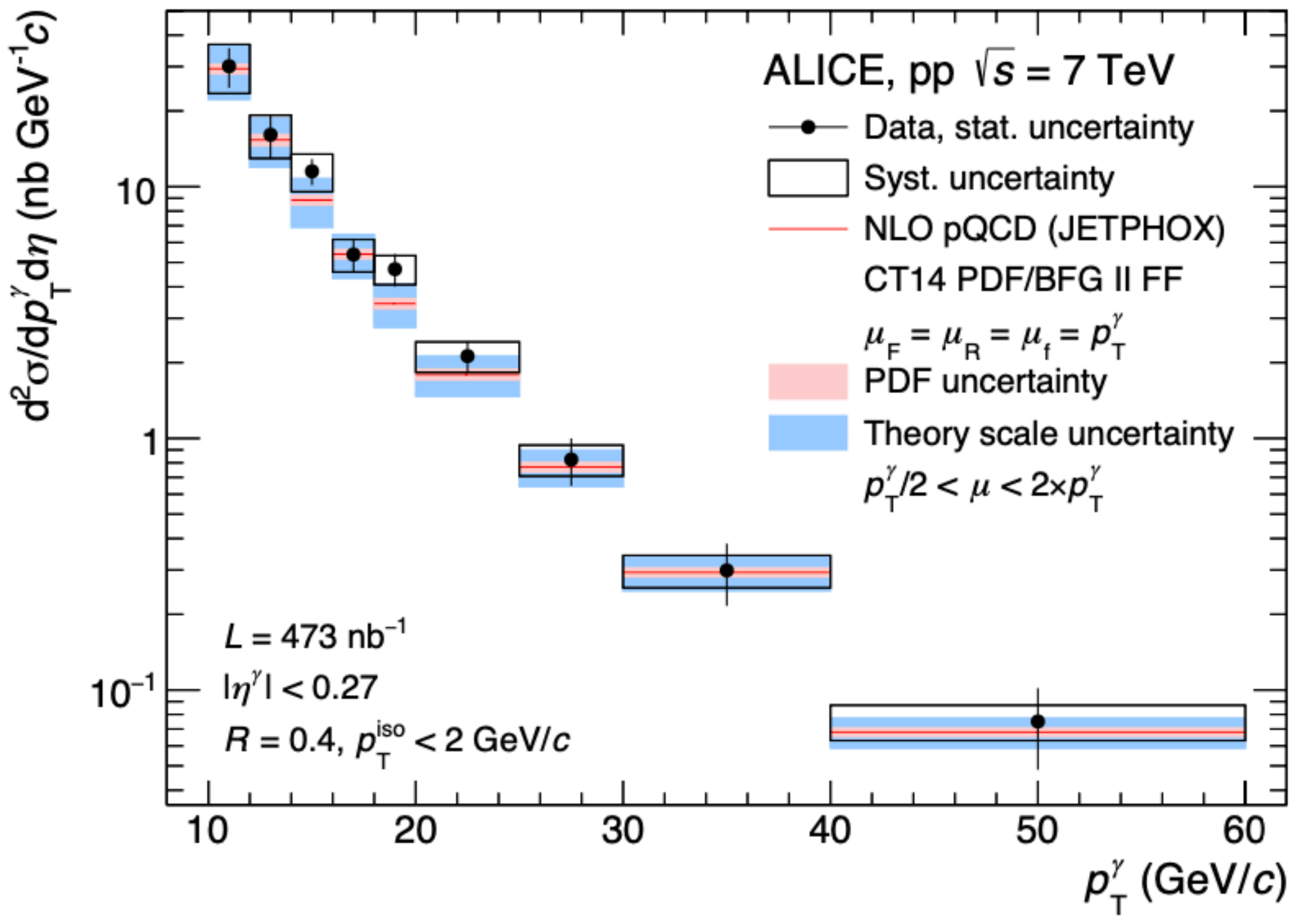

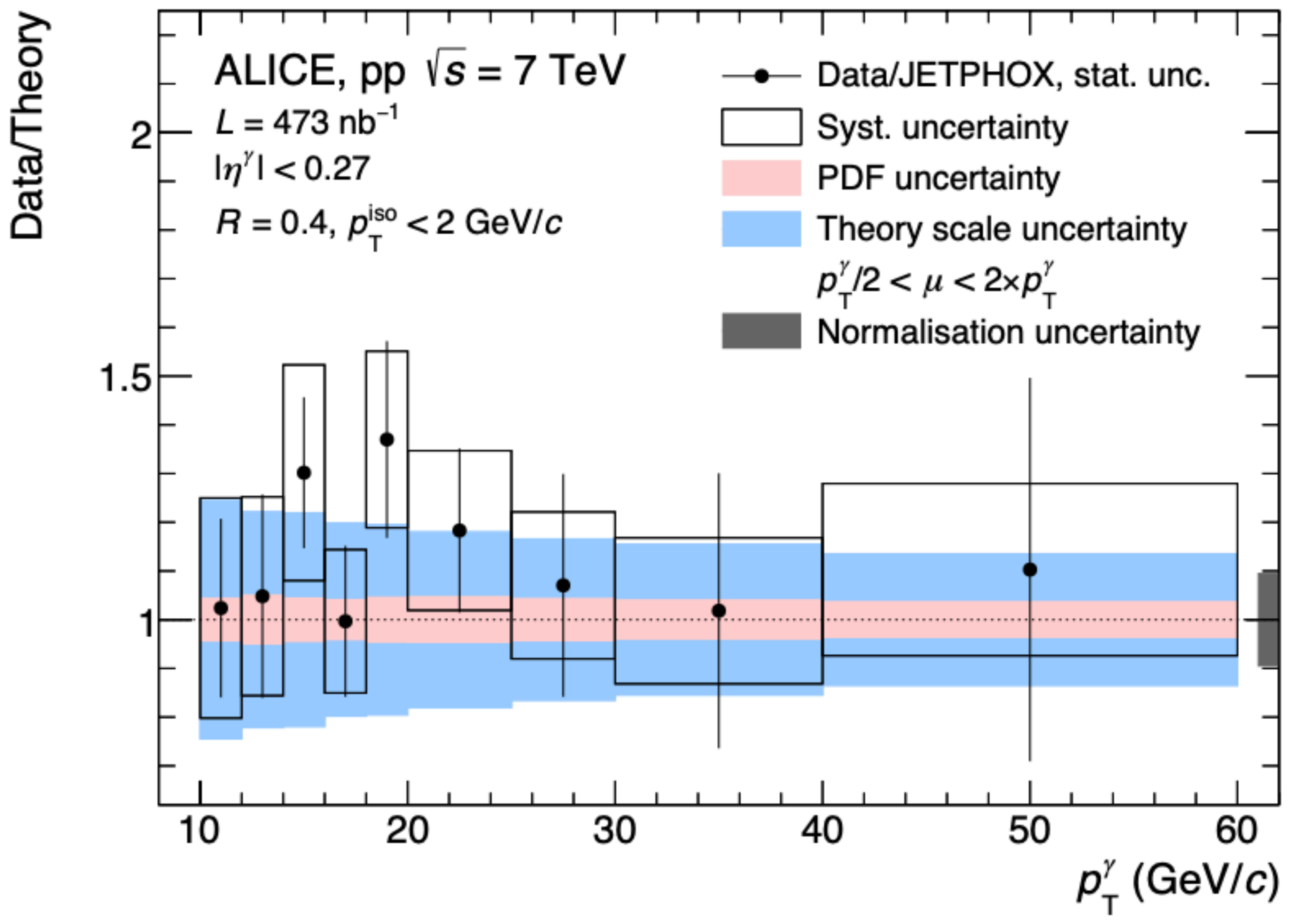

- ➡ arXiv:1906.01371
- ➡ Eur. Phys. J. C 79, 896 (2019)

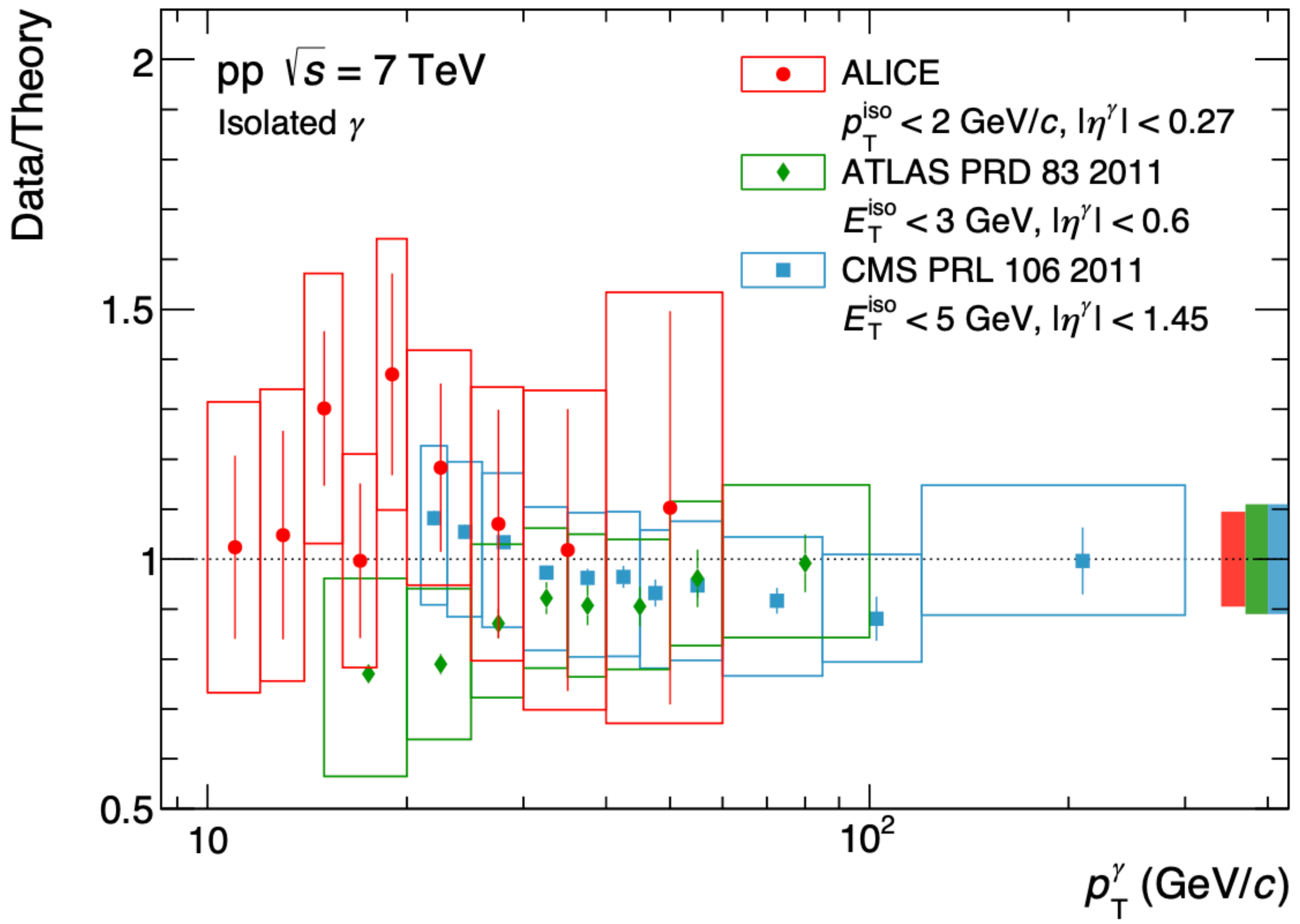

Cross section ratios in pp collisions

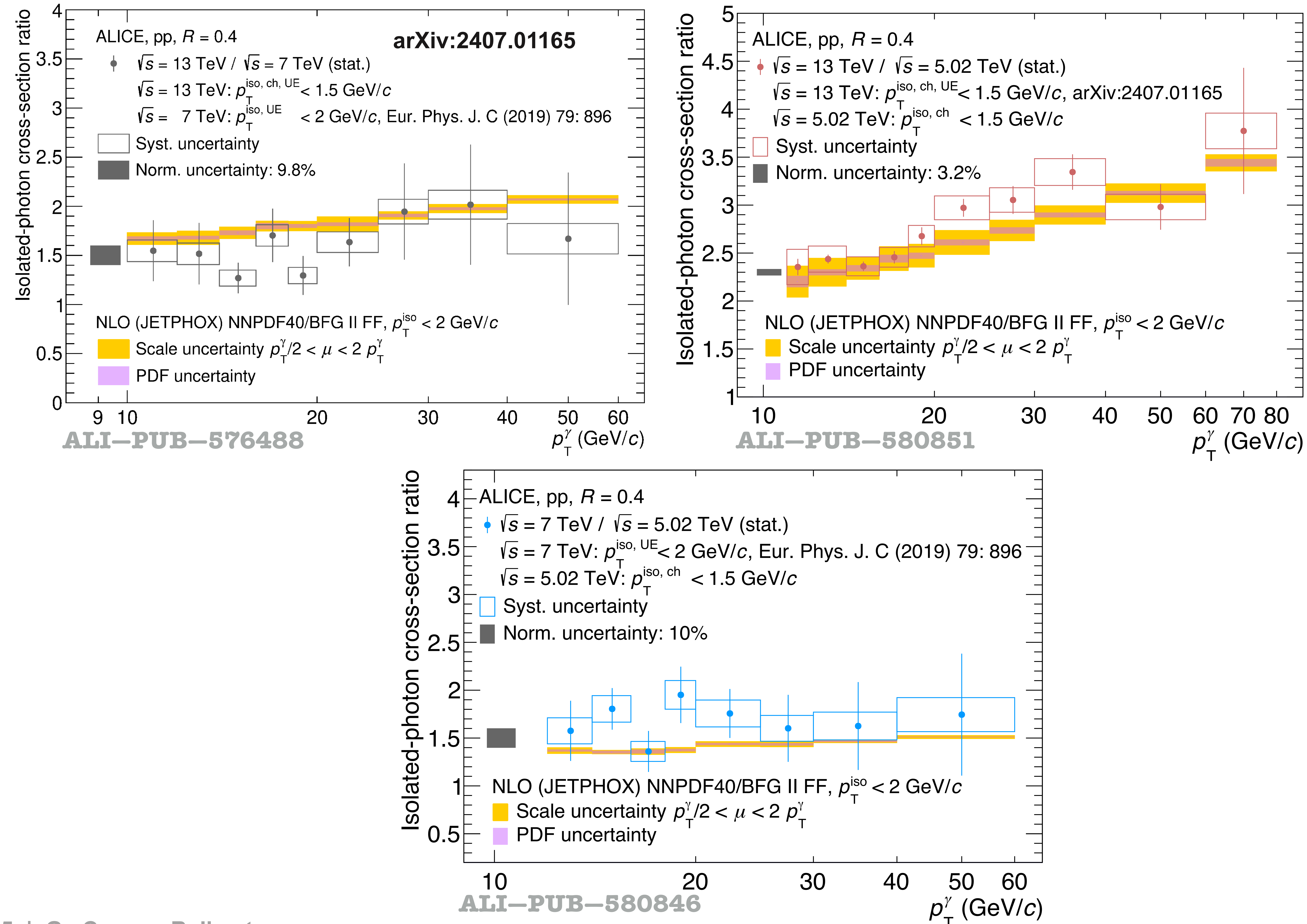

Cross section and purity at different $\sqrt{s}$

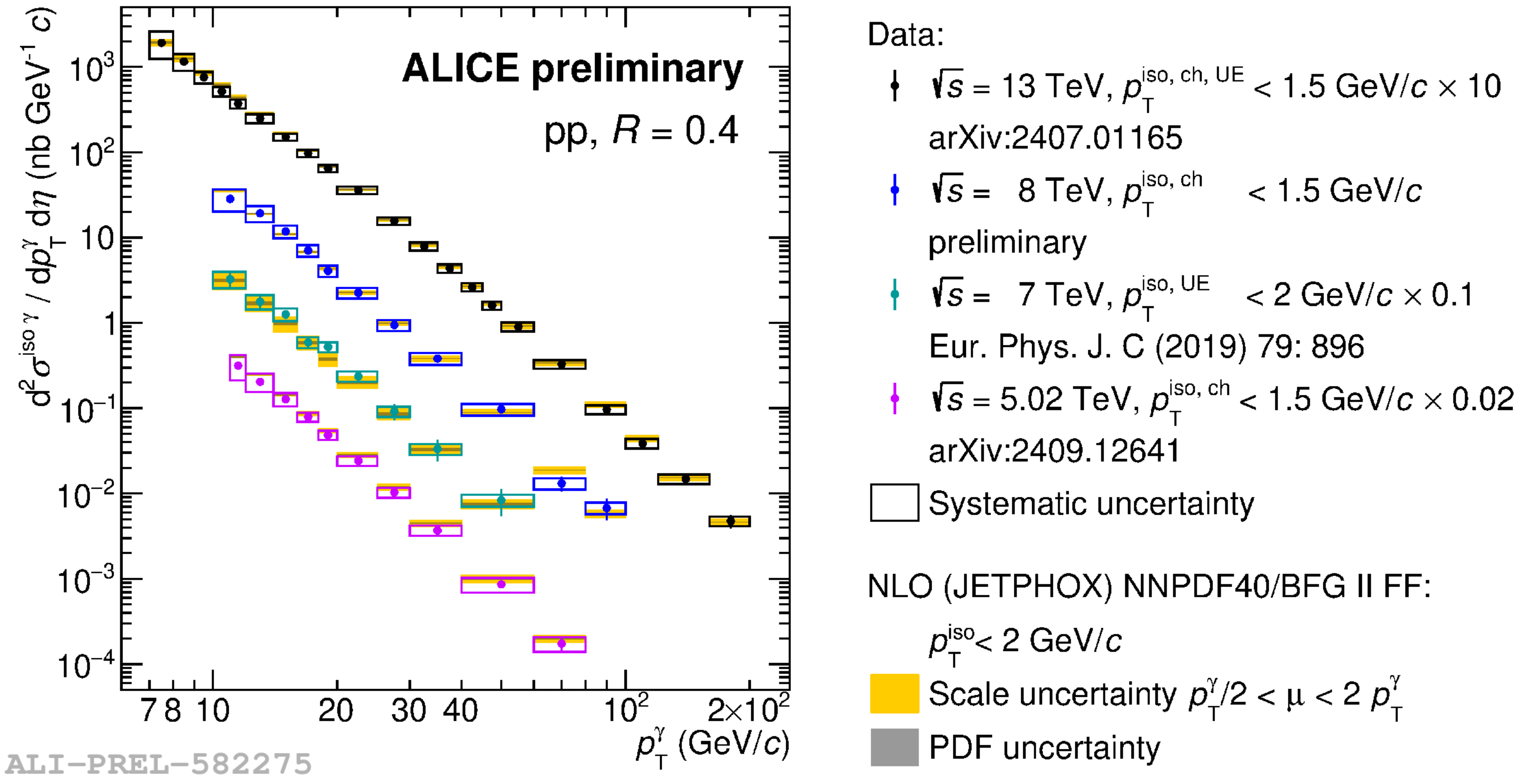

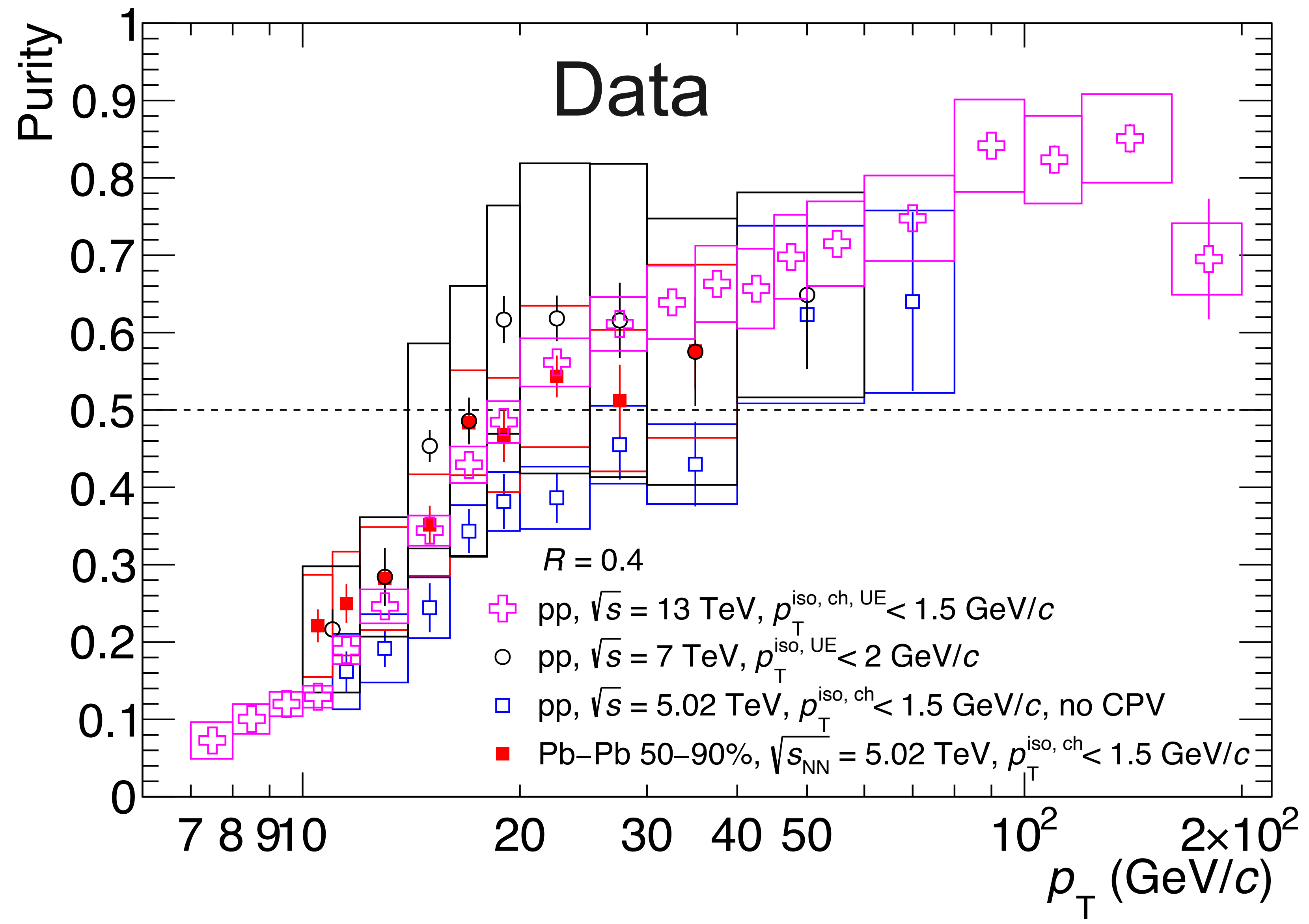

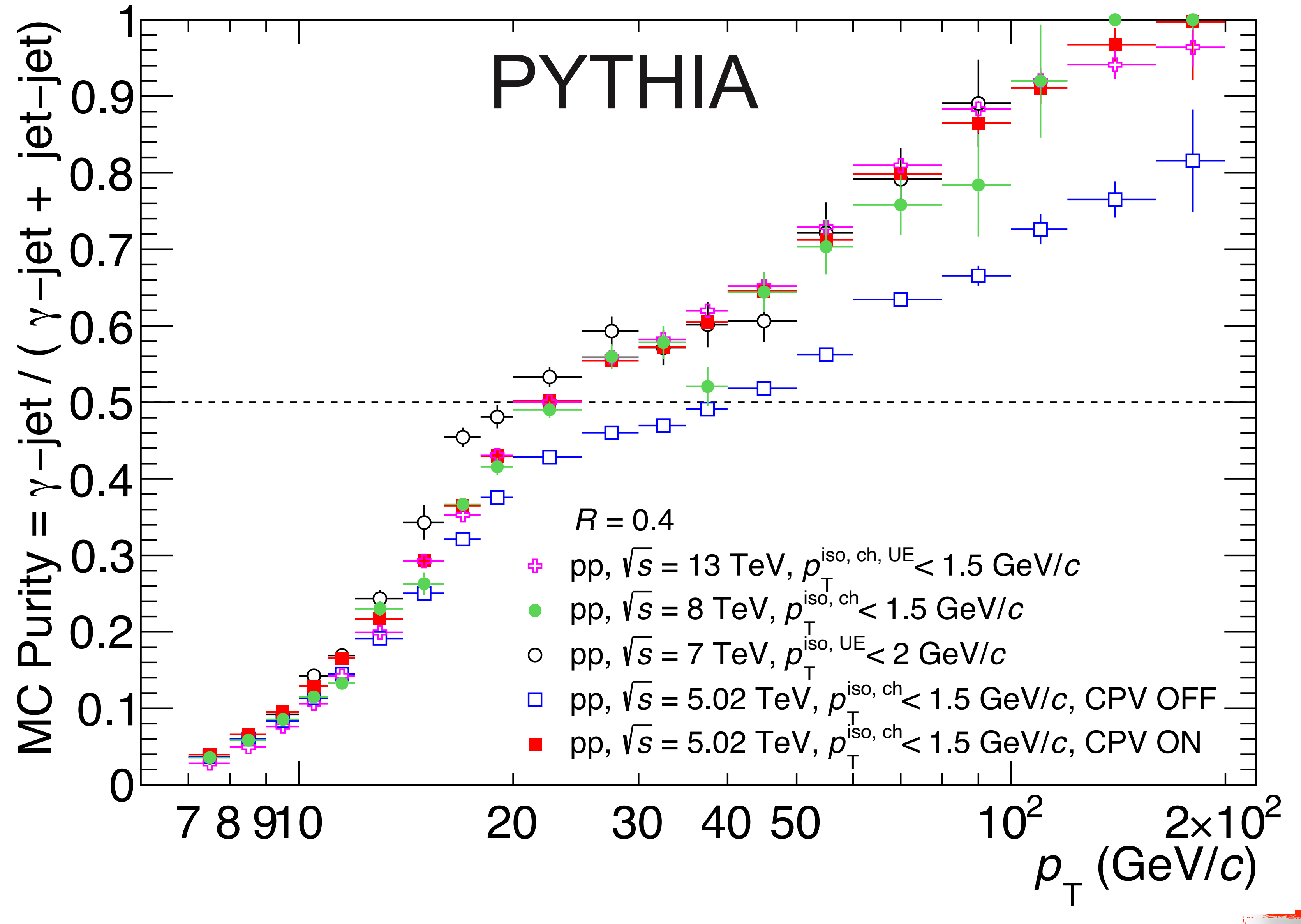

Isolated γ purity in p–Pb collisions, R = 0.4

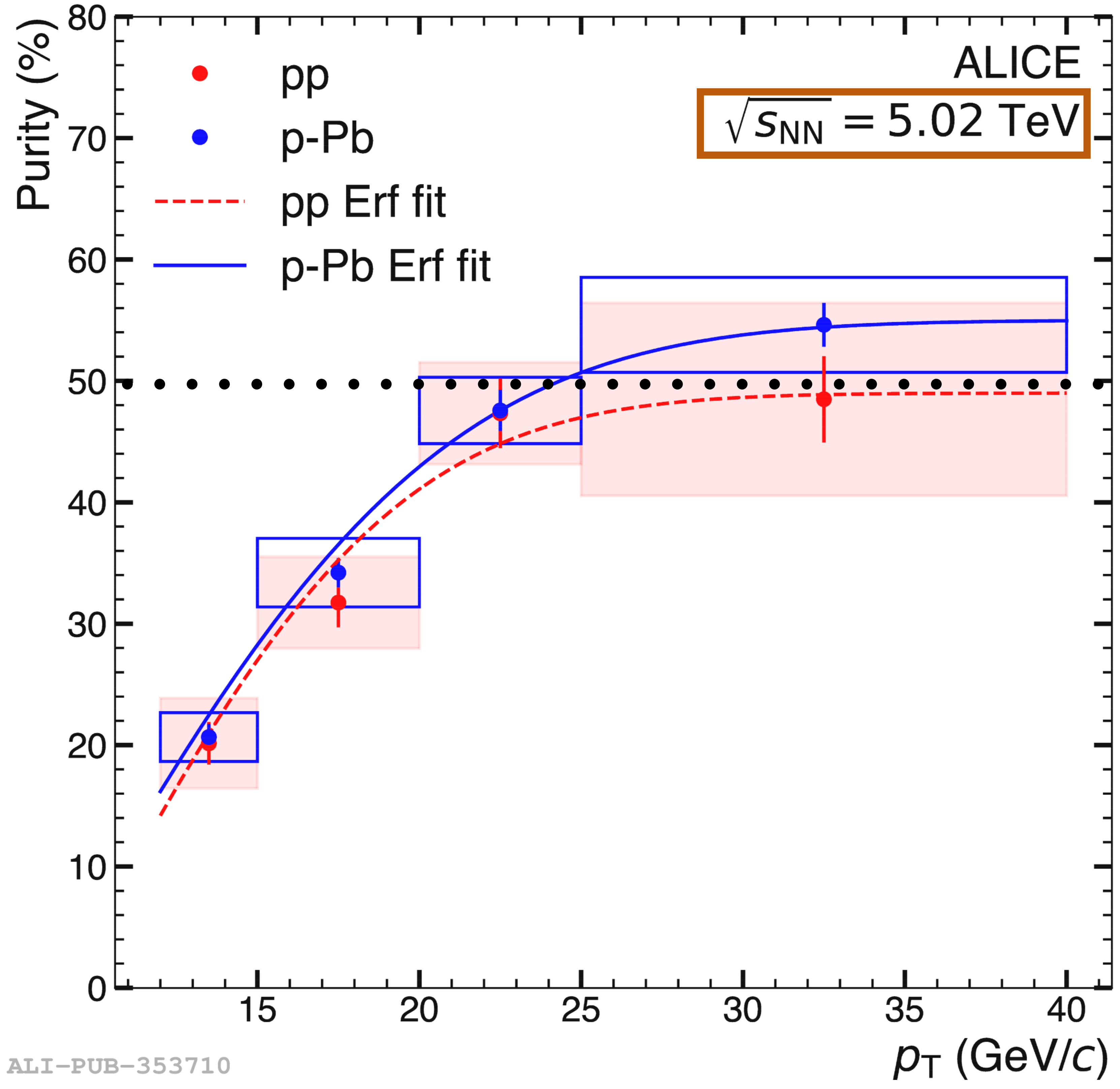

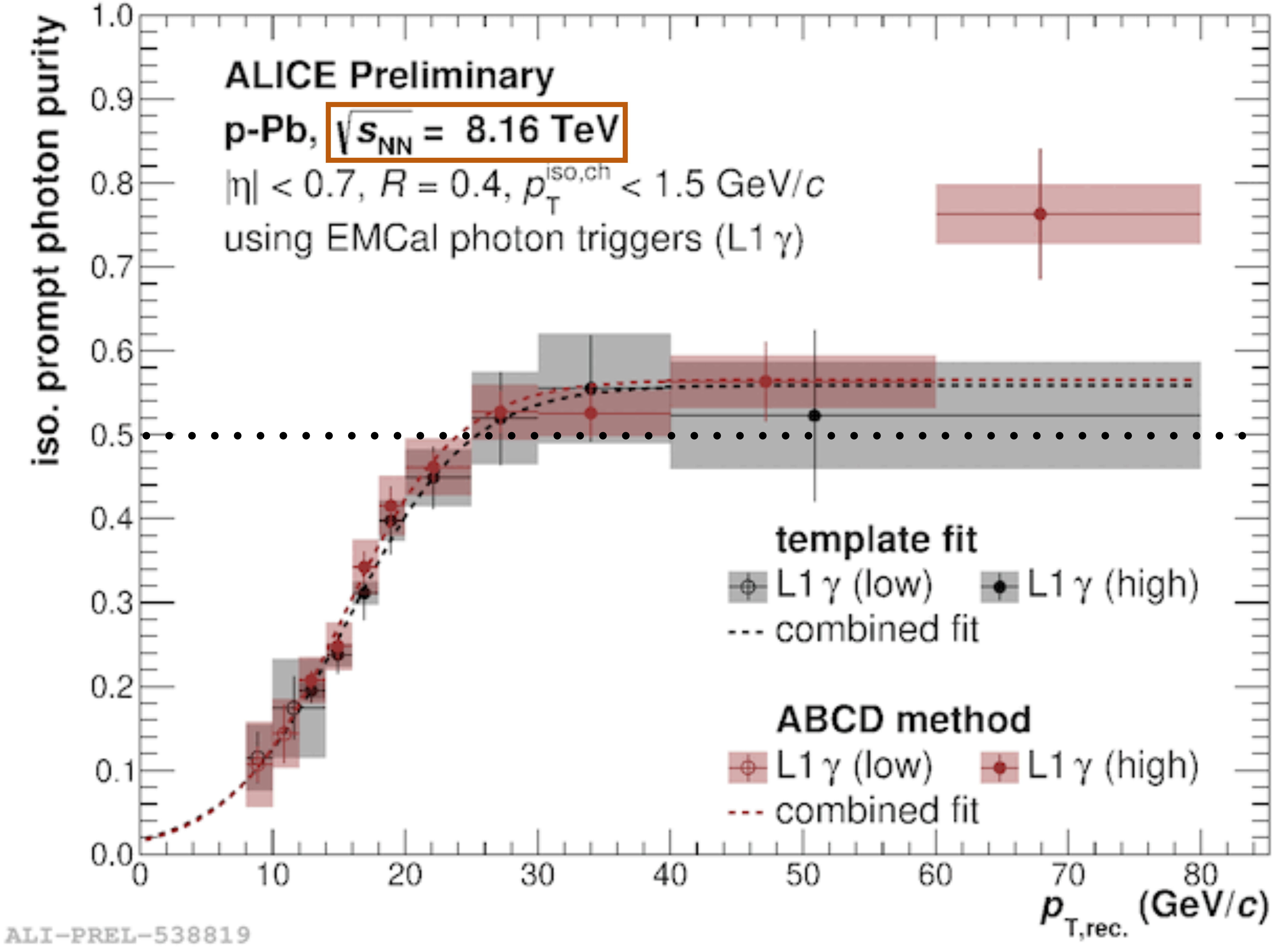

Cross section, p–Pb

Paper in preparation

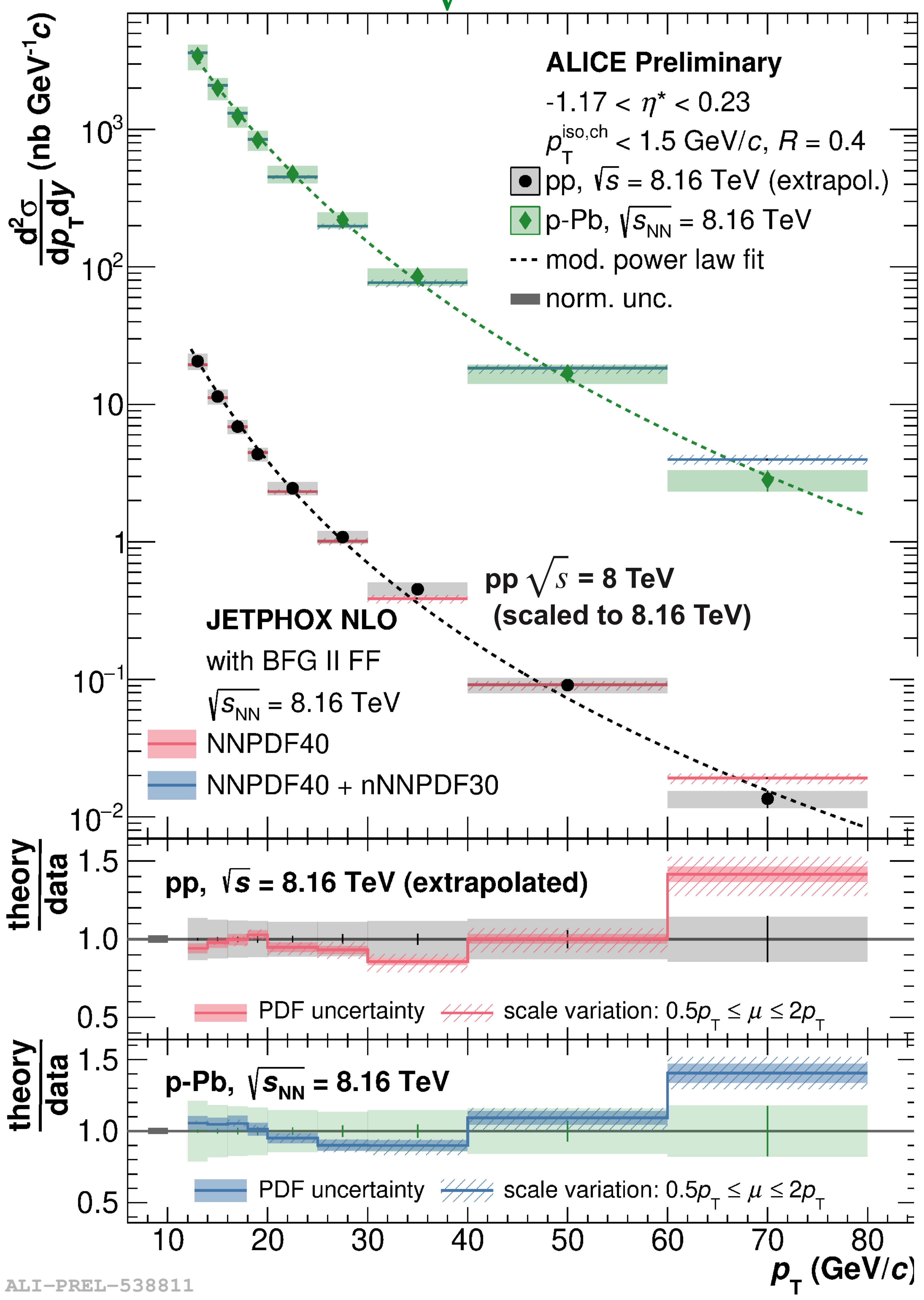

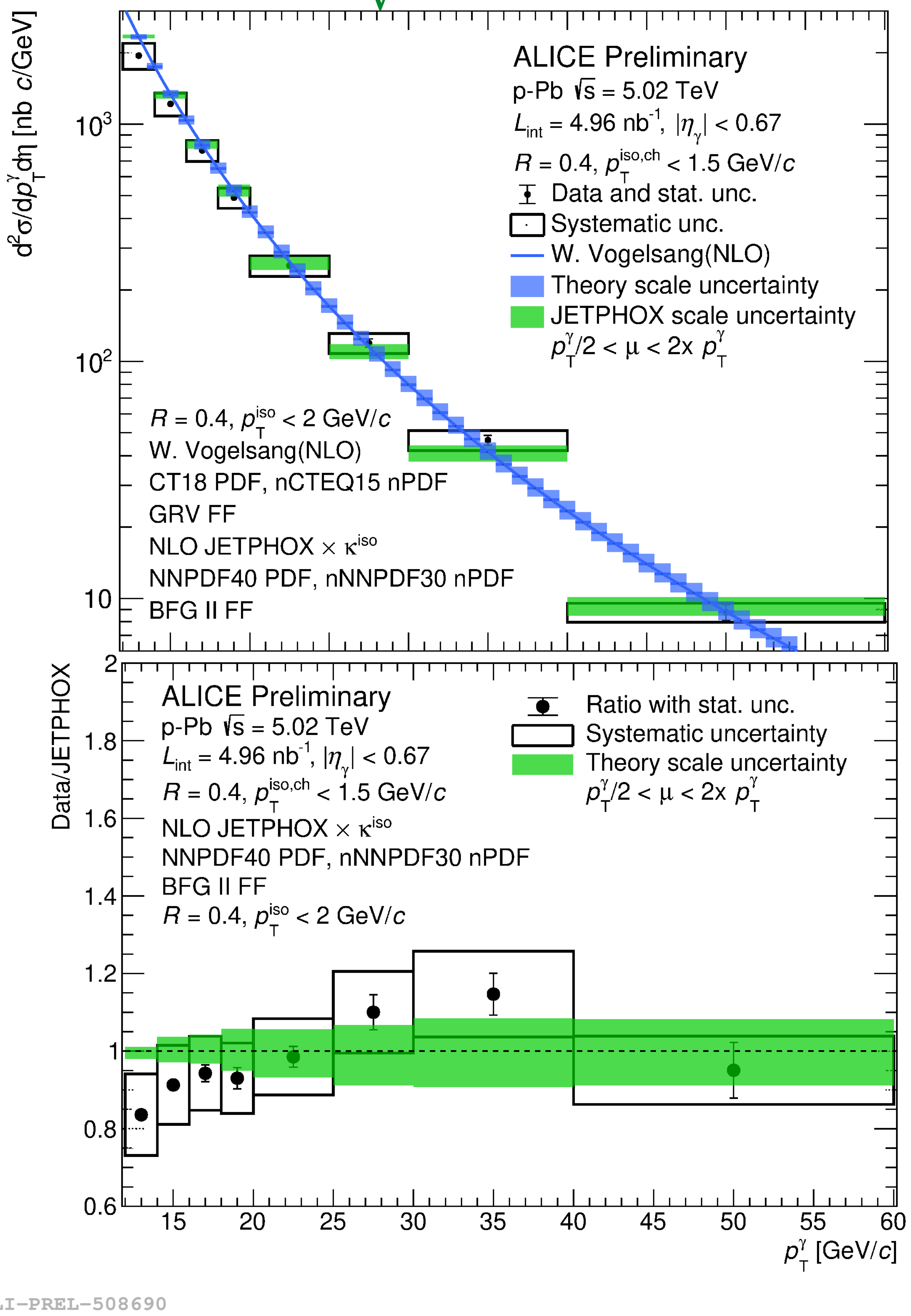

➡ NLO pQCD predictions (JETPHOX) and data agree

Nuclear modification factor R_{pA}

Paper in preparation

ALICE

$$R_{pA} = \frac{d^2\sigma^{\gamma}_{pA}/dp_T\,dy^*}{A_{Pb} \times d^2\sigma^{\gamma}_{pp}/dp_T\,dy^*}$$

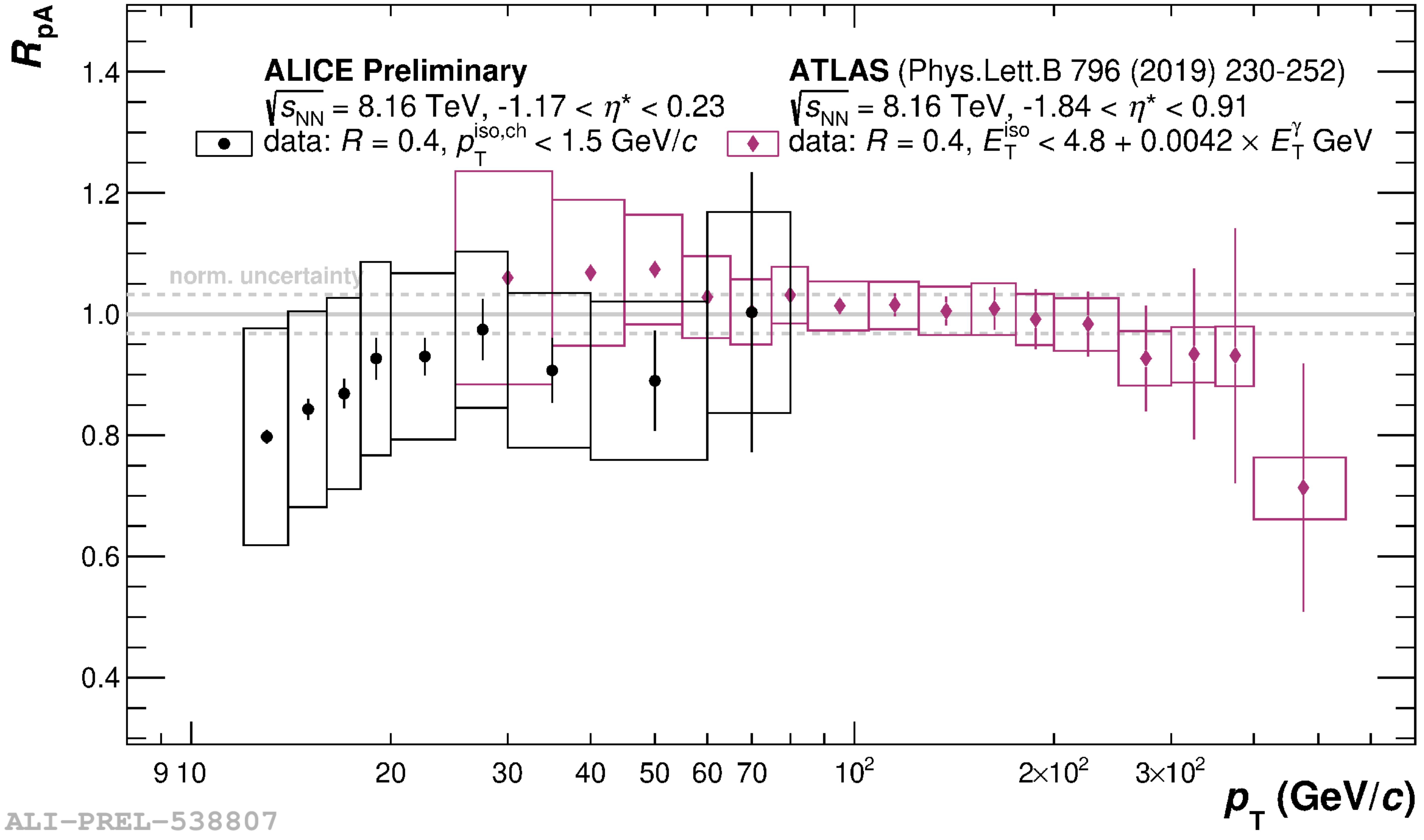

- R_{pA} in agreement with unity
  - No suppression at high p_T, agreement with ATLAS
  - Hints of lower than unity for $p_T < 20$ GeV/c, expected in theory, cold nuclear matter effects, shadowing

Nuclear modification factor R_{pA}

Paper in preparation

$$R_{pA} = \frac{d^2\sigma^{\gamma}_{pA}/dp_T\,dy^*}{A_{Pb} \times d^2\sigma^{\gamma}_{pp}/dp_T\,dy^*}$$

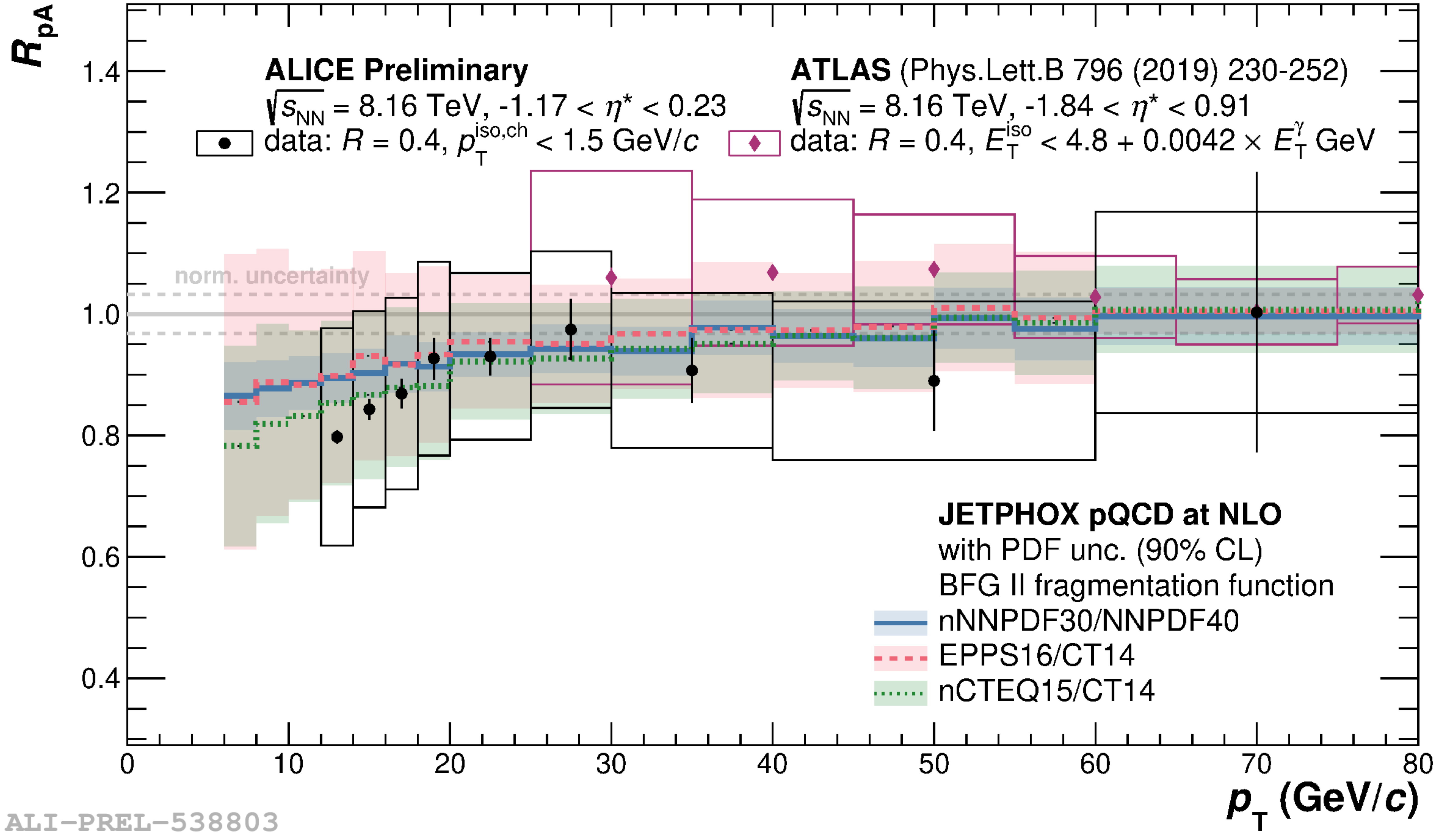

- R_{pA} in agreement with unity
  - No suppression at high p_T, agreement with ATLAS
  - Hints of lower than unity for $p_T < 20$ GeV/c, expected in theory, cold nuclear matter effects, shadowing

EMCal trigger performance, pp $\sqrt{s}$ = 13 TeV

$$RF^{\rm trig}_{\varepsilon_{\rm trig}} = \frac{1}{\varepsilon^{\rm clus}_{\rm trig}} \frac{1/N^{\rm L1\text{-}\gamma}_{\rm evt} \times {\rm d}N^{\rm L1\text{-}\gamma}/{\rm d}p_T}{1/N^{\rm MB}_{\rm evt} \times {\rm d}N^{\rm MB}/{\rm d}p_T}$$

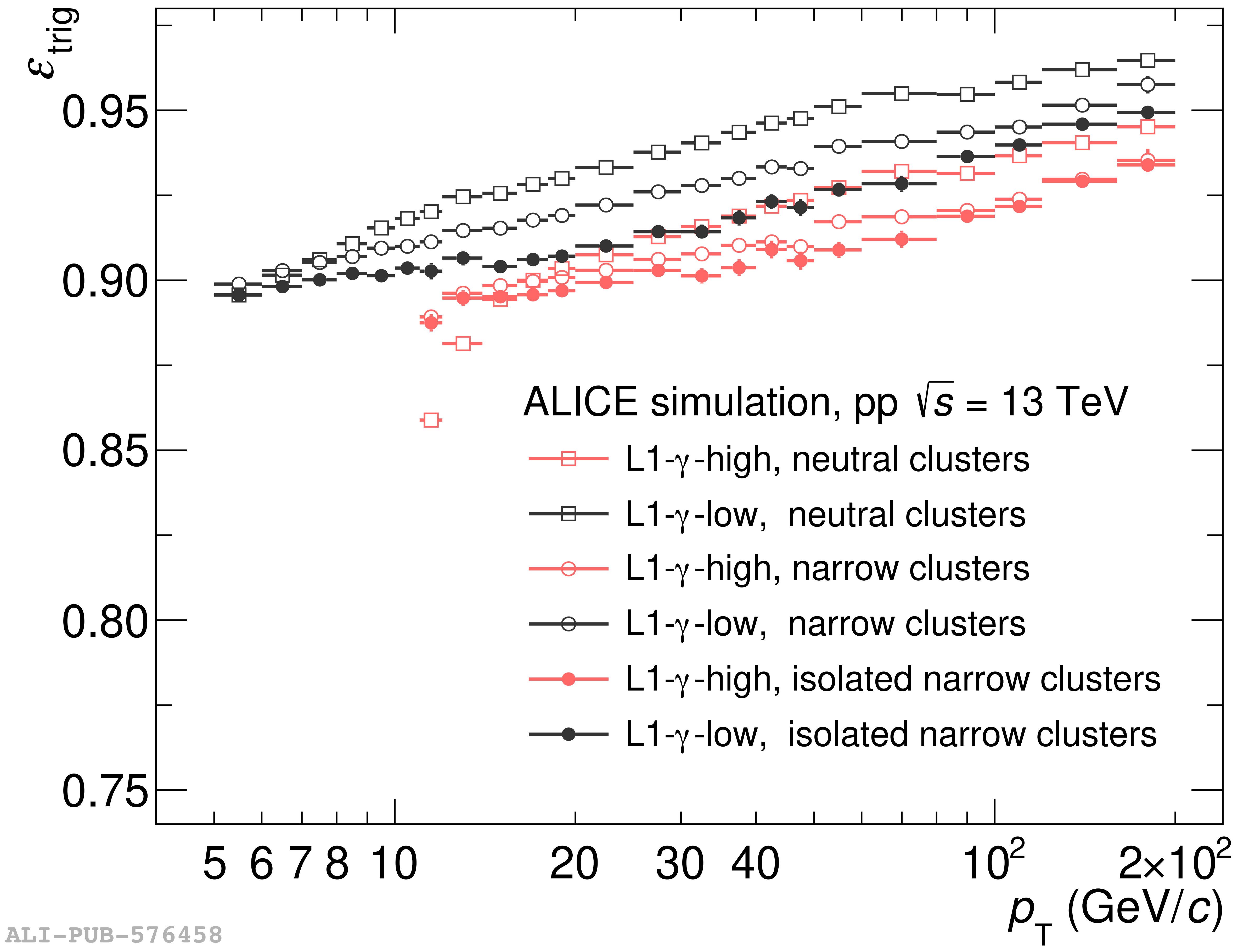

ALI-PUB-576458

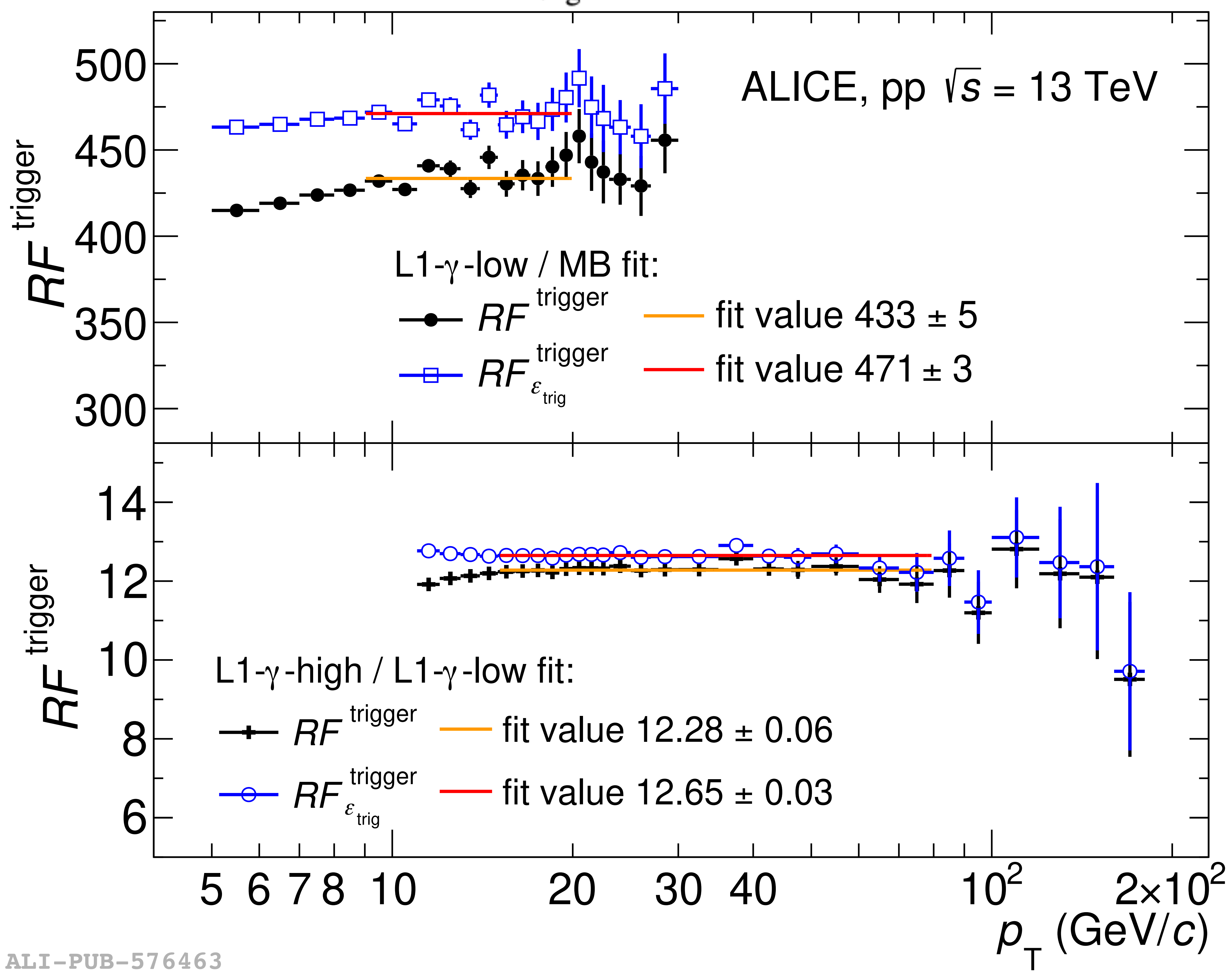

ALI-PUB-576463

EMCal trigger performance, pp & Pb–Pb $\sqrt{s_{NN}}$ = 5.02 TeV

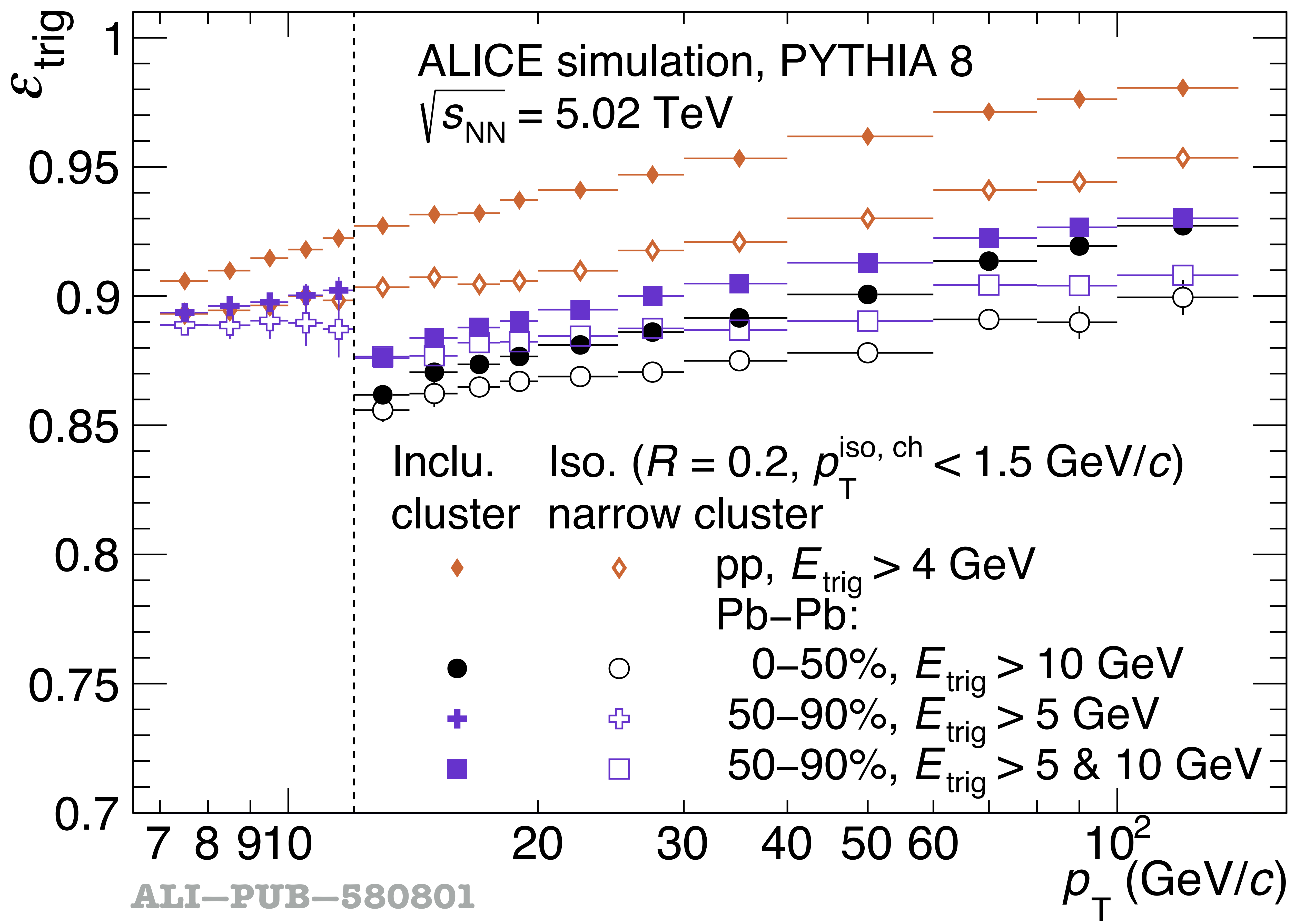

$$RF^{trig}_{\varepsilon_{trig}} = \frac{1}{\varepsilon^{clus}_{trig}} \frac{1/N^{L1-\gamma}_{evt} \times dN^{L1-\gamma}/dp_T}{1/N^{MB}_{evt} \times dN^{MB}/dp_T}$$

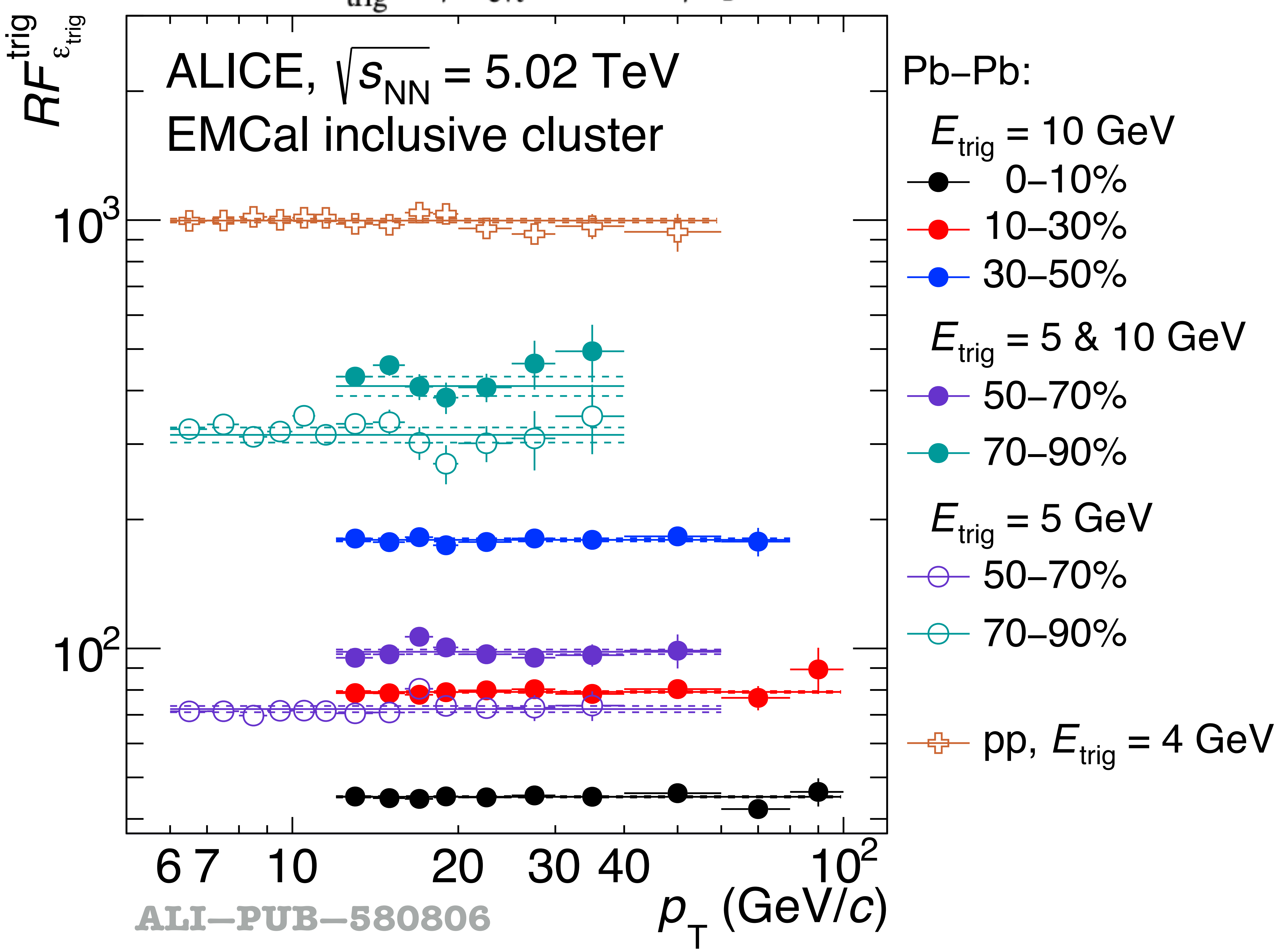

EMCal cluster shower lateral dispersion parameter

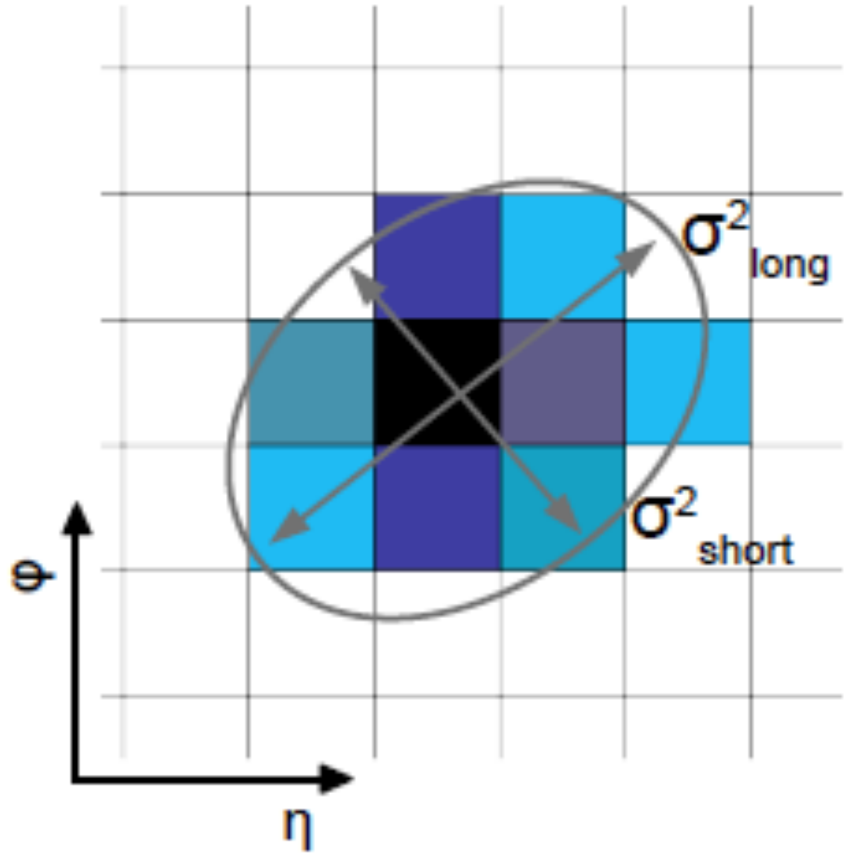

- Shower shape parameter σ^2_{long} is related to the longer axis of the cluster ellipse
- Parameter depends on cluster cells location and its energy

$$w_i = \text{Maximum}(0, w_0 + \ln(E_{\text{cell},\ i}/E))$$

$$\sigma^2_{\alpha\beta} = \sum_i \frac{w_i \alpha_i \beta_i}{w_{\text{tot}}} - \sum_i \frac{w_i \alpha_i}{w_{\text{tot}}} \sum_i \frac{w_i \beta_i}{w_{\text{tot}}}$$

$$w_{\text{tot}} = \sum_i w_i,$$

$$\sigma^2_{\text{long}} = 0.5(\sigma^2_{\varphi\varphi} + \sigma^2_{\eta\eta}) + \sqrt{0.25(\sigma^2_{\varphi\varphi} - \sigma^2_{\eta\eta})^2 + \sigma^2_{\eta\varphi}},$$

$$\sigma^2_{\text{short}} = 0.5(\sigma^2_{\varphi\varphi} + \sigma^2_{\eta\eta}) - \sqrt{0.25(\sigma^2_{\varphi\varphi} - \sigma^2_{\eta\eta})^2 + \sigma^2_{\eta\varphi}},$$

- V2 clusters: Used in pp & Pb–Pb at $\sqrt{s_{\text{NN}}}$ = 5.02 TeV to get *E* and position
  - In other pp and p–Pb measurements V1 clusters are used
- For the σ^2_{long} calculation: consider the neighbour cells around the highest energy cell in a 5x5 fixed window
  - Increase meson decay merging but limiting UE merging

ALICE-PUBLIC-2024-003

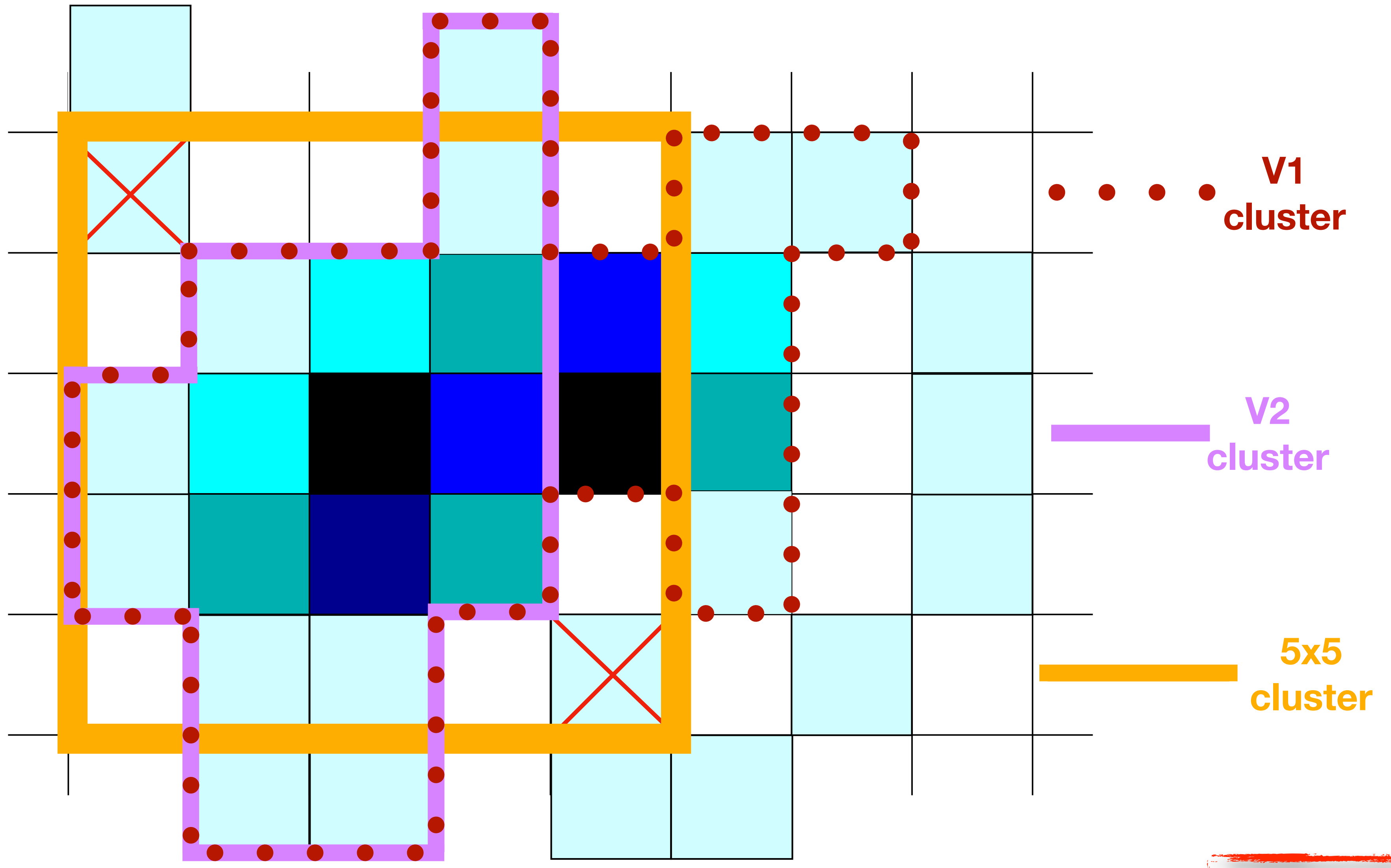

EMCal cluster shower shape, pp & Pb–Pb $\sqrt{s_{NN}}$ = 5.02 TeV

ALICE-PUBLIC-2024-003

EMCal cluster shower shape, pp $\sqrt{s}$ = 13 TeV

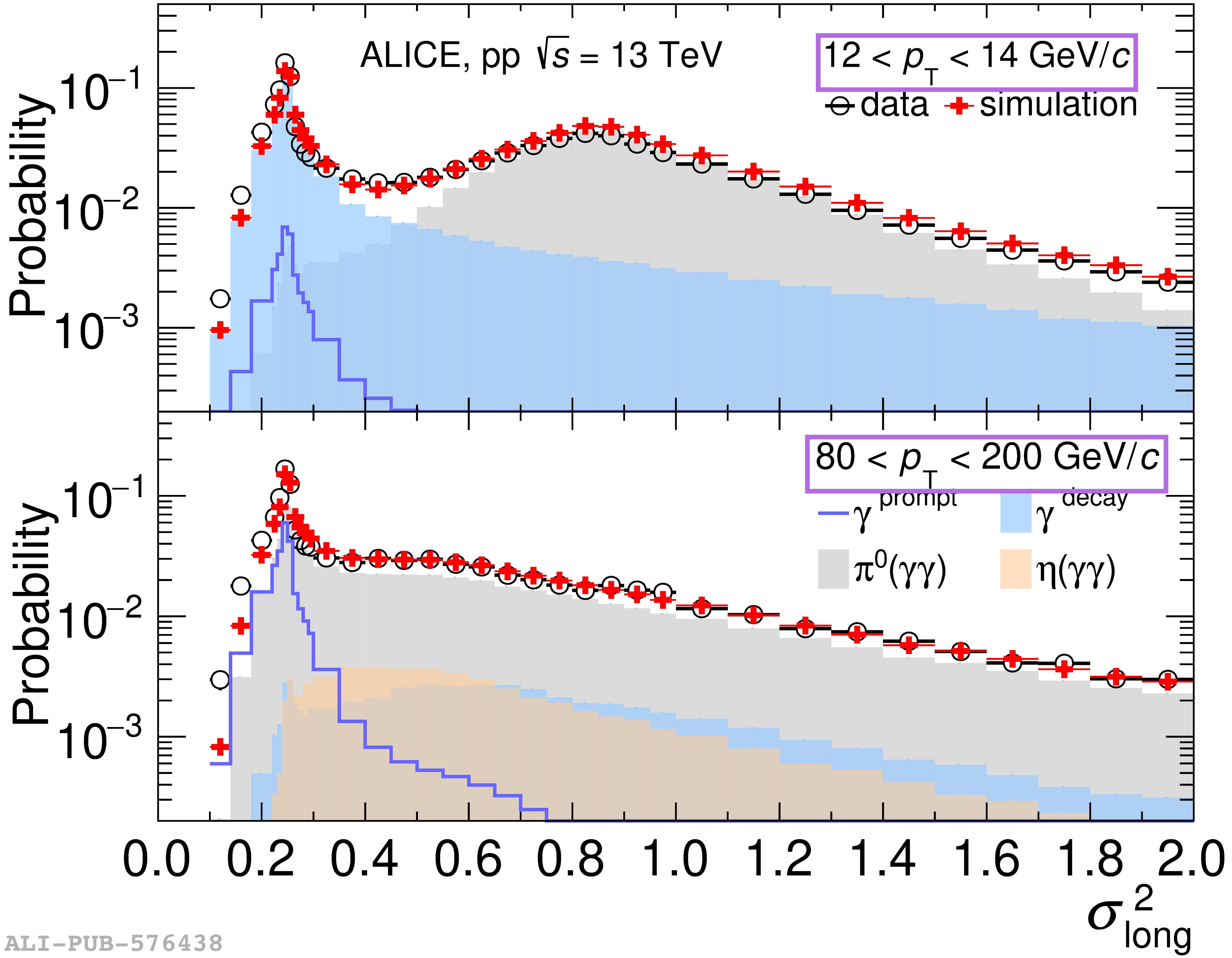

ALI-PUB-576438

EMCal cluster shower shape, pp & Pb–Pb $\sqrt{s_{NN}}$ = 5.02 TeV

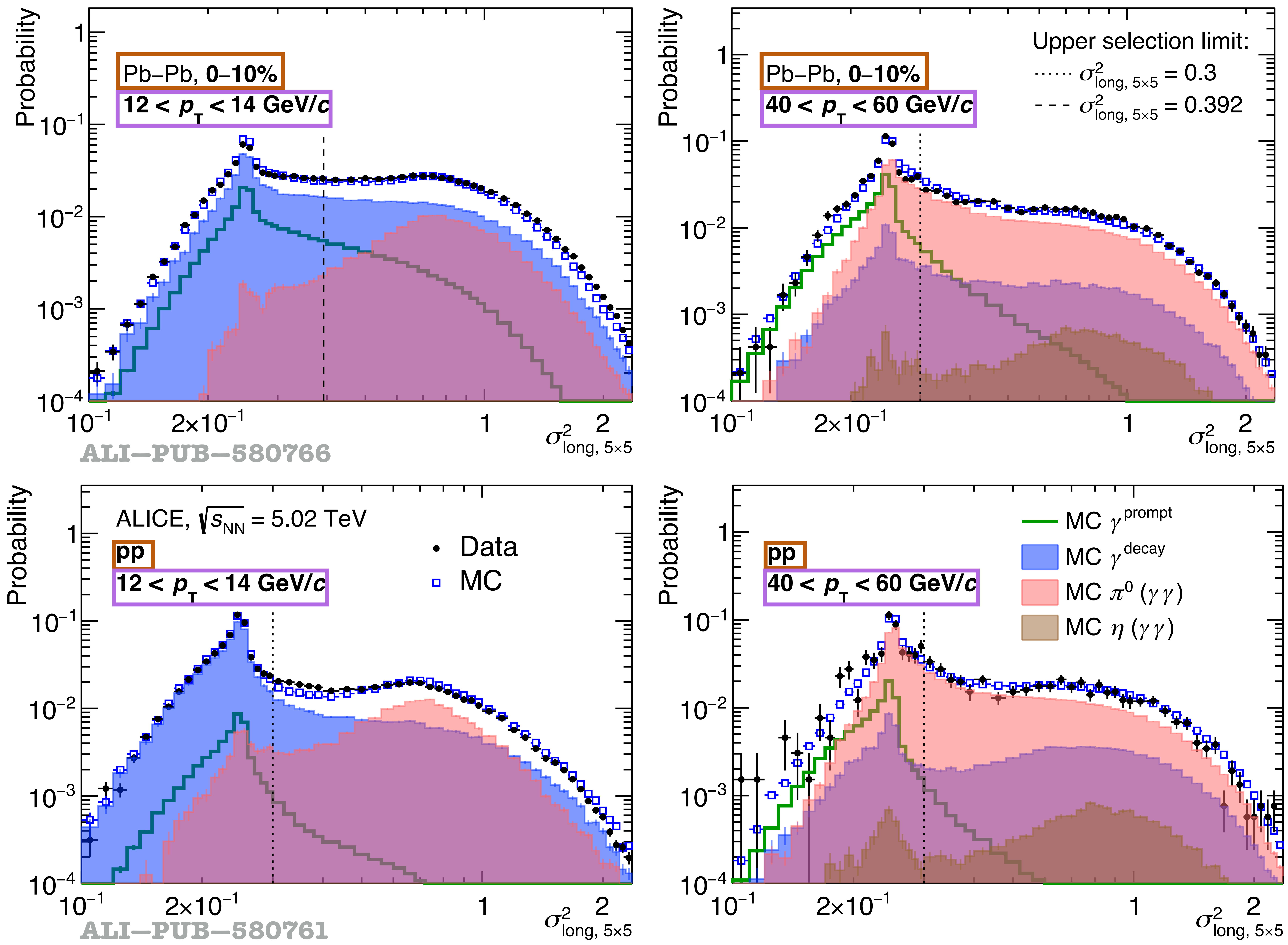

ABCD regions, R = 0.2, pp & Pb–Pb $\sqrt{s_{NN}}$ = 5.02 TeV

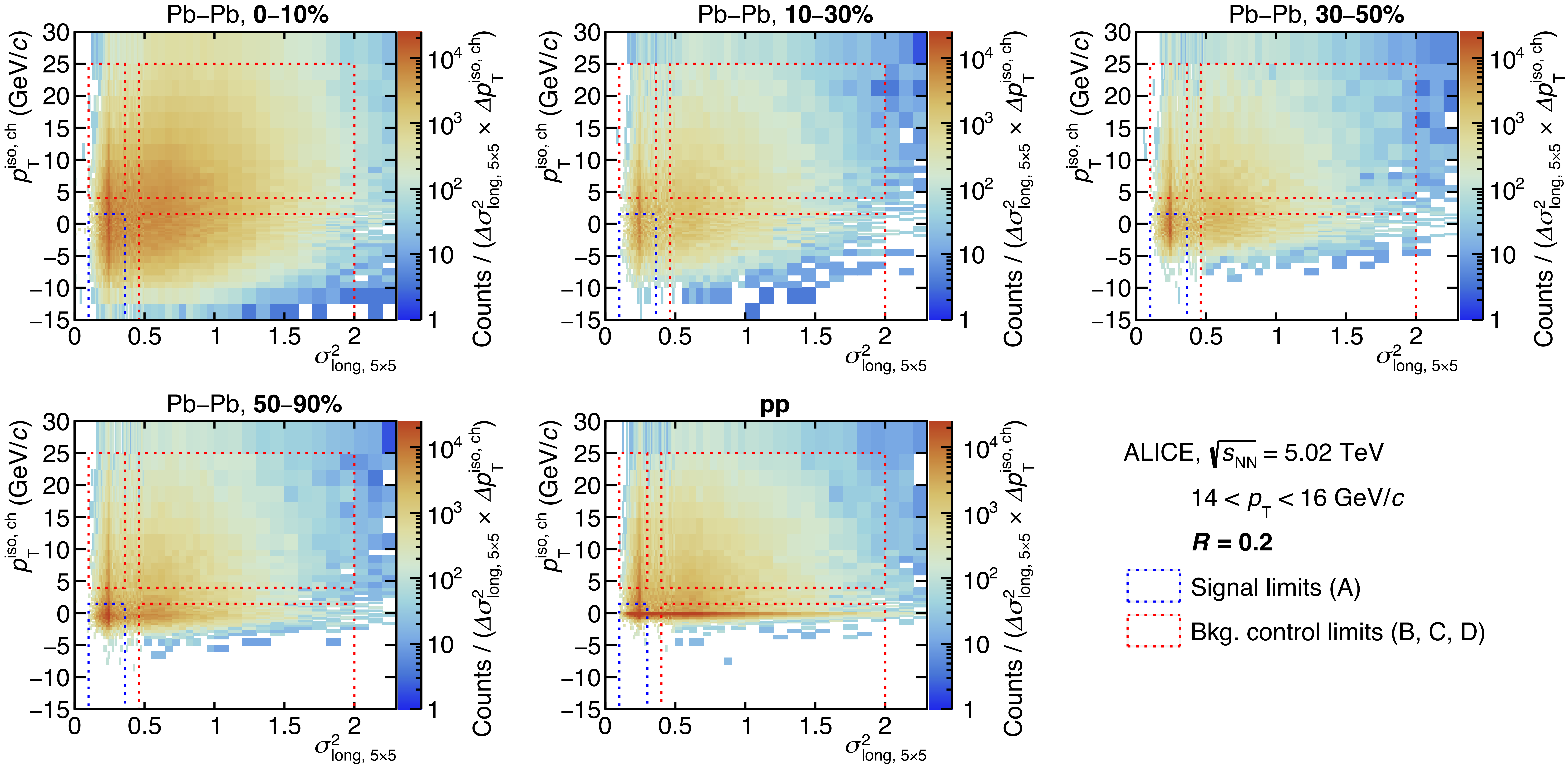

ALICE-PUBLIC-2024-003

ABCD regions, R = 0.4, pp & Pb–Pb $\sqrt{s_{NN}}$ = 5.02 TeV

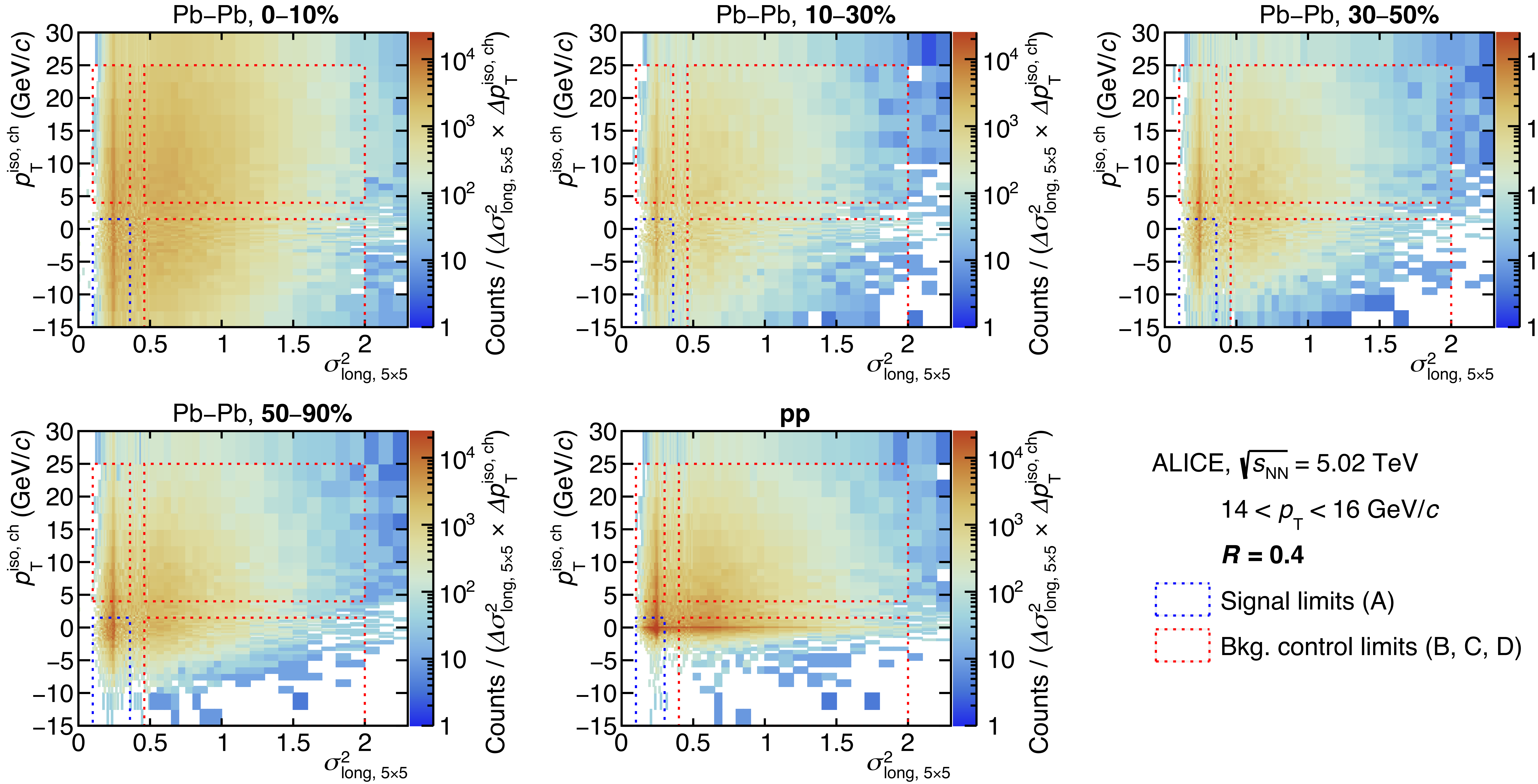

ALICE-PUBLIC-2024-003

Isolation momentum in cone, pp & Pb–Pb $\sqrt{s_{NN}}$ = 5.02 TeV

ALICE-PUBLIC-2024-003

Isolation momentum in cone, different UE areas

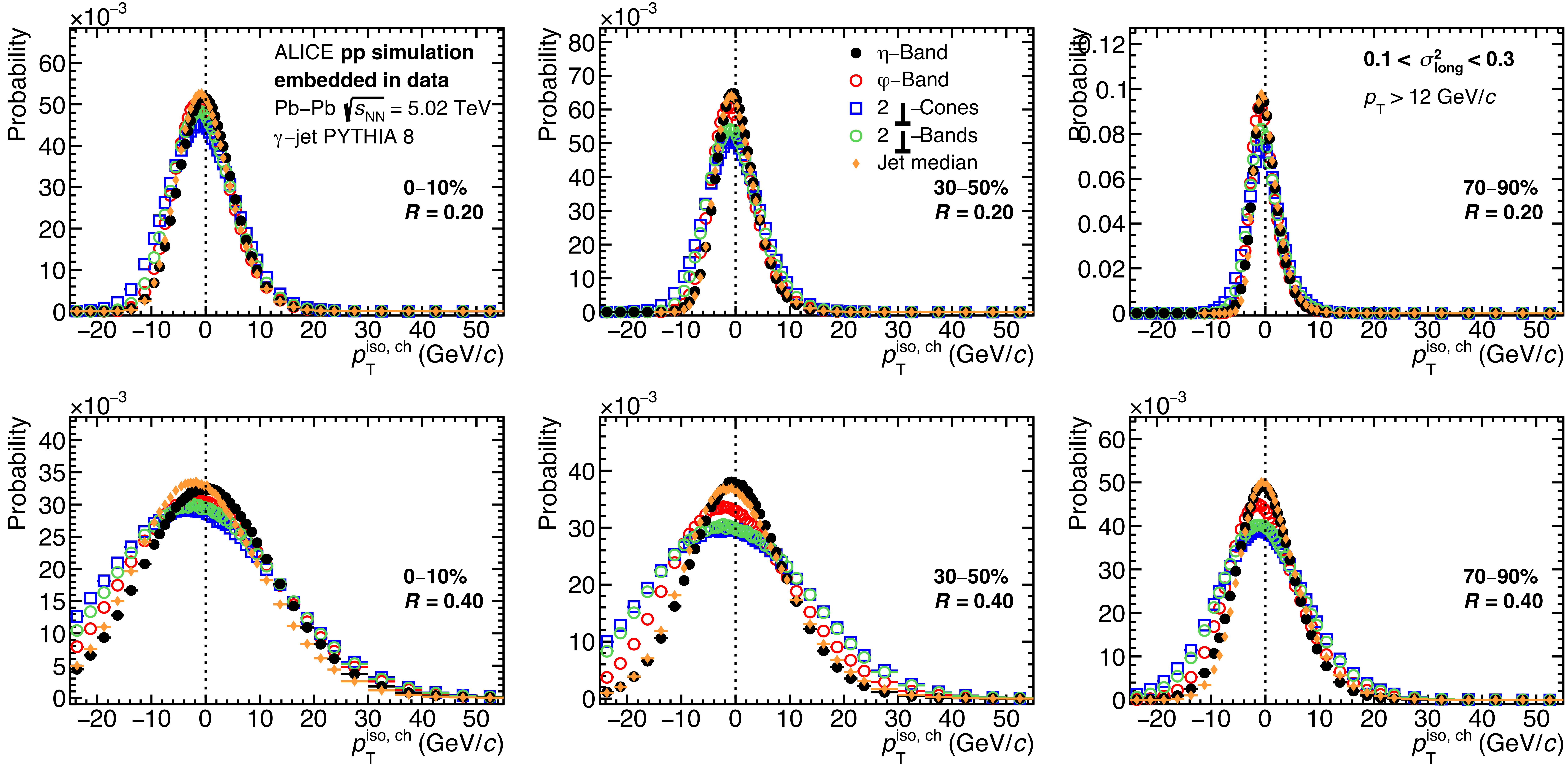

pp PYTHIA 8 γ-jet process simulation embedded into data

ALICE-PUBLIC-2024-003

Purity for R = 0.2 & 0.4, pp & Pb–Pb $\sqrt{s_{NN}}$ = 5.02 TeV

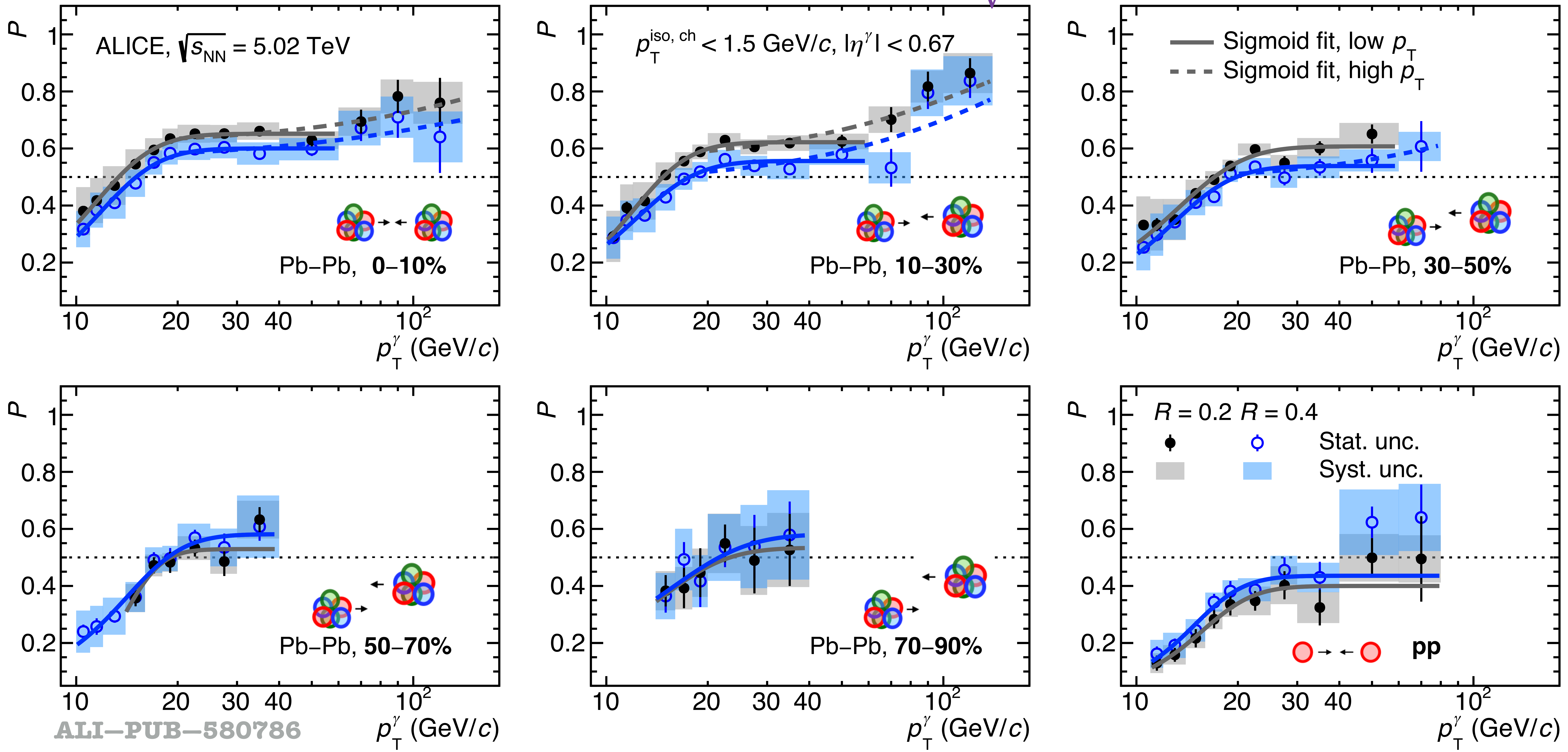

- Distributions fitted to sigmoid function to reduce influence of fluctuations, fits used to correct the spectra
- P (R = 0.4) > P (R = 0.2) in pp collisions, more jet particles in cone, but decreasing centrality P (R = 0.2) > P (R = 0.4), due to UE fluctuations, although not significantly different
- P (Pb–Pb) > P (pp) due to better tracking and higher $N(\gamma)$ / $N(\pi^0)$ ratio ($R_{AA}(\pi^0) << 1$)

Isolated γ efficiency components, pp $\sqrt{s}$ = 13 TeV

$$\varepsilon^{\mathrm{sel}} = \frac{\mathrm{d}N^{\text{cluster sel.}}_{\gamma_{\mathrm{prompt}}}/\mathrm{d}p_{\mathrm{T}}^{\mathrm{rec}}}{\mathrm{d}N^{\text{gener.}}_{\gamma_{\mathrm{prompt}}}/\mathrm{d}p_{\mathrm{T}}^{\mathrm{gen}}}$$

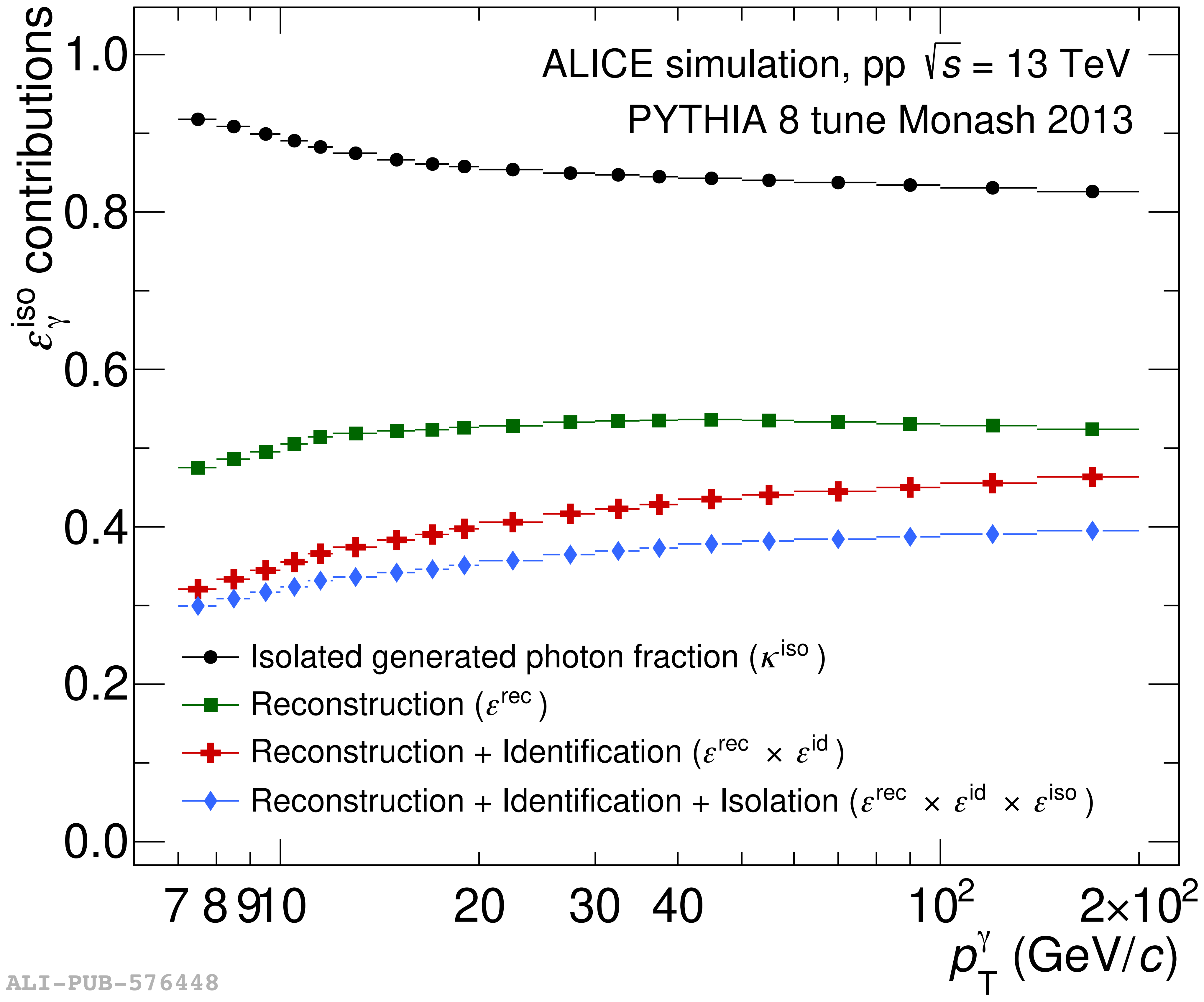

$$\varepsilon^{\mathrm{iso}}_{\gamma} = \frac{\mathrm{d}N^{\text{cluster iso. narrow}}_{\gamma_{\mathrm{prompt}}}/\mathrm{d}p_{\mathrm{T}}^{\mathrm{rec}}}{\mathrm{d}N^{\text{gener. iso.}}_{\gamma_{\mathrm{prompt}}}/\mathrm{d}p_{\mathrm{T}}^{\mathrm{gen}}}$$

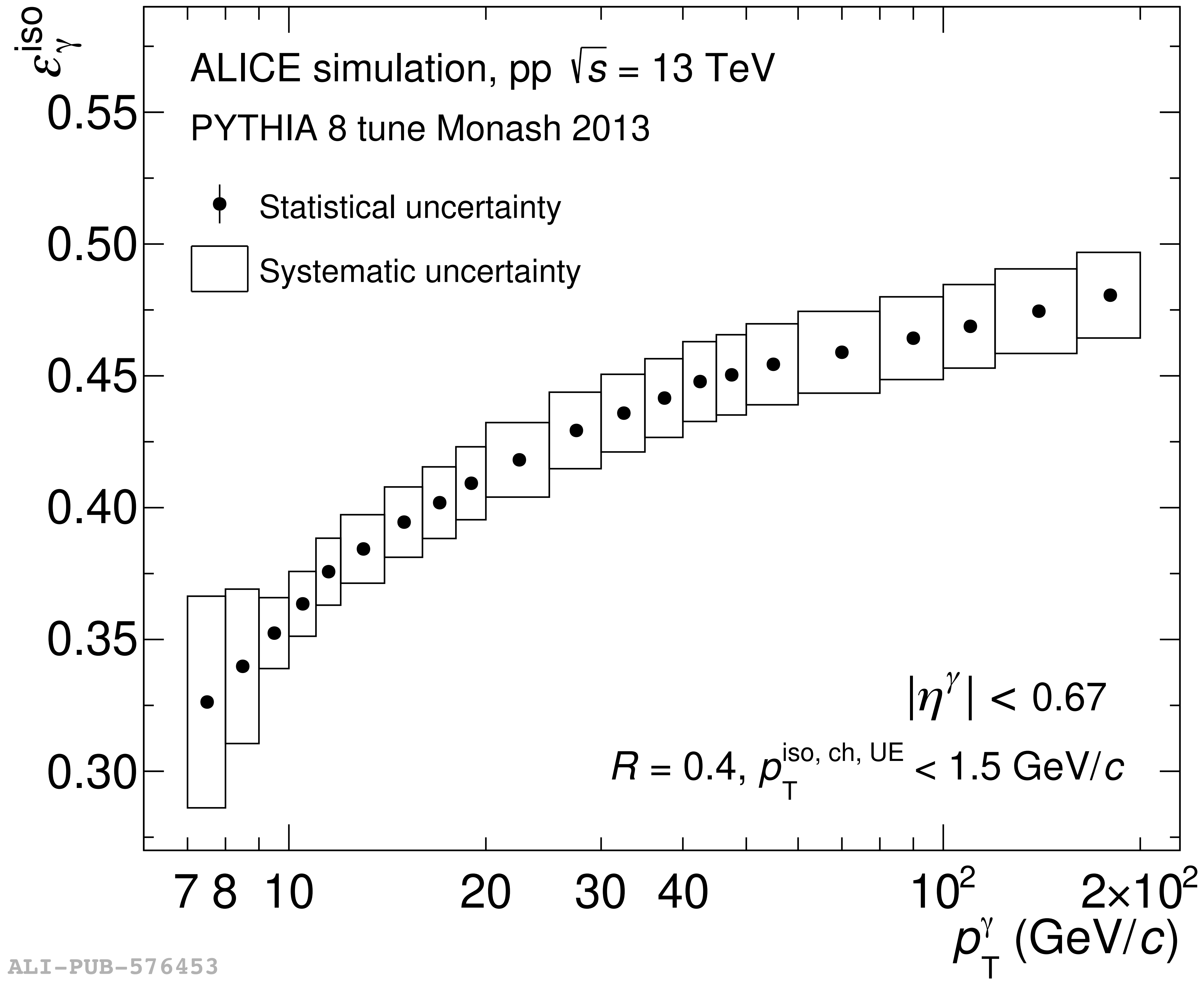

Isolated γ efficiency components, pp & Pb–Pb $\sqrt{s_{\rm NN}}$ = 5.02 TeV

$$\varepsilon^{\rm sel} = \frac{{\rm d}N^{\rm cluster\ sel.}_{\gamma_{\rm prompt}}/{\rm d}p_{\rm T}^{\rm rec}}{{\rm d}N^{\rm gener.}_{\gamma_{\rm prompt}}/{\rm d}p_{\rm T}^{\rm gen}}$$

ALICE-PUBLIC-2024-003

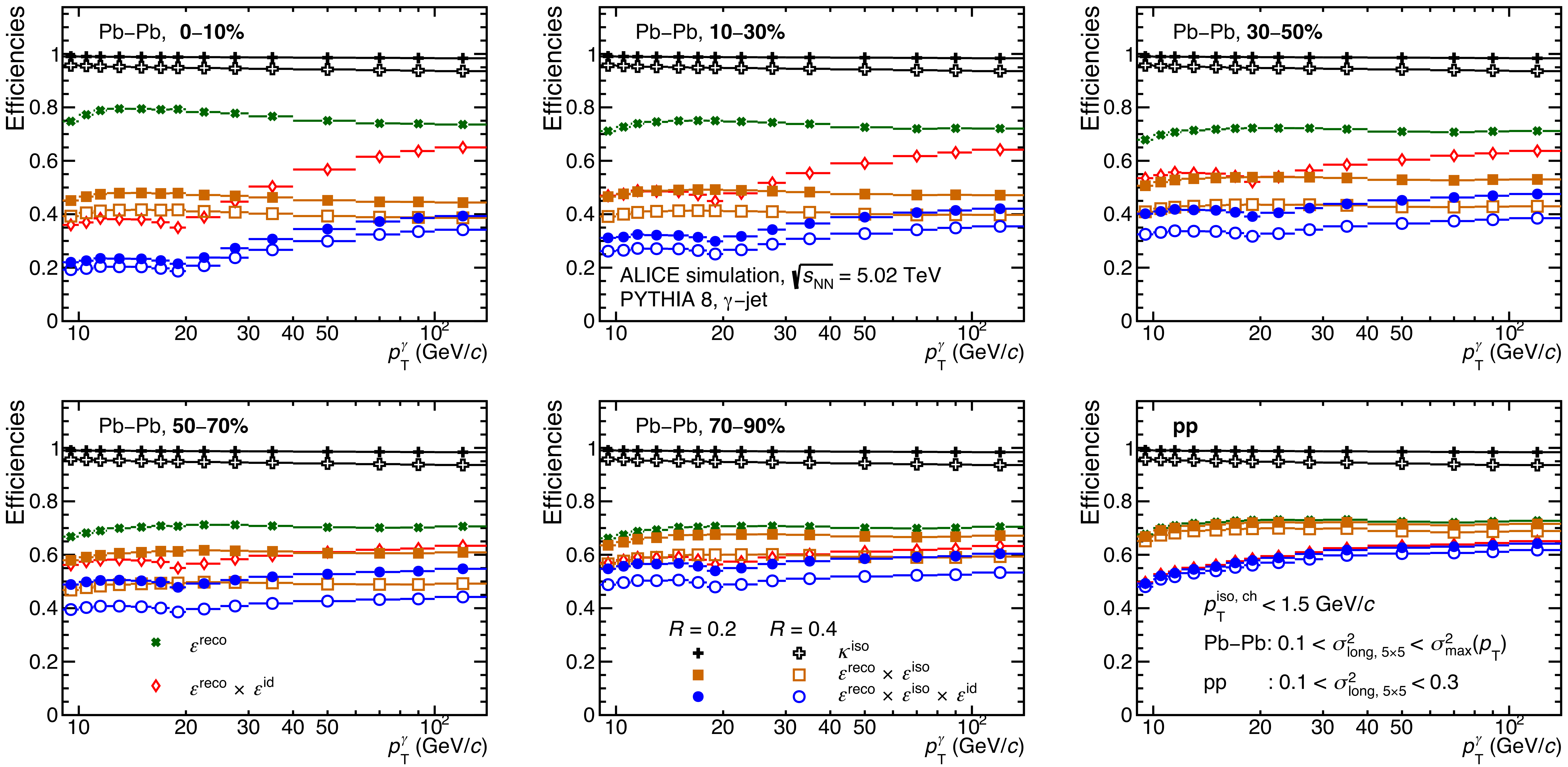

Selection probability depending isolation threshold, R = 0.2, pp & Pb–Pb $\sqrt{s_{NN}}$ = 5.02 TeV

ALICE-PUBLIC-2024-003

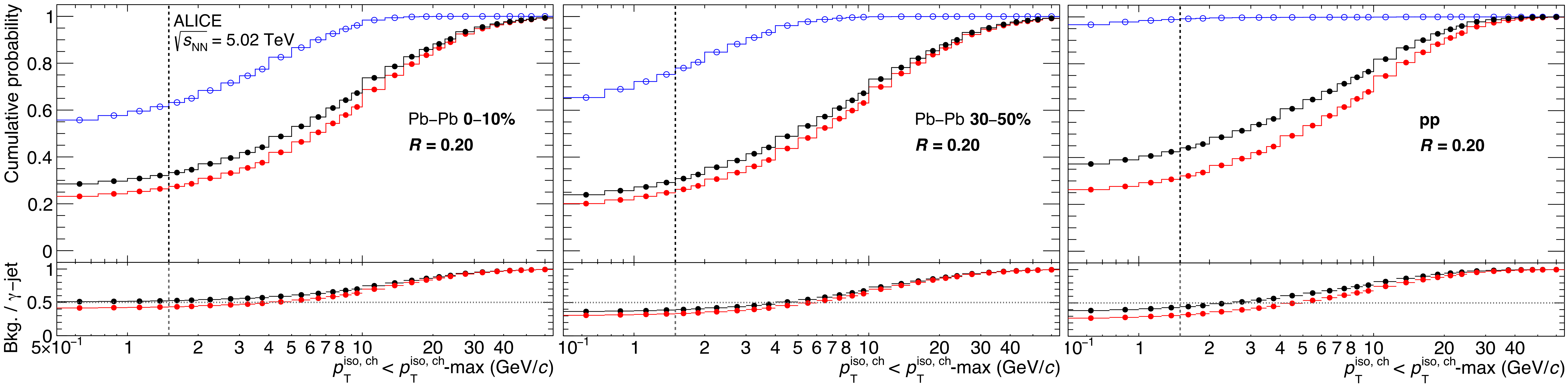

Selection probability depending isolation threshold, R = 0.4, pp & Pb–Pb $\sqrt{s_{NN}}$ = 5.02 TeV

ALICE-PUBLIC-2024-003

Pb–Pb 50-90%: efficiency and purity

ALICE-PUBLIC-2024-003

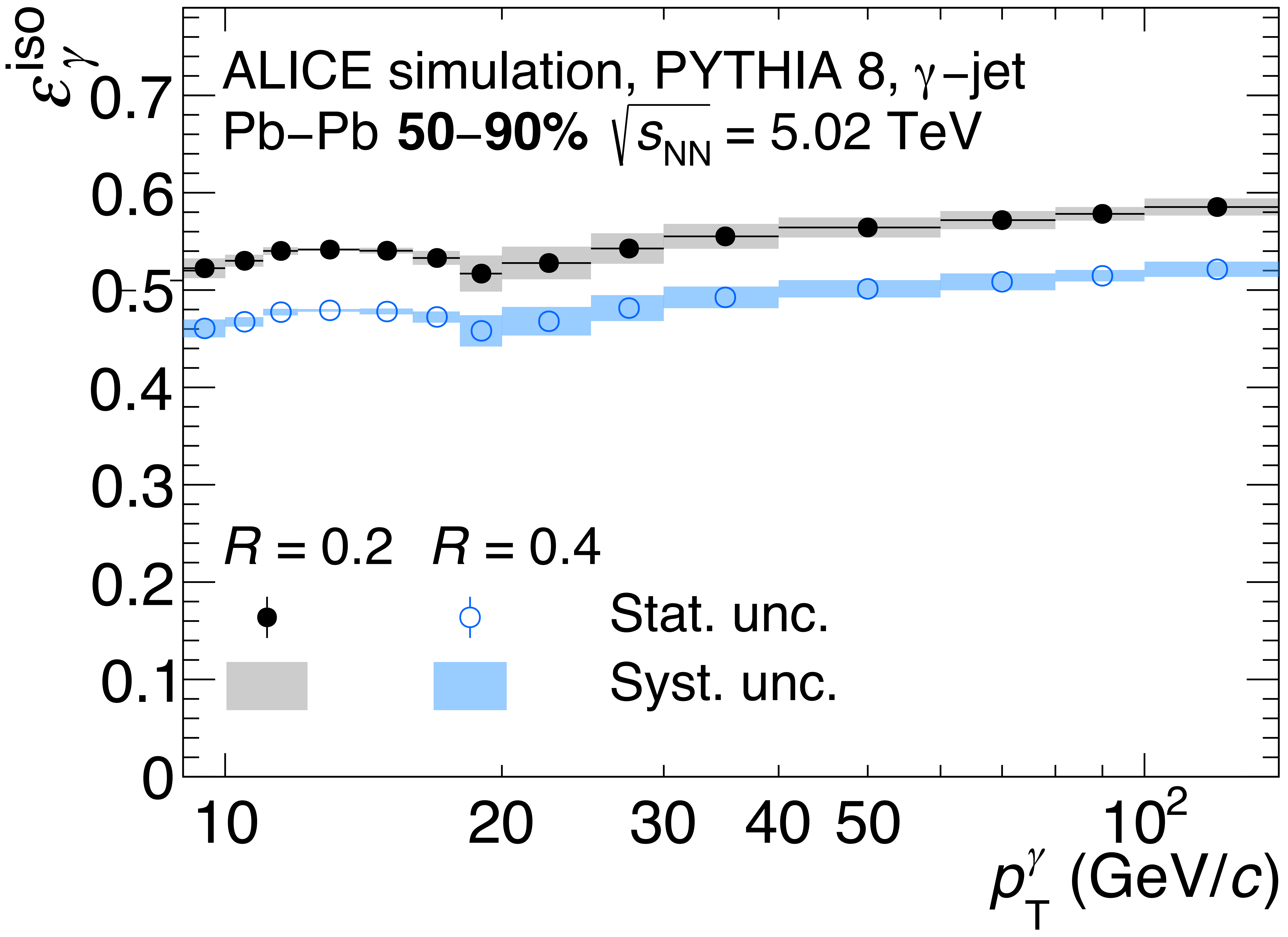

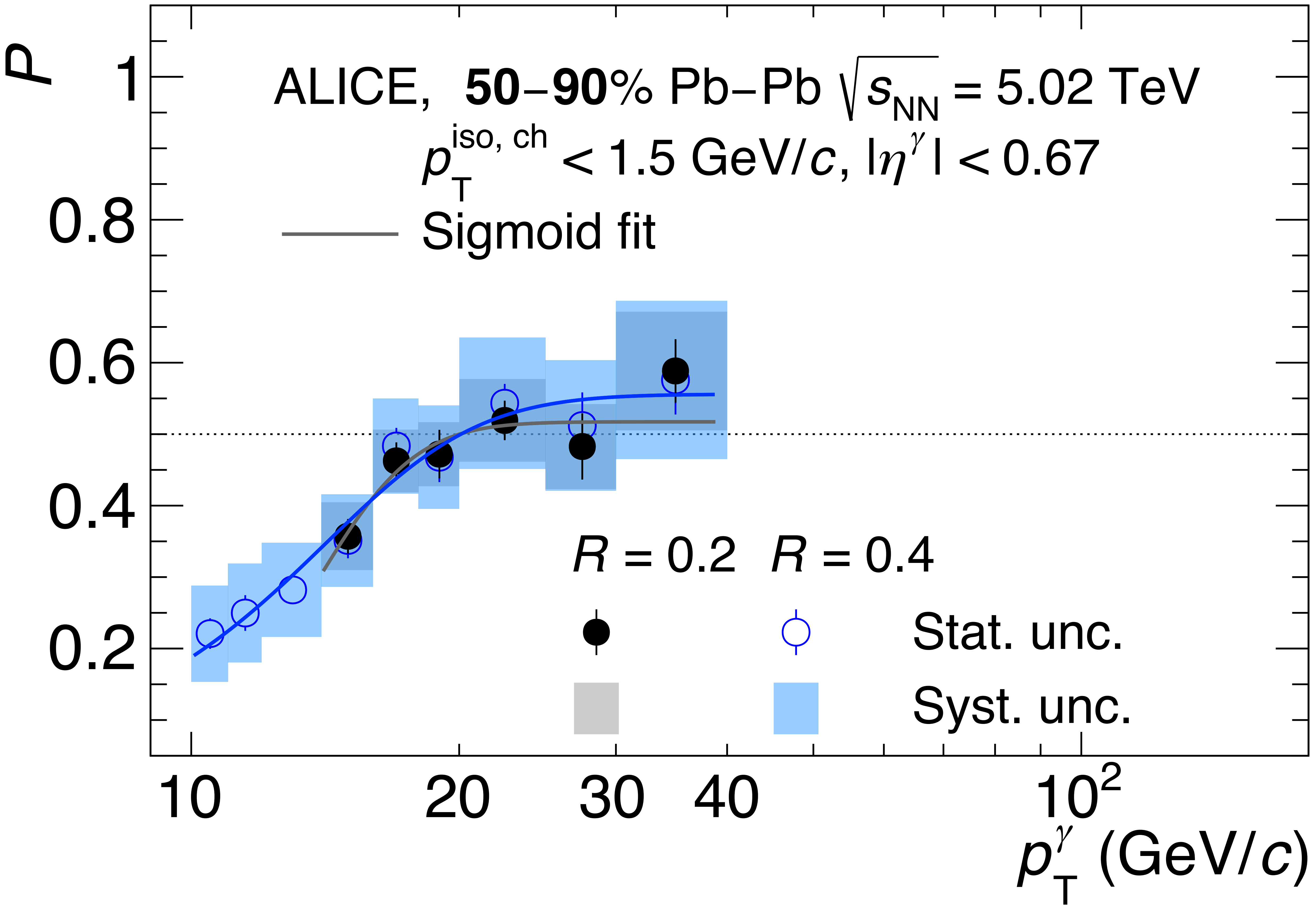

Uncertainties, pp $\sqrt{s}$ = 13 TeV

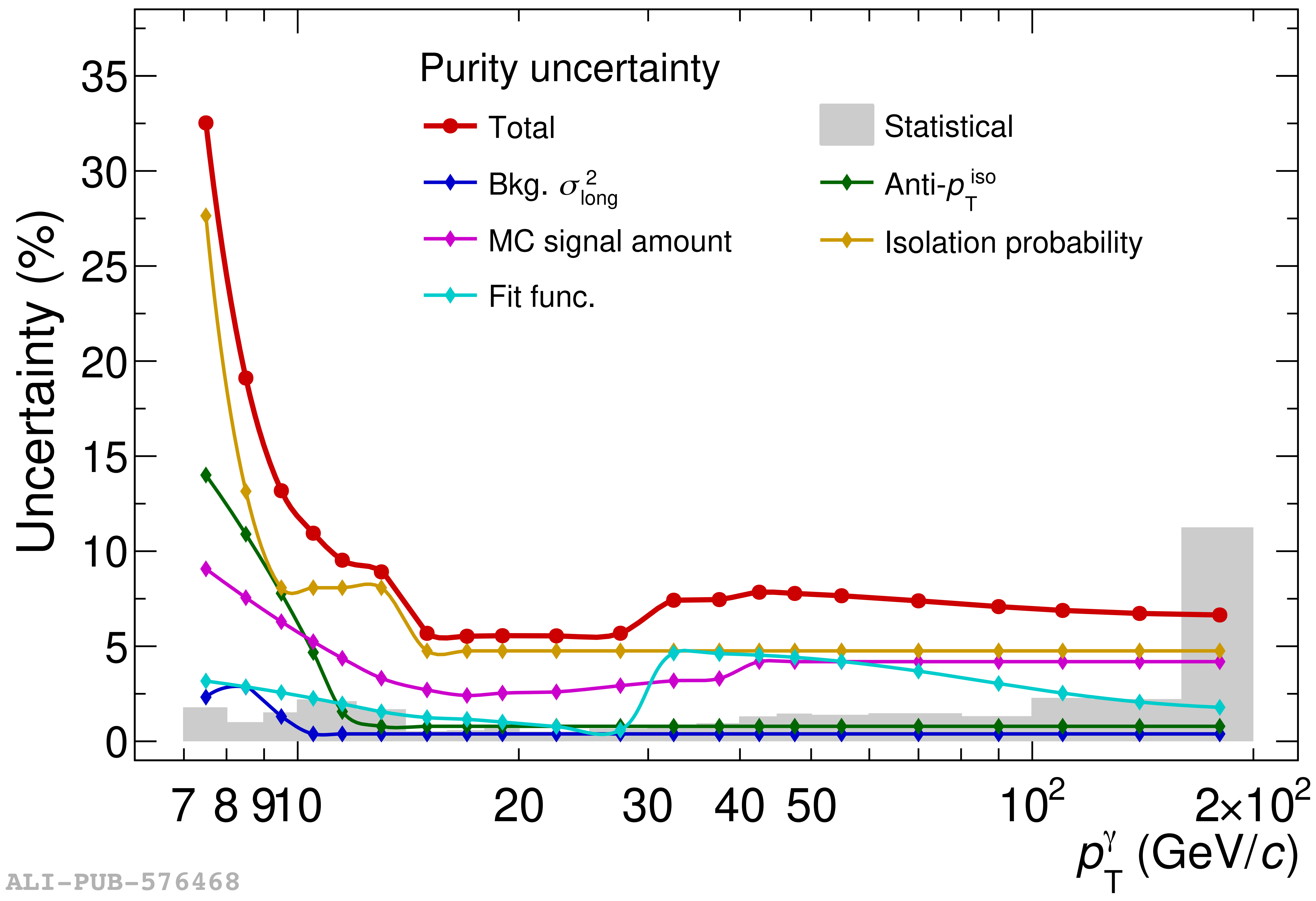

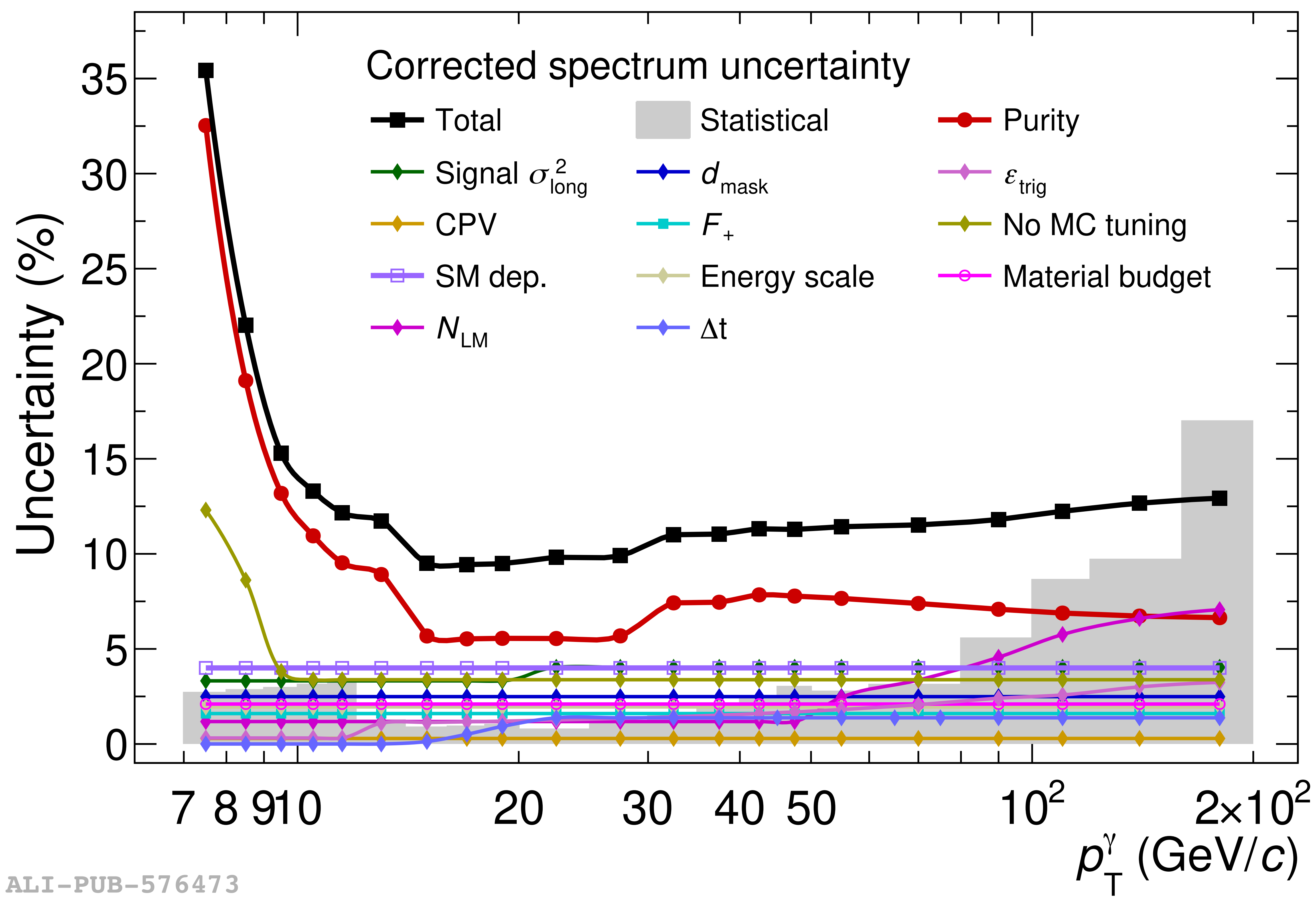

Purity uncertainties, pp & Pb–Pb $\sqrt{s_{NN}}$ = 5.02 TeV, R = 0.2

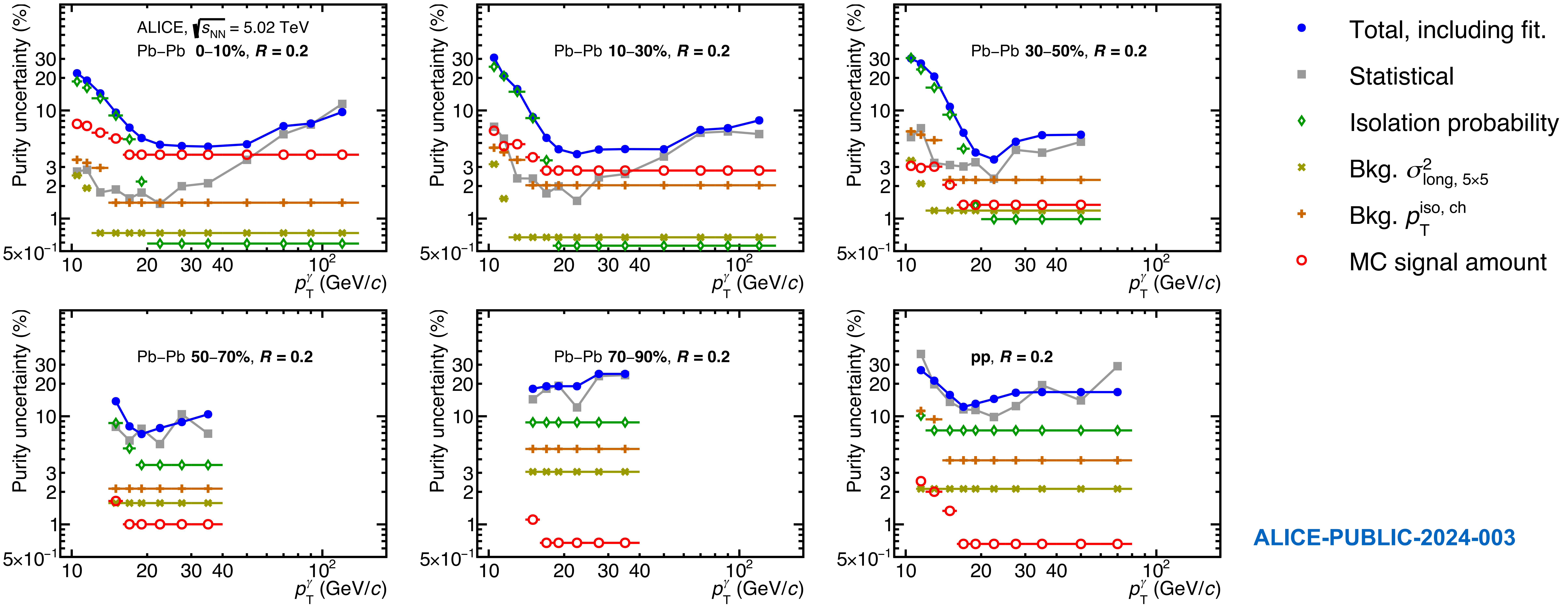

ALICE-PUBLIC-2024-003

Purity uncertainties, pp & Pb–Pb $\sqrt{s_{NN}}$ = 5.02 TeV, *R* = 0.4

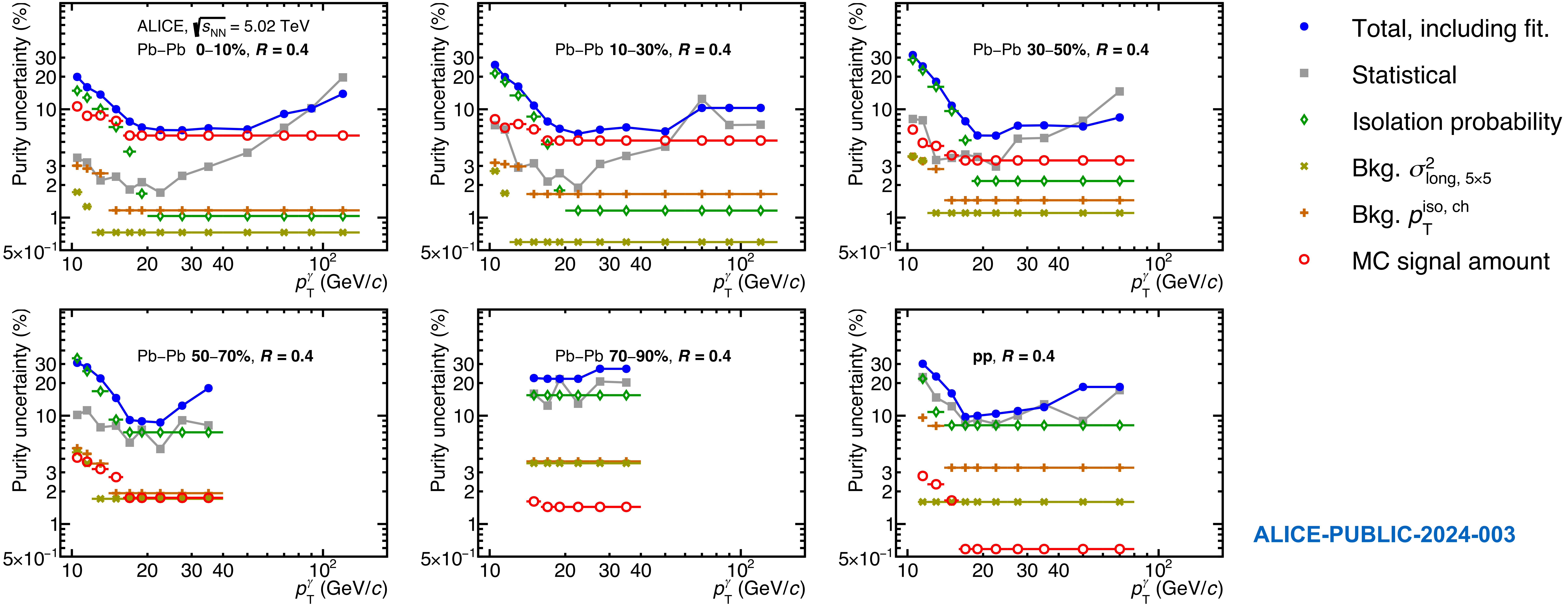

ALICE-PUBLIC-2024-003

Cross section uncertainties, pp & Pb–Pb $\sqrt{s_{NN}}$ = 5.02 TeV, R = 0.2

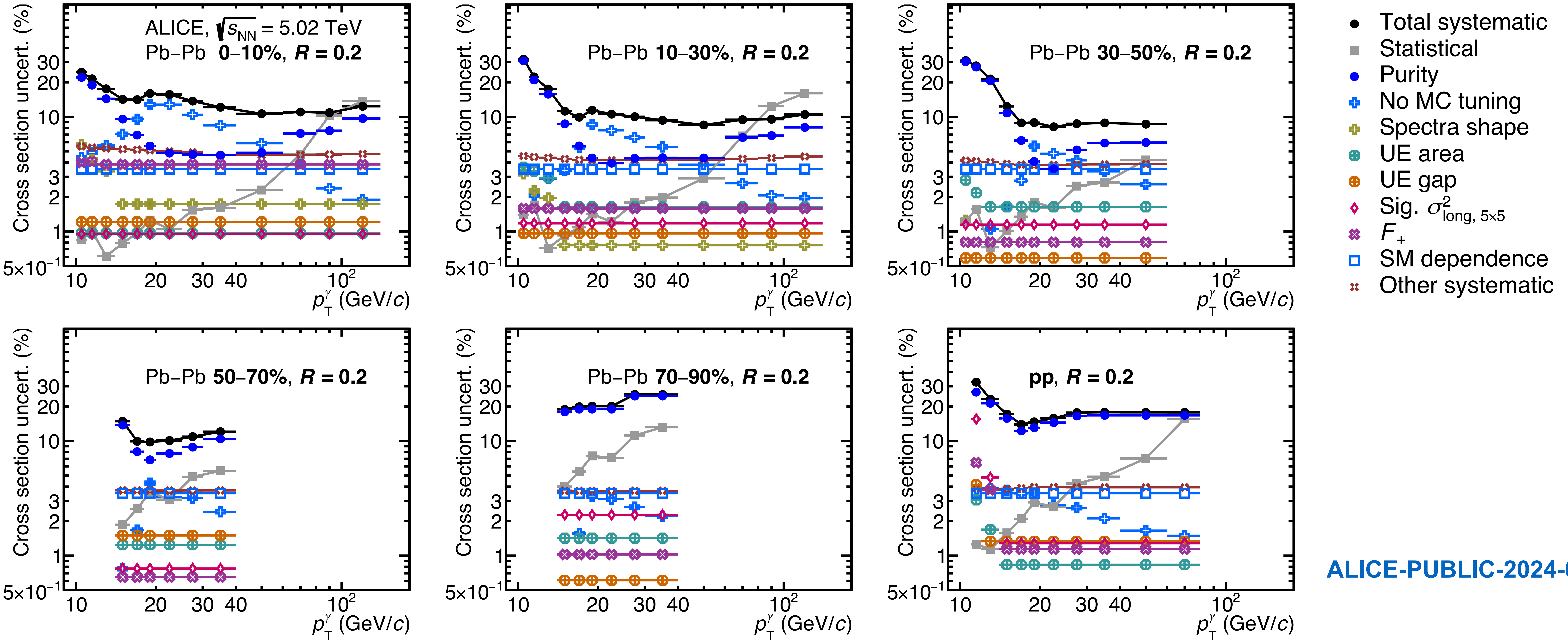

ALICE-PUBLIC-2024-003

Cross section uncertainties, pp & Pb–Pb $\sqrt{s_{NN}}$ = 5.02 TeV, R = 0.4

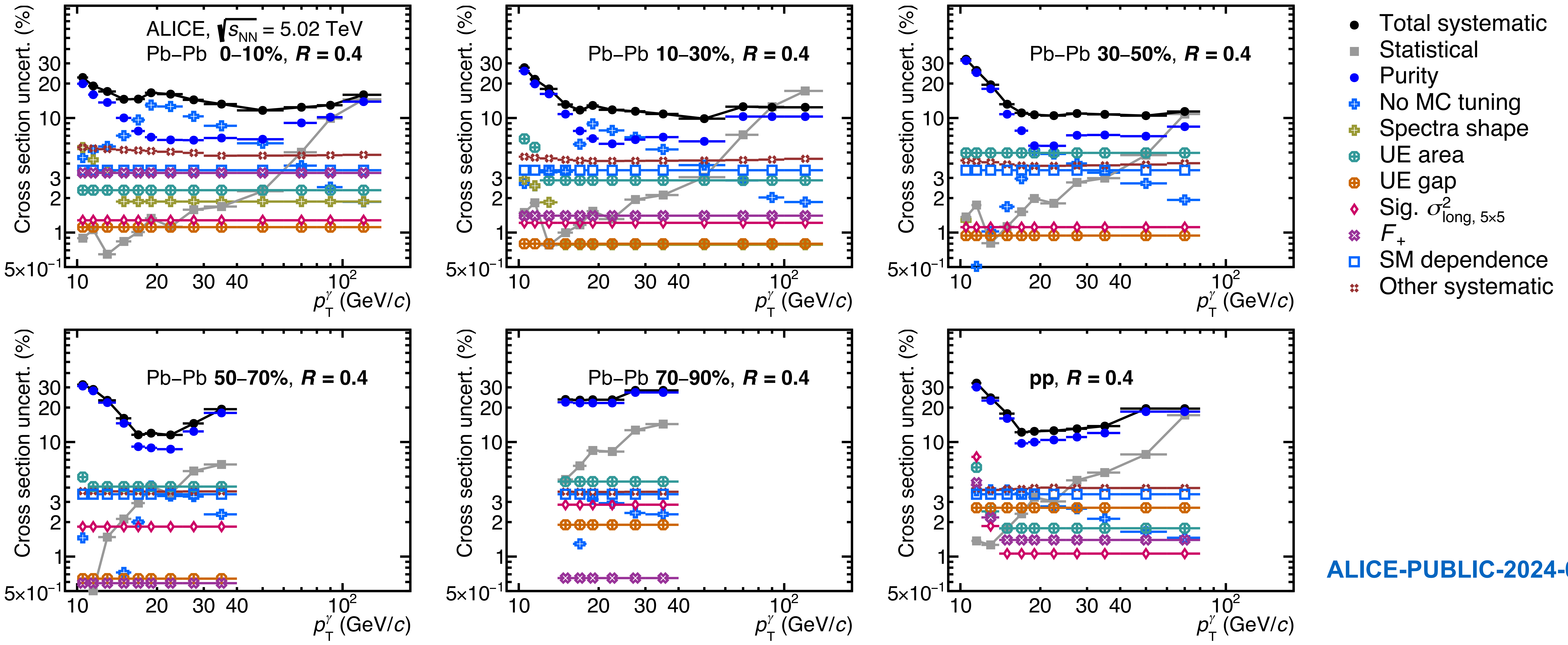

ALICE-PUBLIC-2024-003

R_{AA} uncertainties, R = 0.2

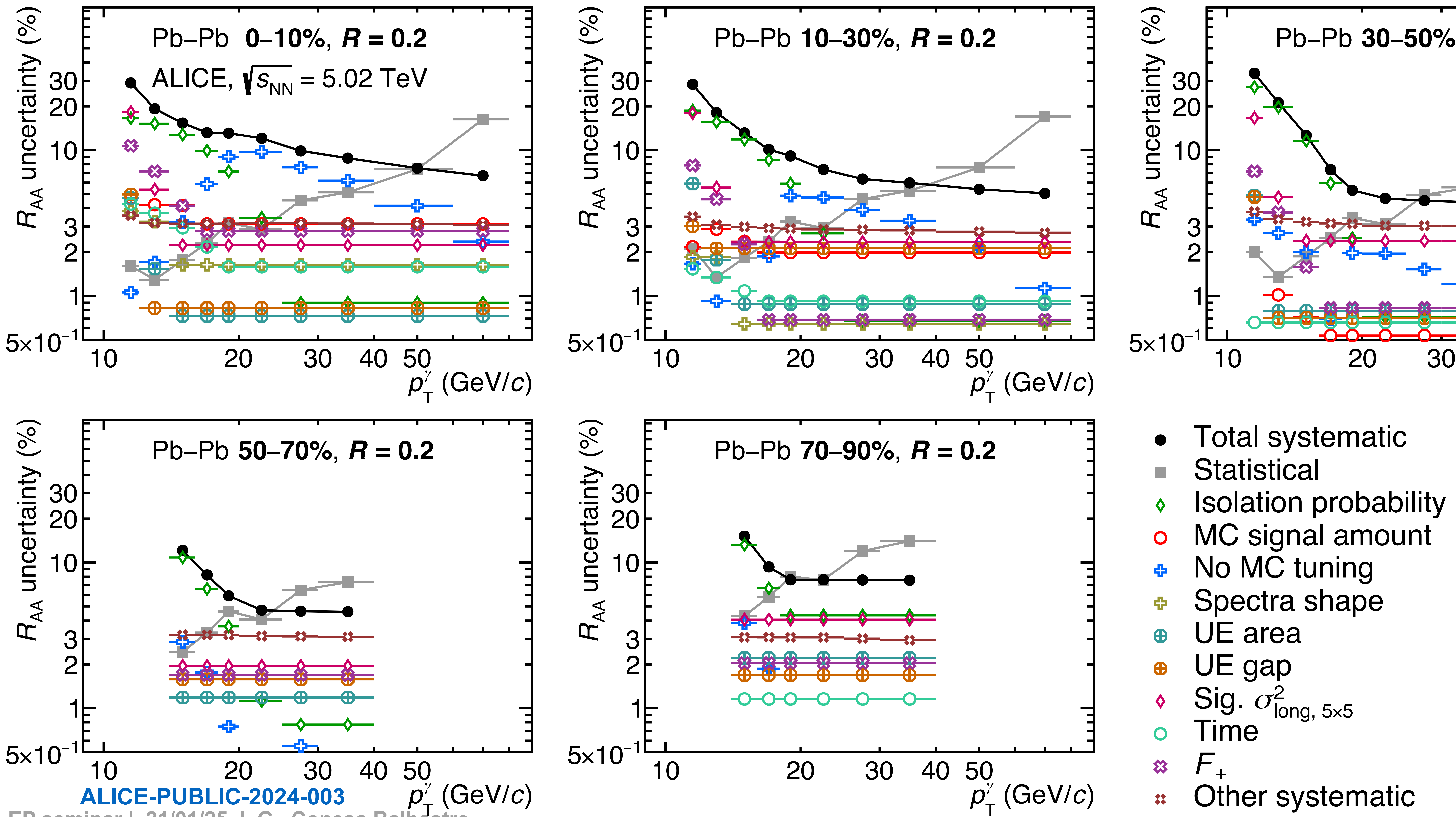

ALICE-PUBLIC-2024-003

R_{AA} uncertainties, R = 0.4

ALICE-PUBLIC-2024-003

R = 0.4 over R = 0.2 ratio uncertainties, pp & Pb–Pb $\sqrt{s_{\mathrm{NN}}}$ = 5.02 TeV

ALICE-PUBLIC-2024-003

Isolated γ–hadron correlations in Pb–Pb: $D(z_T)$

ALICE

I_{pQCD} = Pb–Pb Data / pp pQCD

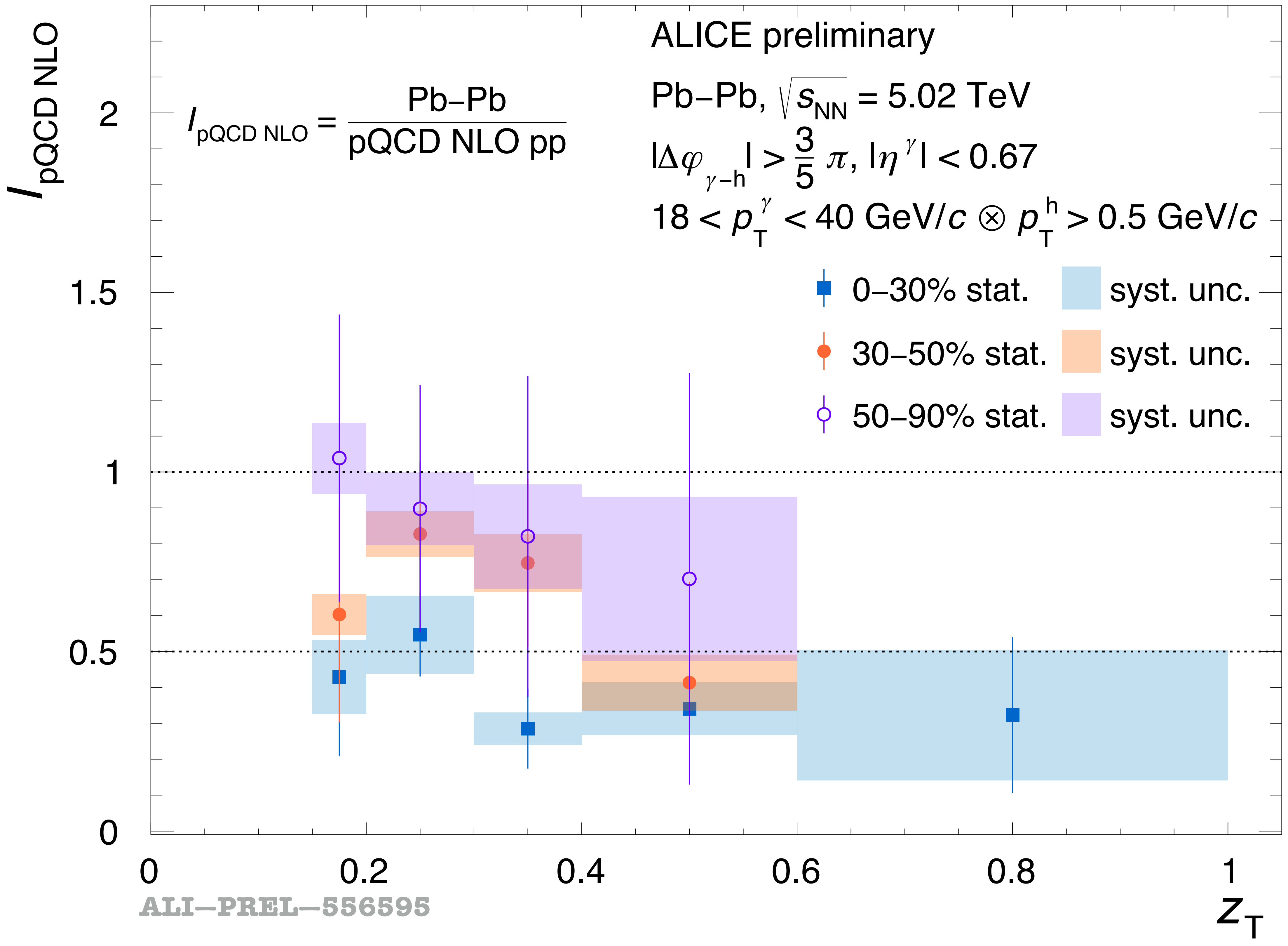

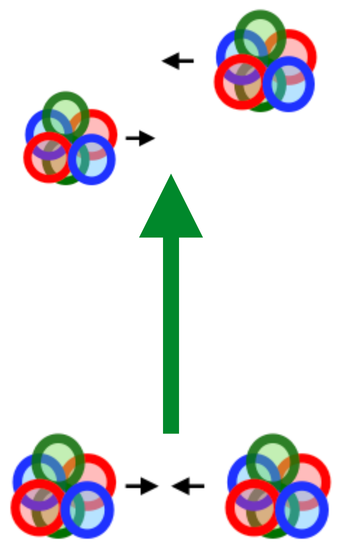

I_{CP} = Pb–Pb (semi) central / peripheral

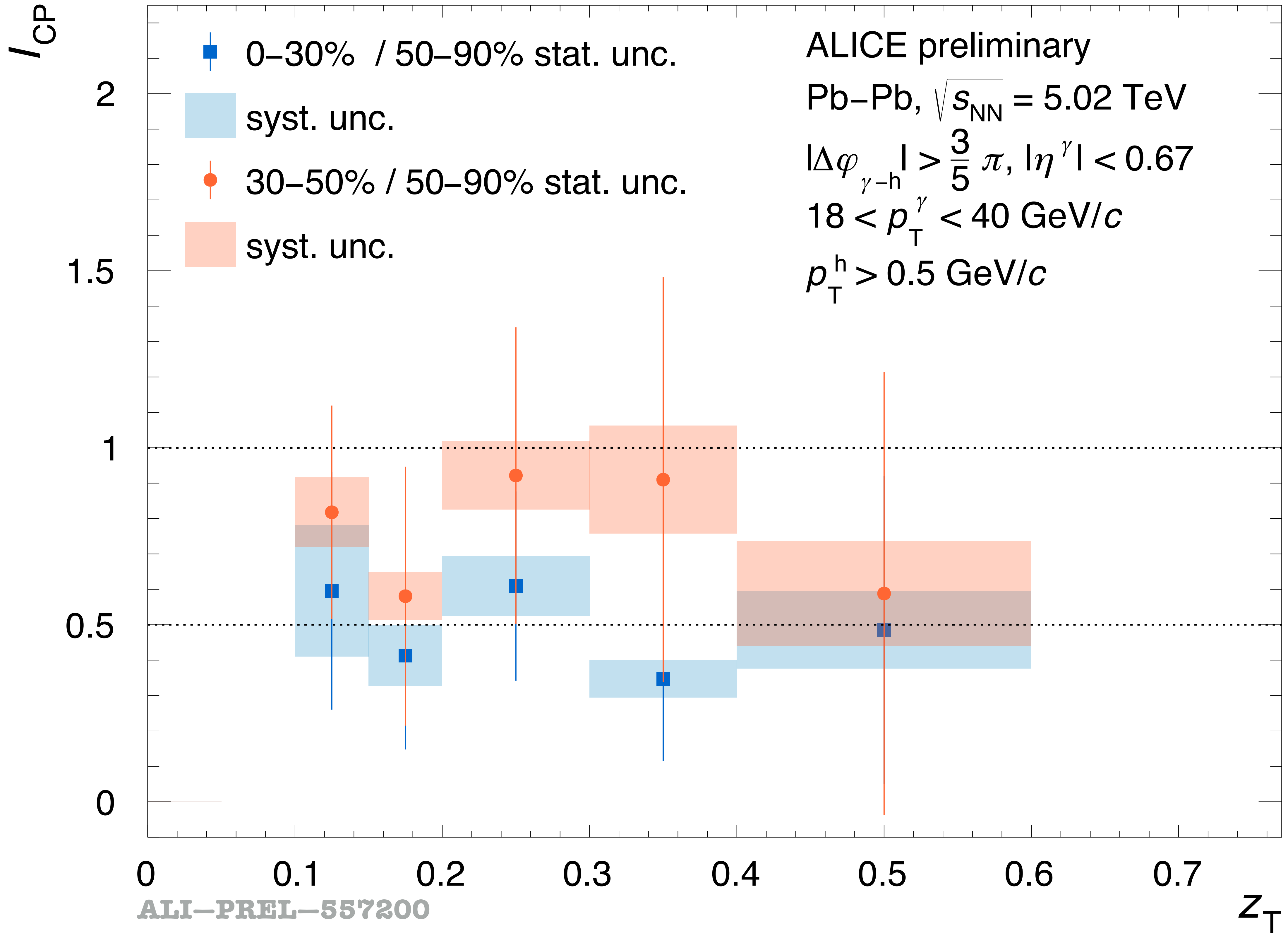

Isolated γ-hadron correlations in Pb–Pb: RHIC & LHC

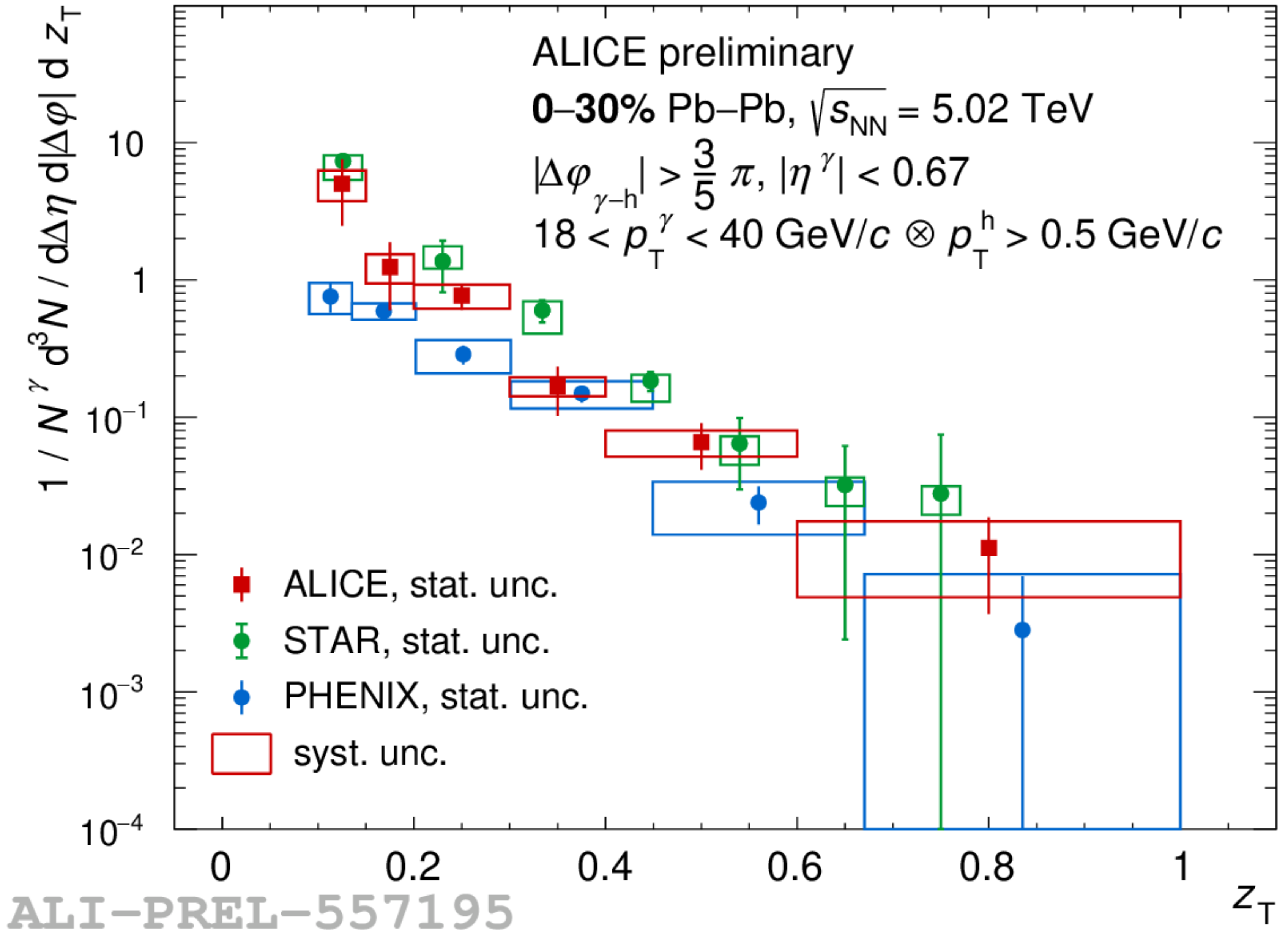

STAR, Phys.Lett.B 760 (2016) 689-696

0–12% Au–Au, $\sqrt{s_{NN}}$ = 200 GeV

$|\Delta\varphi_{\gamma-h} - \pi| \leq 1.4$

$12 < p_T^{\gamma} < 20$ GeV/c ⊗ $p_T^h > 1.2$ GeV/c

PHENIX, PRL 111, 032301 (2013)

0–40% Au–Au, $\sqrt{s_{NN}}$ = 200 GeV

$|\Delta\varphi_{\gamma-h} - \pi| < \pi/2$, $|y| < 0.35$

$5 < p_T^{\gamma} < 9$ GeV/c ⊗ $0.5 < p_T^h < 7$ GeV/c

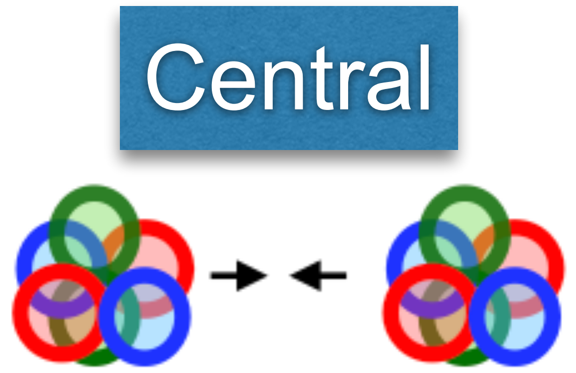

- Similar behaviour as observed at RHIC and LHC experiments

➡ Note: not completely apple-to-apple comparisons!

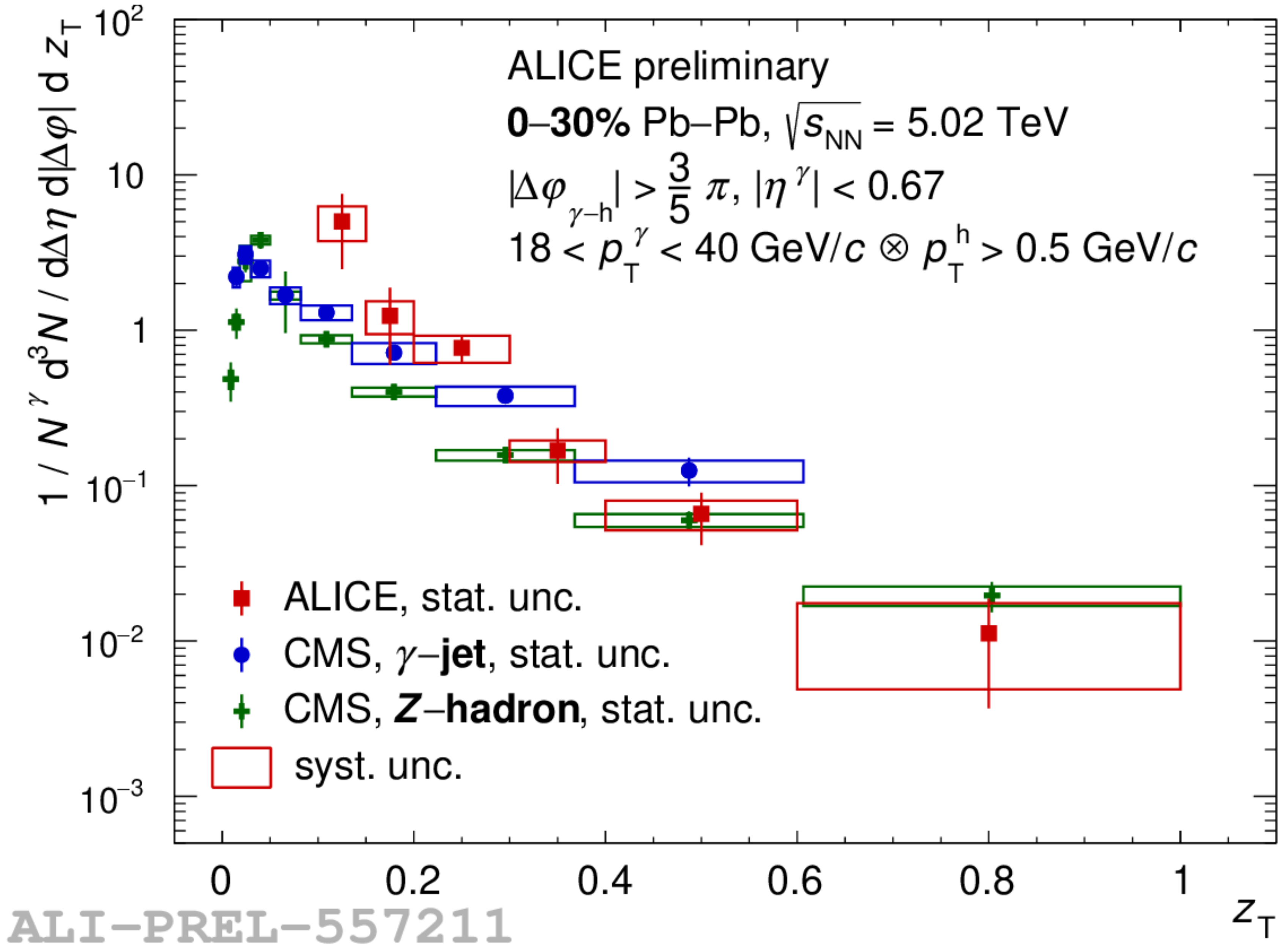

CMS, Phys.Rev.Lett. 121 (2018) 24, 242301, 2018

***γ*–jet, 0–10%**

anti-k_T jet R = 0.3, $p_T^{jet} > 30$ GeV/c, $|\eta^{jet}| < 1.6$

$|\Delta\varphi_{\gamma-jet}| > \frac{7}{8}\pi$, $|\eta^{\gamma}| < 1.44$, $p_T^{\gamma} > 60$ GeV/c ⊗ $p_T^h > 1$ GeV/c

CMS, Phys.Rev.Lett. 128 (2022) 12, 122301, 2022

***Z*–hadron, 0–30%**

$|\Delta\varphi_{Z-h}| > \frac{7}{8}\pi$, $p_T^Z > 30$ GeV/c ⊗ $p_T^h > 1$ GeV/c

Isolated γ-hadron correlations in Pb–Pb: $D(z_T)$

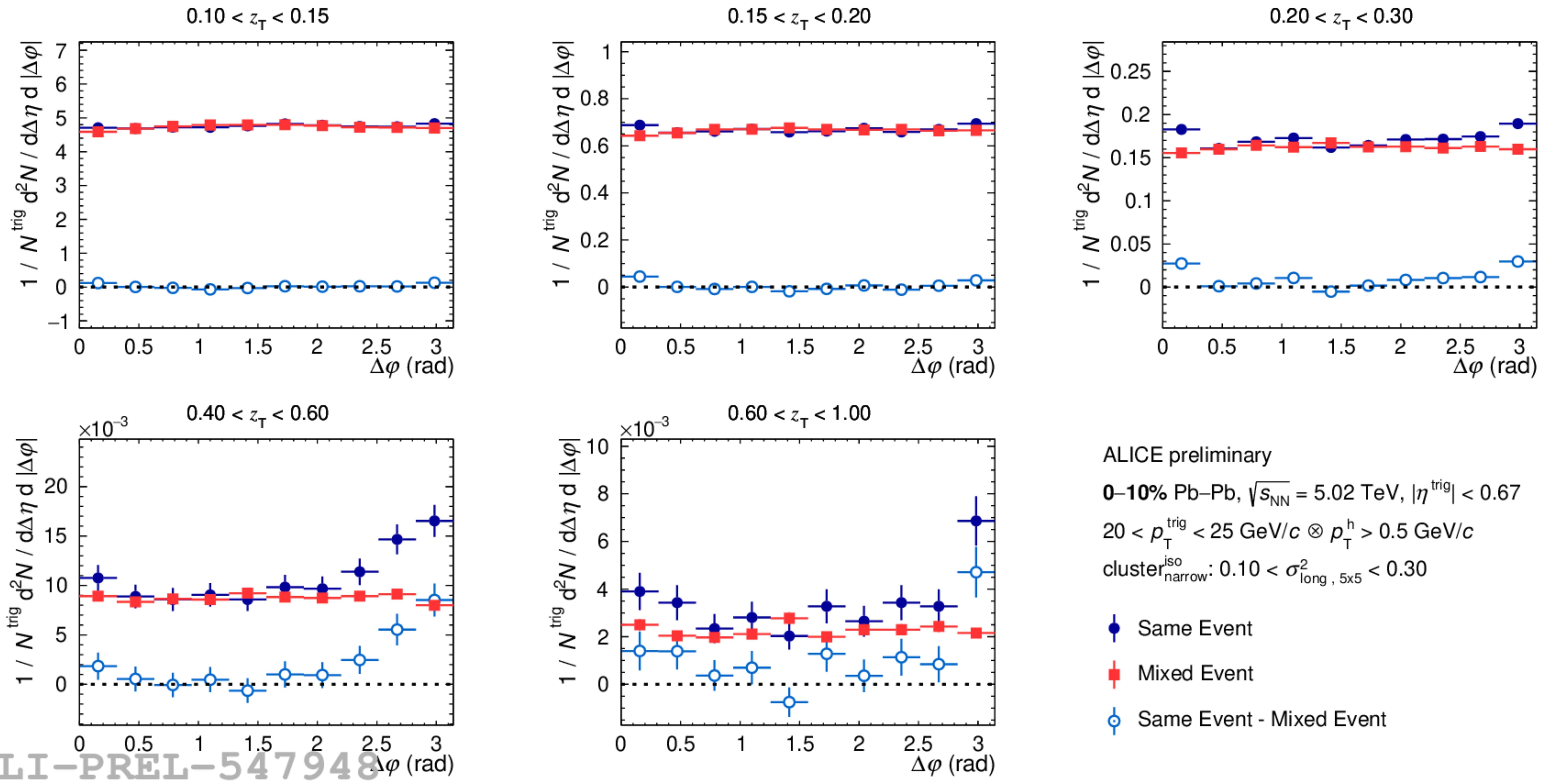

Isolated γ-hadron correlations in Pb–Pb: $D(z_T)$

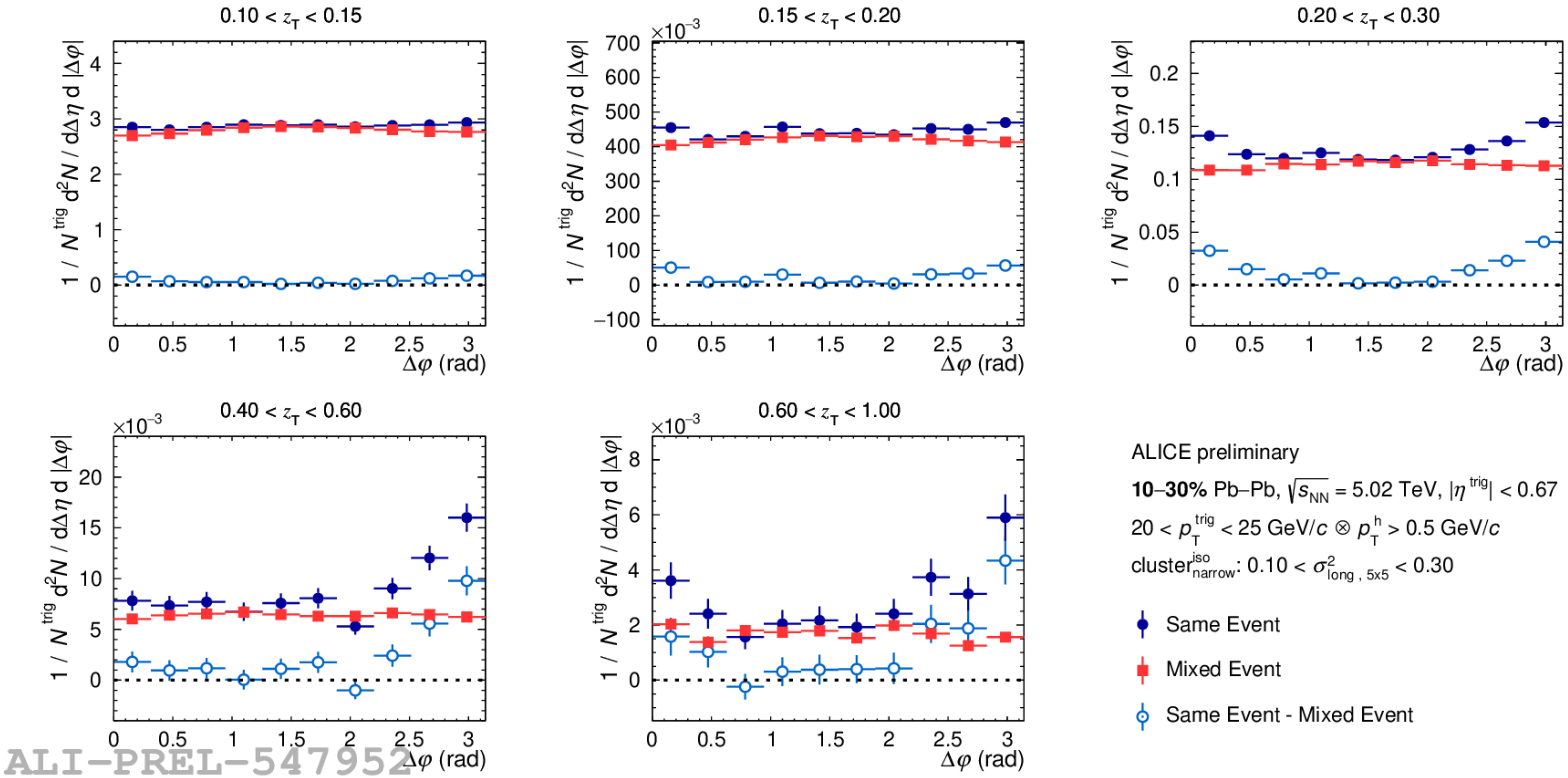

Isolated γ-hadron correlations in Pb–Pb: $D(z_T)$

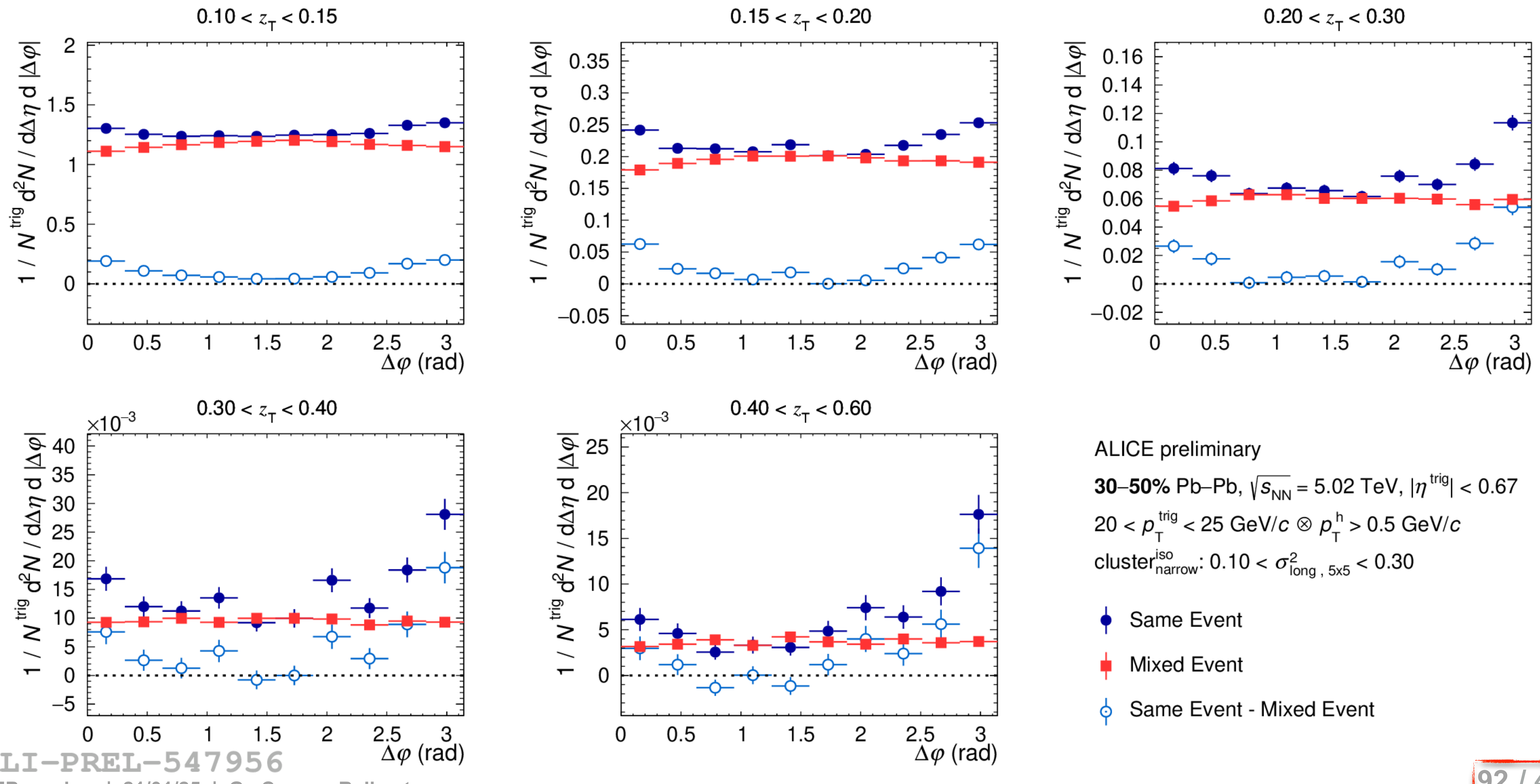

Isolated γ-hadron correlations in Pb–Pb: $D(z_T)$

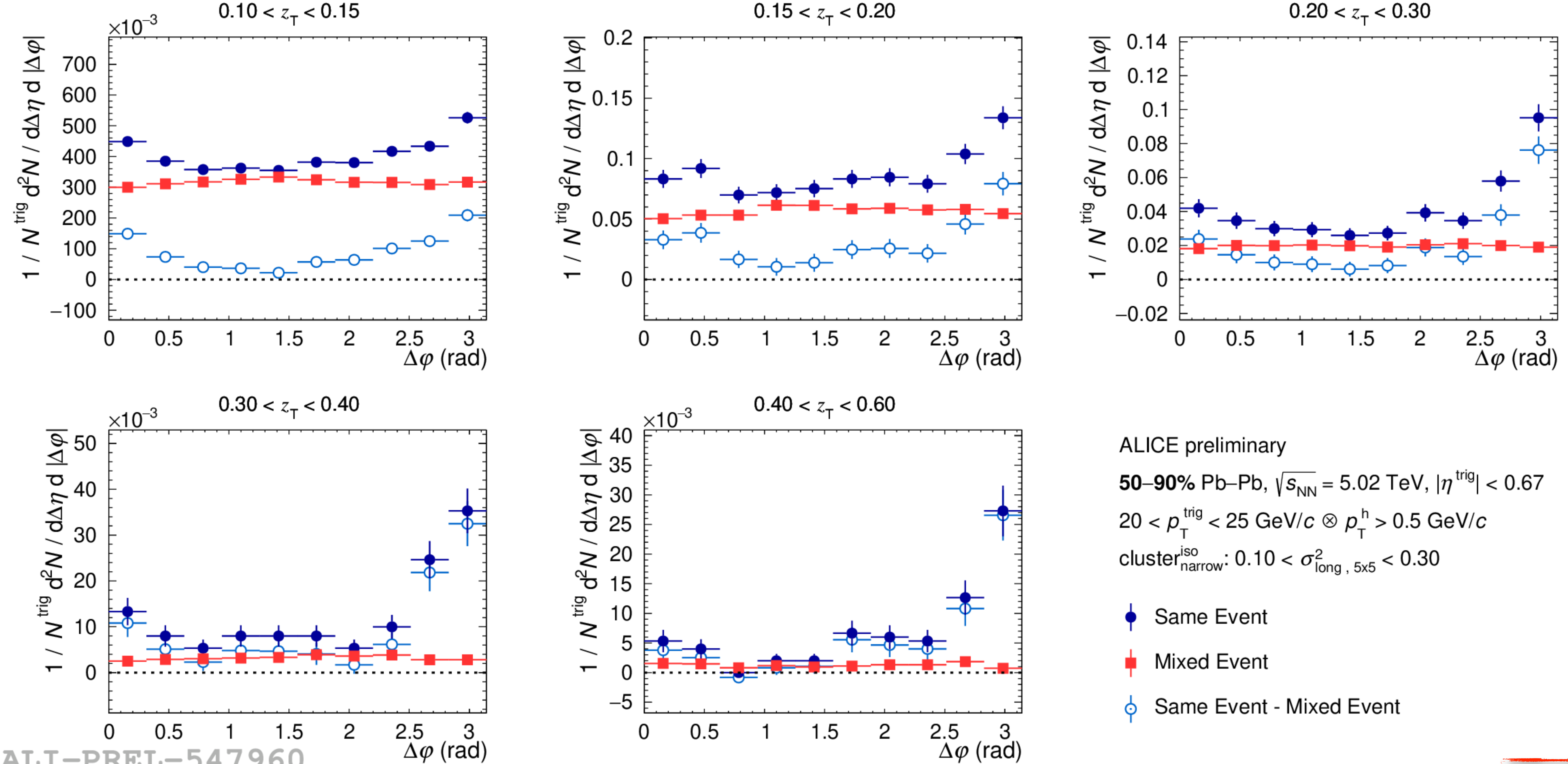

Isolated γ-hadron correlations in Pb–Pb: $D(z_T)$

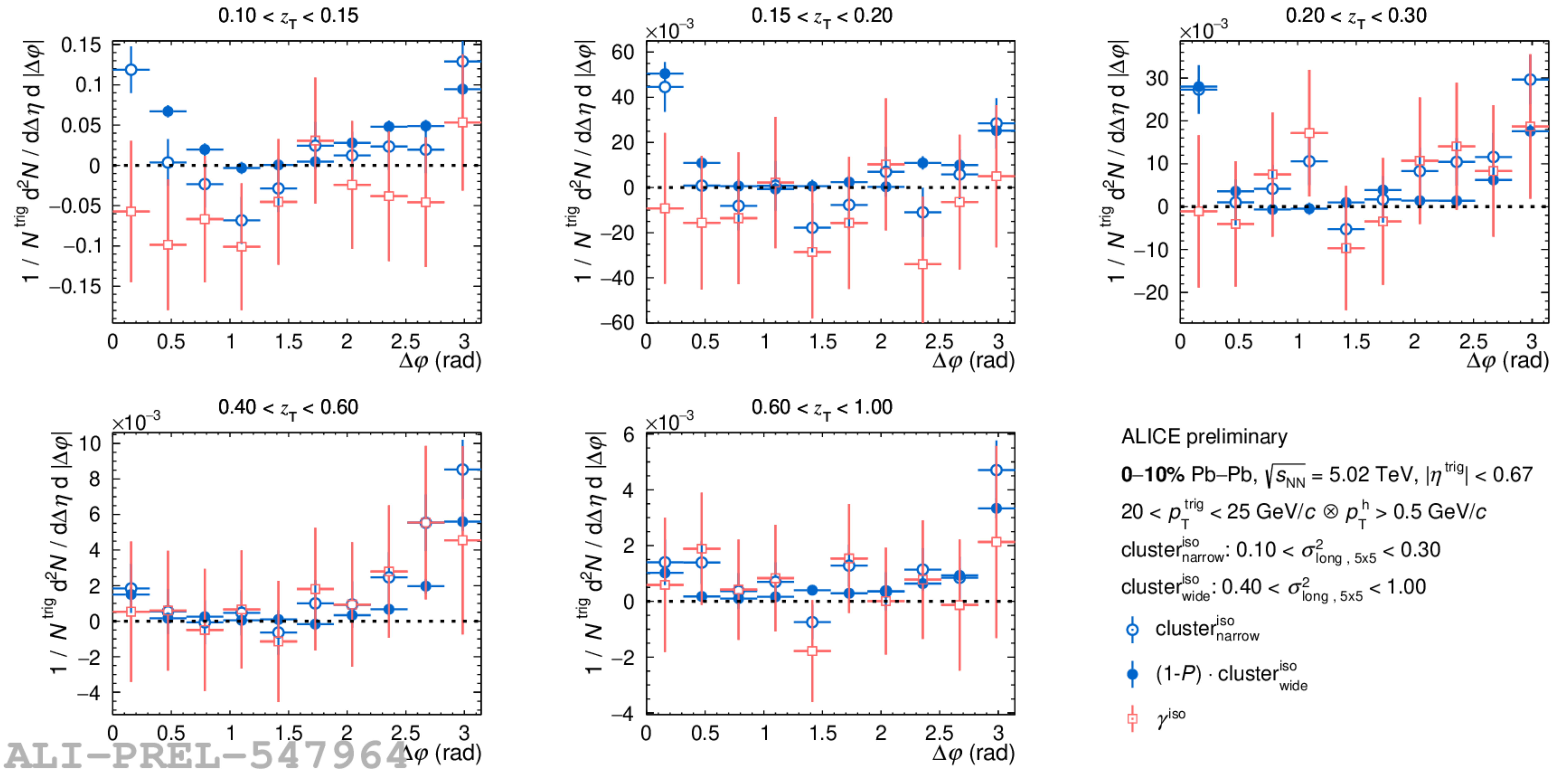

Isolated γ-hadron correlations in Pb–Pb: $D(z_T)$

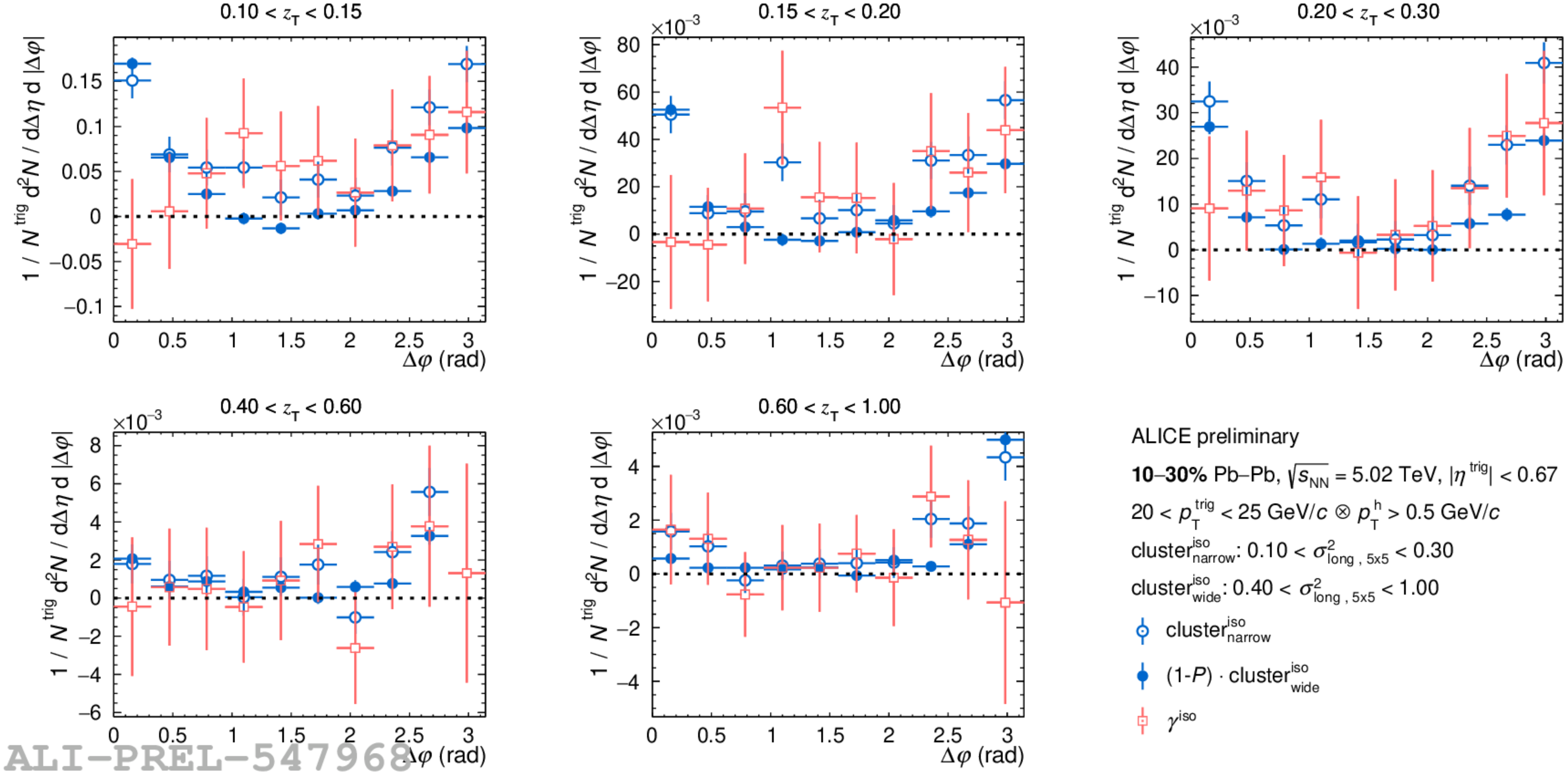

Isolated γ-hadron correlations in Pb–Pb: $D(z_T)$

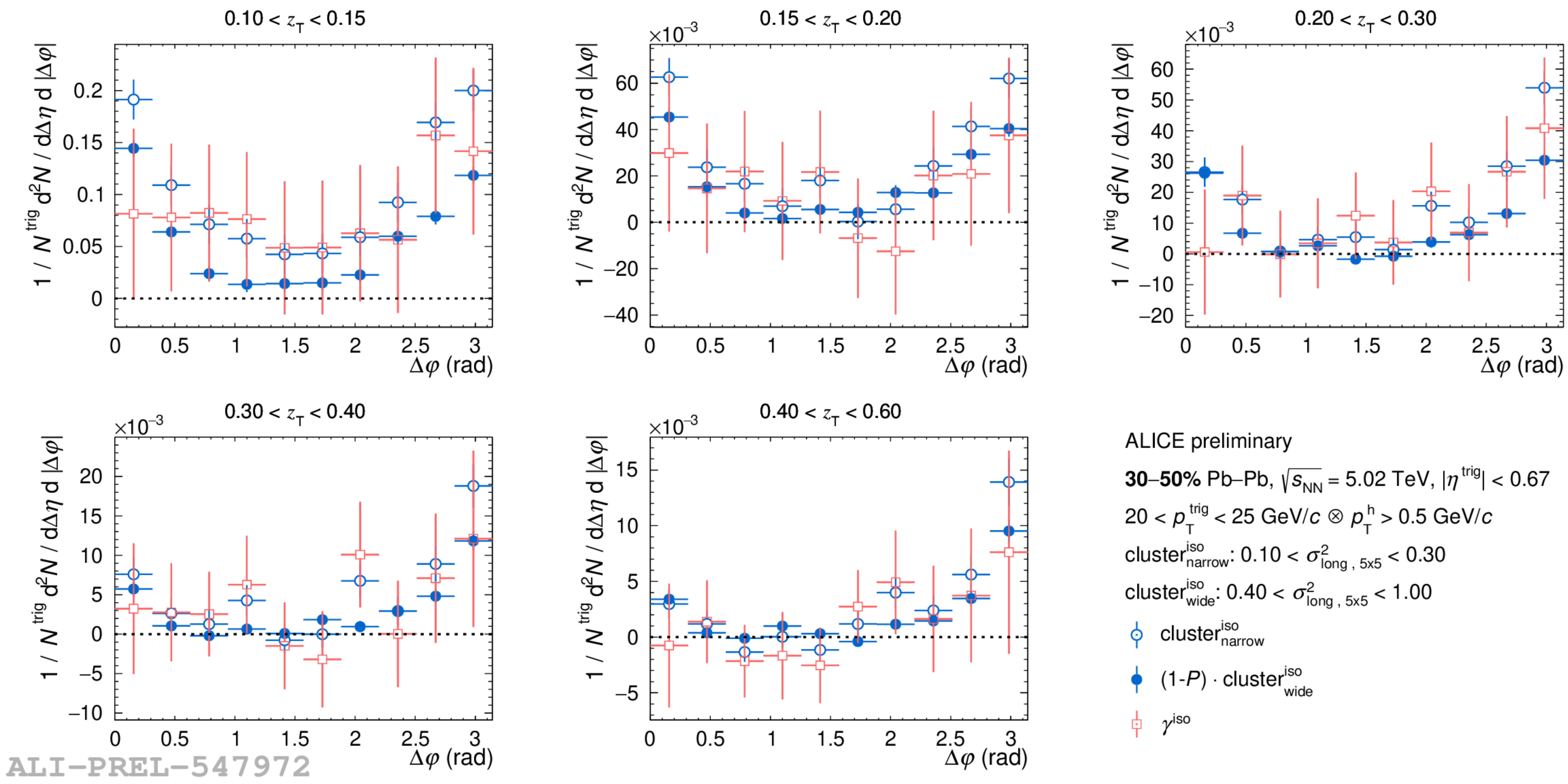

Isolated γ-hadron correlations in Pb–Pb: $D(z_T)$

ALICE

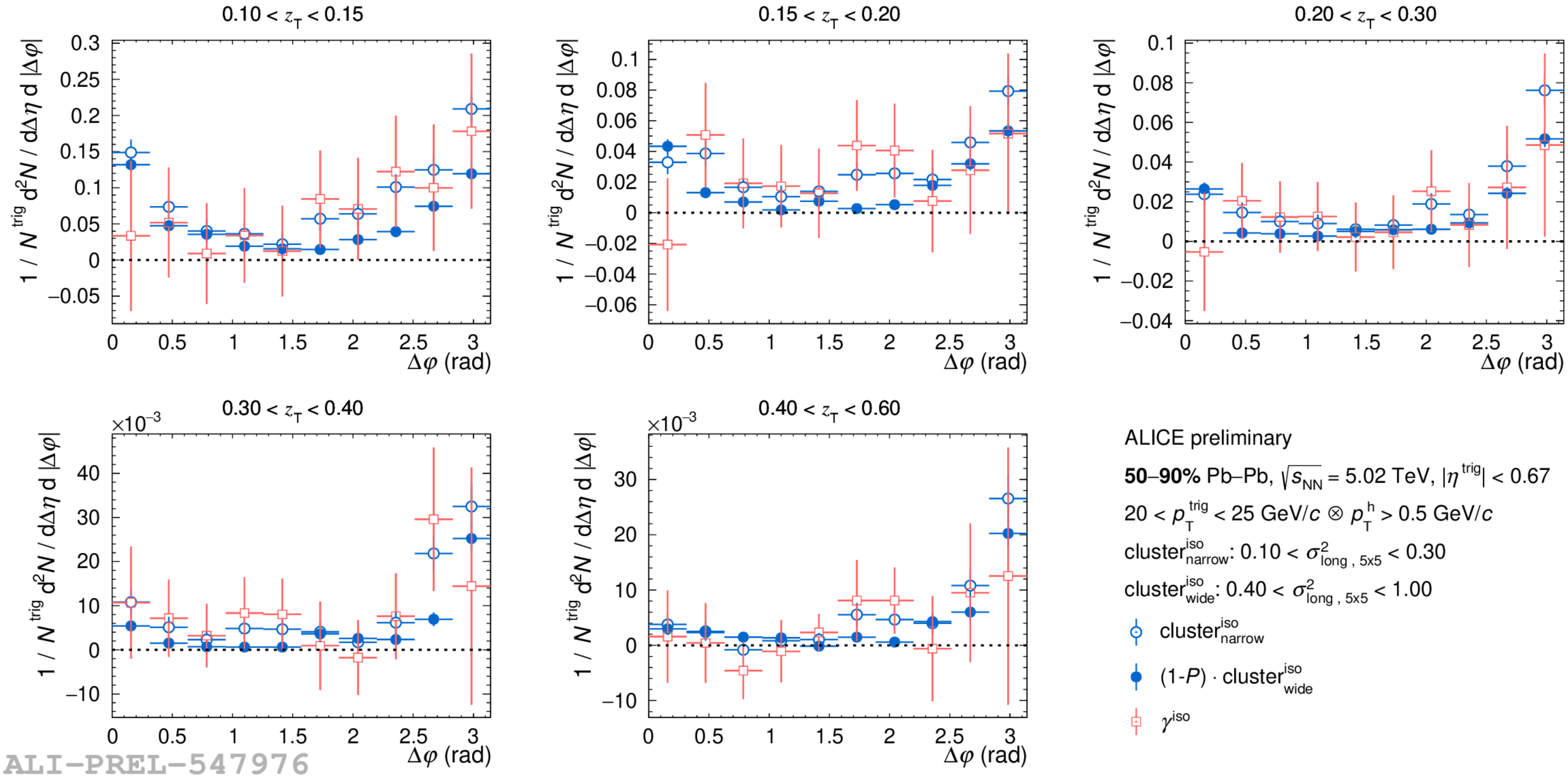

Isolated γ-hadron correlation uncertainty: $D(z_T)$

Isolated γ-hadron correlation uncertainty: I_{CP}

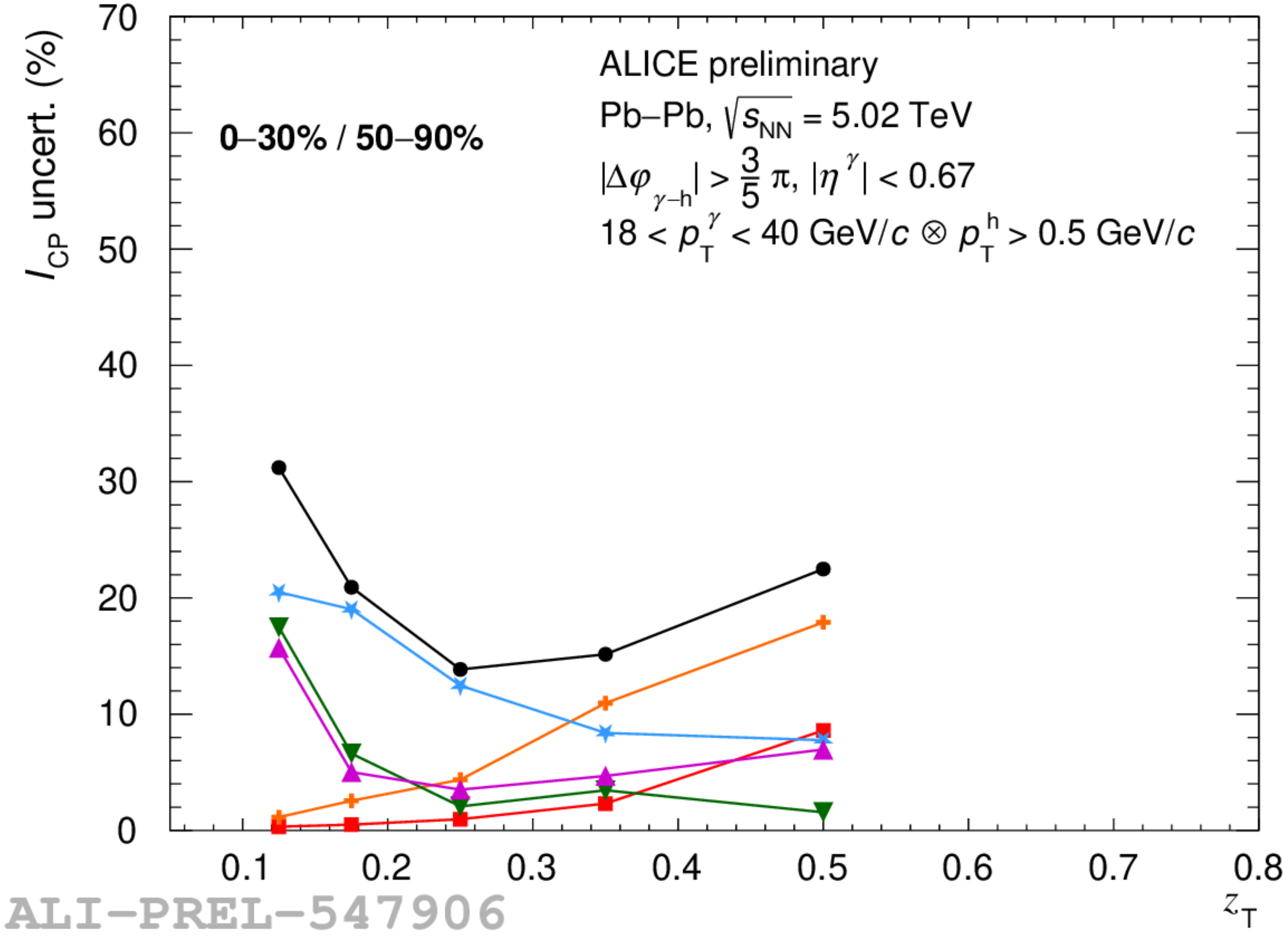

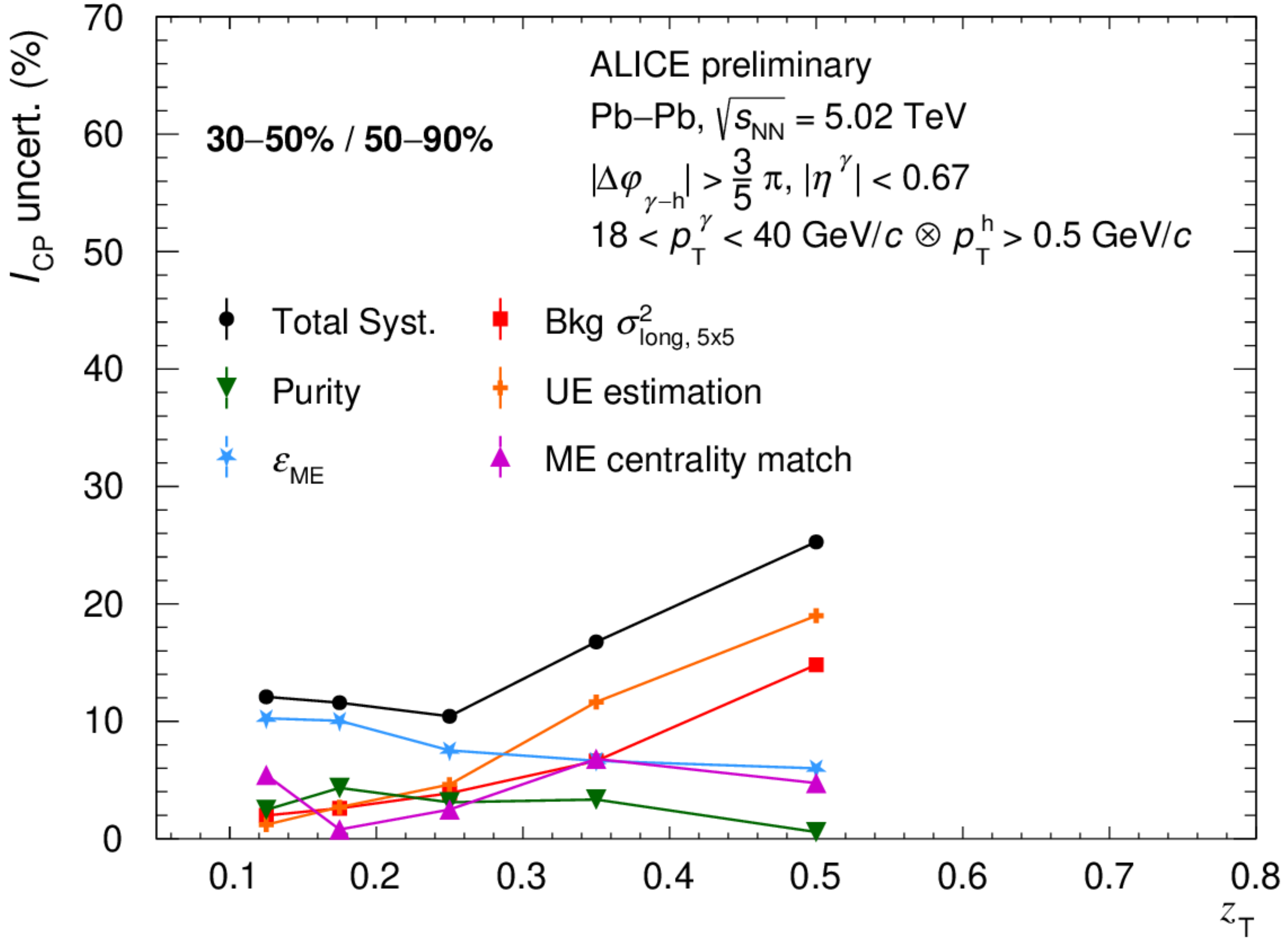

Isolated γ cross section R ratio in ATLAS, pp $\sqrt{s}$ = 13 TeV

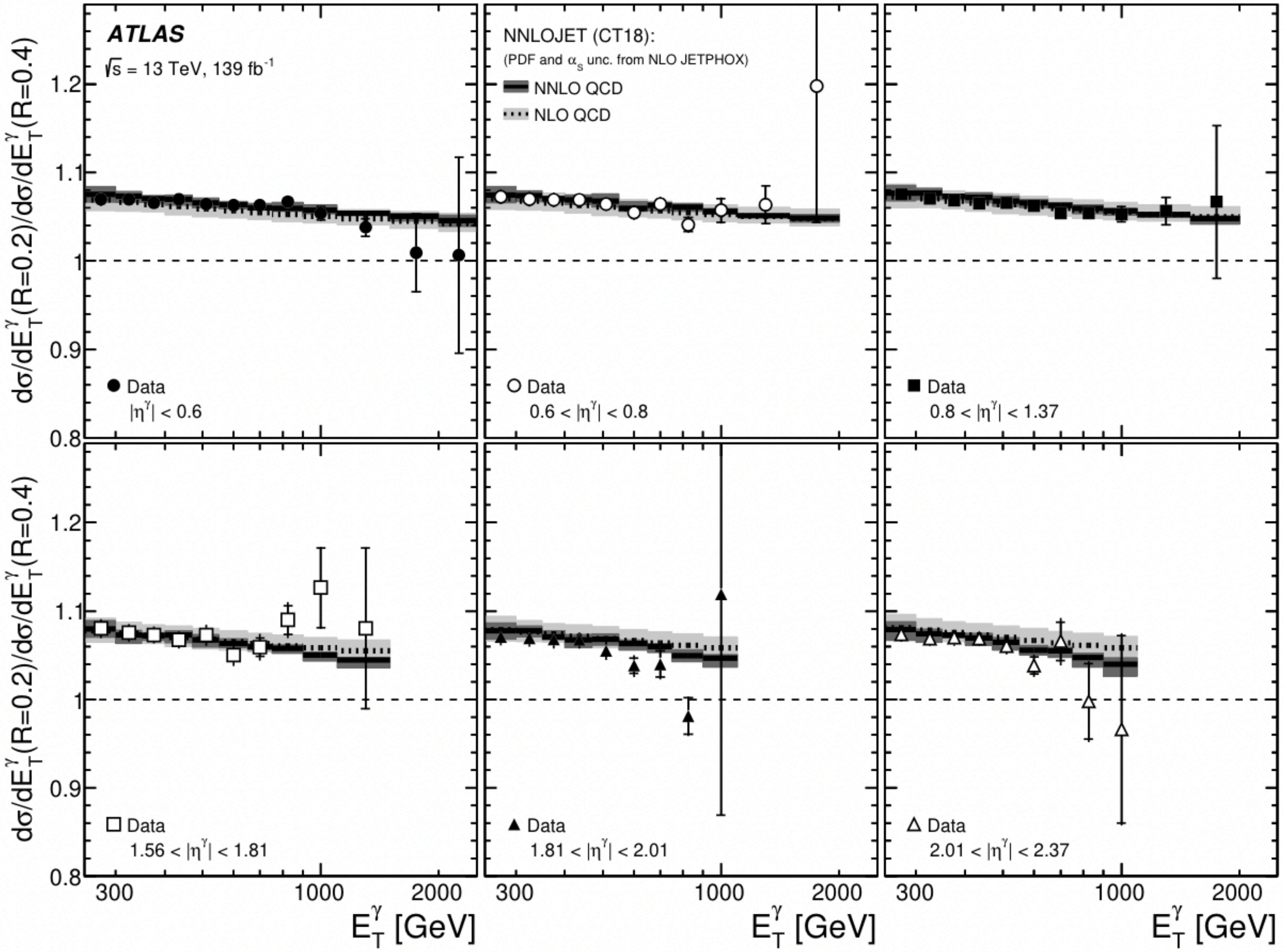

Figure 21: Measured ratios of the differential cross sections for inclusive isolated-photon production for $R = 0.2$ and $R = 0.4$ as functions of E_T^γ in different η^γ regions. The NLO (dotted lines) and NNLO (solid lines) pQCD predictions from NNLOJET based on the CT18 PDF set are also shown. The inner (outer) error bars represent the statistical uncertainties (statistical and systematic uncertainties added in quadrature) and the shaded bands represent the theoretical uncertainties. For some of the points, the inner and outer error bars are smaller than the marker size and, thus, not visible.

JHEP 07 (2023) 86

arXiv:2302.00510

Inclusive prompt γ to π^0 ratio

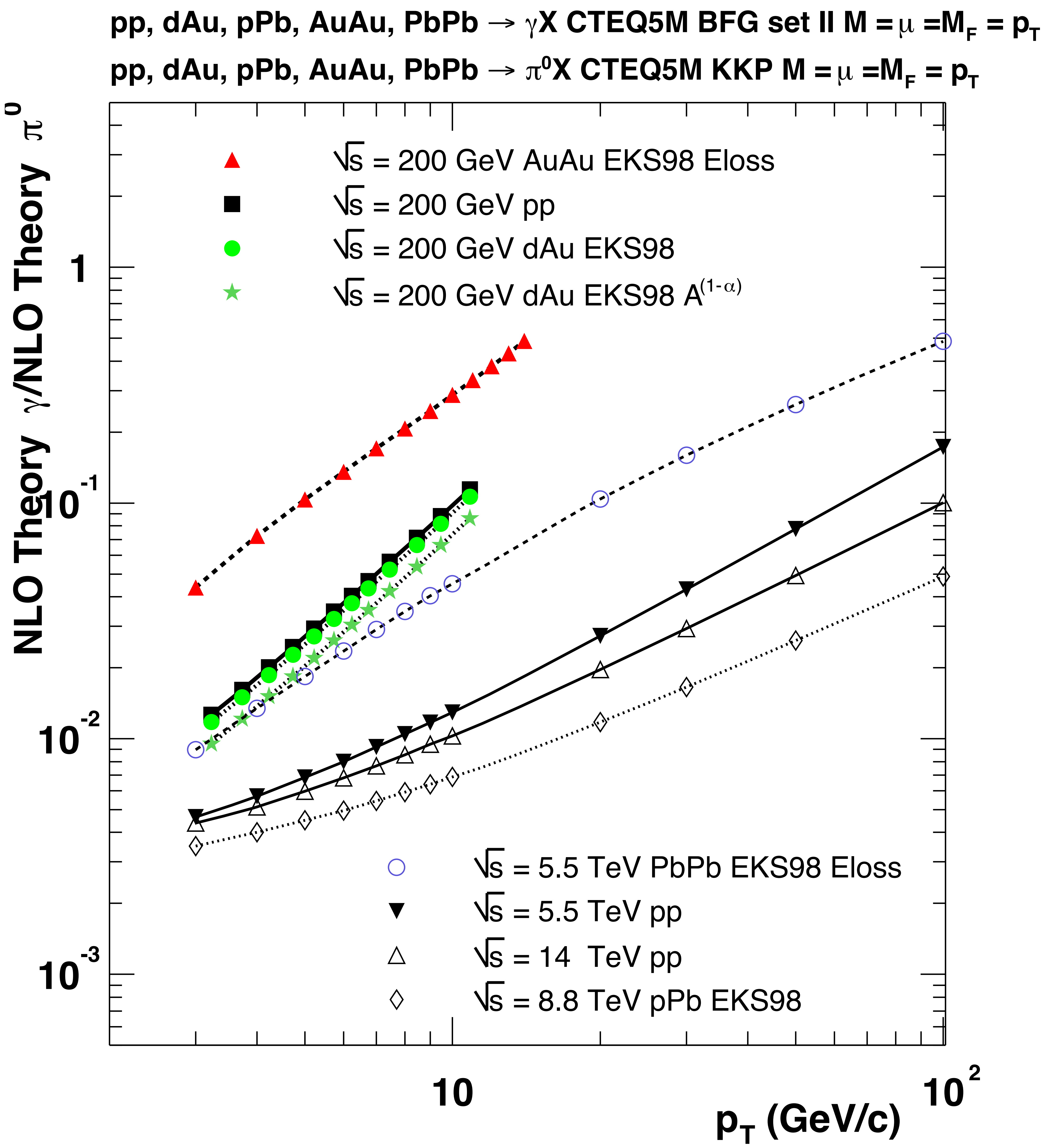

Photon yellow report (2003)
arXiv:hep-ph/031113